Report from Energy Norway

Probabilistic analyses of dams – Experience and recommendations - Phase II

Damsikkerhet i et helhetlig perspektiv (DSHP)

REPORT

Project name:

Damsikkerhet i et helhetlig perspektiv (DSHP)

Document name:

Probabilistic analyses of dams – Experience and recommendations - Phase II

Document number:

EN-01

Date: 15.01.2020

Revision: C01 – For review

Prepared by: Dr.techn. Olav Olsen v/Thomas Konow, Johannes O. Mydland

Norconsult v/Tor K. Sandaker, Hanna Eklund

NORSK SAMMENDRAG

Rapporten er utarbeidet som en del av Energi Norge sitt prosjekt *Damsikkerhet i et helhetlig perspektiv (DSHP),* og inngår som et delprosjekt *Evaluering av eksisterende betong- og murdammer*. Rapporten er utarbeidet i samarbeid mellom Dr. techn. Olav Olsen og Norconsult.

Formålet med dette dokumentet er å evaluere foreløpig praksis for konstruksjonspålitelighet av betong-dammer og komme med anbefalinger til fremtidig arbeid. Målet er på sikt å etablere en veileder for å dokumentere stabilitet av dammer ved hjelp av probabilistiske metoder. Platedammene Viervatn og Eikrebekken har blitt evaluert i denne fasen.

Så langt har Norconsult og Dr. techn. Olav Olsen i to runder gjort uavhengige probabilistiske analyser. Gjennom dette arbeidet har det blitt opparbeidet en bred kompetanse innen konstruksjonspålitelighet av dammer. Presentasjon av prosjektet på ICOLDs kongress i Wien, 2018, viste at temaet er svært relevant. Sammen med rapporten “Probabilistic model code for concrete dams” (PMCD) utarbeidet av Energiforsk i Sverige, representer dette prosjektet nybrottsarbeid som vil være viktig for å videreutvikle regelverk, sikkerhetsvurderinger og generell forståelse av damsikkerhet i Norge og internasjonalt.

I neste fase er det er viktig å konsolidere den kunnskapen som er opparbeidet til nå, der forslaget er at Norconsult og Dr. techn. Olav Olsen samarbeider mot en felles rapport «Best practice» med anbefalinger for probabilistiske analyser. For det fremtidige arbeidet anbefales det å jobbe med valg og dokumentasjon av parametere for probabilistiske beregninger, videre undersøke modelleringsantakelser i beregnings-modellene og antakelser for probabilistiske variabler, samt gjøre flere probabilistiske beregninger på dammer som tilfredsstiller dagens deterministiske regelverk for å etablere akseptverdier for pålitelighet målt med pålitelighet indeks β eller bruddsannsynlighet p_f.

SUMMARY

This report has been prepared as part of Energi Norge's project *Damsikkerhet i et helhetlig perspektiv (DSHP)* and is included in the sub-project *Evaluering av eksisterende betong- og murdammer*. The report has been prepared in collaboration between the consulting engineering firms Dr. techn. Olav Olsen and Norconsult.

The purpose of this document is to evaluate preliminary practices for structural reliability of concrete dams and make recommendations for further work. The long-term goal is to establish a guideline to document the stability of dams using probabilistic methods. The buttress dams Viervatn and Eikrebekken have been evaluated in this phase.

So far Norconsult and Dr. techn. Olav Olsen have performed independent and parallel analyses. Through this work, a broad experience base has been established for the use of probabilistic analyses on dams. Presentation of the project at the ICOLD Congress in Vienna, 2018, showed that the topic is highly relevant, but so far less applied for dams. Together with the report *Probabilistic model code for concrete dams* (PMCD) by Energiforsk in Sweden, this project represents innovative work that will be important for further development of regulations, safety assessments and general understanding of dam safety in Norway and internationally.

For the next phase, it is considered important to consolidate the experience achieved regarding this analysis method, focus should be on further development of a "Best practice" guideline including recommendations for probabilistic analyses. For the future work, it is recommended to work with selection and documentation of parameters for probabilistic analyses, investigation of modelling assumptions in the calculation models and assumptions for probabilistic variables, as well as include more probabilistic calculations on dams that meet the current deterministic rules. This to establish acceptance criteria for the reliability based on the reliability index β or fracture probability p_f.

CONTENTS

1 INTRODUCTION

It is the aim of this document to evaluate the current practice of structural reliability of concrete dams and provide suggestions for further work. The two buttress dams Viervatn and Eikrebekken are evaluated in this phase.

Safety factors calculated according to the dam safety regulations do not necessarily give a clear picture of the safety of a dam. Dams with the same calculated safety factor may have different probabilities of failure. Probabilistic analyses of existing dams are considered a suitable method for assessing reliability, e.g. against sliding and overturning. The calculations result in a reliability index, β, as an expression of the probability of failure.

Calculations based on probabilistic analysis can provide a clear and transparent representation of variables that affect the dam's safety against failure. The analyses indicate which variables are the most sensitive and thus to a greater extent affect the probability of failure.

2 BACKGROUND

2.1 Motivation

As history has shown multiple times, the failure of a dam can lead to catastrophic consequences for the nearby area, with a potential loss of human lives. Also, the loss of a dam and its reservoir can potentially cripple the national power production. The reliability of the structure is therefore of the outmost importance to ensure the safety of humans and the surrounding ecosystem.

In Norway dams and waterways are classified with respect to the consequences due to potential failure. The purpose is to differentiate the dams in terms of safety requirements and to establish an emergency plan in case of a disaster. The five classes are summarized in Table 2.1.

Table 2.1 Classification criteria §4-2 translated from Norwegian Dam Safety Regulations [1]

Consequence class	Housing units	Infrastructure, public functions	Environment and property
4	> 150		
3	21-150	Damage to heavily trafficked road and railway, or other infrastructure with particular large importance to life and health.	Large damage with particular importance to environmental values or particular large damage to foreign property.
2	1-20	Damage to medium trafficked road and railway or other infrastructure with large importance to life and health.	Large damage to important environmental values or large damage to foreign property.
1	Temporary habitat equivalent to < 1 permanent housing unit	Damage to less trafficked road or other infrastructure with importance to life and health.	Damage to environmental values or foreign property.
0 *)	Insignificant consequences		

*) This class is not included in the original Table 4-2.1.

It is stated in the Norwegian Dam Safety Regulations §5-1 that the watercourse facility shall have sufficiently high safety level at all time such that breach, failure or malfunction shall not occur. In the case of existing facilities where it's not possible to satisfy the technical requirements in §5, compensatory structural measures shall be implemented to ensure adequate high safety level.

Although explicit requirements are given in the current regulation, the safety level is rather loosely defined. The consequence class is mostly tied to the flood calculations, i.e. the external loads. Furthermore, the impression may be that the uncertainty and reliability is fully contained within the safety factor. However, this is a false assumption since the technical requirements given in §5 mostly increases the reliability of the structure, and thus obscuring the correlation between the safety factor and the required safety level. The safety factor is also highly dependent on the engineering assumption done in the calculations and may lead to large spread in results depending on the assumptions made by the analyst.

The lack of a clear understanding of the uncertainties tied to the safety level poses a challenge when evaluating existing structures. For an older dam it might be expected that the material has degraded, and the loads may change due to changes in the way the dam is regulated or in climate. On the other hand, with each passing year new knowledge is accumulated and thus reducing the uncertainties in other areas.

It's the total sum of the changes and new knowledge which is of importance when evaluating the current and future safety level of the structure.

As has been the case for other civil engineering fields, the traditional safety factor has mostly been based on rather empirical and/or intuitive notations. According to Melchers the realization that the notion "factor of safety" had little philosophical or theoretical justification, has been the driving force in the development of structural reliability theory [2]. In fact, modern standards as the Eurocode and newer DNV guidelines are built upon the theory of structural reliability. This implies that the safety factor, or the more refined partial factor method, can be estimated and calibrated through probabilistic analysis. One should however be aware that current Eurocodes are primarily based on historical and empirical methods and not on probabilistic methods (Appendix C4(4), [3])

2.2 Structural reliability

It's expected by the general society that man-made structures are reliable. Ideally the structure shall not fail, however, due to various reasons, this is impossible to achieve. One is therefore forced to accept some risk that a failure may occur. This implies a safety level must be defined, either qualitatively or quantitatively, such to reflect the societal perception of required safety.

As previously mentioned, the Eurocode is a modern standard which employs the theory of structural reliability. Another key reference is the world's first "material-independent" design code [4]. Although the Eurocode allows for design by probabilistic methods (3.5(5) [3]), the preferred method, and common practice, is the partial factor method (3.5(4) [3]).

The partial factor method is similar to the safety factor method in the sense that fixed values are used to a large degree to define the required safety level. In the partial factor method, the uncertainty is tied directly to the load and separately to the capacity. The partial factors can also be related to probabilistic methods (chapter 9 [5]). Note for simplified conditions the safety factor can even be related to the partial factors and probabilistic method as shown in subchapter 9.4.2 by Melchers.

In principle the partial factor could be calibrated from probabilistic methods as shown in Figure C1 in Eurocode 0 [3]. Figure C1, and such exercises have been performed as illustrated in the doctoral thesis Appendix B [6]. So far, the calibration is mostly based on the method a, i.e. historical and/or empirical methods.

Eurocode also gives additional guidance for reliability with appendix B. Reliability classes is suggested with minimum reliability level measured in β for ultimate capacity (B3.2 [3]). One should however be careful with utilizing these values directly for other structures than buildings, since stricter requirements can be necessary for special structures as dams (1.1(2) [3]). Similarly, differentiation in reliability can be achieved using the K_{FI} load factor which is tied to the reliability class. Note that appendix B is in Norway informative and is only used indirectly in the National Appendix. The minimum β-values for the different is not used explicitly.

2.3 Previous work

In recent years attention has been paid to probabilistic analyses of dams mainly with focus on research and work done in Sweden at KTH and Swedish Energiforsk. The Probabilistic Model Code for Concrete dams (PMCD) is a first attempt to establish the necessary ground rules for performing probabilistic calculations of dam stability.

Previous experience of the subproject of DSHP, Probabilistic analysis of dams which is financed by Energy Norway, has shown that the PMCD is not suitable for all Norwegian dams. Experience from dam Reinoksvatn showed that the proposed method for modelling water load in PMCD is not suitable for multi-annual reservoirs. The current proposed formulation for ice load also gives much higher ice-loads than compared to the guidelines used in Norway and is thus problematic. For this reason, a lower variance was used at dam Hensfoss in order to better assess the structural reliability of the dam.

In both cases only one single section was evaluated, which may or may not be representative for the reliability of the whole structure, depending on the system reliability.

2.4 Scope of the report

This document is essentially divided into three parts. The first part in Section 3 is meant to give some basic theoretical background and addresses some topics that should be considered when performing reliability analysis of dams, and potentially establishing design codes within this framework. For more thorough details of structural reliability, the reader is referred to the literature. Two recommended books are Structural reliability analysis and prediction [5] and Structural Reliability Methods [7].

The second part in Section 4 and Section 5 is a summary of the reports for Dam Viervatn and Dam Eikrebekken respectively. The third part looks at possible further work.

3 PROBABLISTIC METHOD

3.1 Overall structural probability of failure

The structural reliability is directly linked to the probability of failure and thus attention should be given to the driving factors. The reliability is the sum of the engineering decisions, quality assurance, organization, experience, quality of work during construction, etc. An approximation of the structural failure probability is suggested as following [2] and a short description is given in Figure 3.1.

$$p_F = p_T + p_U + p_{TU} + p_{UT}$$

In recent years most structural failures are due to human error, which implies $p_U \gg p_T$. However, most focus is given to the “technical safety” p_T that can be estimated with structural reliability theory and thus more easily quantifiable. The focus of this document is to primarily address the “technical safety”. One should be aware that a good design on paper does not necessarily reflect the true reliability of the actual structure after construction.

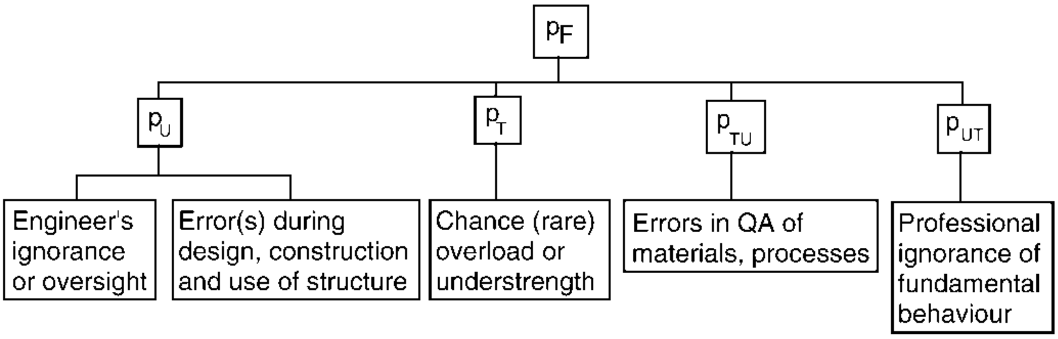

> *Figure 3.1 Classification of human and other errors (adapted from Baker and Wyatt), [2].*

Note that the Norwegian Dam Safety Regulation has explicit requirements with regards to organizational requirements to watercourse facilities and technical qualifications of personnel. Additionally, every flood calculation, dam reassessment and technical design shall be approved by NVE. However, there is still room for improvement with regards to third party control, as is the common practice for major civil infrastructures (roads and railways) in Norway.

A relevant example of error during construction is the installation of rock bolts in dam. It’s known that in several cases that improper grouting has occurred (i.e. pouring from the top) and illustrates how a good designed can be voided by bad workmanship. A probabilistic analysis can in such cases be used to estimate the impact on the reliability.

3.2 Target reliability

In order to perform design based on probabilistic methods, predefined reliability targets must be determined. As described in section 2.1, this should depend on the consequences and reflect the safety level set by the society.

A short summary of some target reliability used in design codes is given below with focus on the ultimate load capacity. With regards to section 3.1, these values are related to the technical reliability and does not necessarily reflect the actual failure rate of a structure, i.e. $p_T = p_f$ in the tables below.

3.2.1 Eurocode

Appendix B suggests minimum values for the reliability index associated with reliability classes. However, as indicated in a paper of reliability levels in Eurocode [8], the suggested target reliabilities can also be interpreted as average target values. The reasoning for this is that many engineers considers the value of $\beta = 3.8$ in 50 years as a calibration target value for partial factors.

As discussed in section 2.2, one should be careful using these values directly, especially when considering other structures as dams where the minimum values for β should perhaps even be larger. This will be dependent on the assumptions used in code calibration.

The probability of failure is related to the β through the relationship

$$p_f = \Phi(-\beta)$$

where Φ is the cumulative function of the standard normal distribution.

> *Table 3.1 Recommended minimum values for reliability index β (ULS), Table B2 [3]*

Reliability Class	**Minimum values of β**	
	1-year reference period	**50 years reference period**
RC3	5,2	4,3
RC2	4,7	3,8
RC1	4,2	3,3

3.2.2 JCSS – Probabilistic Model Code

The Probabilistic Model Code by JCSS is an attempt to create a consistent way of performing probabilistic analysis based on rules, regulations and reliability theory. The target reliability provided by JCSS are built on optimization procedures and the ultimate limit state shown in the table below are obtained from a cost benefit analysis, chapter 7.2 [9]

It is also stated that the shadowed value in the table should be considered as the most common design situation. Furthermore, guidelines for selecting the “right” target reliability should be tied to the consequence class, failure mode (brittle/ductile), relative cost of safety measures, degree of uncertainty, quality assurance, etc.

> *Table 3.2 Tentative target reliability indices β (and associated target failure rates) related to one year reference period and ultimate limit states. [9]*

1	2	3	4
Relative cost of safety measure	Minor consequences of failure	Moderate consequences of failure	Large consequences of failure
Large (A)	β=3.1 ($p_F \approx 10^{-3}$)	β=3.3 ($p_F \approx 5\ 10^{-4}$)	β=3.7 ($p_F \approx 10^{-4}$)
Normal (B)	β=3.7 ($p_F \approx 10^{-4}$)	β=4.2 ($p_F \approx 10^{-5}$)	β=4.4 ($p_F \approx 5\ 10^{-6}$)
Small (C)	β=4.2 ($p_F \approx 10^{-5}$)	β=4.4 ($p_F \approx 5\ 10^{-6}$)	β=4.7 ($p_F \approx 10^{-6}$)

3.2.3 DNV

Structural reliability is also practiced within offshore engineering, and guidelines are given by DNV [10], [11]. In appendix B for “Guideline for Offshore Structural Reliability Analysis – General”, the tables below are provided. The annual probability given in Table B.3 is to be used when no calibration against well-established practice or similar designs are available.

> *Table 3.3 Recommended failure probabilities in DNV. [11]*

Table B.3 Target Annual Failure Probabilities in DNV

	Consequences	
Class of Failure	Less Serious	Serious
I - Redundant Structure	10^{-3}	10^{-4}
II - Non-redundant structure, significant warning before failure	10^{-4}	10^{-5}
III - Non-redundant structure, no warning before failure	10^{-5}	10^{-6}

Skjong,R., E.B.Gregersen, E.Cramer, A.Croker, Ø.Hagen, G.Korneliussen, S.Lacasse, I.Lotsberg, F.Nadim,K.O.Ronold (1995) “Guideline for Offshore Structural Reliability Analysis-General”, DNV:95-2018

In the same appendix the following annual target failure probability is provided by the Nordic Committee for Safety of Structures (NKB).

> *Table 3.4 Recommended failure probabilities in NKB. [11]*

Table B.4 Target Annual Failure Probabilities in NKB

	Type of failure		
Consequences of failure	Ductile with reserve capacity	Ductile without reserve capacity	Brittle instability
Not serious	10^{-3}	10^{-4}	10^{-5}
Serious	10^{-4}	10^{-5}	10^{-6}
Very serious	10^{-5}	10^{-6}	10^{-7}

3.2.4 PMCD

The target safety index from PMCD has been defined from calibration to existing dams that fulfil the deterministic requirement with the corresponding assumptions suggested in PMCD. The calibration is documented in “Dammsäkerhetsannolikhetsbaserad bedömning av betongdammars stabilitet, Rapport 2016:291” [12] using the assumptions and methods described in PMCD [13]. One can observe that the reliability index is similar to the ones in Table 3.1. Note that due to different regulation the required reliability index for Norwegian dams might be different from the ones listed here.

> *Table 3.5 Recommended minimum values for β in ultimate limit states. Reference period 1 year*

Dam consequence class	Minimum β	Equivalent P_f
A	5.2	$\approx 10^{-7}$
B	4.8	$\approx 10^{-6}$
C	4.2	$\approx 10^{-5}$
U	3.8	$\approx 5 \cdot 10^{-4}$

3.3 Limit state functions

The main objective of a reliability analysis in structural engineering is to ensure that the estimated probability of failure of the structure is below a certain target value. The classical and simplest approach to this problem is to define a Limit State Function (LSF) given as G = R − S, where R is the resistance and S is the load action. The variables R and S are uncertain and are often assigned appropriate probability density functions. Once these functions are known, the probability of failure, P (G ≤ 0), can be calculated.

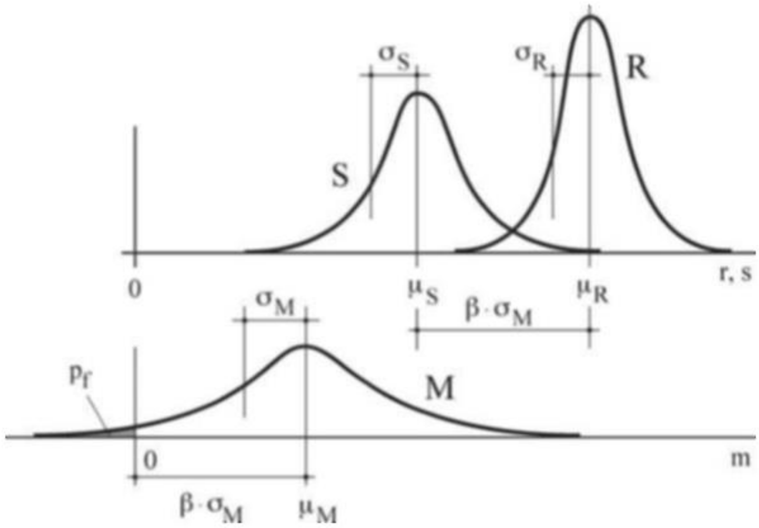

> *Figure 3.2 Probability density function of resistance, load and safety margin. [14]*

The limit state can also be expressed as the safety margin M = R −S, as shown in Figure 3.2. The method developed by Basler [15] and presented in the notation of Cornell [16], can be used to find the exact probability of failure assuming the variables are normally distributed.

In general, there might be many variables involved in the calculations. The variables can also be correlated, as for an instance the stress being a function of the strain. Once the limit state function is defined, the generalized reliability can be calculated as

$$p_f = P[G(x \leq 0)] = \int \dots \int_{G(x \leq 0)} f_x(x)dx$$

where $f_x(x)$ is the joint probability density function for n variables.

3.4 System reliability

Primarily structural design is focused on component behaviour looking at a single mode of failure for a single component. However, most structures are an assembly of structural components and even individual components may be susceptible to several possible failure modes. A probabilistic approach provides a better platform from which system behaviour can be explored and utilised. This can be of benefit in assessment of existing structures where strength reserves due to system effects can alleviate the need for expensive strengthening. [17]

System failure is described with a combination of several limit state functions, each representing one single failure mode and structural component. It is generally distinguished between system configurations that corresponds to a purely parallel or series arrangement of failure modes and components. A combination of both is also possible

4 DAM VIERVATN

4.1 Summary

Reliability indices for stability, sliding and overturning, of one dam pillar have been calculated as an expression of the pillar's probability of failure at dam Viervatn. Stochastic variables have been carefully selected and a density function for each parameter has been chosen based on collected data and literature. Also, a sensitivity study has been performed, determining the stochastic variables' impact on the result.

A probabilistic model based on Monte Carlo simulations has been used and the results are products of 10^8 simulations. The resulting reliability indices for sliding ranges from 2.8 and up, while the probability indices for overturning ranges from 4.6 and up. The resulting reliability indices of the design situation which include bolt capacity and cohesion are higher than the minimum target reliability given in the *Probabilistic model code for concrete dams* and the Eurocode. A target reliability has not been calibrated to accurately compare the results to.

The sensitivity study shows that the friction angle, water level, angle of sliding plane and dam height are the most sensitive parameters for the analyses performed in this report. These parameters are also the ones expected to carry the most uncertainty.

4.2 Case configuration

4.2.1 General

Viervatn is located approximately 9 km south east of Øvre Årdal in the municipality Årdal in Sogn og Fjordane county. The magazine is a regulated magazine connected to Tyin power plants belonging to Hydro Energi.

The dam consists of a buttress dam (slab) with massive connections and an overflow threshold designed as a gravity dam in concrete. The dam is owned and operated by Hydro Energi Sogn. Year of construction for dam Viervatn is 1953. The dam is classified as level 1 in NVE's consequence classes [18].

A deterministic stability control has been performed by Norconsult AS. This control shows that certain pillars do not satisfy the safety demands set by *Norges vassdrag- og energidirektorat* (NVE). The reliability assessment will focus on pillar 11.

Figure 4.1 Dam Viervatn. Picture taken by Norconsult in August 2019.

4.2.2 Probabilistic model

The Monte Carlo (MC) method is used to evaluate the stability of dam Viervatn and compute the reliability index. The calculation model for sliding and overturning are based on limit equilibrium as described in NVE's *Retningsliner for betongdammer* [19].

The design situations applied are shown in Table 4.1. All situations are analysed with and without the contribution of cohesion and bolts.

> *Table 4.1 Design situations for stability.*

Design situation	Self-weight	HRV	DFV	Ice load
1	x	x		
2	x	x		x
3	x		x	

The stochastic variables and the assumptions for their probability density function are summarized in Table 4.2. For further details of the stochastic variables, see **Error! Reference source not found.**.

> *Table 4.2 Summary of stochastic variables.*

Parameter	Distribution	μ	CoV	σ	Upper limit	Lower limit	Peak
k_{bot}	Normal	1222 m	0.00038	0.46 m			
α	Normal	-1.7 °	1	-1.7 °			
h_o/v_o	Normal	8.5/10	0.004	0.034/10			
b_{eff1}	Normal	4.95 m	0.05	0.248 m			
b_{eff2}	Normal	4.7 m	0.05	0.235 m			
γ_b	Normal	23.5 kN/m^3	0.034	0.8 kN/m^3			
φ	Normal	50 °	0.05	2.5 °			
c	Normal	0.29 MPa	0.15	0.0435 MPa			
f_y	Lognormal	180 MPa	0.07	12.6 MPa			
$k_{w.DFV}$	Triangular				1231.5 m	1230.1 m	1231.16 m
$k_{w.HRV}$	Triangular				1230.1 m	1208.1 m	1215.0 m
q_i	Lognormal	100 kN/m	1	100 kN/m	222.5 kN/m		

4.3 Results

4.3.1 Reliability index

The results of the 10^8 Monte Carlo simulations are shown in Table 4.3 to Table 4.6. As expected, design situation 2 without the contribution of cohesion and bolts result in the lowest reliability index of 2,8. Dam Viervatn can be assumed to fall under consequence class C in the PMCD, which suggest a target reliability index of 4,2. Neither design situation 2 nor 3 satisfy this condition in sliding when cohesion and bolts are not included. The calibration of target reliabilities from the PMCD are based on a calculation model that includes rock bolts. The results given in Table 4.5 are therefore more adequate for comparison. In this case the reliability indices all satisfy the minimum β. With regards to the target reliabilities given in Eurocode 0, Dam Viervatn could be classified as RC1. Eurocode gives a target reliability like the PMCD of 4,2, and the same considerations as above can be made.

Table 4.3 Results for limit states without contribution of bolts and cohesion.

Design situation	Sliding		Overturning		Stability	
	β	**P_f**	**β**	**P_f**	**β**	**P_f**
1	4.5	3.18E-06	> 5.6	< 1.00E-08	4.5	3.18E-06
2	2.8	2.42E-03	4.6	1.79E-06	2.8	2.42E-03
3	3.8	6.41E-05	> 5.6	< 1.00E-08	3.8	6.41E-05

Table 4.4 Results for limit states included contribution from cohesion.

Design situation	Sliding		Overturning		Stability	
	β	**P_f**	**β**	**P_f**	**β**	**P_f**
1	> 5.6	< 1.00E-08	> 5.6	< 1.00E-08	> 5.6	< 1.00E-08
2	> 5.6	< 1.00E-08	4.6	1.63E-06	4.6	1.63E-06
3	> 5.6	< 1.00E-08	> 5.6	< 1.00E-08	> 5.6	< 1.00E-08

Table 4.5 Results for limit states included contribution from bolts.

Design situation	Sliding		Overturning		Stability	
	β	**P_f**	**β**	**P_f**	**β**	**P_f**
1	> 5.6	< 1.00E-08	> 5.6	< 1.00E-08	> 5.6	< 1.00E-08
2	4.2	1.43E-05	> 5.6	< 1.00E-08	4.2	1.43E-05
3	5.3	6.00E-08	> 5.6	< 1.00E-08	5.3	6.00E-08

Table 4.6 Results for limit states included contribution from cohesion and bolts.

Design situation	Sliding		Overturning		Stability	
	β	**P_f**	**β**	**P_f**	**β**	**P_f**
1	> 5.6	< 1.00E-08	> 5.6	< 1.00E-08	> 5.6	< 1.00E-08
2	> 5.6	< 1.00E-08	> 5.6	< 1.00E-08	> 5.6	< 1.00E-08
3	> 5.6	< 1.00E-08	> 5.6	< 1.00E-08	> 5.6	< 1.00E-08

4.3.2 Sensitivity

Results of the calculation of sensitivity measurements are shown in Figure 4.2 to Figure 4.4.

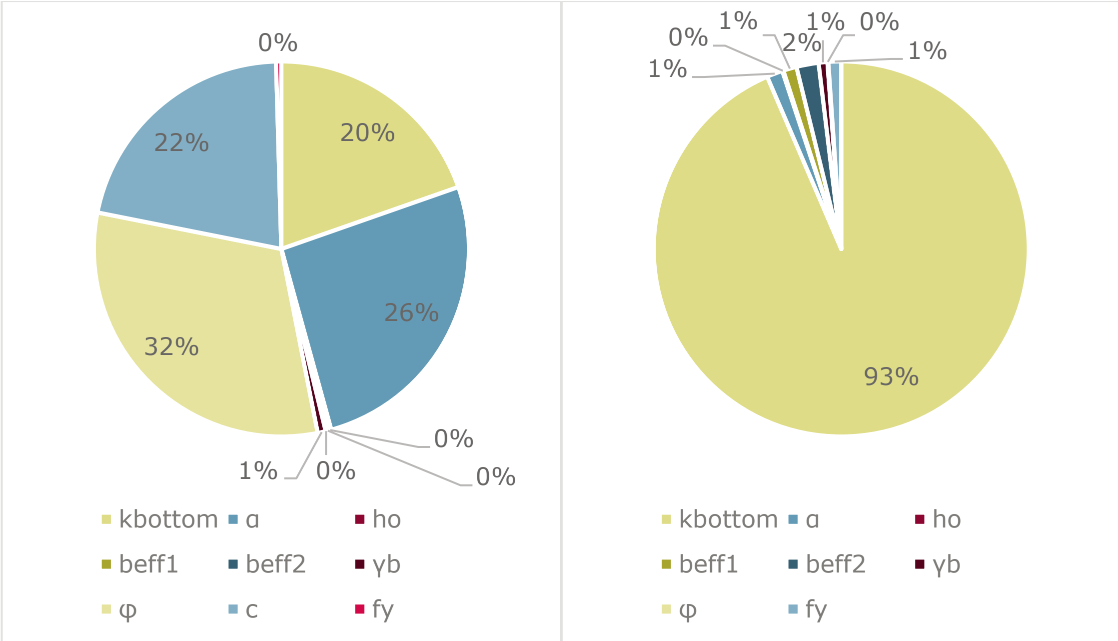

> *Figure 4.2 Sensitivity indices for design situation 1, sliding (left) and overturning (right).*

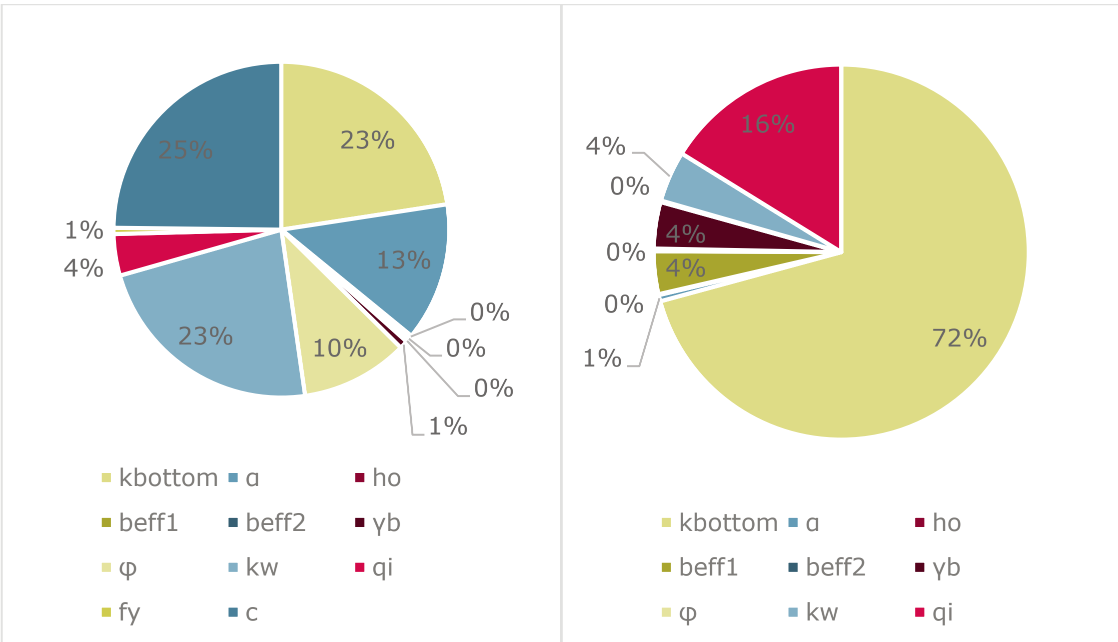

> *Figure 4.3 Sensitivity indices for design situation 2, sliding (left) and overturning (right).*

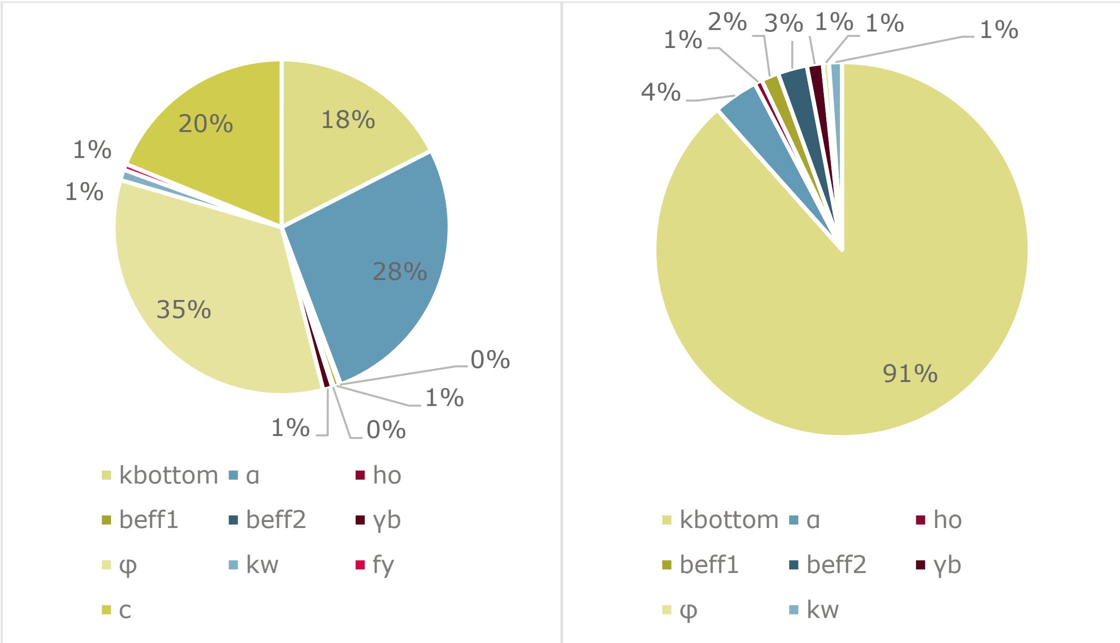

> *Figure 4.4 Sensitivity indices for design situation 3, sliding (left) and overturning (right).*

Based on the results of the sensitivity indices, the most sensitive parameters introduced in the design situations for sliding are the friction angle, the dam height (level at bottom of dam), the angle of the sliding plane, cohesion, the water level and the ice load. The other parameters, the effective width, slope of the front plate and mass density of concrete, and their distribution has only a small effect on the results. The results are as expected more sensitive to the parameters which are introduced to the analysis with a larger uncertainty.

4.4 Conclusion

In order to develop a guideline similar to the PMCD in Sweden for existing dams in Norway in the future phases of this project, a set of assumptions must be agreed upon. Future analysis must be based on the same assumptions, design situations, calculation model and probabilistic model in order to calibrate a target reliability. These assumptions must be made such that the methods in the guideline can be applied by the common engineer.

Based on the discoveries of this report assumptions for the water level, friction and sliding angle, ice load, cohesion and bolt capacity should be further investigated. These parameters have large influence on the result and are also highly sensitive when introduced to the analysis with large uncertainties.

A probabilistic model applying FORM analysis is advantageous when seeking more accurate sensitivity studies, and a suggestion is to use this approach in combination with Monte Carlo simulations. If a calculation model of limit equilibrium, as used in this report, is applied the calculation time of Monte Carlo simulations is acceptable.

5 DAM EIKREBEKKEN

5.1 Summary

Experience from the work carried out in 2017 of dam Reinoksvatn showed that the method proposed for calculating the exterior water load in Probabilistic Model code for Concrete dams (PMCD) is not suitable for all dams. Furthermore, the stochastic modelling of ice load was also an issue due to limited capability of the software, which in turn lead to a simplification of the ice load.

The main motivation of this report was to test the underlaying assumptions with regards to probabilistic modelling and how it reflected the reliability of dams. The second motivation was to show how testing and increased knowledge, i.e. less uncertainty, can improve the calculated structural reliability.

Both FORM and Crude Monte Carlo analyses has been performed for two cross-sections with different assumptions regarding the stochastic modelling of ice load, design flood level and the contribution from cohesion and rock bolts.

A simplified base case was established based on deterministic analyses and was used as a reference when comparing probabilistic results. Due to initial conservative assumptions, the calculated reliability index for the base case, and thereby most cases, was rather low in the order of $\beta \approx 2$ caused by sliding. It was also shown that by reducing the uncertainty due to hypothetical testing, and new assumptions of the water load, the calculated reliability index can be increased to roughly $\beta \approx 4$ in sliding. It's also believed that it can be further increased by accounting for macro-asperity and the buried part of the slab in the foundation.

5.2 Case configuration

The dam is located at the border of Hemsedal and Gol municipality in Norway on the river Hemsil. The dam is a conventional concrete slab buttress dam constructed between 1958-59. On each side of the buttress dam, there is a concrete gravity section between the slab buttress and then an embankment dam at the far end to the abutment.

> *Figure 5.1 Dam Eikrebekken. Picture taken by Dr. Techn. Olav Olsen in June 2019.*

The in-house developed model for dam stability calculations has been used in probabilistic analyses, which is based on common limit equilibrium calculations. The model assumes a linear sliding plane at the foundation. A drawback with the model is that one cannot easily model gate failure, and the model only calculates the sliding capacity at the assumed foundation, which is not necessarily the weakest plane. The analyses are thus restricted to only consider global equilibrium (EQU), while failure in the concrete (STR) or rock (GEO) is not considered.

The cross-section P.47 (overflow spillway and footway), and P.55 (general cross-section) were selected for probabilistic analyses. It's assumed that the slab transfers the exterior load, water pressure, directly to the buttresses. I.e. no forces are transferred from the slab to the bedrock trench. Due to the choice of calculation model the parametrization of geometry is limited, i.e. no cut-outs, footbridge etc.

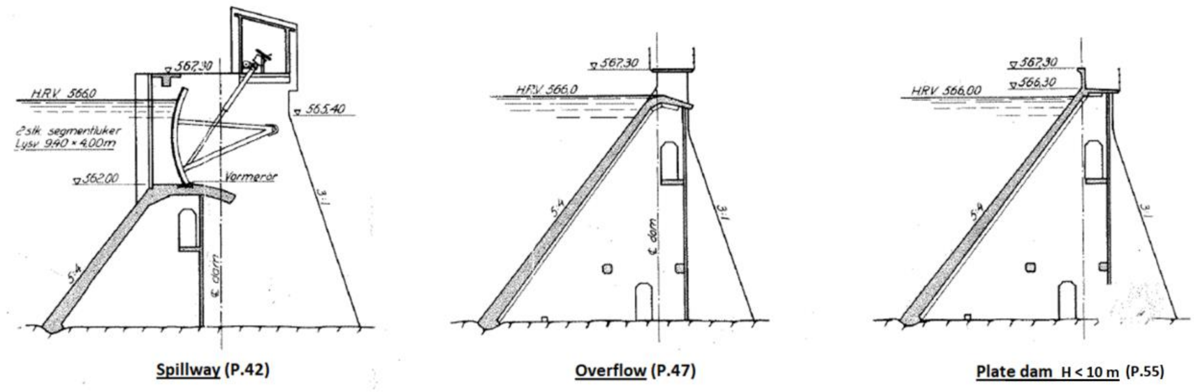

> *Figure 5.2 Cross section used in deterministic and probabilistic analyses.*

For comparison some initial deterministic calculations were performed for P.47 and P.55. This was also done to compare the results with previous stability calculations from the reassessment of the dam done by Norconsult in 2004. The deterministic results for the load combination of HRV and 100 kN/m ice load is critical with respect to sliding for a friction coefficient of 50°.

Different assumptions for the ice load have been studied. The recommended ice load with truncation according to PMCD, without truncation and ice load with reduced variance is assumed in the probabilistic analyses.

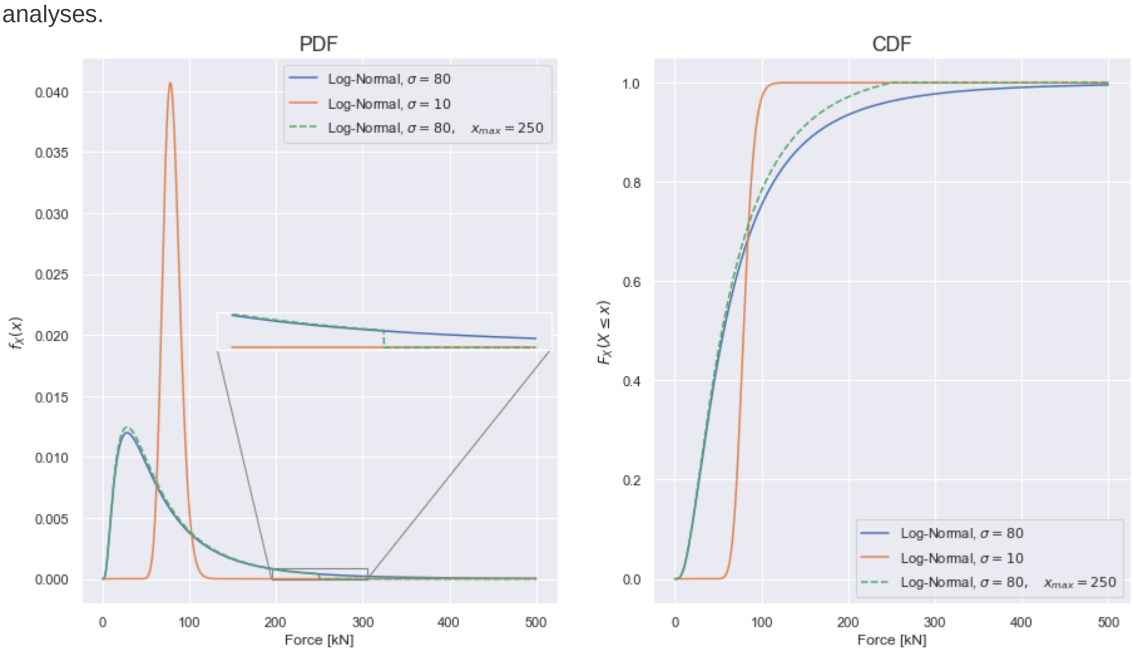

> *Figure 5.3 PDF and CDF of different Ice-load assumptions.*

An alternative approach for determining the stochastic maximum flood level based on extreme value theory, measured data on site and spillway capacity is here suggested. Lastly the effect of cohesion and rock bolts is compared to the base case that is established.

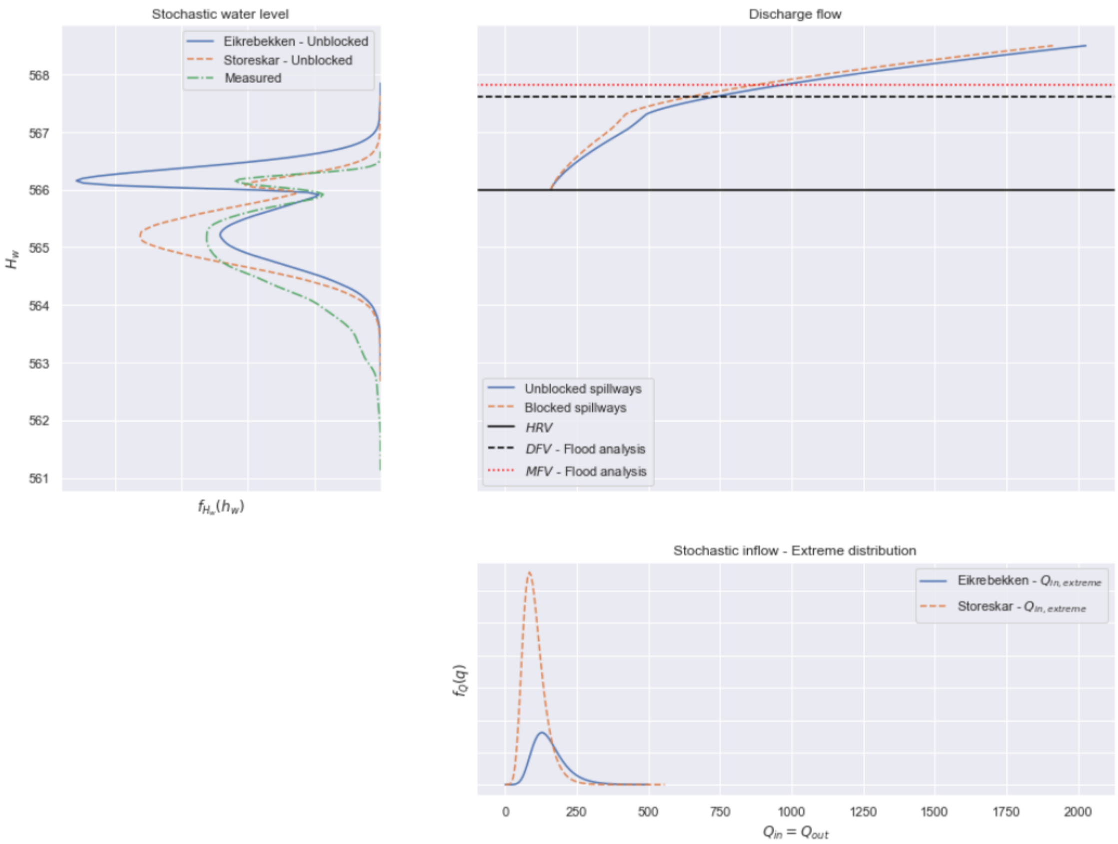

Figure 5.4 Water level calculated from extreme distribution inflow assuming unclogged spillways.

5.3 Results

For the base case bolts and cohesion are included in the calculations. The ice load is normally truncated using the values in PMCD which corresponds to a 1 m ice thickness. Furthermore, the water levels are given an unreasonably high variance due to ignorance of the analyst. The combined effects results in a low calculated reliability level as summarized in Table 5.5.1. However, the results also show how the reduced uncertainty by examining the important parameters can improve the structural reliability. Table 5.5.2 is an example of the calculated values from a FORM analysis of load case I and the corresponding sensitivity plot is given in Figure 5.6. Figure 5.5 illustrates how the friction angle relates to the failure probability based on Crude Monte Carlo simulations.

Table 5.5.1 Summary of calculated probability of failure and corresponding reliability index.

	Load combination	FORM Overturning	FORM Sliding	Crude Monte Carlo
I	DFV + clogged spillways (ULS)	$p_f = 2.5e-8$ $\beta = 5.4495$	$p_f = 0.0254$ $\beta = 1.953$	$p_f = 0.0176$ $\beta = 2.1050$
II	HRV + Ice load (ULS)	$p_f = 4.8e-8$ $\beta = 5.3354$	$p_f = 0.0165$ $\beta = 2.131$	$p_f = 0.0134$ $\beta = 2.2120$
IV	MFV (ALS)	$p_f = 3.7e-8$ $\beta = 5.379$	$p_f = 0.0278$ $\beta = 1.914$	$p_f = 0.0193$ $\beta = 2.0691$

> *Table 5.5.2 Summary of value at MPP, gradient vector and sensitivity values for load case "DFV with blocked spillways" using FORM.*

	Sliding				Overturning		
Variables	x_{MPP}	α_i	α_i^2		x_{MPP}	α_i	α_i^2
Conc_density	23.955	-0.035	0.001		23.867	-0.037	0.001
phi	**40.645**	**-0.799**	**0.638**		50.006	-0.000	0.000
cohesion	56.556	-0.186	0.034		67.120	-0.000	0.000
bolt_capacity	110.029	-0.135	0.018		72.168	-0.150	0.022
HRV	566.001	-0.000	0.000		566.001	-0.000	0.000
DFV	**570.651**	**0.548**	**0.300**		**582.667**	**0.973**	**0.947**
PMF	567.813	-0.000	0.000		567.813	-0.000	0.000
Ice_load	53.851	-0.000	0.000		54.984	-0.000	0.000
c/c	5.026	0.053	0.003		5.038	0.028	0.001
inc_upstream	0.799	-0.040	0.002		0.797	-0.070	0.005
inc_downstream	0.330	-0.004	0.000		0.329	-0.032	0.001
b_crown	1.997	-0.017	0.000		1.940	-0.110	0.012
h_vert_down	1.501	0.004	0.000		1.511	0.027	0.001
plate_t_top	0.300	-0.008	0.000		0.299	-0.009	0.000
plate_t_bot	0.600	0.007	0.000		0.608	0.046	0.002
column_t_top	0.350	-0.008	0.000		0.349	-0.006	0.000
column_t_bot	0.657	-0.046	0.002		0.656	-0.022	0.000
top_height	565.996	-0.019	0.000		565.954	-0.081	0.007

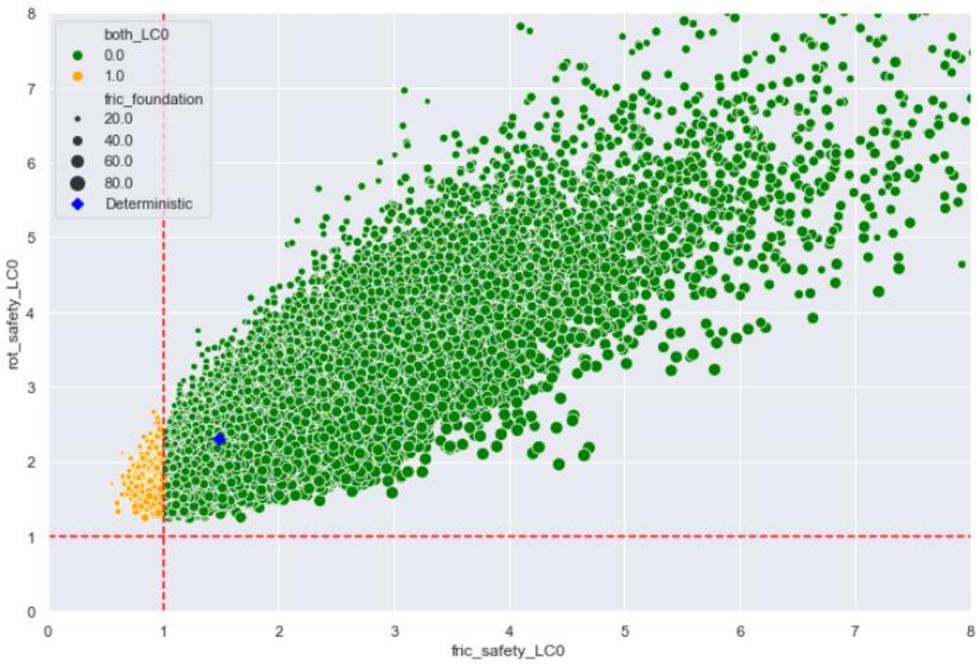

> *Figure 5.5: Safety factor from Monte Carlo simulations (a) DFV, (b) Friction angle for load case I.*

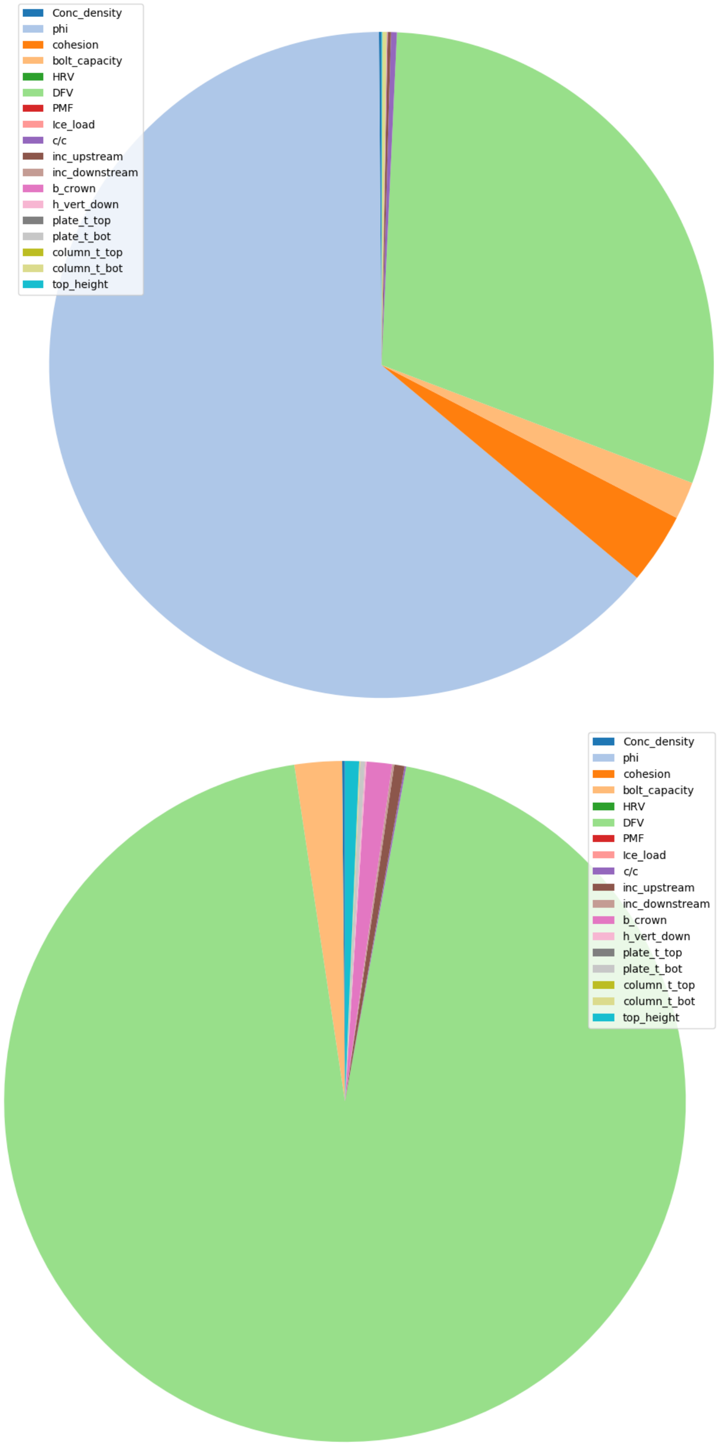

Figure 5.6: Sensitivity plots of basic variables (a) Sliding, (b) Overturning for load case I.

It can be seen from *Table 5.5.3* that the different assumptions regarding the ice load considerably changes the outcome of the structural reliability. As is expected, the non-truncated increases the risk of failure and vice versa with lower variance. It's expected that the research project Stable Dams done at Norut will improve our knowledge of the ice load mechanism.

Table 5.5.3 Comparison of FORM sensitivity values for load case "HRV + Ice load"

	PMCD	Non-truncated	Low variance
Sliding	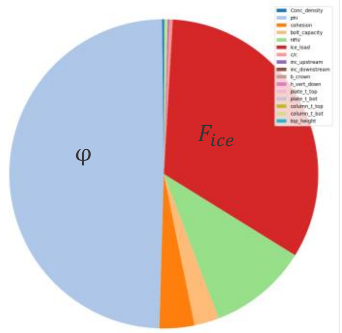	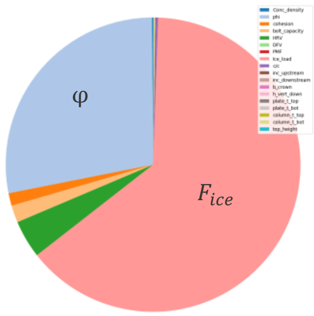	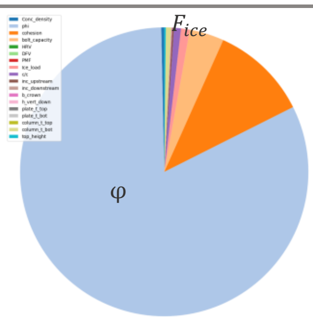
Overturning	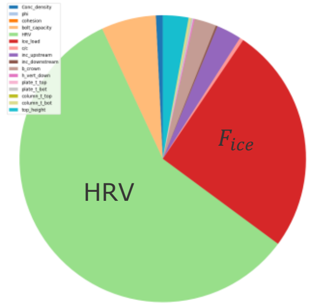	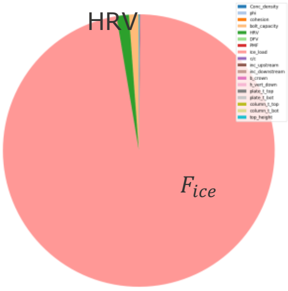	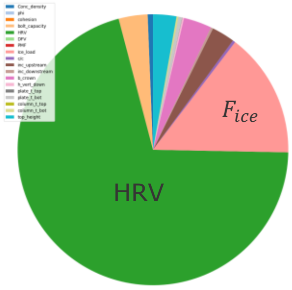

In the case of no contribution of rock bolts the reliability reduces as expected. The change is subjectively judged to be small and indicates that there are other variables that are more important to the structural reliability. Results shows that the cohesion does in fact contribute to the sliding reliability considerably, compared to rock bolts. The cohesion is according to common practice neglected due to its uncertainty. However, with probabilistic methods this can be accounted for and considerably improve the reliability against sliding.

The method of establishing extreme water level distribution from on-site measurements, shows that the reliability is improved with these assumptions. However, this is believed to be primarily caused by the reduction of both the mean value and the variance, rather than the method itself, as the variance on the water level used in the base case is extremely unrealistic.

A hypothetical case where the friction angle has been studied has been assumed, where the mean value and variance. The increased certainty of the friction angle shows that the reliability against sliding failure is substantially improved.

5.4 Conclusion

The deterministic results show that the safety factor against sliding is generally low, which is confirmed by the probabilistic analyses. For Eikrebekken the reliability can be improved considerably by increasing the knowledge of the friction capacity in the foundation.

In general, for probabilistic analyses the proposed ice loads in PMCD gives high loads compared to the Norwegian guidelines. It is also shown that the truncation is of large importance since it skews the result in a non-conservative direction. Thus, further study of the stochastic process of ice load is required.

An approach for determining the design flood level based on extreme value theory from data on site is proposed with the assumption $Q_{in} = Q_{out}$. The calculations show that by decreasing the uncertainty of the water level, the reliability is improved.

6 FURTHER WORK

Please refer to the following DSHP reports:

- Probabilistic analyses of dams - Experience and recommendations. January 16, 2019
- Probabilistic analyses of dams - Experience and recommendations – Phase II. January 2020.

So far have Norconsult and Dr. techn. Olav Olsen performed independent and parallel analyses. Through this work, a broad experience base has been established for the use of probabilistic analyses on dams.

Presentation of the project at the ICOLD Congress in Vienna, 2018, showed that the topic is highly relevant, but so far less applied for dams. Together with the report *Probabilistic model code for concrete dams* (PMCD) by Energiforsk in Sweden, this project represents innovative work that will be important for further development of regulations, safety assessments and general understanding of dam safety in Norway and internationally.

The next phase should focus on further development of a “Best practice” guideline similar to the PMCD for Norwegians dams. This “Best practice” guideline can lead to a calibration of a target reliability index which existing dams can be classified according to. An overview of topics for the next phase is shown below.

1. **Parameter selection and documentation**

   The results from previous phases of the project indicates which parameter uncertainties that affects the analysis the most. It may be appropriate to remove some of the lesser sensitive stochastic parameters from the analysis. The more sensitive parameters should be further investigated in order to develop a common set of assumptions for their distribution. It should also be determined if parameter assumptions should be based on experience data, recorded data or a combination of both. If measured data is relevant, suggestions for the type of examination and documentation should be developed.

2. **Model assumptions**

   The choice of calculation model and type of probabilistic analysis may be important for the result, the calculation time and the desired output. In order to calibrate a target reliability, these methods must be agreed upon and be standard for all analyses. A further investigation of which methods are most fitting for a “Best practice” guideline should be done.

3. **Recommendations for probabilistic calculations of dams**

   The recommendations will be based on descriptions in the Eurocode and PMCD and the findings of the two above mentioned topics. The recommendations may include a description of the following:

   - Proposed method for calculating reliability index.
   - Proposed method for producing sensitivity of the various parameters.
   - Proposed acceptance criteria for the reliability index (β). Acceptance criteria should be adapted to NVE's classification of reservoirs in different breach consequence classes. Note that a calibration requires investigation of several dams.

REFERENCES

[1] OED, “Forskrift om sikkerhet ved vassdragsanlegg (damsikkerhetsforskriften),” Olje- og energidepartementet, 2009.

[2] R. E. Melchers, “Structural reliability theory in the context of structural safety,” 2006.

[3] Eurocode 0, “NS-EN 1990:2002+A1:2005+NA:2016”.

[4] H. Gulvanessian, “EN 1990 Eurocde - Basis of structural design,” Civil Engineering, 2001.

[5] R. E. Melchers and A. T. Beck, Structural reliability analysis and prediction, Wiley, 2018.

[6] M. Baravalle, “Risk and Reliability Based Calibration of Structural Design Codes,” NTNU, 2017.

[7] O. D. a. H. Madsen, “Structural Reliability Methods,” 2007.

[8] R. S. N.E. Meinen, “Reliability levels obtained by Eurocode partial factor design - A discussion on current and future reliability levels,” 2018.

[9] JCSS, “Probabilistic Model Code - Part I,” 2001.

[10] DNV, “Structural reliability analysis of marine structures,” 1992.

[11] DNV, “Guideline for Offshore Structural Reliability Analysis,” 1996.

[12] W. Westberg, M. Westberg and F. Johansson, “SANNOLIKHETSBASERAD BEDÖMNING AV BETONGDAMMARS STABILITET,” 2016.

[13] W. M. W. Westberg and F. Johansson, “PROBABILISTIC MODEL CODE FOR CONCRETE DAMS,” 2016.

[14] J. Schneider, Introduction to safety and reliability of structures, IABSE-AIPC-IVBH, 2006.

[15] E. Basler, “Untersuchungen über den sicherheitsbegriff von bauwerken,” *Schweizer Archiv für angewandte Wissenschaft und Technik,* no. 4, 1961.

[16] A. C. Cornell, “A probability based structural code,” *ACI Journal,* no. 12, 1969.

[17] The Joint Committee on Structural Safety (JCSS), “Probabilistic Model Code,” The Joint Committee on Structural Safety, 2015.

[18] Norges vassdrags- og energidirektorat, *Klassifisering av Hydro Energi AS sine dammer i Luster, Årdal og Vang kommuner - vedtak,* Oslo: Norges vassdrags- og energidirektorat, 2015.

[19] Norges vassdrags- og energidirektorat, «Retningslinjer for betongdammer, utgave 2,» Norges vassdrags- og energidirektorat, 2005.

[20] NVE, “Retningslinjer for flomberegninger,” Norges vassdrags- og energidirektorat, 2011.

[21] R. V. Whitman, “Evaluating calculated risk in geotechnical engineering,” American Society of Civil Engineers, 1981.

[22] D. E. Newland, An Introduction to Random Vibrations, Spectral & Wavelet Analysis, Dover Books, 1993.

[23] Norconsult, “Hemsil II Kraftverk, Dam Eikrebekken - Revurdering av dam og luker,” 2004.

[24] E. Adolfi and J. Eriksson, “Islastens inverkan på brottsannolikheten för glidning och stjälpning av betongdammar,” KTH, 2013.

[25] Dr. techn. Olav Olsen, “Recommendations for existing concrete dams - Probabilistic analysis of stability,” 2017.

[26] M. W. Wilde and F. Johansson, “Probabilistic model code for concrete dams,” Energiforsk, 2016.

APPENDIX A REPORT – DAM VIERVATN

Energi Norge

Reliability assessment of stability

Recommendations for existing concrete dams

Dam Viervatn

Assignment no.: **5195694** Document no.: **NO-01** Version: **D01** Date: **2020-01-13**

Norconsult

Client:	Energi Norge
Client's Contact Person:	Johnny Bruheim
Consultant:	Norconsult AS,Vestfjordgaten 4, NO-1338 Sandvika
Assignment Manager:	Tor Kristian Sandaker
Technical Advisor:	Tor Kristian Sandaker
Other Key Personnel:	Hanna Eklund

D01	2020-01-13	For approval	HaEkl	TKS	TKS
Version	**Date**	**Description**	**Prepared by**	**Checked by**	**Approved by**

Summary

Reliability indices for stability, sliding and overturning, of one dam pillar have been calculated as an expression of the pillar's probability of failure at dam Viervatn. Stochastic variables have been carefully selected for different influencing parameters and a density function for each parameter has been chosen based on collected data and literature. Also, a sensitivity study has been performed, determining the stochastic variables' impact on the result.

A probabilistic model based on Monte Carlo simulations has been used and the results are products of 10^8 simulations. The calculation model applied is based on the limit equilibrium described in NVE's *Retningslinjer for betongdammer.* The resulting reliability indices for sliding ranges from 2.8 and larger, while the indices for overturning ranges from 4.6 and larger. The resulting reliability indices of the design situation, which include bolt capacity and cohesion, are higher than the minimum target reliability given in the *Probabilistic model code for concrete dams* and the Eurocode. A target reliability has not been calibrated to accurately compare the results.

The sensitivity study shows that the friction angle, water level, angle of sliding plane, ice load and dam height are the most sensitive parameters for the analyses performed in this report, depending on the considered load situation. These parameters are also the ones expected to carry the largest amount of uncertainty.

Contents

1 References

[1] Norges vassdrags- og energidirektorat, *Klassifisering av Hydro Energi AS sine dammer i Luster, Årdal og Vang kommuner - vedtak,* Oslo: Norges vassdrags- og energidirektorat, 2015.

[2] Standard Norge, NS-EN 1992-1-1:2004+NA:2008 Prosjektering av betongkonstruksjoner - Del 1-1: Allmenne regler og regler for bygninger, 2004.

[3] Norges vassdrag- og energidirektorat, «Retningslinjer for flomberegninger,» Norges vassdrag- og energidirektorat, 2011.

[4] RIDAS TA, "Kraftföretagens riktlinjer för dammsäkerhet, tillämpningshänvisningar - Swedish Hydropower companies guidelines for dam safety,," Svensk Energi, 2012.

[5] Norges vassdrags- og energidirektorat, "Retningslinje for laster og dimensjonering," Norges vassdrags- og energidirektorat, 2003.

[6] H. Eklund, A. Skorve and A. Strand, *Reliability assessments of concrete structures using non-linear finite element analyses,* Trondheim: Norwegian University of Science and Technology, Department of Structural Engineering, 2017.

[7] J. Schneider, Introduction to safety and reliability of structures, IABSE-AIPC-IVBH, 2006.

[8] E. Basler, "Untersuchungen über den sicherheitsbegriff von bauwerken," *Schweizer Archiv für angewandte Wissenschaft und Technik,* no. 4, 1961.

[9] A. C. Cornell, "A probability based structural code," *ACI Journal,* no. 12, 1969.

[10] The Joint Committee on Structural Safety (JCSS), "Probabilistic Model Code," The Joint Committee on Structural Safety, 2015.

[11] J. Köhler, *Lecture Notes - Safety Aspects in Civil Engineering - L07 – System Reliability,* Trondheim: Norwegian University of Science and Technology, 2016.

[12] A. Saltelli, M. Ratto, T. Andres, F. Campolongo, J. Cariboni, D. Gatelli, M. Saisana and S. Tarantola, Global Sensitivity Analysis. The primer, Sussex: John Wiley & Sons Ltd, 2008.

[13] Standard Norge, NS-EN 1990:2002+A1:2005+NA:2016 Grunnlag for prosjektering av konstruksjoner, 2002.

[14] M. W. Wilde and F. Johansson, "Probabilistic model code for concrete dams," Energiforsk AB, Stockholm, 2016.

[15] Norges vassdrags- og energidirektorat, «Retningslinjer for betongdammer, utgave 2,» Norges vassdrags- og energidirektorat, 2005.

[16] Norges vassdrags- og energidirektorat, «Tillegg til retningslinjer for betongdammer, utgave 2. Glidekontroll for betongdammer uten medvirkende fjellbolter,» Norges vassdrags- og energidirektorat, 2019.

[17] H. Schlune, K. Gylltoft and M. Plos, "Safety formats for non-linear," *Magazine of Concrete Research,* vol. 64, no. 7, 2012.

[18] Norges Geologiske Undersøkelse, *Bergart 1:50 000,* Norges Geologiske Undersøkelse.

[19] K. Y. Lo and A. Hefny, "Statistical analysis of the strength of the contac tbetween 609 concrete dams and rock foundations," in *Proc., 1st Annual Conf.*, Toronto, 1998.

[20] Den norske Ingeniørforening, NS 427 Regler for utførelse av arbeider i armert betong, Norges Standardiserings Forbund, 1939.

[21] Statens Vegvesen, Håndbok N200 Vegbygging, Vegdirektoratet, 2018.

[22] F. Johansson and M. W. Wilde, "Sannolikhetsbaserad bedömning av betongdammars stabilitet," Energiforsk, Stockholm, 2016.

[23] Norges vassdrags- og energidirektorat, "Veileder nr. 3/2014 - Veileder for klassifisering av vassdragsanlegg," Norges vassdrags- og energidirektorat, 2014.

2 Introduction

Safety factors calculated according to the dam safety regulations in Norway do not necessarily give a clear picture of the real safety of a dam. Dams with the same calculated safety factor may have different probabilities of failure. Probabilistic analyses of existing dams are considered to be a suitable method for assessing reliability, e.g. against sliding and overturning. The calculations result in a reliability index, β, as an expression of the probability of failure.

Calculations based on probabilistic analysis can provide a clear and transparent representation of variables that affect the dam's safety against failure. The analyses indicate which variables are the most sensitive and thus to a greater extent affect the probability of failure.

This report includes reliability assessment and probabilistic analysis of the buttress dam (slab) at Viervatn. The calculations are performed as an alternative to traditional deterministic calculation methods according to guidelines from NVE and current standards. Pillar 11 of dam Viervatn has the lowest safety against sliding based on deterministic calculations of all the pillars and is therefore used as a base for the calculations of this report.

3 Case configuration

3.1 General

Viervatn is located approximately 9 km southeast of Øvre Årdal in the municipality Årdal in Vestland county. The magazine is a regulated magazine connected to Tyin waterpower plants belonging to Hydro Energi.

The dam consists of a buttress dam (slab) with massive connections and an overflow threshold designed as a gravity dam in concrete. The dam is owned and operated by Hydro Energi Sogn.

Figure 3.1 Dam Viervatn. Picture taken by Norconsult in August 2019.

Year of construction for dam Viervatn is 1953. The dam is classified as level 1 in NVE's consequence classes [1]. Flood calculations have been performed by Norconsult AS, the present water levels for dam Viervatn are shown in Table 3.1.

Table 3.1 Water levels at dam Viervatn.

Water level	m a.s.l.
Highest retention water level (HRV)	+ 1230,10
Lowest retention water level (LRV)	+ 1208,10
Water level at design flooding, Q_{500} (DFV)	+ 1231,16
Water level at maximum flooding, 1,5 x Q_{500} (MFV)	+ 1231,50

A deterministic stability control has been performed by Norconsult AS. This control shows that certain pillars do not satisfy the safety demands set by *Norges vassdrag- og energidirektorat* (NVE). One of these pillars are pillar number 11, see Figure 3.2. The reliability assessment of this report will further focus on this pillar.

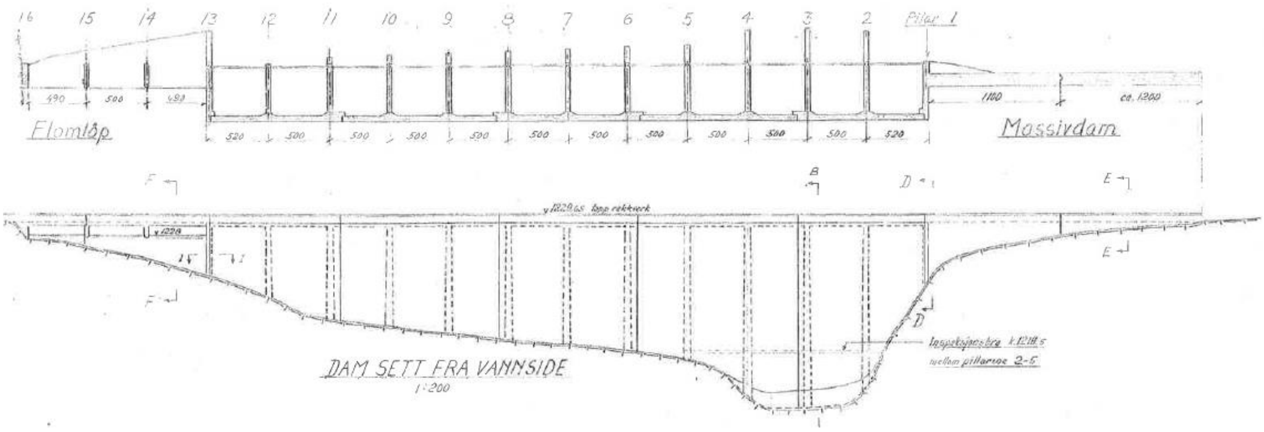

Figure 3.2 Dam Viervatn. From drawing number 3526.

Norconsult AS and Hydro Energi performed a dam inspection of dam Viervatn on August 28, 2019. Measurements of geometry and material from this inspection are further used in the reliability assessment.

3.2 Geometry

The front plate stretches 60,4 m along 13 pillars with approximately 5 m distance between each pillar. The general pillar geometry is shown in Figure 3.3. Pillar 11 has 4 rock bolts with diameter 25 mm.

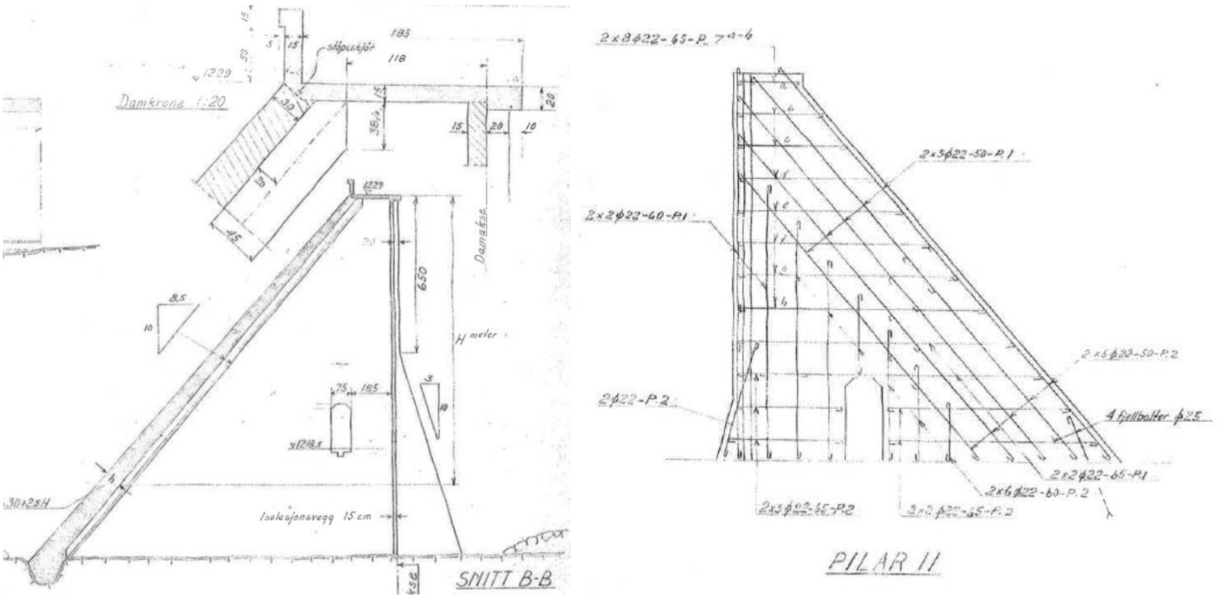

Figure 3.3 Pillar geometry and reinforcement. From drawing number 3526 and 3541.

3.3 Material

Drawings indicate the following concrete quality

- Front plate: “A” – Approximate B25 from Eurocode 2 [2].
- Pillars: “B” – Approximate B20 from Eurocode 2.

The rock bolts are of steel quality “St 37”.

3.4 Load

The dam is subject to the following loads:

1. Self-weight
2. Water pressure
3. Uplift
4. Ice load

3.4.1.1 Self-weight

The self-weight is calculated as $G = \gamma_b V$, where γ_b is the weight density of concrete and V is the total volume of the dam.

3.4.1.2 Water pressure

The water levels used in calculating the water pressure is given in Table 3.1. Considering dam Viervatn is in consequence class 1, it should be checked for a DFV corresponding to a Q_{500} flooding and the accident loading corresponding to $1{,}5 \times Q_{500}$ [3].

3.4.1.3 Uplift

Uplift is distributed as shown in Figure 3.4. Dam Viervatn has no tail water head on the downstream side, thus the uplift is only acting beneath the front plate.

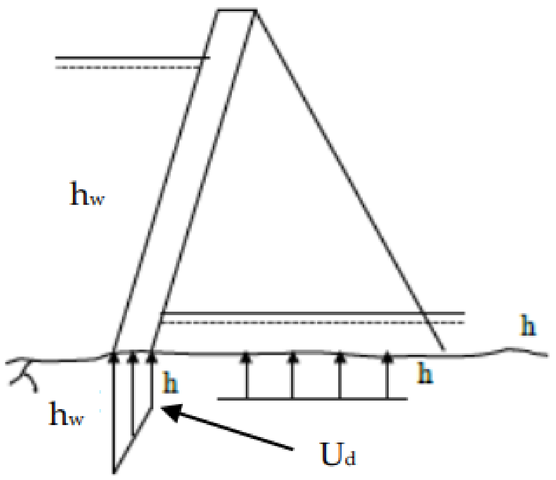

Figure 3.4 Design assumption for uplift for buttress dam. [4]

3.4.1.4 Ice load

The ice load is assumed to be a line load acting 250 mm below the water level as suggested in NVE's *Retningslinje for laster og dimensjonering* [5].

4 Structural reliability

4.1 Limit states

The main objective of a reliability analysis in structural engineering is to ensure that the estimated probability of failure of the structure is below a certain target value. The classic solution to this problem is to define a Limit State Function (LSF) given as G = R − S, where R is the resistance and S is the load action. The variables R and S are uncertain and are often assigned appropriate probability density functions. Once these functions are known, the probability of failure, P (G ≤ 0), can be calculated. [6]

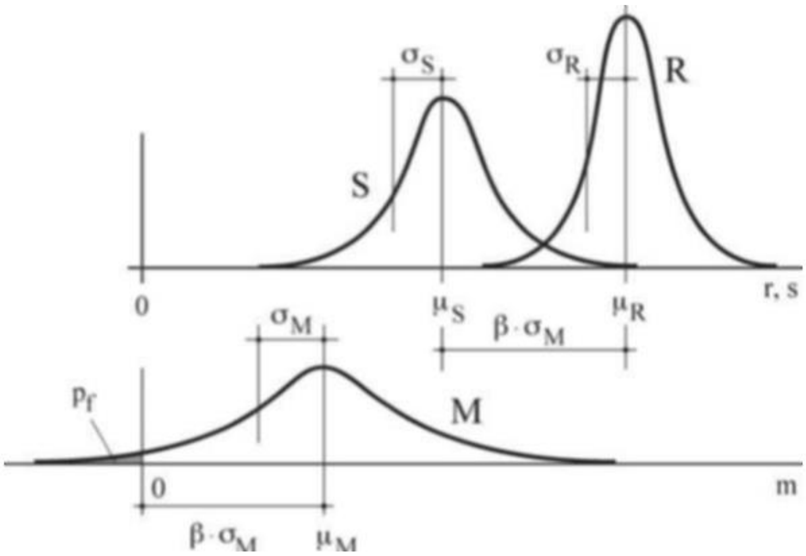

Figure 4.1 Probability density function of resistance, load and safety margin. [7]

The limit state can also be expressed as the safety margin M = R −S, as shown in Figure 4.1. The method developed by Basler [8] and presented in the notation of Cornell [9], can be used to find the exact probability of failure assuming the variables are normally distributed. If the resistance and load are normally distributed, so is the safety margin, and all variables can be introduced by their mean and standard deviation only. The mean and standard deviation of the safety margin, μ_M and σ_M, can now be represented by the mean and standard deviation of the resistance, μ_R and σ_R, and load, μ_S and σ_S, as shown below

$$\mu_M = \mu_R - \mu_S$$

$$\sigma_M = \sqrt{\sigma_R^2 + \sigma_S^2}$$

In these equations it is assumed that R and S are uncorrelated. The reliability index, β, and the probability of failure, P_f, is determined as

$$\beta = \frac{\mu_M}{\sigma_M}$$

$$P_f = \Phi(-\beta).$$

The resistance and load action defining the LSF are functions of load, material and geometry parameters. These parameters are subject to uncertainties and can be represented by random variables, X. In this context the probability of failure can be expressed as

$$P_f = Prob\{G(\boldsymbol{X}) \leq 0\}$$

In most engineering applications, complete statistical information about the basic random variables X is not available and, furthermore, the function G (X) is a mathematical model which idealizes the limit state. A model uncertainty should be added to include these uncertainties in the result. A consideration of the model uncertainty will not be done in this report but is highly relevant for further work.

4.2 Reliability analysis

Primarily structural design is focused on component behaviour looking at a single mode of failure for a single component. However, most structures are an assembly of structural components and even individual components may be susceptible to several possible failure modes. A probabilistic approach provides a better platform from which system behaviour can be explored and utilised. This can be of benefit in assessment of existing structures where strength reserves due to system effects can alleviate the need for expensive strengthening. [10]

System failure is described with a combination of several limit state functions, each representing one single failure mode and structural component. It is generally distinguished between system configurations that corresponds to a purely parallel or series arrangement of failure modes and components. A combination of both is also possible, see Figure 4.2.

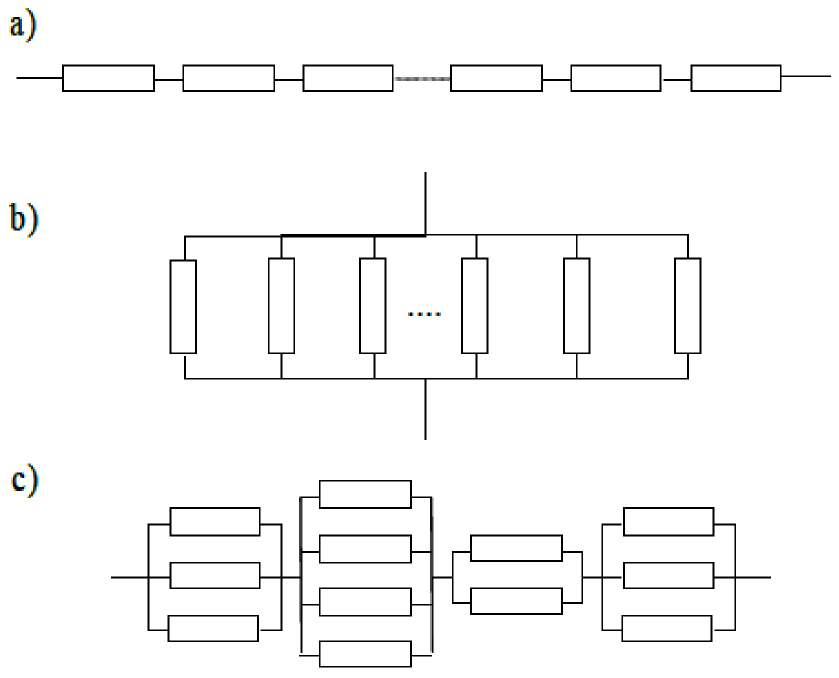

Figure 4.2 Different logical arrangements of failure modes to a) serial system, b) parallel system, and c) mixed system. [11]

The simple bounds for system reliability of series and parallel systems may be determined as listed in Table 4.1.

Table 4.1 Probability of failure for series and parallel systems [11].

System	Independent components	Dependent components
Series	$\Pr(F_{Sys}) = 1 - \prod_{i=1}^{n}(1 - \Pr(F_{comp,i}))$	$\Pr(F_{Sys}) = \max(\Pr(F_{comp,i}))$
Parallel	$\Pr(F_{Sys}) = \prod_{i=1}^{n}(\Pr(F_{comp,i}))$	$\Pr(F_{Sys}) = \min(\Pr(F_{comp,i}))$

This report will mainly focus on the component reliability of a single pillar in sliding and overturning as separate failure modes. The system reliability of the pillar's stability will also be included by combining the two failure modes as a series system of independent components. A component reliability analysis is outlined in the following main steps [10]

1. Select appropriate limit state function
2. Specify appropriate time reference
3. Identify basic variables and develop appropriate probabilistic models
4. Compute reliability index and failure probability.

4.3 Monte Carlo

The Monte Carlo (MC) method is used to evaluate the stability of dam Viervatn and compute the reliability index. The Monte Carlo simulation technique is based on a series of analyses, each with random realizations of the stochastic variables **X**. The probability of failure is simply the number of failures divided by the number of simulations. The reliability index was calculated using the inverse of the normal cumulative distribution $\beta = \Phi^{-1}(P_f)$.

In structural reliability problems, where low probabilities of failure and coefficients of variation are sought, a large number of simulations are needed to cover the tail region of the distributions. Running 10^8 simulations is considered enough to achieve this accuracy [7].

4.4 Sensitivity studies

In order to identify certain parameters' influence on the final reliability index, a sensitivity analysis is performed. The studies chosen in this report is based on conditional variances as mentioned in *Global Sensitivity Analysis. The Primer* [12]. This method is based on fixing factor X_i at a value, x_i^*, while letting the other parameters vary during the analysis. The generic model

$$G = f(X_1, X_2, \dots, X_n)$$

with a fixed factor, gives the variance of G taken over all factor but X_i as $V_{\sim X_i}(G|X_i = x_i^*)$. This variance will, in a set of uncorrelated, normal distributed variables, be less than the corresponding total or unconditional variance $V(G)$. One could therefore conceive using $V_{\sim X_i}$ as a measure of the relative importance of X_i, giving us a sensitivity factor

$$S_i = \frac{V_{\sim X_i}(G|X_i = x_i^*)}{V(G)}.$$

Two problems appear with this approach; First, the sensitivity measure becomes dependent on the position of the point x_i^*. Second, there are cases where $V_{\sim X_i}(G|X_i = x_i^*) > V(G)$. If $\sum S_i = 1$ the approach above has been considered adequate in this report.

On other hand, if $\sum S_i \neq 1$, then the problems have been solved by taking the average of this measure over all possible points x_i^*, $E_{X_i}(V_{\sim X_i}(G|X_i = x_i^*))$. The sensitivity measure becomes

$$S_i = \frac{V(G) - E_{X_i}(V_{\sim X_i}(G|X_i = x_i^*))}{V(G)}.$$

The sensitivity has also been checked by inspecting trends and shapes of scatter plots.

4.5 Target reliability

In order to do design based on probabilistic methods, predefined reliability targets must be determined. This should depend on the consequences and reflect the safety level set by society. The connection between probability of failure and reliability index is shown in Table 4.2.

Table 4.2 Probability of failure and corresponding reliability index.

P_f	1.00E-01	1.00E-02	1.00E-03	1.00E-04	1.00E-05	1.00E-06	1.00E-07	1.00E-08
β	1.3	2.3	3.1	3.7	4.3	4.8	5.2	5.6

Examples of target reliabilities applied in Eurocode [13] and *Probabilistic model code for concrete dams* [14] are shown in the tables below.

Table 4.3 Minimum values for β in ultimate limit states. Reference period 1 year. [14]

Dam consequence class	Minimum β
A	5,2
B	4,8
C	4,2
U	3,8

Table 4.4 Recommended minimum values for the reliability index. [13]

Reliability Class	Minimum values of β	
	1-year reference period	50 years reference period
RC3	5,2	4,3
RC2	4,7	3,8
RC1	4,2	3,3

Similar target reliabilities should be determined for concrete dams in Norway in order to do probabilistic design.

5 Probabilistic model

The probabilistic model is defined in the following subchapters. Limit states of the sliding and overturning are defined, the time reference is set by choosing design situations and the stochastic variables are selected.

5.1 Sliding

The Norwegian Water Resources and Energy Directorate (NVE) defines safety against sliding in *Retningslinjer for betongdammer* [15] as

$$S_f = \frac{F}{\sum H}$$

where S_f is the safety factor, F is the resistance load and ∑H is the sum of the horizontal drifting forces. The resistance load is expressed as

$$F = \frac{cA}{cos\alpha(1 - tan\varphi tan\alpha)} + \sum V \tan(\varphi + \alpha) \text{ ,}$$

where

φ	= Friction angle.
α	= Sliding plane angle with regards to the horizontal plane.
c	= cohesion.
A	= Contact area.
∑V	= Sum of vertical loads.

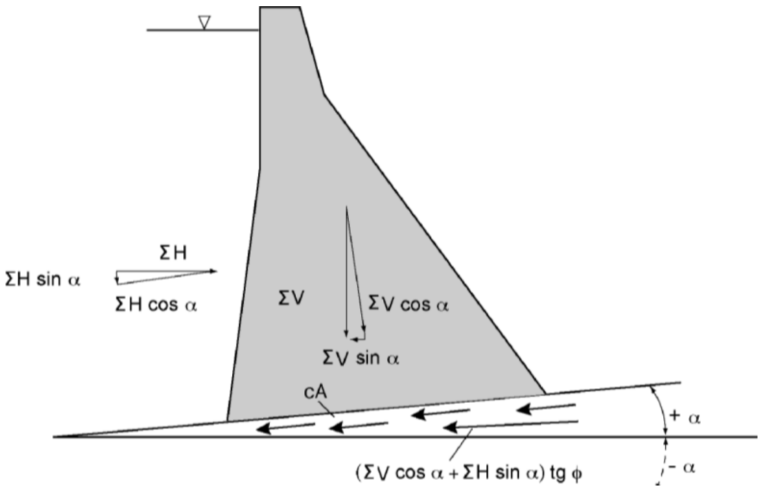

Figure 5.1 Limit state configuration for sliding. [15]

Including the bolts' capacity, the expression becomes

$$F = \frac{cA}{cos\alpha(1 - tan\varphi \cdot tan\alpha)} + \sum V \tan(\varphi + \alpha) + f_y A_s[sin\theta \cdot \tan(\alpha + \varphi) + cos\theta] \text{ ,}$$

where

f_y	= Yield strength of bolts.
A_s	= Area of bolts.
θ	= Bolts angle with regards to the horizontal plane.

Applying this to the limit state function described in Section 4 we get the following LSF for sliding

$$G = R - S = F - \sum H.$$

5.2 Overturning

The Norwegian Water Resources and Energy Directorate (NVE) defines safety against overturning in *Retningslinjer for betongdammer* [15] as

$$S_f = \frac{M_S}{M_V}$$

where S_f is the safety factor, M_S is the stabilizing moment and M_V is the drifting moment.

All forces are decomposed into vertical and horizontal components to calculate stabilizing and driving moments. The moments are taken about the downstream edge of the cross-section as highlighted in Figure 4.1.

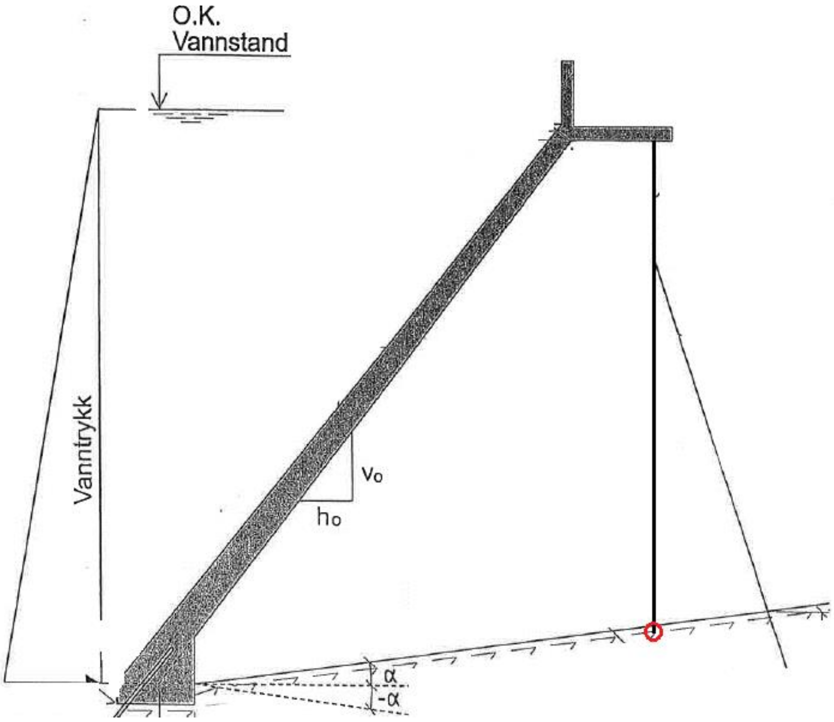

Figure 5.2 Center for moment equilibrium.

Applying this to the limit state function described in Section 4 we get the following LSF for overturning

$$G = R - S = M_S - M_V.$$

5.3 Design situations

According to NVE [16], [15] stability of concrete buttress dams should be checked for the load combinations listed in Table 5.1.

Table 5.1 Check of sliding for buttress dams. [15] [16]

	ULS	Accidental situation	DFV without bolts
Without cohesion	$S_f > 1,4$	$S_f > 1,1$	$S_f > 1,1$
With cohesion	$S_f > 3,0$	$S_f > 2,0$	-

Control of overturning should be performed for the following load combinations.

Table 5.2 Check of overturning for buttress dams. [15]

	ULS	Accidental situation
H > 7 m without bolts	$S_f > 1,4$	$S_f > 1,3$
H < 7 m without bolts	$S_f > 1,1$	$S_f > 1,1$

According to Table 2-1 in *Retningslinje for laster og dimensjonering* [5] checks of accidental load combinations are not necessary for dams in consequence class 1. Possible design situations for stability are listed in Table 5.3.

Table 5.3 Design situations for stability.

Design situation	Self-weight	HRV	DFV	Ice load
1	x	x		
2	x	x		x
3	x		x	

This results in twelve possible analyses, all shown in Table 5.4.

Table 5.4 Overview of analyses.

Analysis no.	Design situation 1	Design situation 2	Design situation 3	Included cohesion	Included bolts
A1					
A2					
A3					
A4					
A5					
A6					
A7					
A8					
A9					
A10					
A11					
A12					

5.4 Stochastic variables

The parameters considered to carry the most uncertainty in determining the load action and resistance are listed in Table 5.5 The geometry parameters are further described in Figure 5.3.

Table 5.5 Stochastic variables.

Category	Parameter		Unit
Geometry	Level of bottom dam upstream	k_{bot}	m a.s.l.
	Angle of sliding plane	α	°
	Slope of front plate	h_o/v_o	-
	Effective width of front plate considering self-weight	b_{eff1}	m
	Effective width of front plate considering water pressure and ice load	b_{eff2}	m
Material	Mass density of concrete	γ_b	N/m^3
	Friction angle	φ	°
	Cohesion	c	Pa
	Yield strength bolts	f_y	Pa
Load	Water level	k_w	m a.s.l.
	Ice load	q_i	N/m

These parameters will in further analyses be considered as stochastic variables with certain probability density functions (PDF). The PDFs are based on assumptions, literature and measurements from the actual dam. Correlation between the parameters are not included in this report.

The safety formats in Eurocode 2 [2] are used in the cases of insufficient tests and measurements of the geometry. These safety formats are based on a 5 % coefficient of variation for geometry [17].

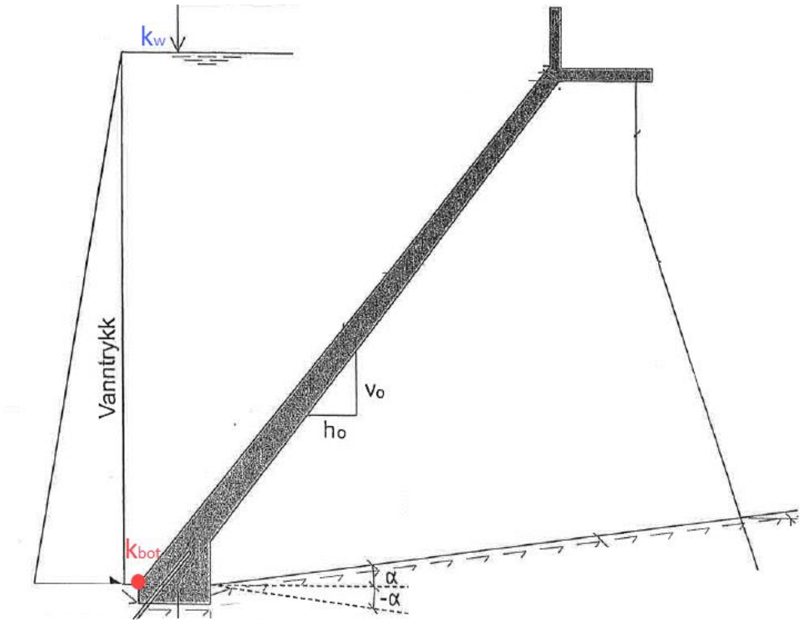

Figure 5.3 Geometric stochastic variables.

5.4.1 Level of bottom dam, upstream, k_{bot}

The level of the bottom end of the front plate is assumed to be normal distributed. Measurements upstream of the bottom of the front plate have not been performed on Dam Viervatn. The mean value is set to level +1222 as indicated on drawings. The coefficient of variation for the dam height have been set to 5%. Assuming a dam height of 9,3 m the standard deviation becomes 0,5 m.

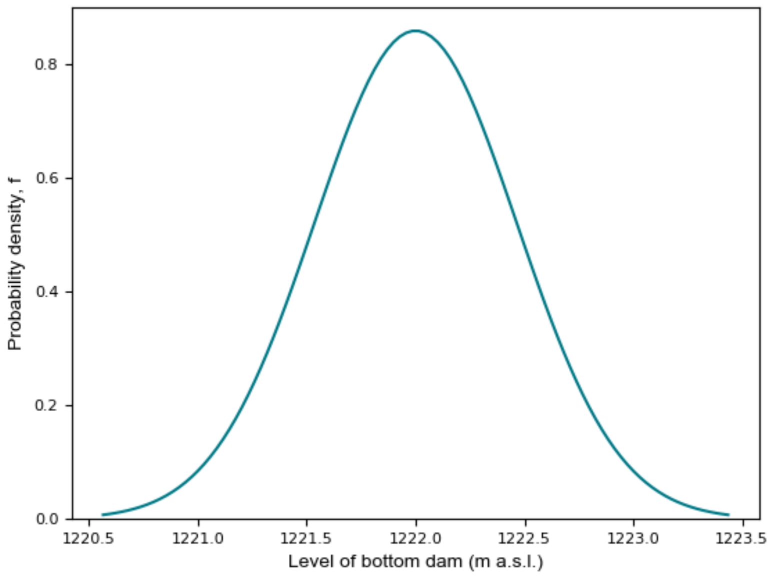

Figure 5.4 Probability density function – Level of bottom front plate.

5.4.2 Slope of front plate, h_o/v_o

The slope of the front plate is assumed to be normal distributed. The mean has been set to 0,85 as indicated on drawings, and the coefficient of variation has been set to 5%.

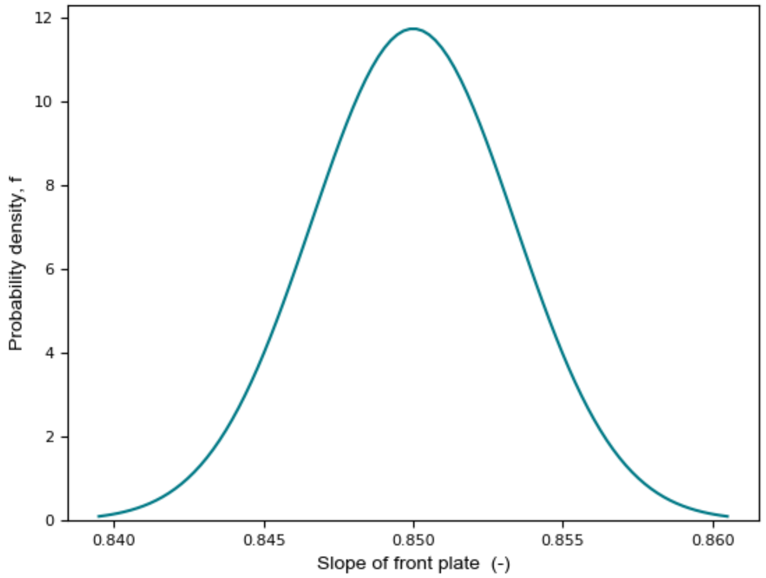

Figure 5.5 Probability density function for slope of front plate.

5.4.3 Angle of sliding plane, α

The angle of the sliding plane is assumed to be normal distributed. Measurements of the concrete-rock interface have been performed, with the results for pillar 11 shown in Figure 5.6.

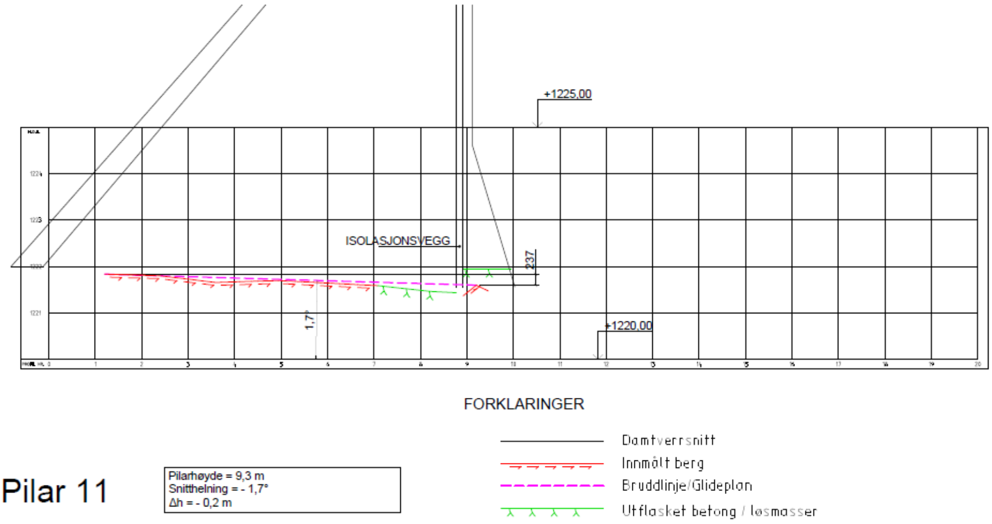

Figure 5.6 Test results of the rock-concrete interface geometry for pillar 11.

The pink line indicates the average sliding angle of 1,7 °. The red lines show measurements of the rock surface, while the green line shows measurements of the soil surface. Due to the uncertainty of the location of the rock surface below the soil, a standard deviation of 1,7 ° is chosen for the angle of the sliding plane.

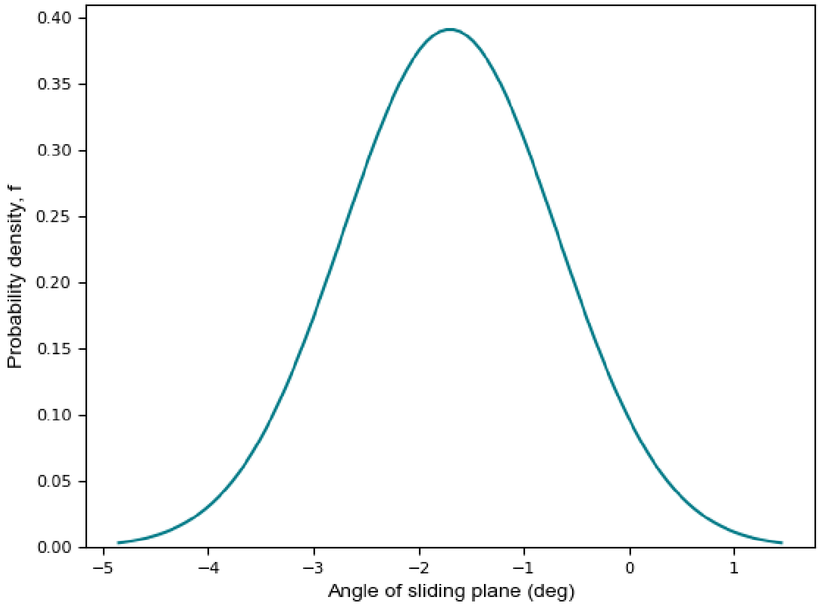

Figure 5.7 Probability density function – Angle of sliding plane.

5.4.4 Effective width of front plate, b_{eff}

The effective width of the front plate affects both the vertical and the horizontal forces of the limit state. The effective width considering the vertical forces are a product of the stabilizing mass, while the effective width considering the horizontal forces are a product of position of the front plate joints. Hence, the effective width for the vertical forces is assumed to be the distance between each pillar, and the effective width for the horizontal forces are calculated from the static system of the pillars, see Appendix A. Measurements of the distance between pillars have been performed, measuring 4,955 m between pillar 9 and 10 and 4,950 m between pillar 10 and 11.

Based on the above, the effective width is assumed to be normal distributed with a coefficient of variation of 5 %. The mean is set to 4,95 m and 4,7 m respectively for the vertical and horizontal load configurations.

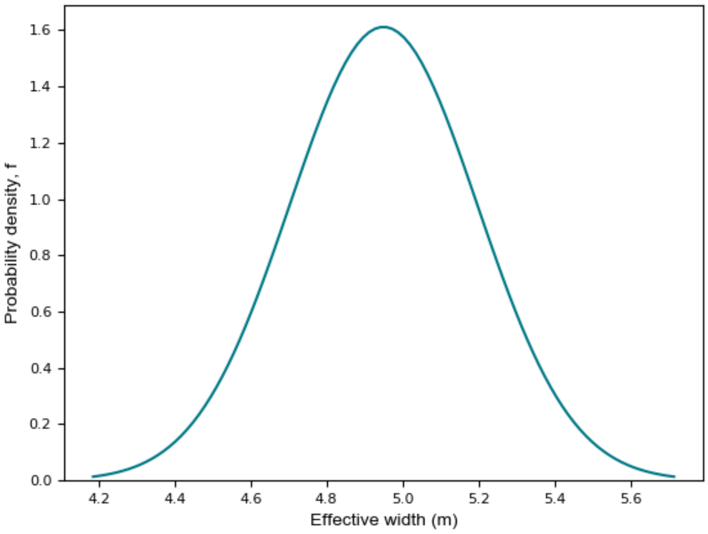

Figure 5.8 Probability density function - Effective width for vertical load.

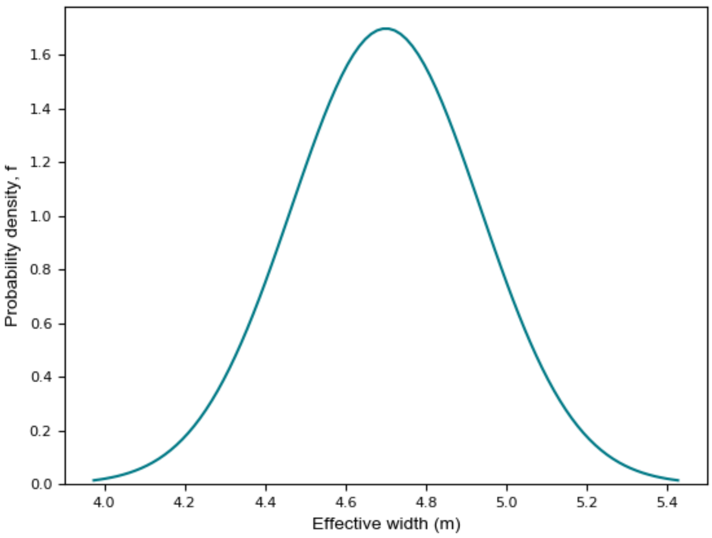

Figure 5.9 Probability density function – Effective width for horizontal load.

5.4.5 Mass density concrete, γ_b

As suggested in *Probabilistic model code for concrete dams* [14] the weight density is assumed to have a normal distribution. It also suggests a mean value of 23,5 kN/m^3. The coefficient of variation (CoV) suggested by JCSS [10] is 4 %.

For large structures consisting of many "members" the variability of the global weight density may be taken as $V_G \cdot \rho_o \cdot \rho_m$, where ρ_o is 0,85 and ρ_m is 0,7 [10]. This results in a CoV of 3,4 %.

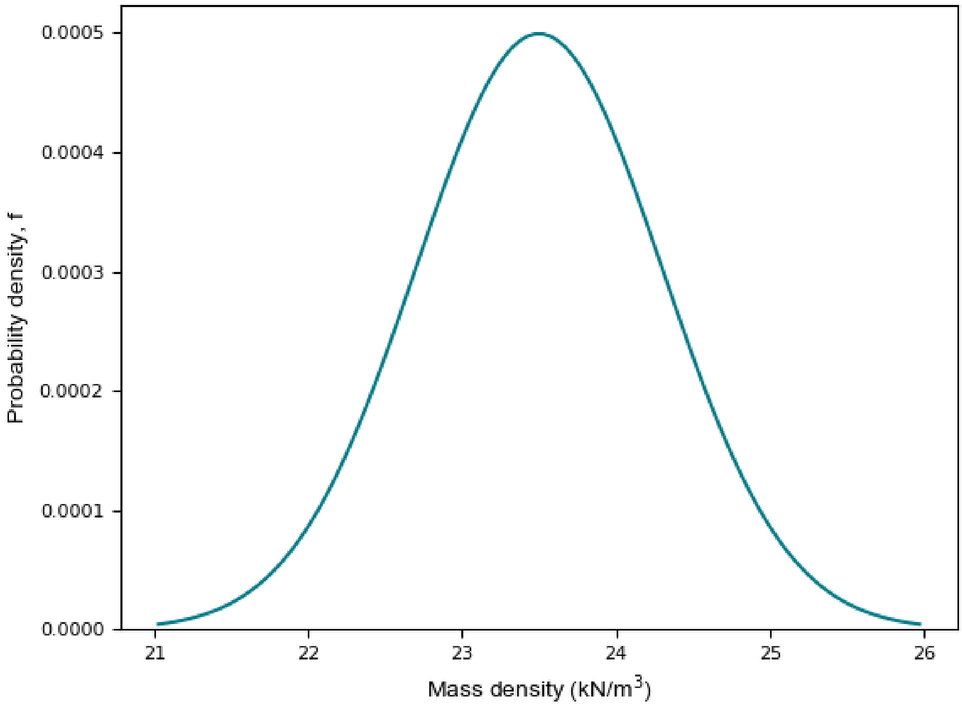

Figure 5.10 Probability density function - Mass density of concrete.

5.4.6 Friction angle, φ

The dam has a concrete-rock interface. The bedrock map shows that the rock in the area consists of gneiss and syenitic to monzonitic composition [18]. Gneiss is usually considered to be a hard rock with a rough surface. Based on this, the mean friction angle is set to 50° as suggested in NVE's *Retningslinjer for betongdammer* [15].

Based on the results of Lo & Hefny [19] a coefficient of variation of 5 % can be applied if no tests are performed.

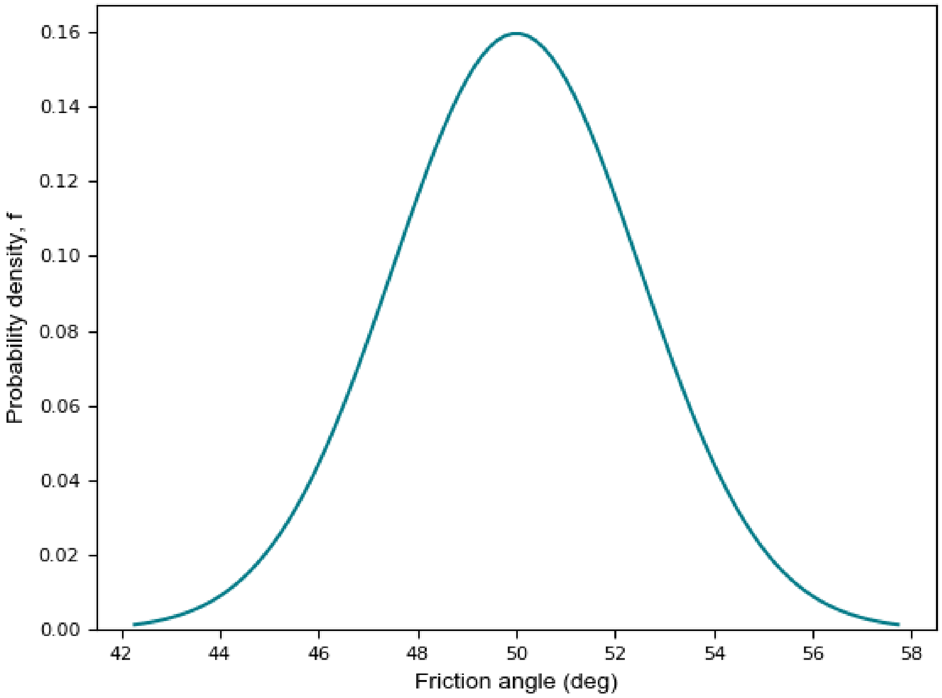

Figure 5.11 Probability density function - Friction angle.

5.4.7 Water level, k_w

The water level is described by three load situations based on the *Probabilistic model code for concrete dams* [14], the design situations listed in Table 5.3 and data collected at dam Viervatn.

1. Water level at HRV (Highest regulated water level).

   Since a water level at, or very close to, HRV may be expected nearly every year the probability of this to occur is close to 1. The water level is deterministic and fixed at HRV.

2. Water level above HRV, also called DFV (flooding situation).

   Occurs with a small probability that is dependent on natural variation, operation, availability of gates and power station. The water level will vary between HRV and MFV (maximum flooding), with a peak at DFV.

3. Water level below HRV with ice loading.

   When the water level is proved to be generally lower than retention water level for regulation dams with large reservoirs, an adjustment to HRV can be performed. According to the data shown in Appendix B the water level is rarely at HRV and usually close to LRV in the winter season when we also expect ice loading. A distribution between LRV and HRV is chosen for this situation.

The water level is best described by a triangular distribution [14]. For design situation 2 the upper limit is set to MFV, the lower limit to HRV and the mode to DFV. For design situation 3 the lower limit is set to LRV and the upper limit to HRV. The mode is set to the mean value of the collected data for the winter season, + 1215,0.

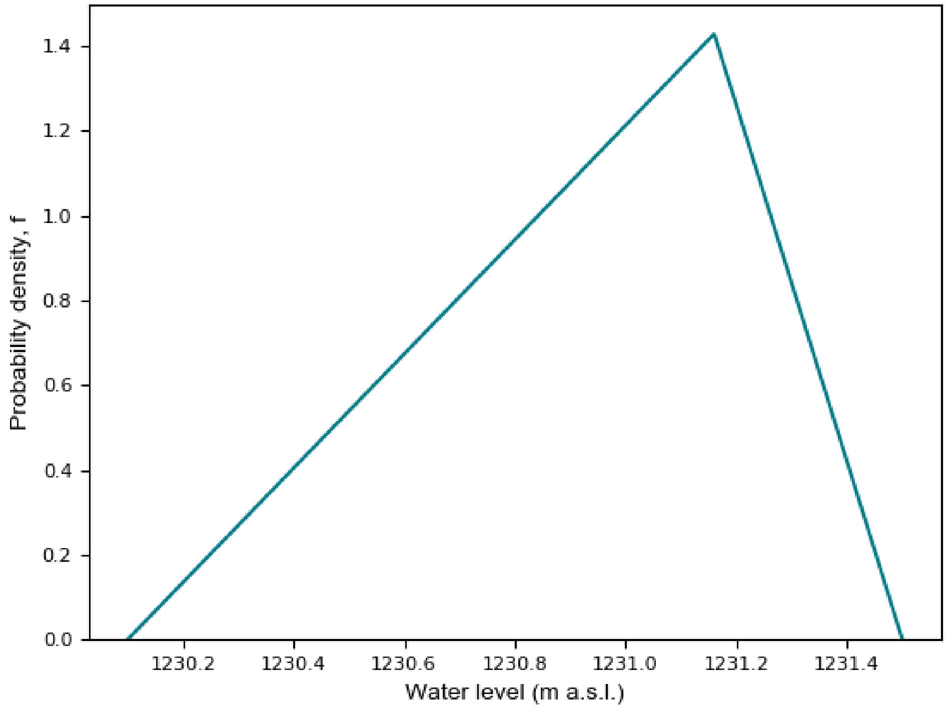

Figure 5.12 Probability density function - Water level for DFV.

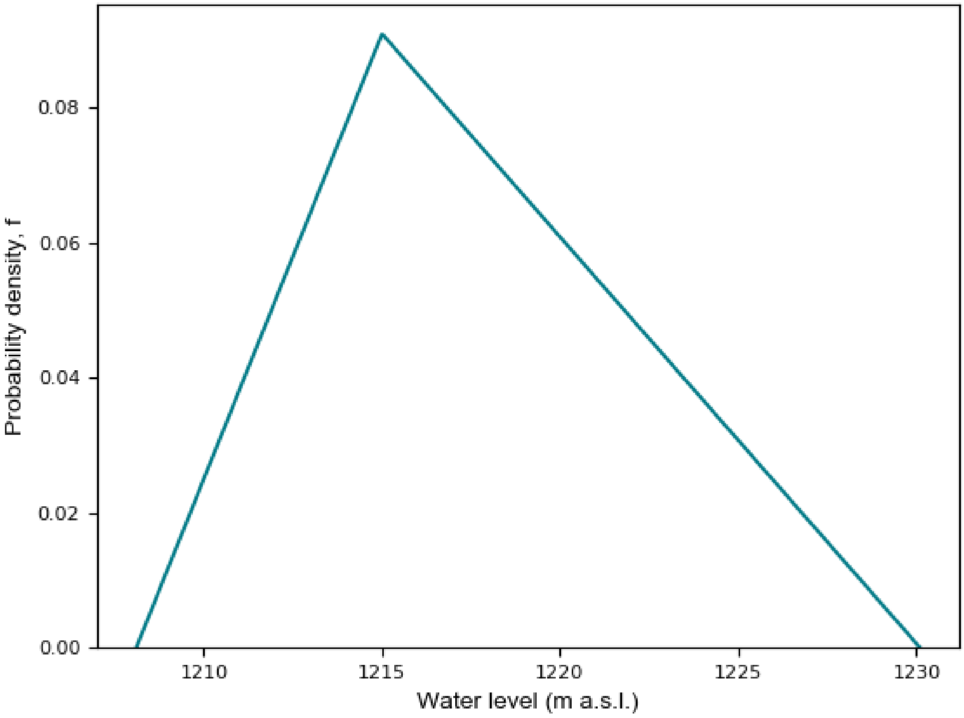

Figure 5.13 Probability density function - Water level for HRV + ice load.

5.4.8 Cohesion, c

According to NVE [15] a cohesion contribution of maximum 0,085·$\sqrt{f_{cd}}$ can be included if no other documentation from tests is available. The drawings of dam Viervatn indicates the concrete grade "B" for the pillars. As shown in Table 5.6, concrete quality "B" has a compressive cube strength, $f_{ck,cube}$, of 23 MPa . Converted to today's standards, this corresponds to a f_{ck} of 20 MPa [2]. This results in

$$c = 0{,}085\sqrt{f_{cd}} = 0{,}085 \cdot \sqrt{0{,}85 \cdot \frac{20}{1{,}5}} = 0{,}29MPa$$

Table 5.6 Concrete grade in NS 427 [20].

Tabell II: Betongkvaliteter.

Betongkvalitet	A	B	C	D
Trykkfasthet K_{T28} kg/cm² efter 28 døgn av 20×20×20 cm betongterninger	290	230	180	140

Anvendes cylindriske prøvestykker med dimensjon 15×30 cm,

Tests with a rebound hammer have been done at dam Viervatn. From 28 tests an average f_{ck} of 30,9 MPa with a standard deviation of 3,81 MPa and coefficient of variation of 12 % was found.

Based on the information above, the cohesion is assumed to be lognormally distributed with a mean value of 0,29 MPa and a coefficient of variation of 15 %.

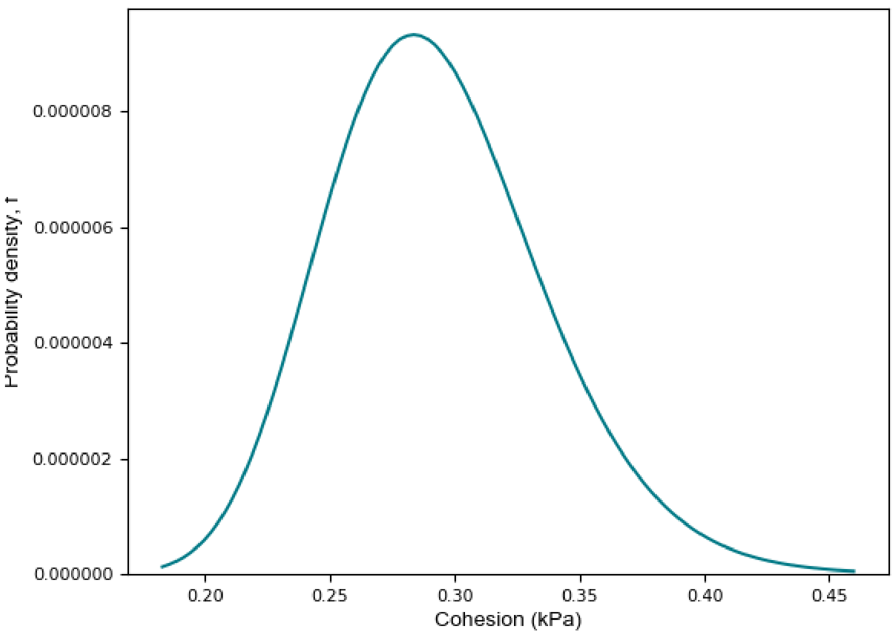

Figure 5.14 Probability density function - Cohesion.

5.4.9 Yield strength bolts, f_y

Pillar 11 has 4 rock bolts of diameter 25 mm according to the drawings. The yield strength of steel quality "St 37" is reckoned to be approximately 2400 kg/cm^2, or 235,4 MPa, according to NS 427 [20]. According to NVE's guidelines a tensile stress of 180 MPa can be used when including bolts in the stability checks [16]. The JCSS [10] and the PMCD [14] suggest the use of a lognormal distribution with a coefficient of variation of 7 %.

Based on the information above, the yield strength is assumed to be lognormally distributed with a mean value of 180 MPa and a coefficient of variation of 7 %.

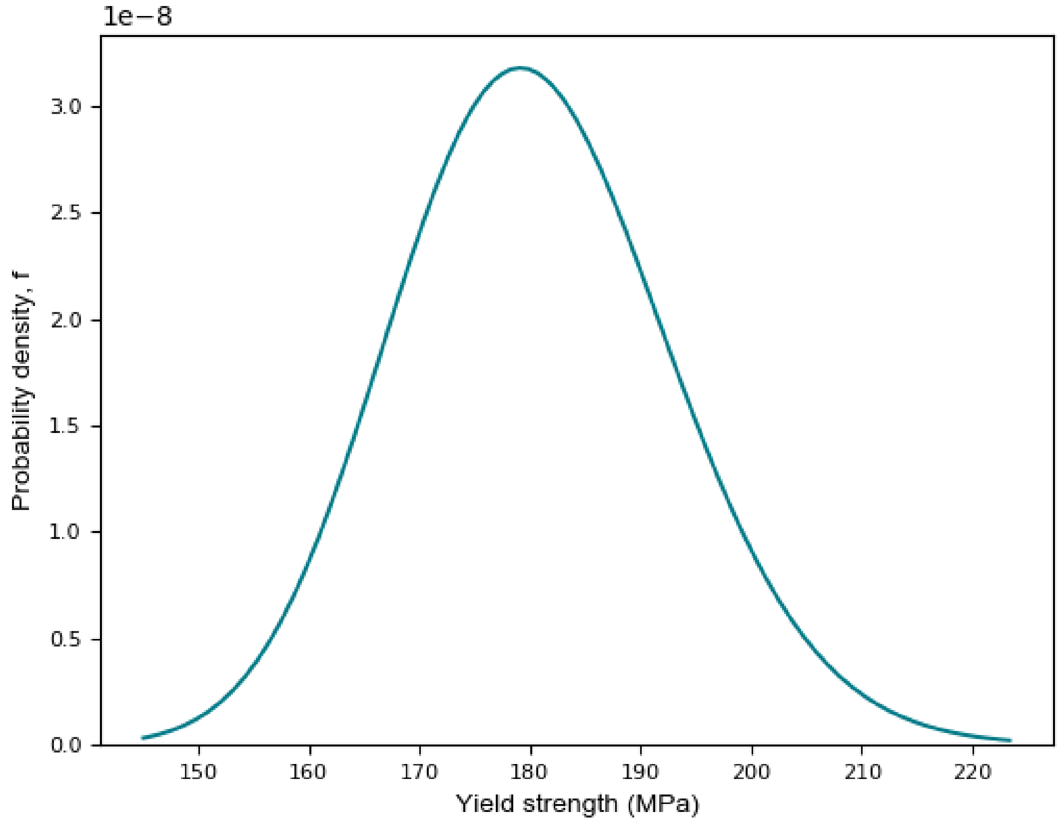

Figure 5.15 Probability density function - Yield strength bolts.

5.4.10 Ice load, q_i

The ice load is normally set to 100-150 kN/m if no further considerations are performed [5]. For dams in the lowest consequence class a value of 100 kN/m is accepted.

The PMCD [14] suggest a truncated lognormal distribution for the ice loading where the truncation of the distribution is set to the maximum ice loading. The maximum ice load is calculated as [5]:

$$P_{is-maks} = 250 \cdot \left(0{,}02 \cdot \sqrt{F_{100}}\right)^{1,5}$$

where F_{100} is the frost level in *°C days*. The frost level at Viervatn is collected from the map given in Statens Vegvesen's *Håndbok N200* [21], see Figure 5.16. Resulting in a maximum ice load of 222,5 kN/m.

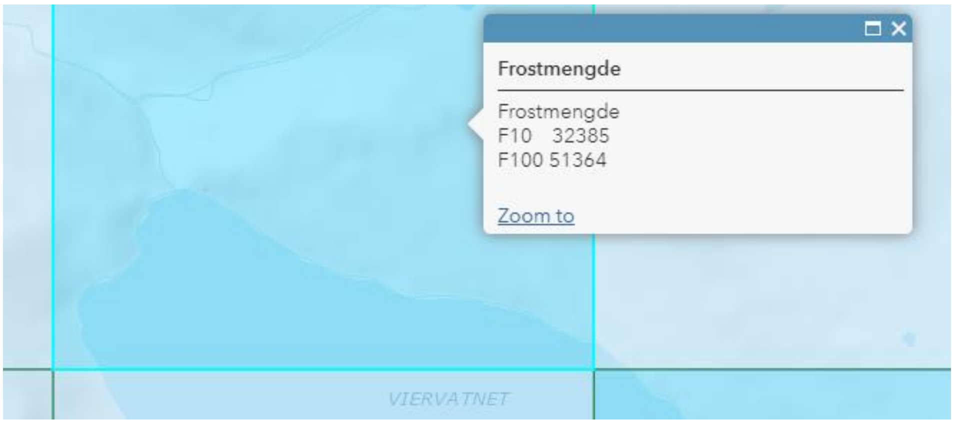

Figure 5.16 Frost levels in °C hours at dam Viervatn.

Based on the above, a truncated lognormal distribution of the ice loading is chosen. The mean is set to 100 kN/m with a coefficient of variation of 100% and a truncation at 222,5 kN/m.

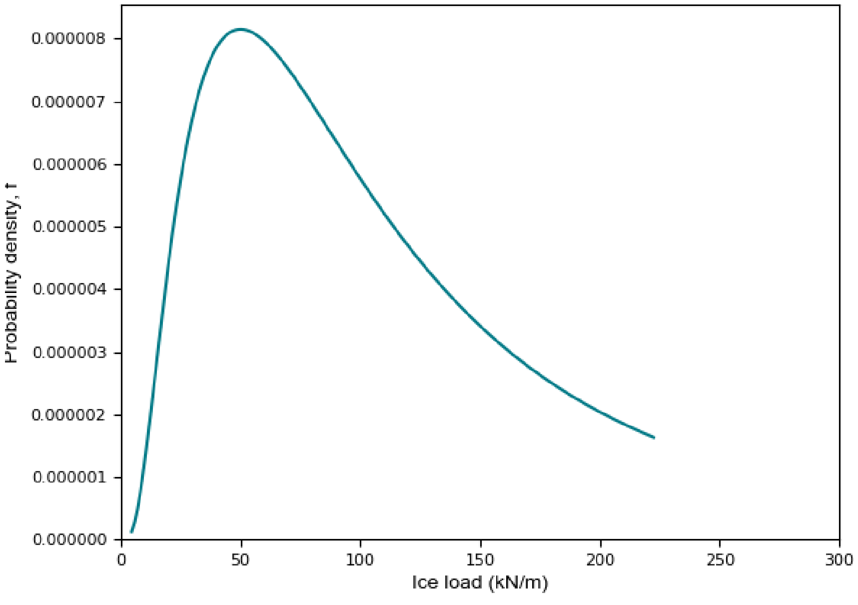

Figure 5.17 Probability density function - Ice load.

5.4.11 Summary

A summary of the chosen stochastic variables and their distributions are shown in Table 5.7.

Table 5.7 Summary of stochastic variables.

Parameter	Distribution	Mean	Coefficient of variation	Standard deviation	Upper limit	Lower limit	Peak
k_{bot}	Normal	1222 m	0.00038	0.46 m			
α	Normal	-1.7 °	1	-1.7 °			
h_o/v_o	Normal	8.5/10	0.004	0.034/10			
b_{eff1}	Normal	4.95 m	0.05	0.248 m			
b_{eff2}	Normal	4.7 m	0.05	0.235 m			
γ_b	Normal	23.5 kN/m³	0.034	0.8 kN/m³			
φ	Normal	50 °	0.05	2.5 °			
c	Normal	0.29 MPa	0.15	0.0435 MPa			
f_y	Lognormal	180 MPa	0.07	12.6 MPa			
$k_{w.DFV}$	Triangular				1231.5 m	1230.1 m	1231.16 m
$k_{w.HRV}$	Triangular				1230.1 m	1208.1 m	1215.0 m
q_i	Lognormal	100 kN/m	1	100 kN/m	222.5 kN/m		

6 Results

6.1 Reliability index

The reliability index has been calculated for stability and overturning of pillar 11 of dam Viervatn. The index for stability is calculated as a series system of the independent components stability and overturning. The tables below summarize the indices for the calculations.

Table 6.1 Results for limit states without contribution of bolts and cohesion.

Analysis no.	Sliding		Overturning		Stability	
	β	P_f	β	P_f	β	P_f
A1	4.5	3.18E-06	> 5.6	< 1.00E-08	4.5	3.18E-06
A2	2.8	2.42E-03	4.6	1.79E-06	2.8	2.42E-03
A3	3.8	6.41E-05	> 5.6	< 1.00E-08	3.8	6.41E-05

Table 6.2 Results for limit states included contribution from cohesion.

Analysis no.	Sliding		Overturning		Stability	
	β	P_f	β	P_f	β	P_f
A4	> 5.6	< 1.00E-08	> 5.6	< 1.00E-08	> 5.6	< 1.00E-08
A7	> 5.6	< 1.00E-08	4.6	1.63E-06	4.6	1.63E-06
A10	> 5.6	< 1.00E-08	> 5.6	< 1.00E-08	> 5.6	< 1.00E-08

Table 6.3 Results for limit states included contribution from bolts.

Analysis no.	Sliding		Overturning		Stability	
	β	P_f	β	P_f	β	P_f
A5	> 5.6	< 1.00E-08	> 5.6	< 1.00E-08	> 5.6	< 1.00E-08
A8	4.2	1.43E-05	> 5.6	< 1.00E-08	4.2	1.43E-05
A11	5.3	6.00E-08	> 5.6	< 1.00E-08	5.3	6.00E-08

Table 6.4 Results for limit states included contribution from cohesion and bolts.

Analysis no.	Sliding		Overturning		Stability	
	β	P_f	β	P_f	β	P_f
A6	> 5.6	< 1.00E-08	> 5.6	< 1.00E-08	> 5.6	< 1.00E-08
A9	> 5.6	< 1.00E-08	> 5.6	< 1.00E-08	> 5.6	< 1.00E-08
A12	> 5.6	< 1.00E-08	> 5.6	< 1.00E-08	> 5.6	< 1.00E-08

6.2 Sensitivity

Results of the calculation of sensitivity measurements are shown in the sections below. The cohesion is not included in the limit state of overturning, which is why there are two less figures for this failure mode. Some of the analysis resulted in $\sum S_i \approx 1$. These results have been deemed acceptable considering some of the variables are not normal distributed.

6.2.1 Sliding

The sensitivity analysis for sliding tends to give a high sensitivity index for the friction angle.

6.2.1.1 <u>Design situation 1 – Only HRV</u>

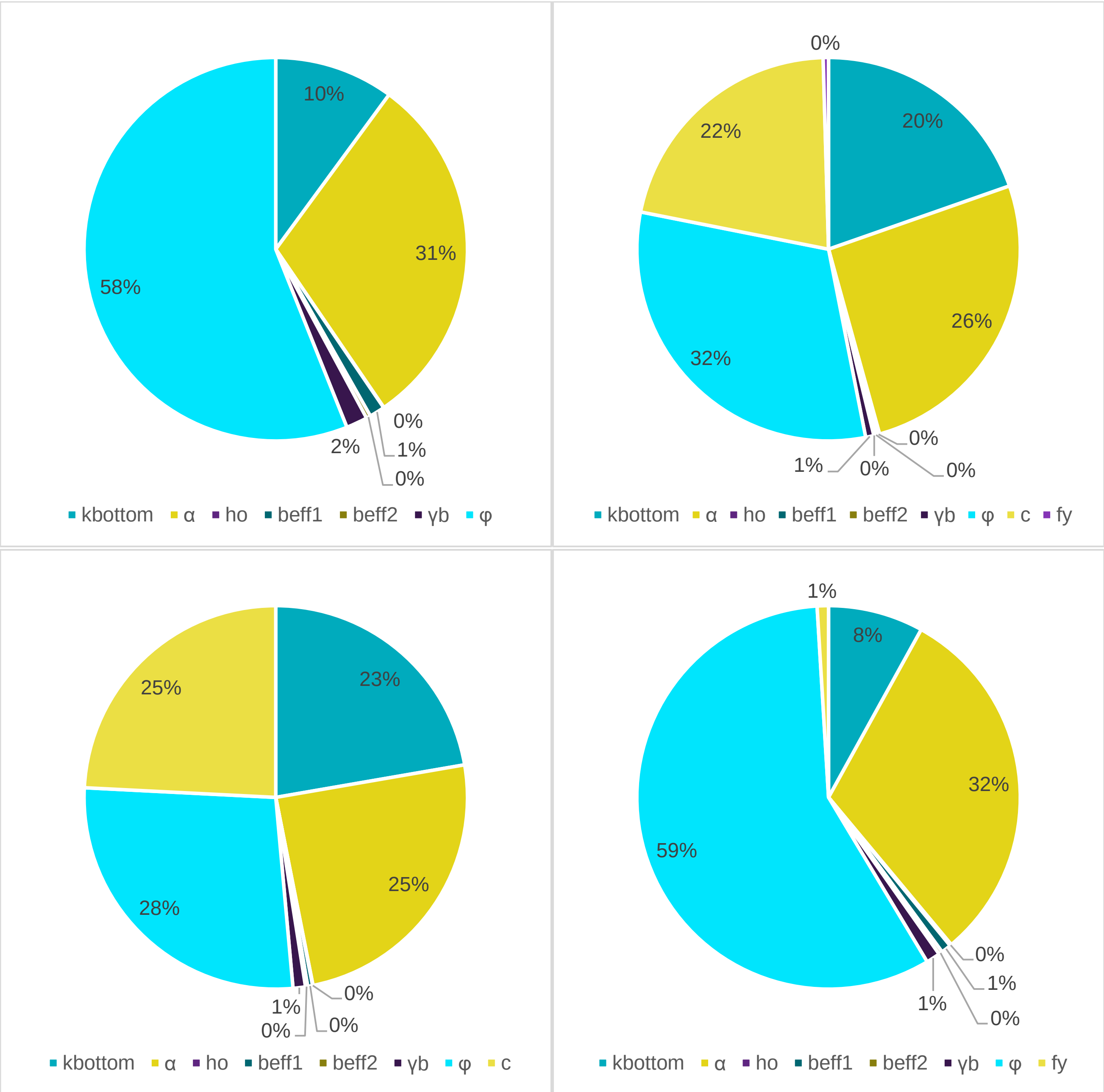

Figure 6.1 Sensitivity indices for design situation 1 in sliding, A1 (upper left), A6 (upper right), A4 (lower left) and A5 (lower right).

6.2.1.2 Design situation 2 – HRV and ice

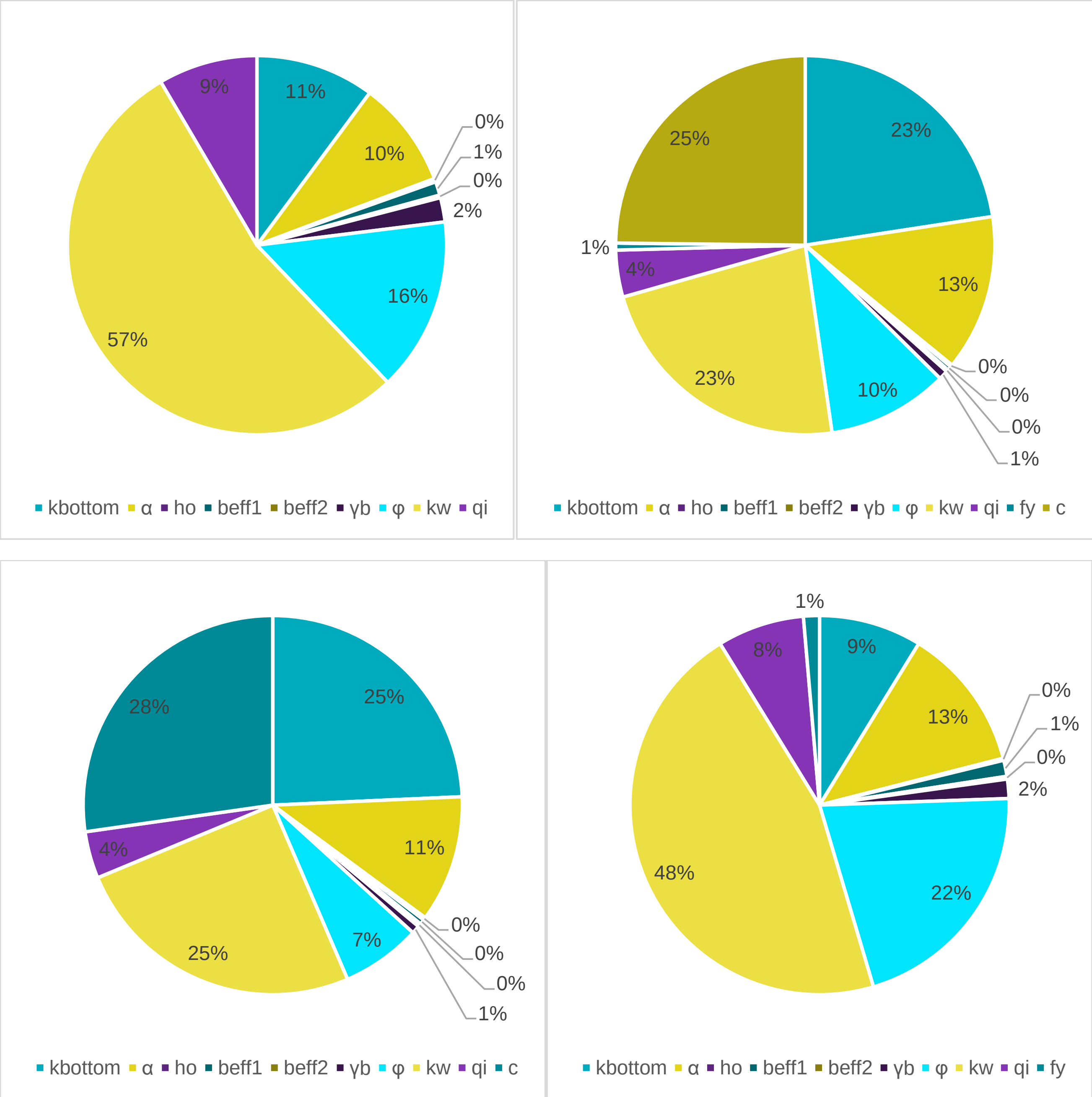

Figure 6.2 Sensitivity indices for design situation 2 in sliding, A2 (upper left), A9 (upper right), A7 (lower left) and A8 (lower right).

6.2.1.3 Design situation 3 – DFV

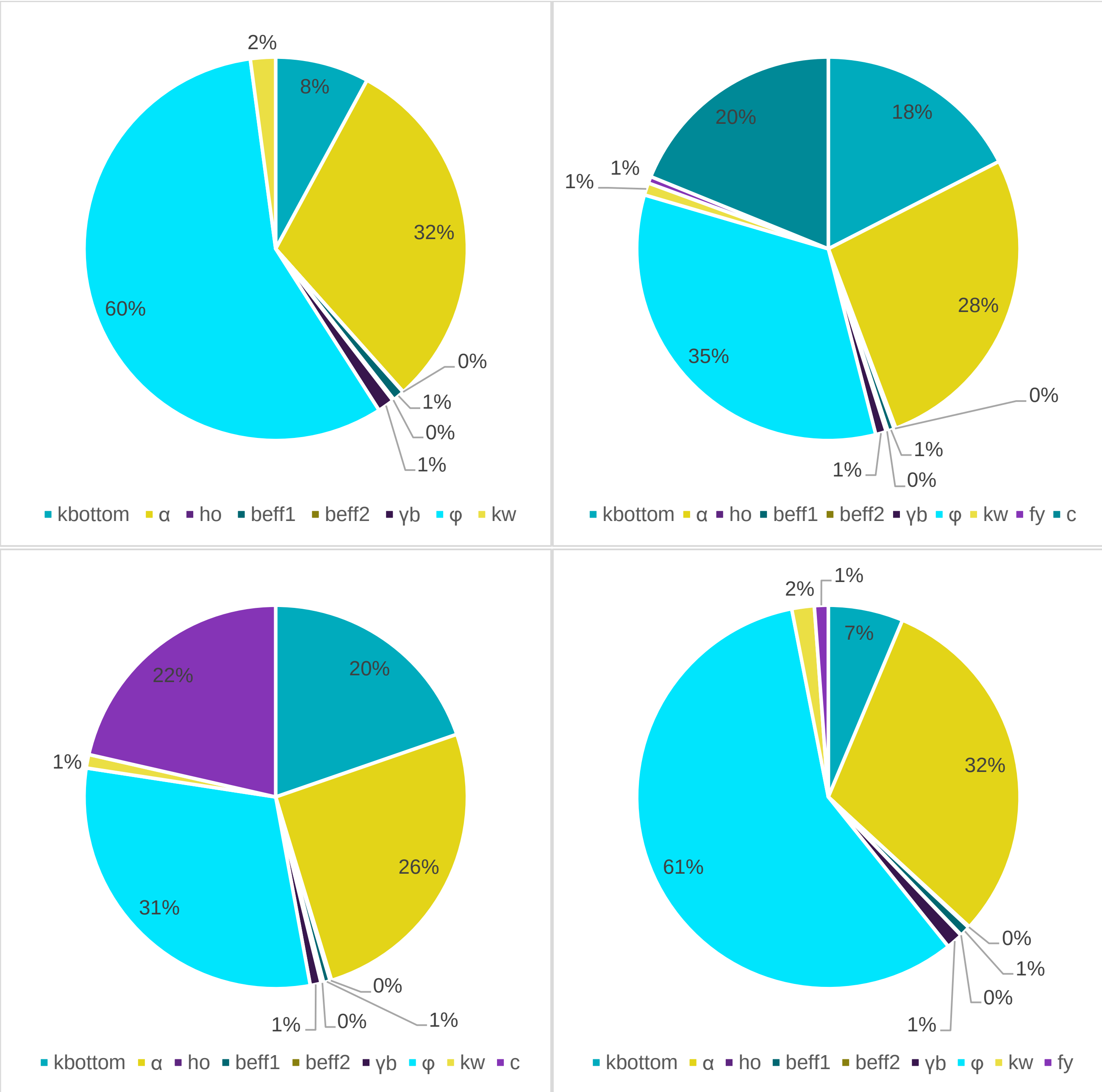

Figure 6.3 Sensitivity indices for design situation 3 in sliding, A3 (upper left), A12 (upper right), A10 (lower left) and A11 (lower right).

6.2.2 Overturning

6.2.2.1 Design situation 1 – Only HRV

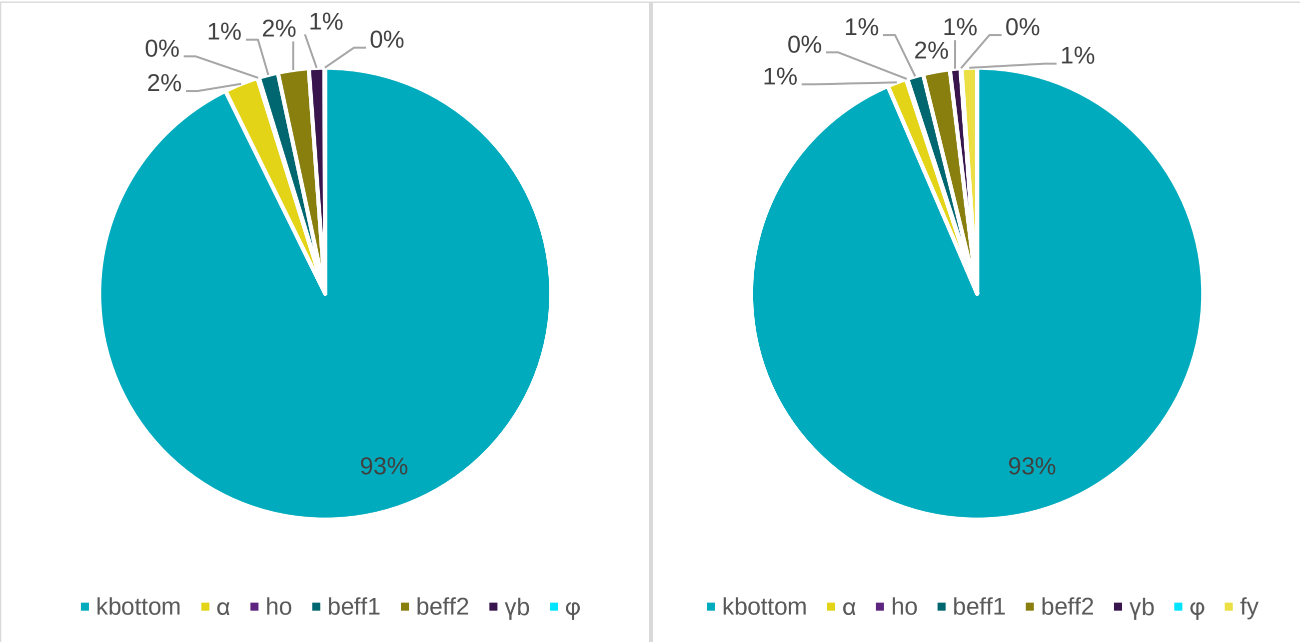

Figure 6.4 Sensitivity indices for design situation 1 in overturning, A1 (left) and A5 (right).

6.2.2.2 Design situation 2 – HRV and ice

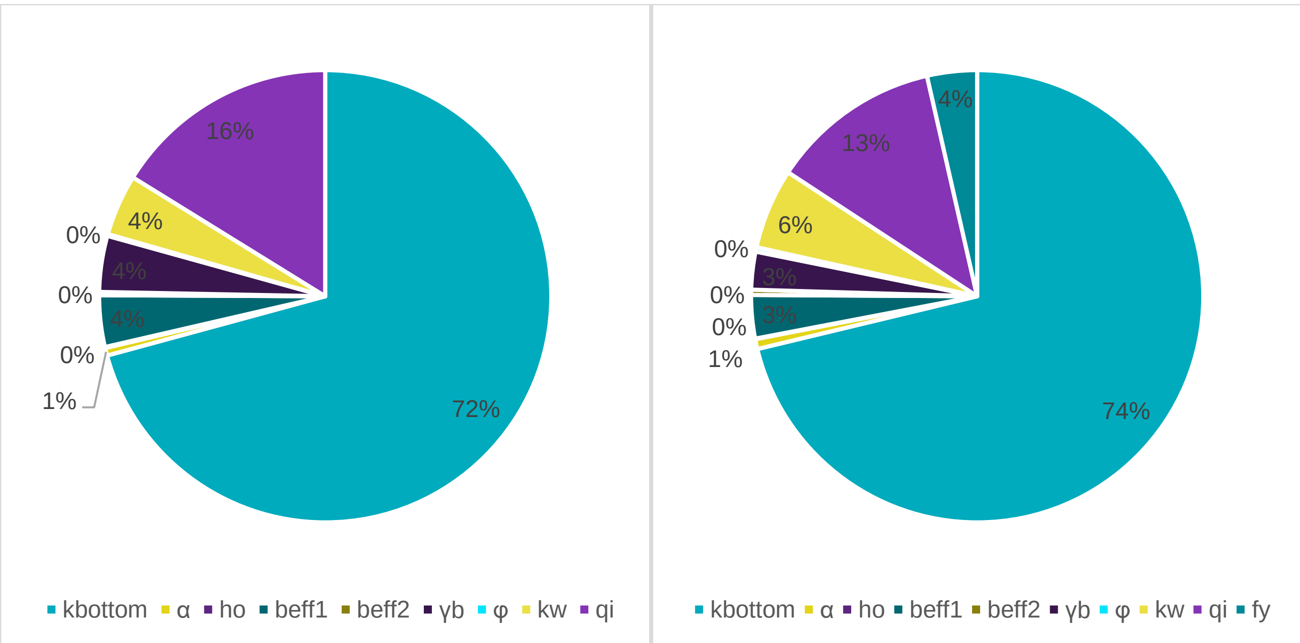

Figure 6.5 Sensitivity indices for design situation 2 in overturning, A2 (left) and A8 (right).

6.2.2.3 Design situation 3 – DFV

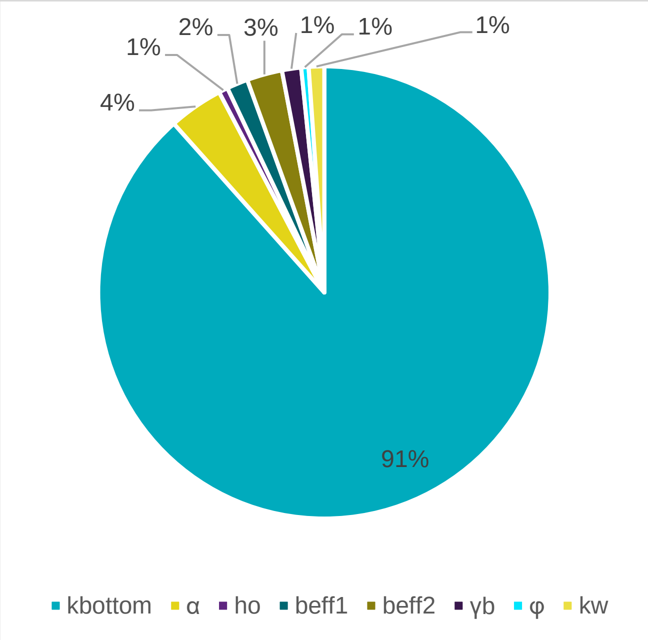

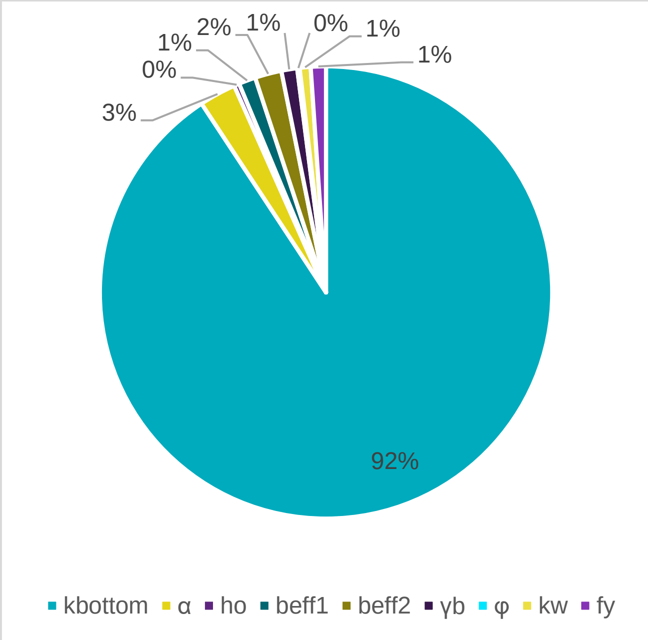

Figure 6.6 Sensitivity indices for design situation 3 in overturning, A3 (left) and A11 (right).

7 Discussion

7.1 Probabilistic model

Direct, or crude, Monte Carlo is used as simulation method in this report. The method requires a large number of trials in order to estimate with a certain degree of confidence the failure probability [10]. The number of trials increases as the failure probability decreases. The Monte Carlo method gives, in principle, correct answers to the reliability problem. As present in most systems, the limit state function used in this report is discontinuous. For these types of limit states the Probabilistic model codes for concrete dams [14] suggest the use of Monte Carlo simulations.

The results given in Section 6.1 are products of 10^8 simulations. The lowest possible probability of failure for this amount of simulations is $1/10^8 = 10^{-8}$. As the tables above show, some of the design situations, especially for overturning, results in an unobtainable probability of failure which is lower than 10^{-8}. Due to the simplicity of the calculation model described in Section 5, the calculation time is not too extreme. The simulation time using multiprocessing with 8 processors are illustrated in Figure 7.1. For a more complex calculation model, e.g. a FEM-model, the Monte Carlo method will not be adequate and first or second order reliability methods (FORM or SORM) should be considered. Still, the validity of FORM-calculation should be determined by comparative MC-simulations.

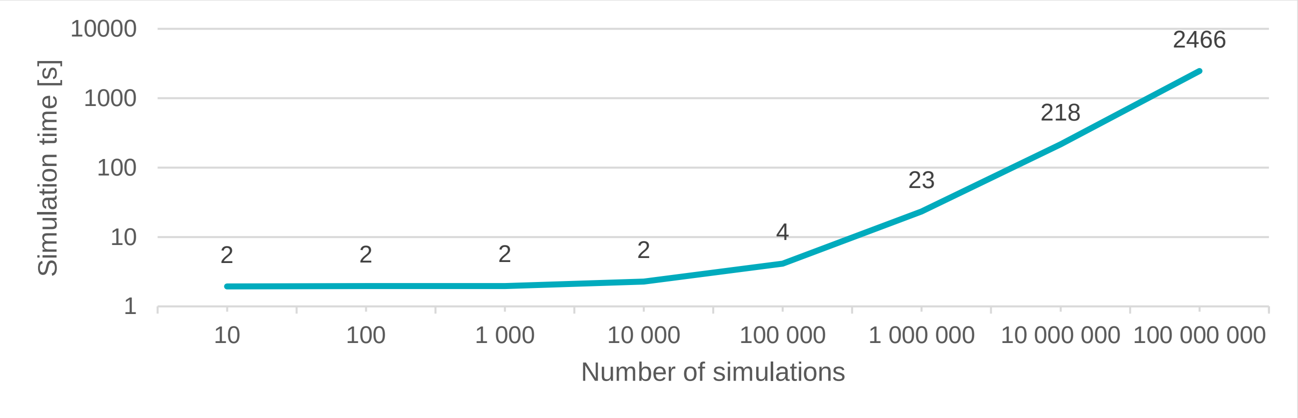

Figure 7.1 Simulation time.

7.2 Target reliability

Target reliabilities are nominal, and dependant of assumptions made in an analysis. Still, it is possible to apply target values from the Eurocode, the JCSS and the PMCD. Therefore, a comparison towards the target reliabilities of the PMCD and Eurocode is done for Dam Viervatn.

Dam Viervatn can be assumed belonging to consequence class C in the PMCD as shown in Table 4.3, which suggest a target reliability index of 4,2. Neither design situation 2 nor 3 satisfy this condition in sliding when cohesion and bolts are not included. The calibration of target reliabilities from the PMCD are based on a calculation model that includes rock bolts. The results given in Table 6.3 are therefore more adequate for comparison. In this case the reliability indices all satisfy the minimum β. With regards to the target reliabilities given in Eurocode 0, Dam Viervatn could be classified as RC1. Table 4.4 gives a target reliability like the PMCD of 4,2, and the same considerations as above can be made. With regards to target reliabilities in the future phases of this project, a calibration similar to the one performed by Westberg and Johansson [22] should be done for Norwegian dams.

In the PMCD, reference period for load parameters is one year (that is statistical parameters of loads should be based on annual maximum values). [10] The adaption of loads for design situation 2 in this report is less conservative and not based on annual maximum values, but on all values in the winter months at Dam Viervatn. A set of standard assumptions for the load model and reference period should be determined in order to calibrate a target reliability in future phases of the project.

7.3 Sensitivity

The results of the sensitivity study are shown in Section 6.2 and Appendix D. The method applied in this report is a simplified approach, as mentioned in Section 4.4. The trends shown in the scatter plots of Appendix D are compared to the results of Section 6.2.

In sliding, the sensitivity indices for design situation 1 and 3 correlates well to the scatter plots. The limit state of design situation 2 is highly non-linear since the distribution of the water level may lead to situations with no load action on the front plate. The results from the sensitivity analyses of A2, A7, A8, and A9, are therefore more uncertain. The trends of the scatter plots are also more difficult to interpret. The indices from overturning does not correlate to the scatter plots.

Based on the results of the sensitivity study, the most sensitive parameters introduced in the design situations for sliding are the friction angle, the dam height (level at bottom of dam), the angle of the sliding plane, cohesion, the water level and the ice load. The other parameters, the effective width, slope of the front plate and mass density of concrete, and their distribution has only a small effect on the results. The results are as expected more sensitive to the parameters which are introduced to the analysis with a larger uncertainty.

8 Conclusion and further work

In order to develop a guideline similar to the PMCD for existing Norwegian dams in the future phases of this project, a set of assumptions must be agreed upon. Future analysis must be based on the same assumptions, design situations, calculation model and probabilistic model in order to calibrate a target reliability. These assumptions must be made such that the methods in the guideline can be applied by the common engineer.

Based on the discoveries of this report assumptions for the water level, friction and sliding angle, ice load, cohesion and bolt capacity should be further investigated. These parameters have large influence on the result and are also highly sensitive when introduced to the analysis with large uncertainties.

A probabilistic model applying FORM analysis is advantageous when seeking more accurate sensitivity studies, and a suggestion is to use this approach in combination with Monte Carlo simulations. If a calculation model of limit equilibrium, as used in this report, is applied, the use of Monte Carlo simulation with regard to calculation time is acceptable.

Appendix A Effective width of front plate

The front plate has joints at the edges, at pillar 1 and 13, and between pillars 10-11, 8-9, 5-6 and 3-4, see Figure 8.1. The spacing between each pillar is 5 m, except between pillars 12-13 and 1-2, where the width measures 5,2 m. The distance from centre pillar to the joints is 850 mm. The static system assumed is shown in Figure 8.2.

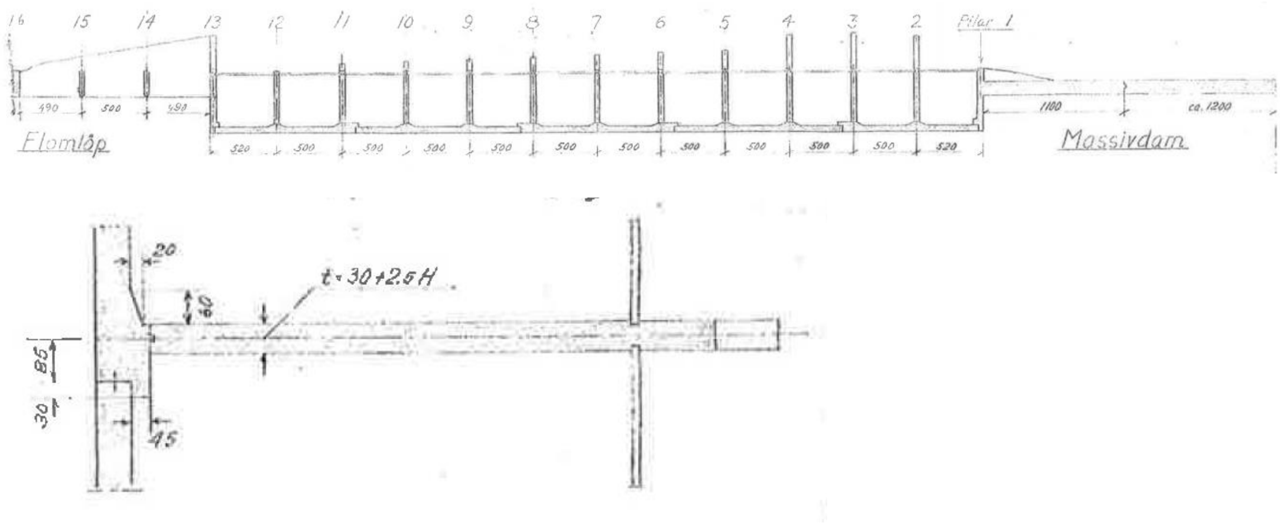

Figure 8.1 Plan view of dam Viervatn, drawing 3526.

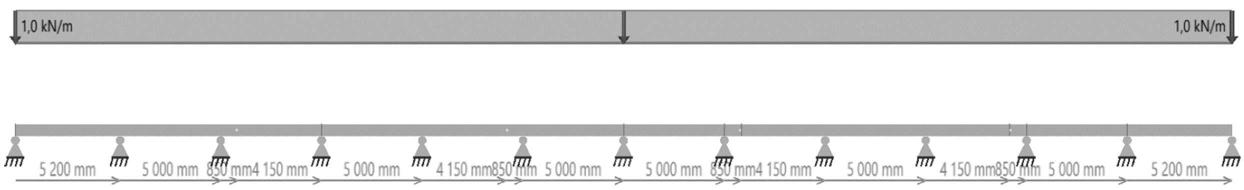

Figure 8.2 Static system for calculation of effective width of front plate.

The effective width is calculated as follows, where R_i is the reaction force in pillar i, R_{Tot} is the total force, $b_{eff,i}$ is the effective width for pillar i and b_{Tot} is the total width of the front plate.

$$\frac{R_i}{R_{Tot}} = \frac{b_{eff,i}}{b_{Tot}}$$

This results in the effective widths shown in Table 8.1.

Table 8.1 Effective width of front plate for each pillar.

Pillar i	1	2	3	4	5	6	7	8	9	10	11	12	13
$b_{eff,i}$ [m]	2.1	5.9	4.7	5.1	5.1	4.8	5.2	4.8	5.1	5.1	4.7	5.9	2.1

Appendix B Water level data

Water level registrations for dam Viervatn have been collected between 2004 and 2019. Data have been collected every hour for the last 15 years. In the below figures the data have been filtered to the "summer" and "winter" months.

The summer months, June, July, August, September, October and November, are most likely to experience flooding and are shown in Figure 8.3. The data shows a higher frequency of water levels close to HRV than the winter months. It also shows that water levels above HRV have not been present during the last 15 years.

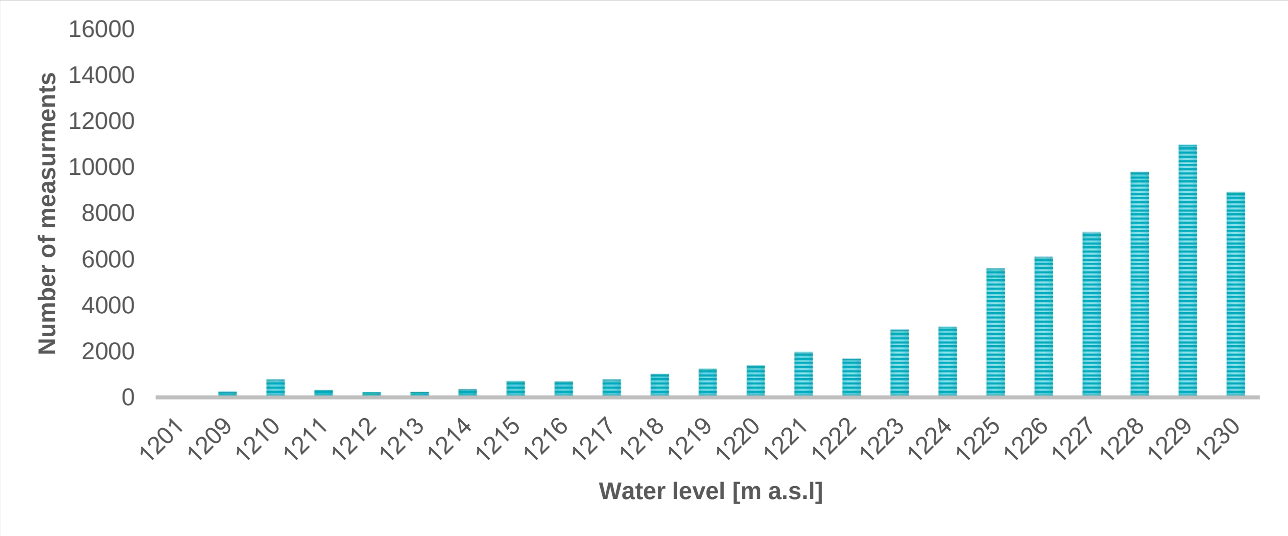

Figure 8.3 Data of water level at dam Viervatn during the summer months.

The winter months, December, January, February, March, April and May, are most likely to experience ice loading on the dam and are shown in Figure 8.4. The data suggests that the water level rarely reaches HRV and that it usually lies in the area of LRV (lowest regulated water level).

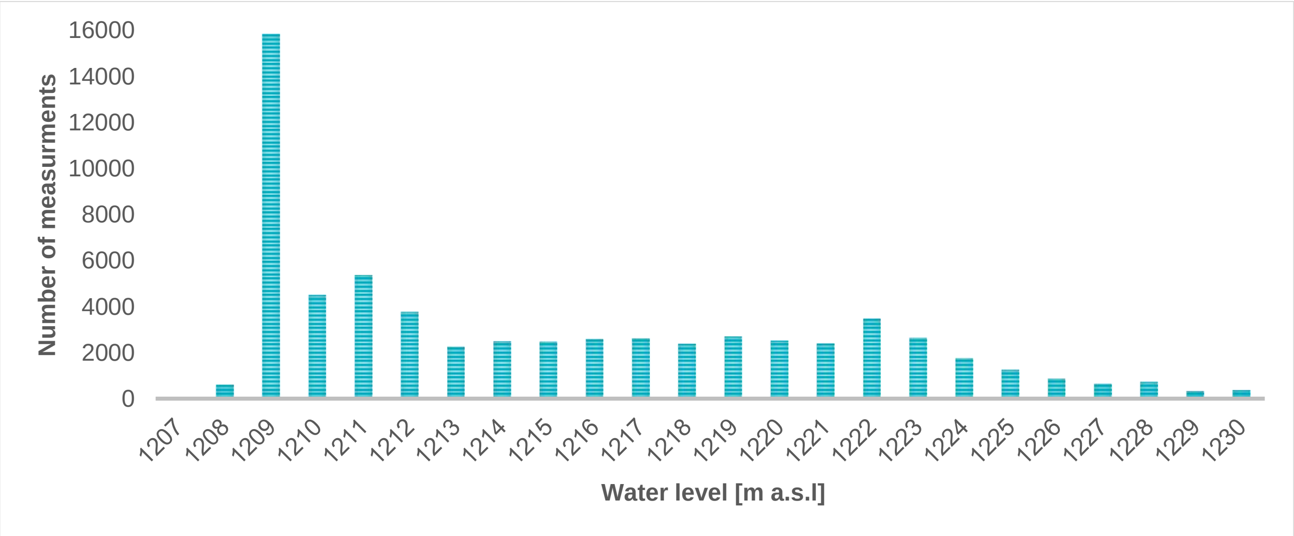

Figure 8.4 Data of water level at dam Viervatn during the winter months.

Appendix C Control of calculations

C.1 Control against deterministic calculations

The python script developed has been controlled against the deterministic calculations for stability already performed during Norconsult's reassessment of dam Viervatn. The results of safety factors for sliding and overturning are given in Table 8.2 and Table 8.3 respectively. The python script results in similar safety factors with small deviations. These deviations are acceptable due to the causes which are the following

- The pore pressure has been halved to better fit the guidelines from NVE in the python script.
- In the reassessment does not include increase and decrease of mass due to the angle of the rock-concrete interface.
- The reassessment only works with heights rounded to nearest whole meter.

The safety factors from the reassessment highlighted in red does not satisfy the demands from NVE. Notice that pillar 11 of Dam Viervatn is "safe" with regards to overturning.

Table 8.2 Control against deterministic calculations - Sliding

	Safety factor for sliding, S_f		
Analysis no.	Reassessment	Python	Deviation
A1	1.57	1.65	-5 %
A2	1.20	1.28	-6 %
A3	1.43	1.5	-5 %
A4	2.48	2.56	-3 %
A5	1.97	1.95	1 %
A7	1.76	1.98	-11 %
A8	1.48	1.51	-2 %
A10	2.14	2.22	-4 %
A11	1.72	1.73	-1 %

Table 8.3 Control against deterministic calculations - Overturning.

	Safety factor for overturning, S_f		
Analysis no.	Reassessment	Python	Deviation
A1	2.33	2.73	-14 %
A2	1.52	1.68	-9 %
A3	2.03	2.31	-12 %
A5	2.77	3.17	-12 %
A8	1.81	1.96	-7 %
A11	2.36	2.64	-10 %

C.2 Convergence of reliability index

As mentioned in Section 4.3, a large number of Monte Carlo simulations are needed to cover the tail region of the distributions. The largest probability of failure is found in design situation 2, with ice load and water pressure. There is a larger probability of failure in sliding than in overturning, this is also reflected in the deterministic results given in Section C.1. In Figure 8.5 and Figure 8.6 the changes in reliability index and covariance of probability of failure for analysis A2 are shown for sliding and overturning respectively.

In sliding the probability of failure is less than 10^{-3}. Using 10^3 simulations, only one of the simulations result in failure. This gives a covariance of p_f equal to 1. As shown in Figure 8.5, the covariance and reliability index stabilize at 10^6 simulations and larger.

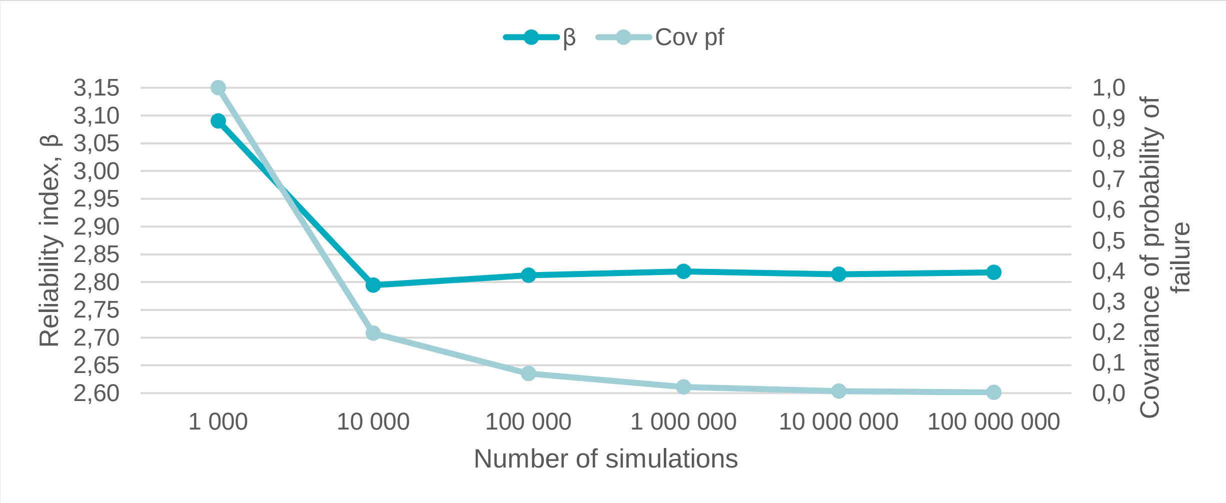

Figure 8.5 Convergence of A2 - Sliding

In overturning the probability of failure is less than 10^{-6}. In order to get one failure, at least 10^6 simulations must be run. Since the probability of failure is so low, a covariance of p_f less than 0,1 is only achieved at 10^8 simulations.

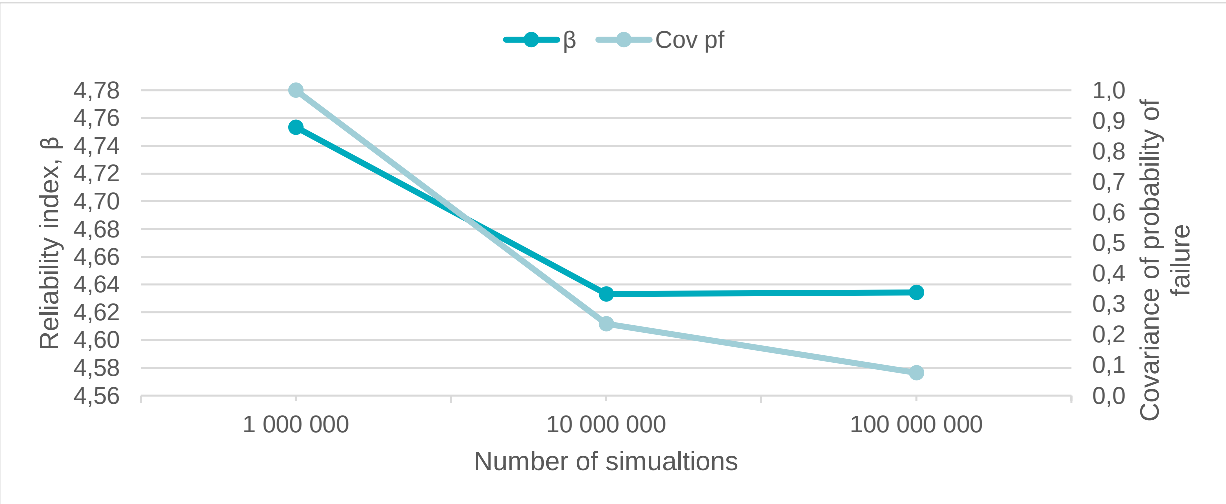

Figure 8.6 Convergence of A2 - Overturning.

Appendix D Scatter plots

D.1 Sliding

Table 8.4 Sensitivity sliding - A6 Design situation 1 with cohesion and bolts.

Parameter	Sensitivity index	Scatter plot
φ	0.32	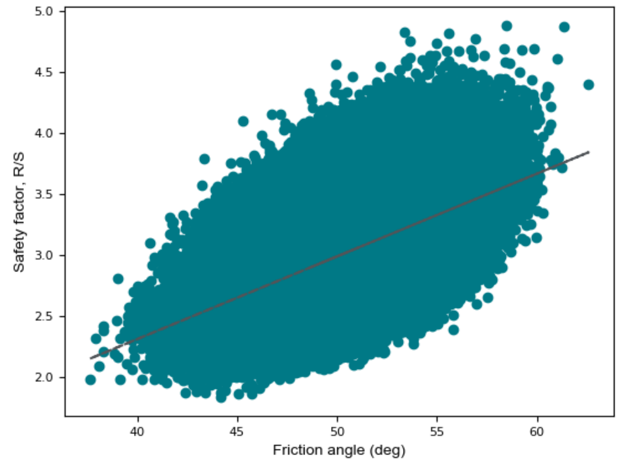
α	0.26	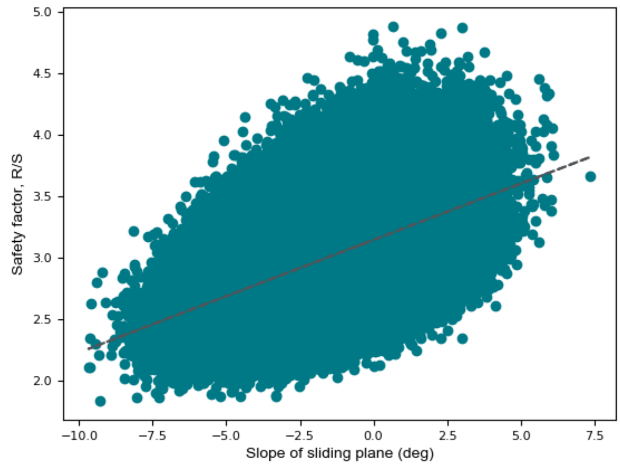
c	0.22	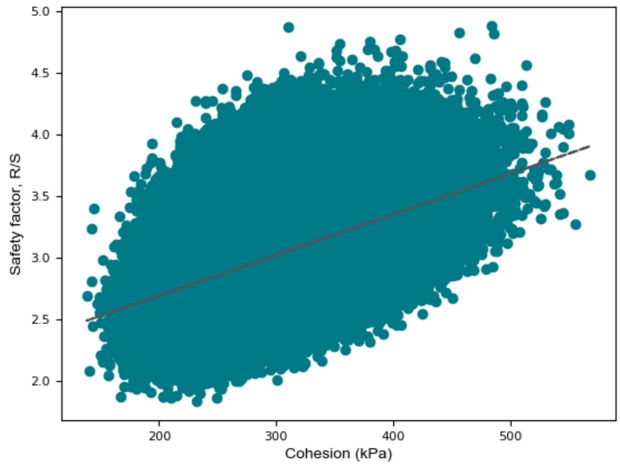

k_{bot}	0.20	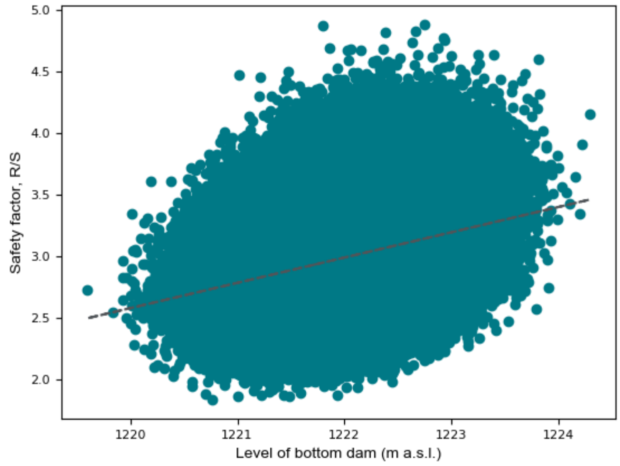
γ_b	0.007	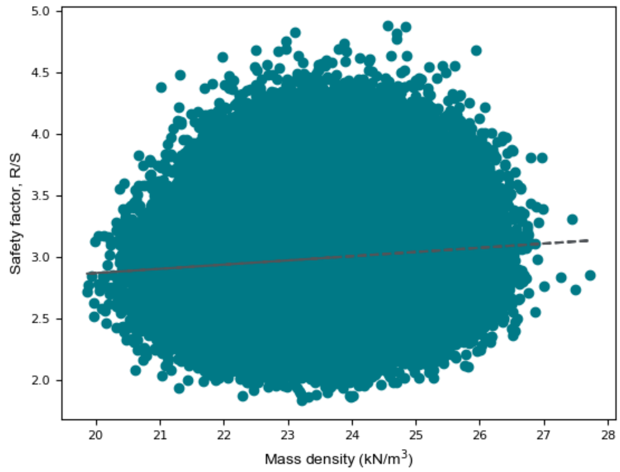
f_y	0.005	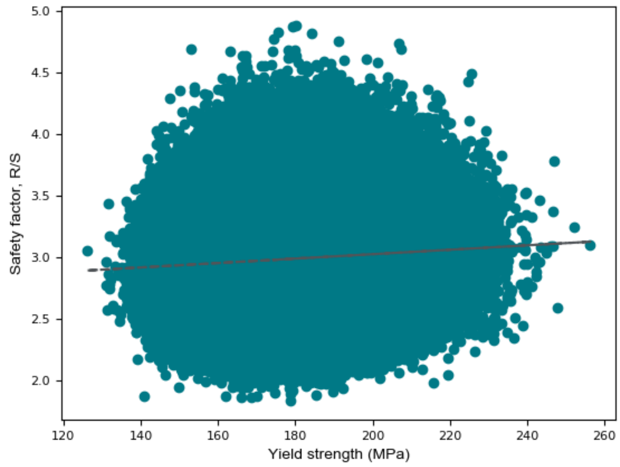

b_{eff1}	0.003	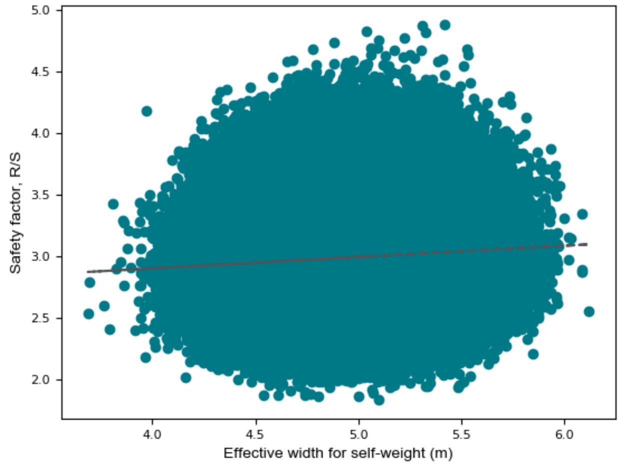
b_{eff2}	0.001	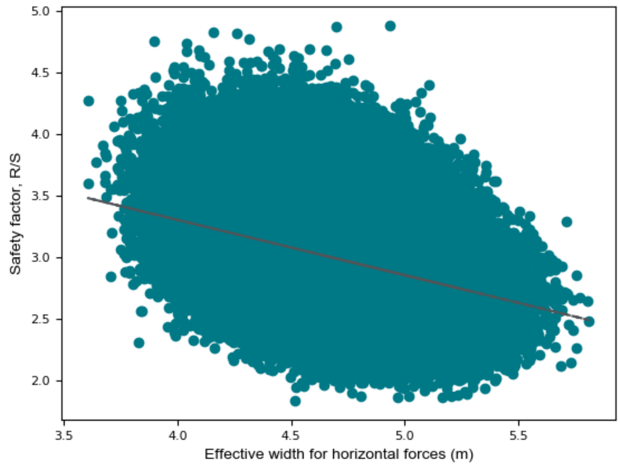
h_o/v_o	0.000	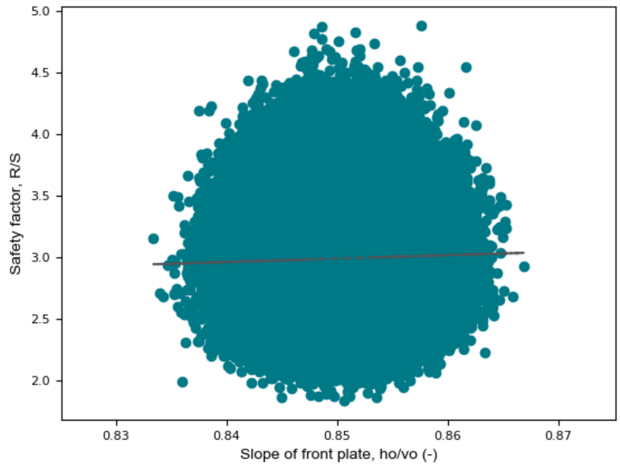

Table 8.5 Sensitivity sliding – A9 Design situation 2 with cohesion and bolts.

Parameter	Sensitivity index	Scatter plot
c	0.25	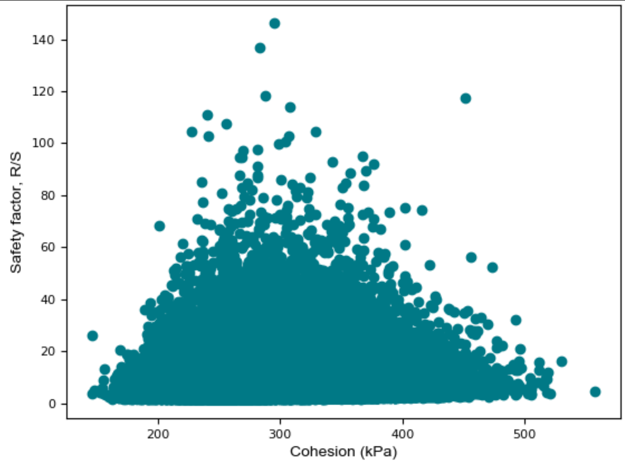
k_w	0.23	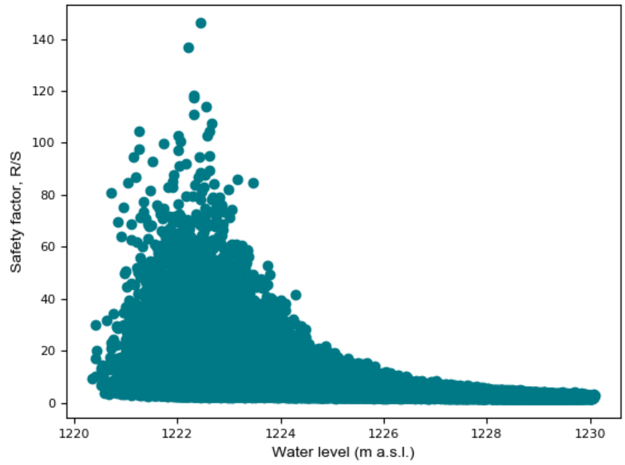
k_{bot}	0.23	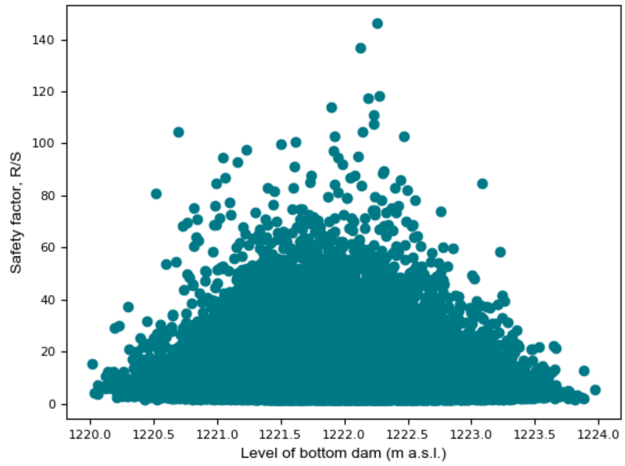

α	0.13	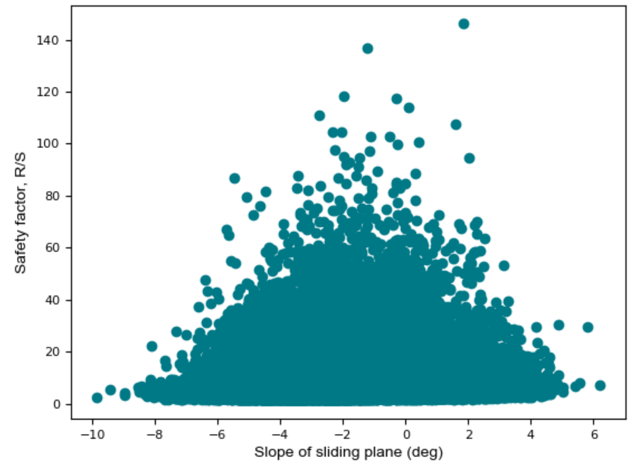
q_i	0.04	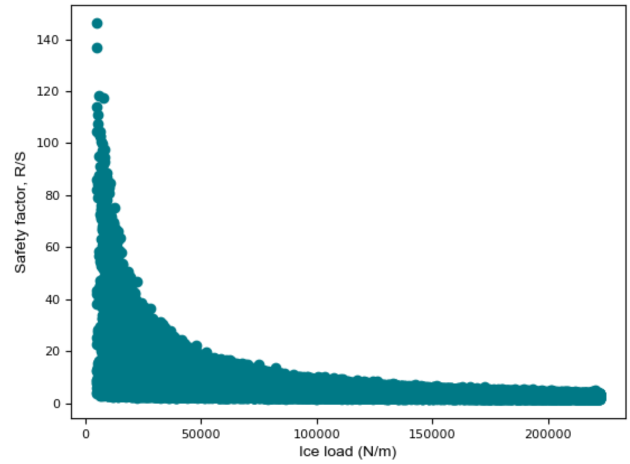
γ_b	0.01	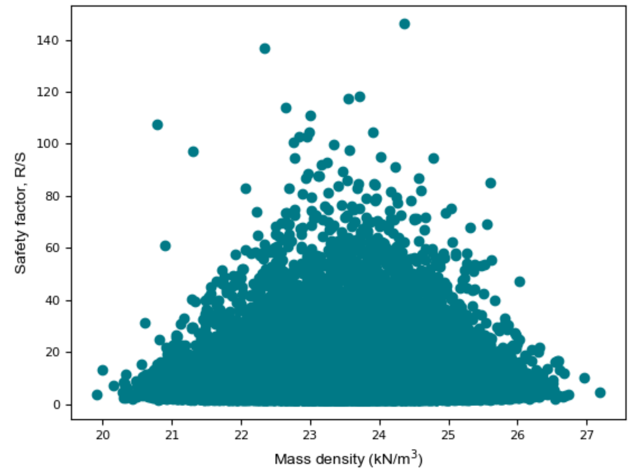

f_y	0.01	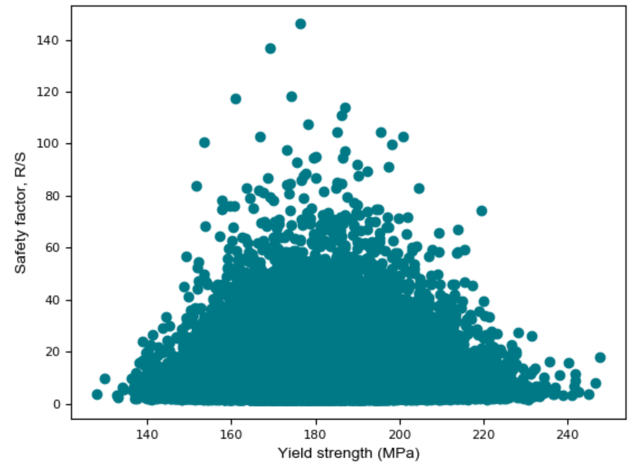
b_{eff1}	0.003	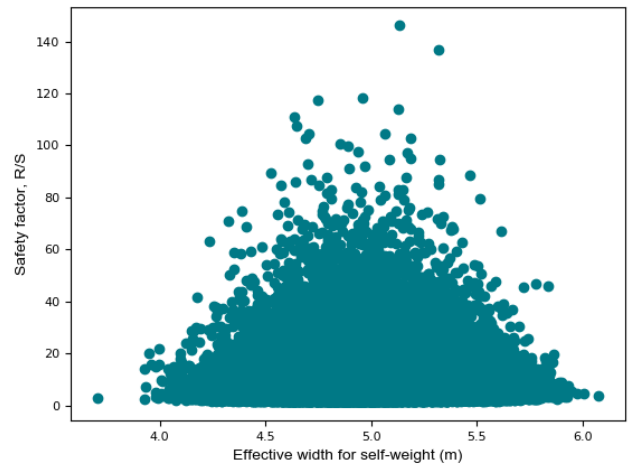
b_{eff2}	0.002	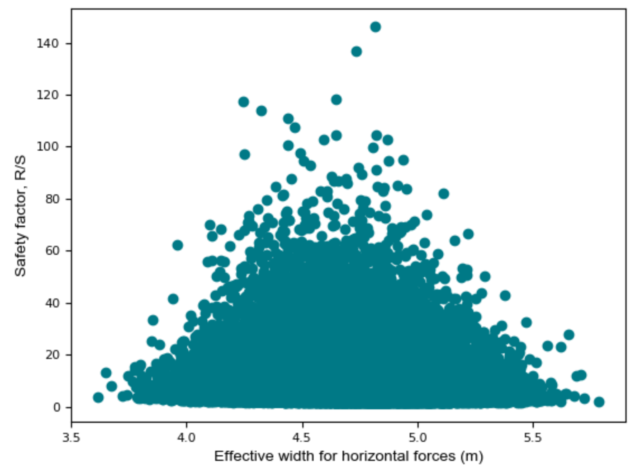

h_o/v_o	0.000	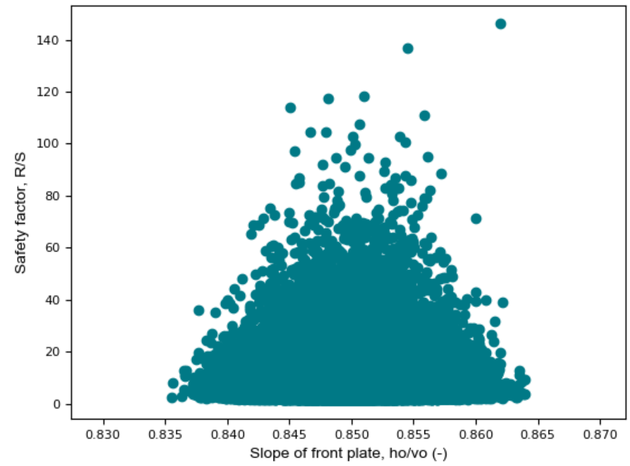

Table 8.6 Sensitivity sliding – A12 Design situation 3 with cohesion and bolts.

Parameter	Sensitivity index	Scatter plot
φ	0.35	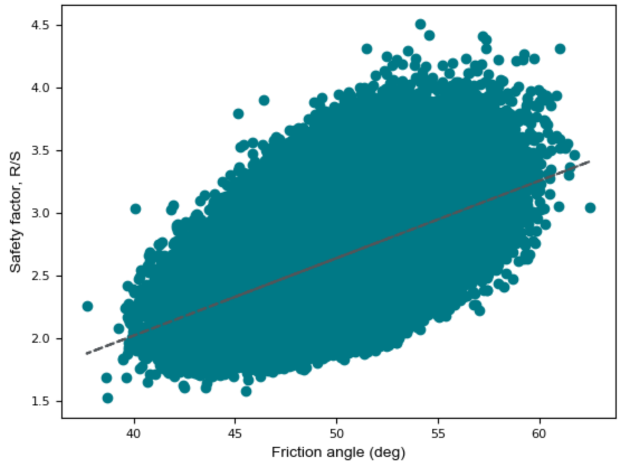
α	0.28	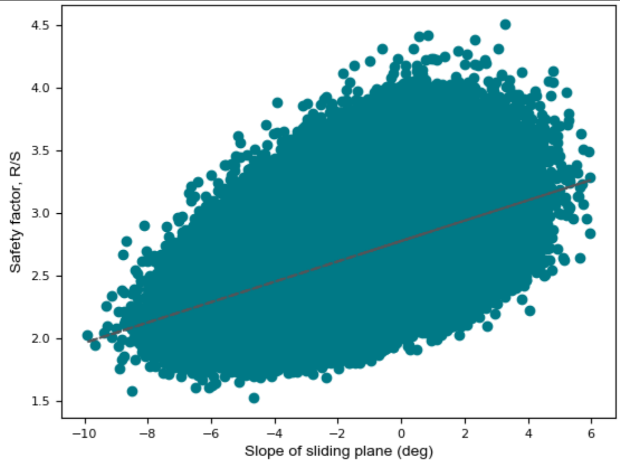

c	0.20	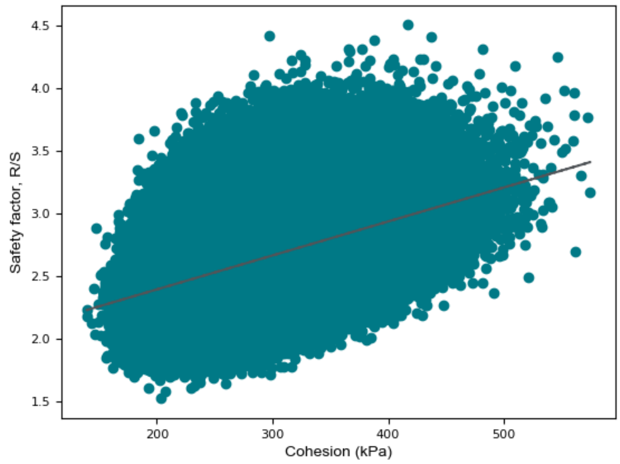
k_{bot}	0.18	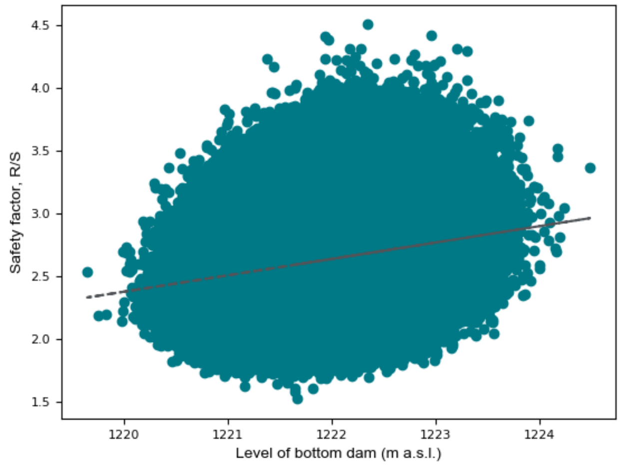
k_w	0.01	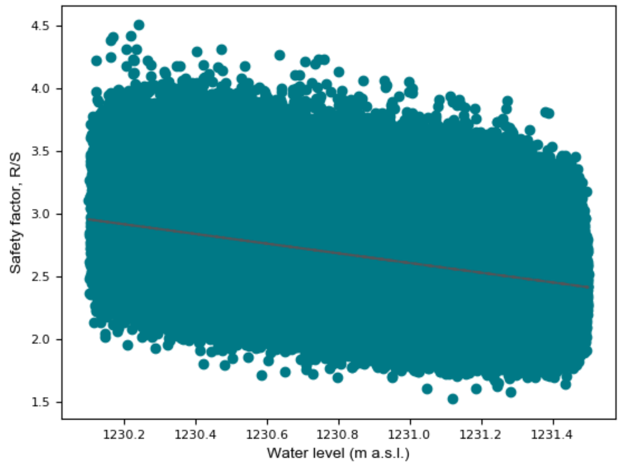

γ_b	0.01	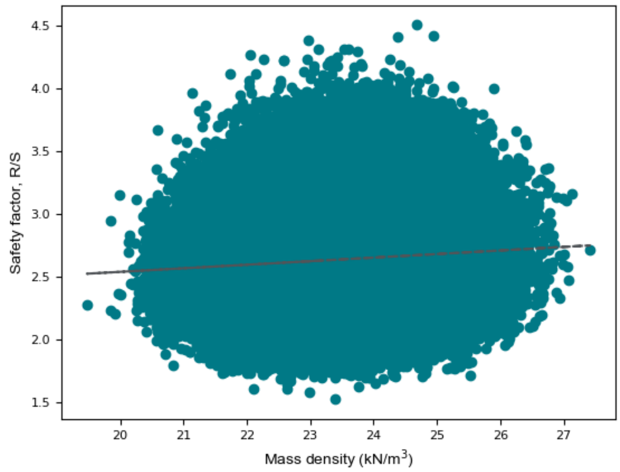
f_y	0.01	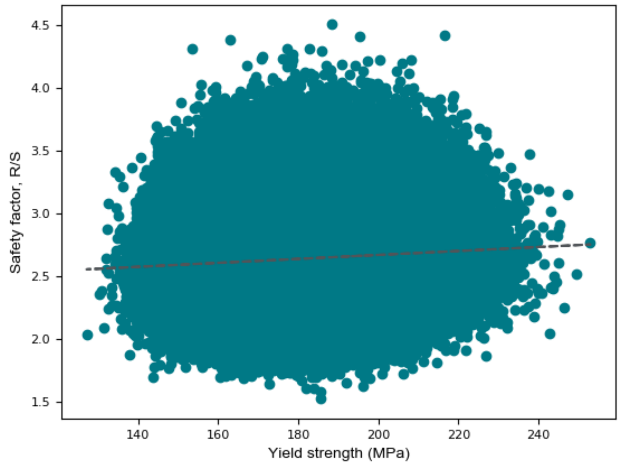
b_{eff1}	0.01	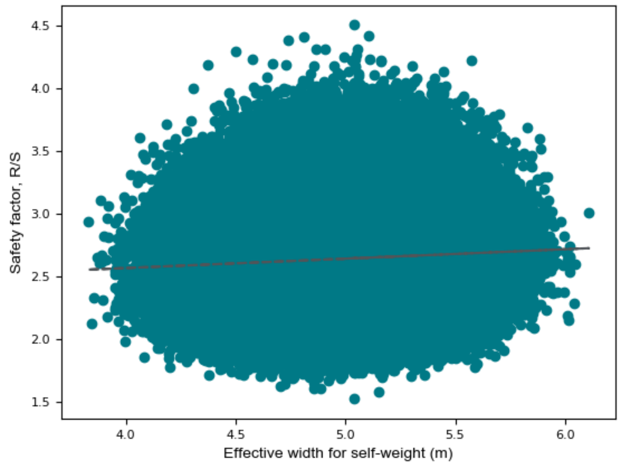

b_{eff2}	0.002	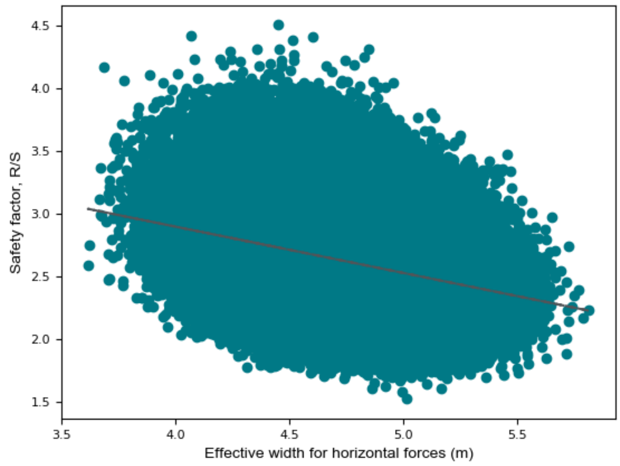
h_o/v_o	0.002	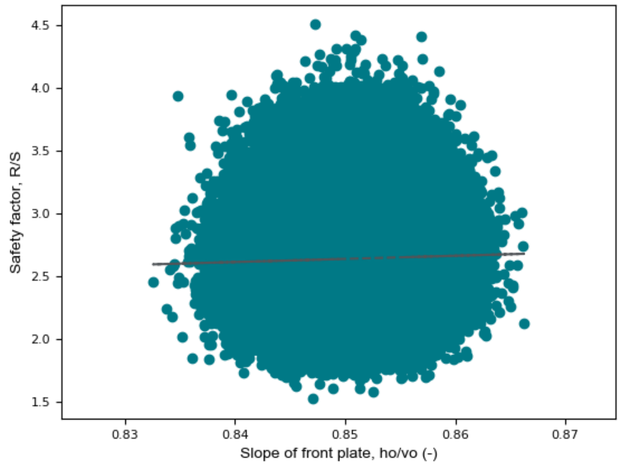

D.2 Overturning

Table 8.7 Sensitivity overturning – A5 Design situation 1 with bolts.

Parameter	Sensitivity index	Scatter plot
k_{bot}	0.93	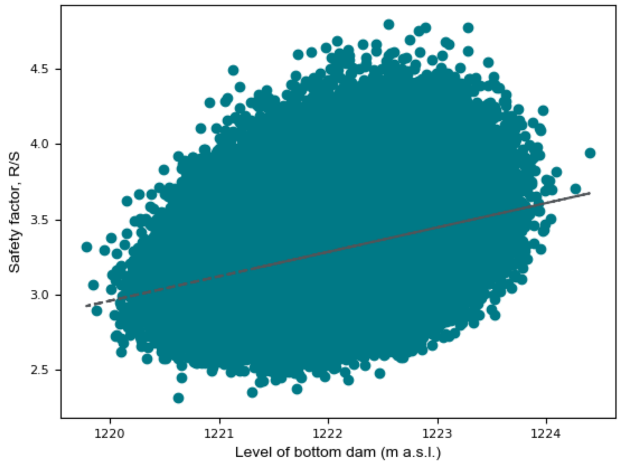
b_{eff2}	0.02	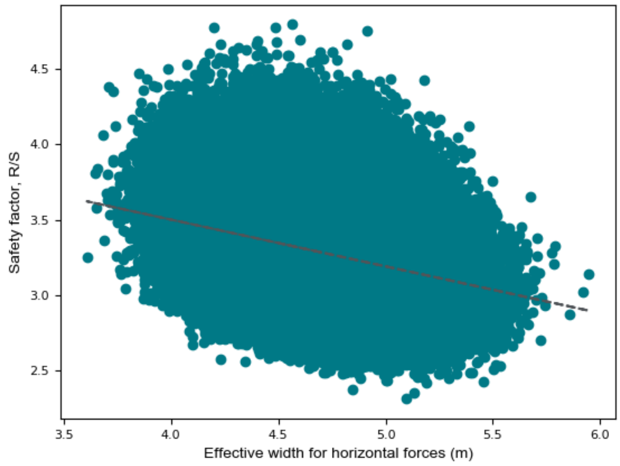
γ_b	0.01	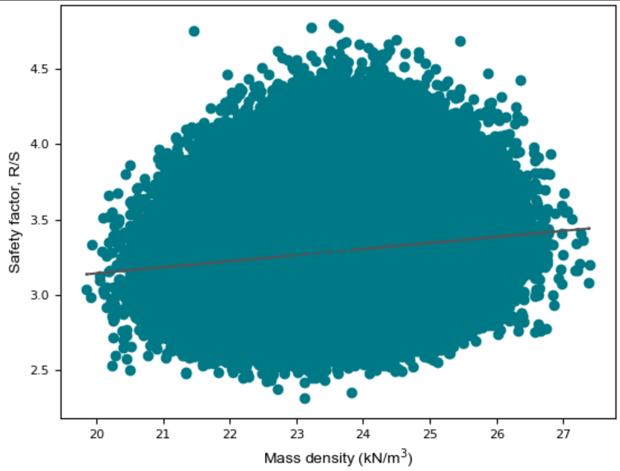

f_y	0.01	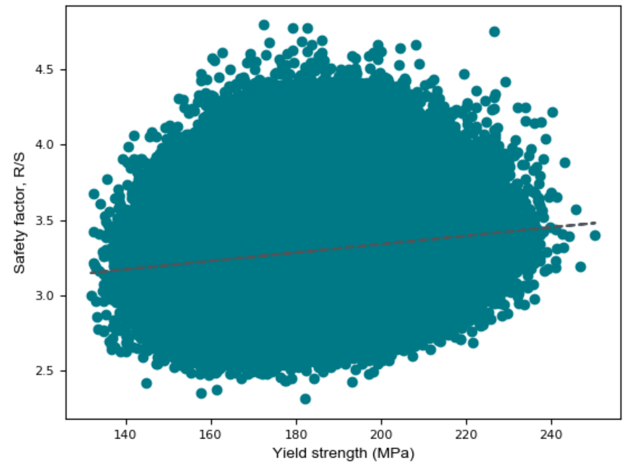
b_{eff1}	0.01	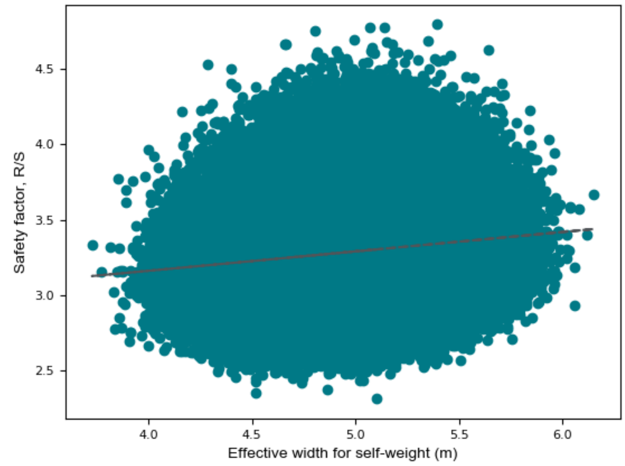
α	0.01	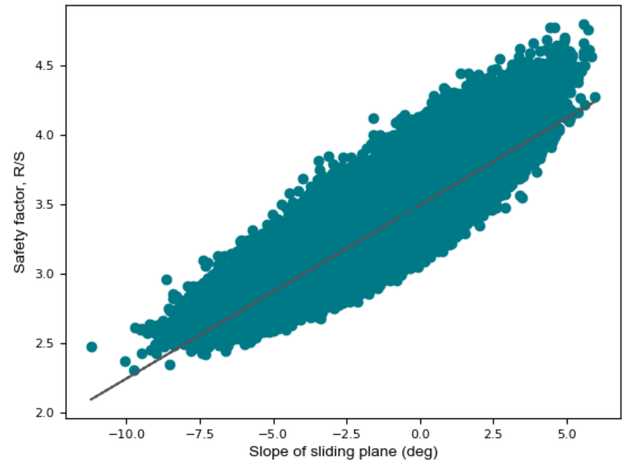

h_o/v_o	0.00	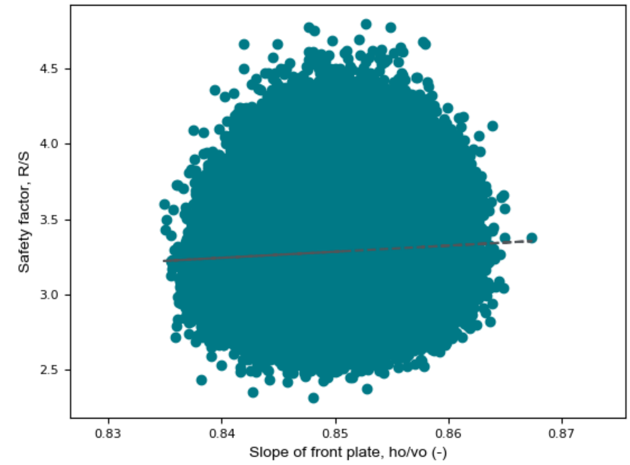

Table 8.8 Sensitivity overturning – A8 Design situation 2 with bolts.

Parameter	Sensitivity index	Scatter plot
k_{bot}	0.74	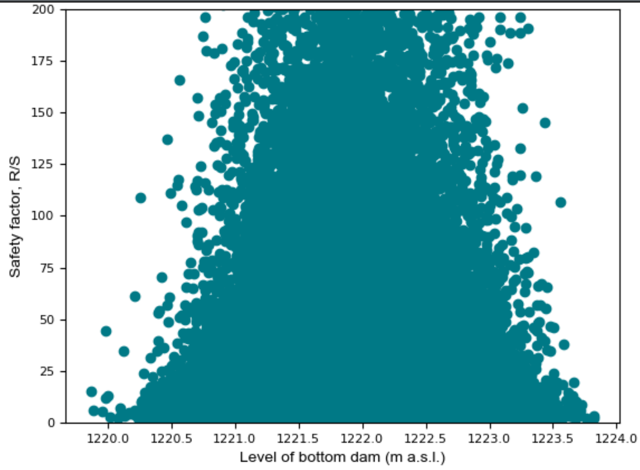
q_i	0.13	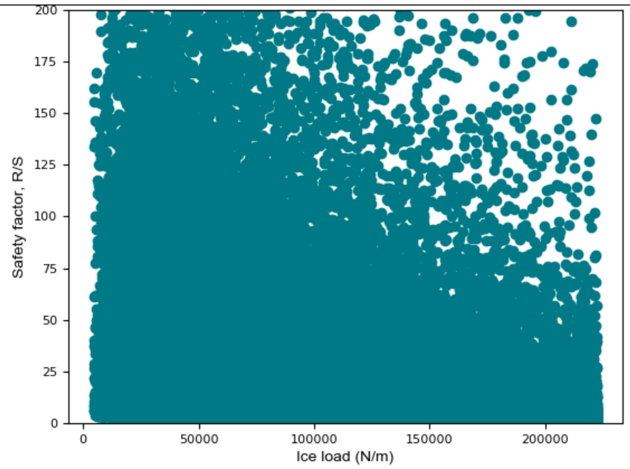

k_w	0.06	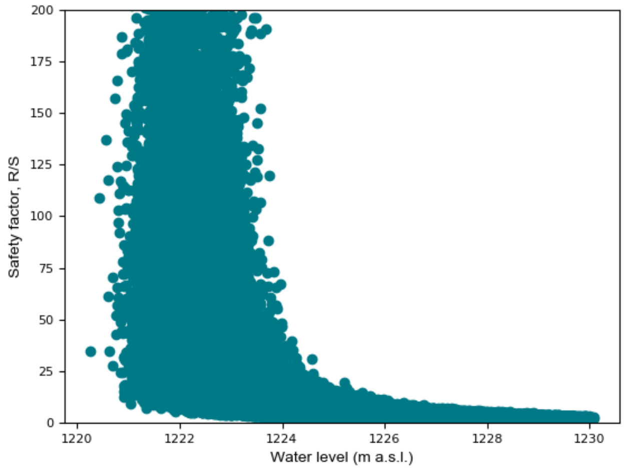
f_y	0.04	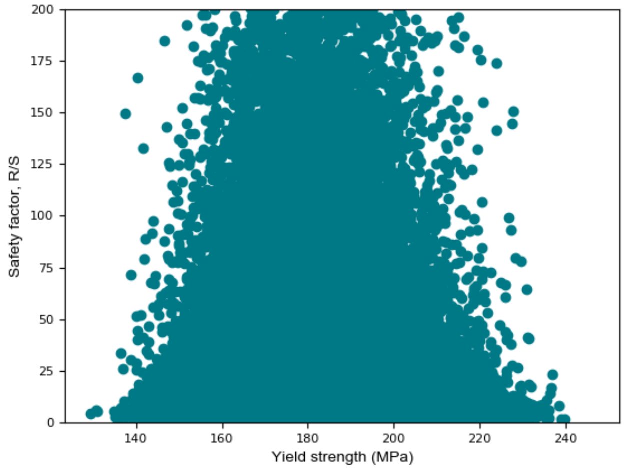
b_{eff1}	0.03	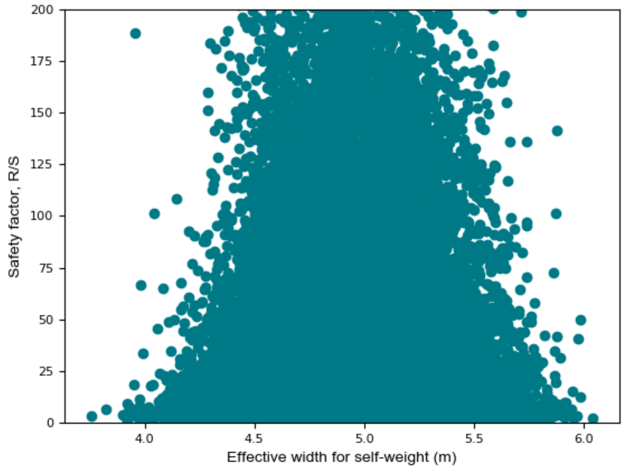

γ_b	0.03	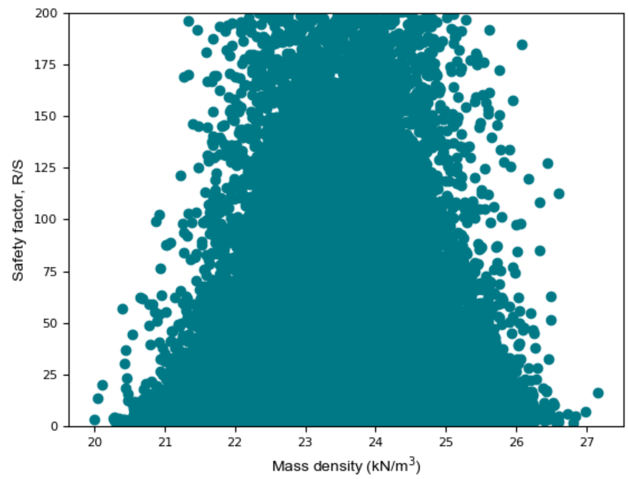
α	0.01	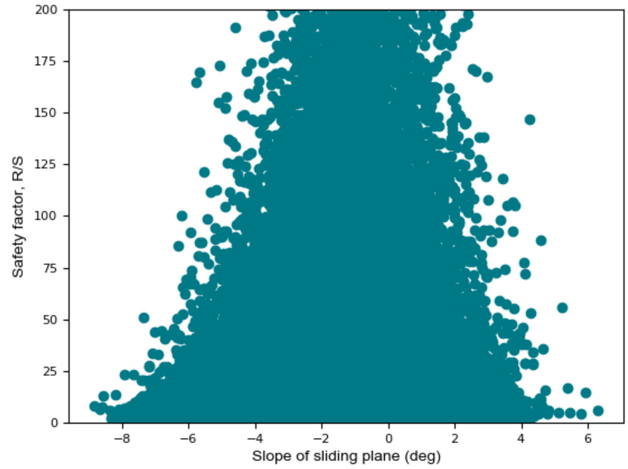
h_o/v_o	0.00	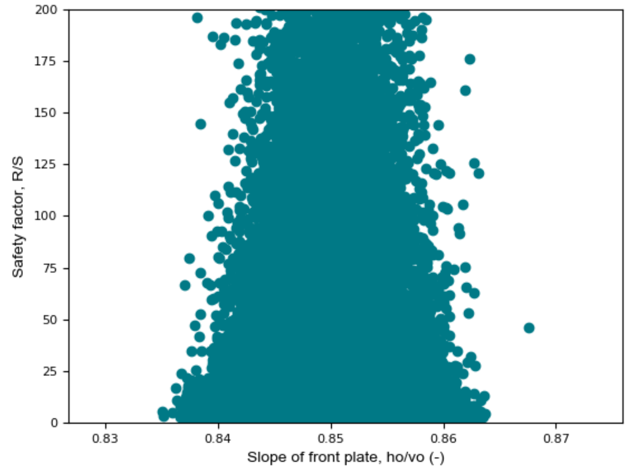

b_{eff2}	0.00	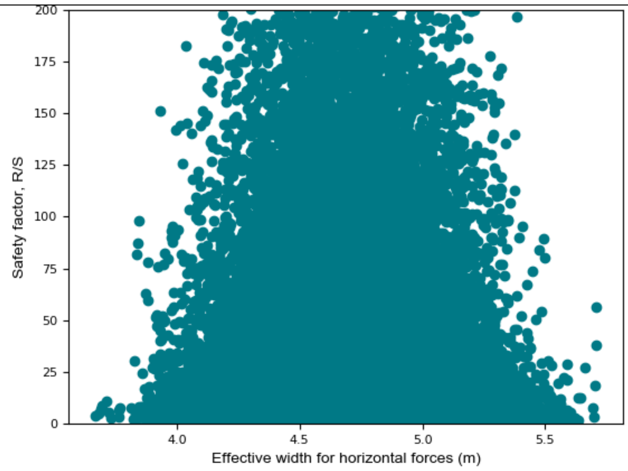

Table 8.9 Sensitivity overturning – A11 Design situation 3 with bolts.

Parameter	Sensitivity index	Scatter plot
k_{bot}	0.92	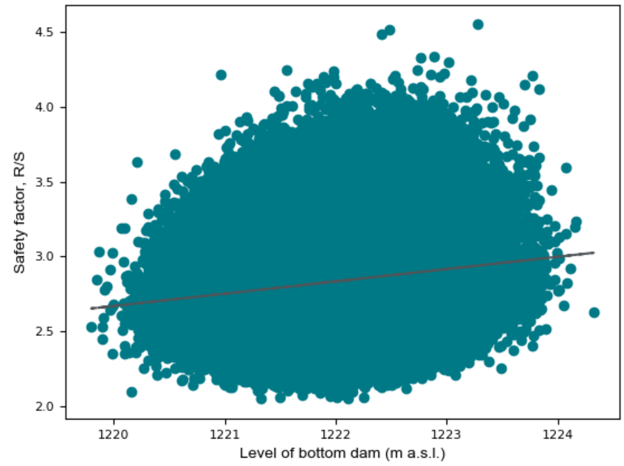
α	0.03	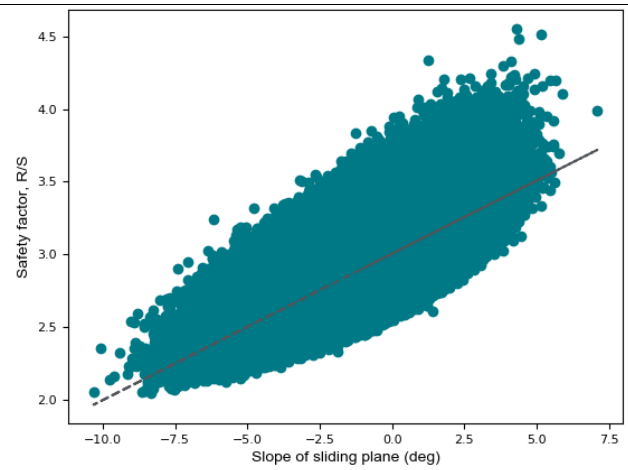

b_{eff2}	0.02	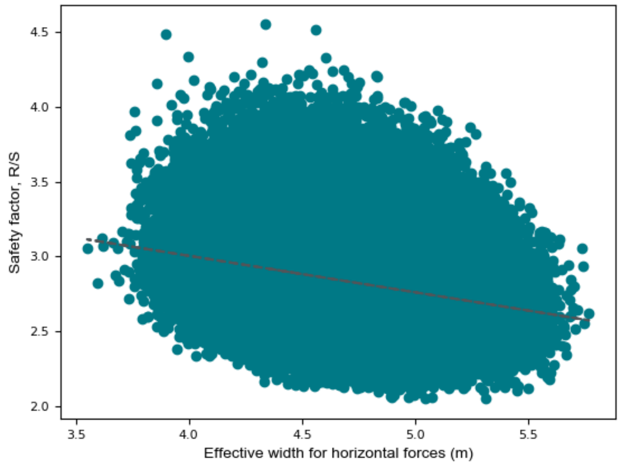
k_w	0.01	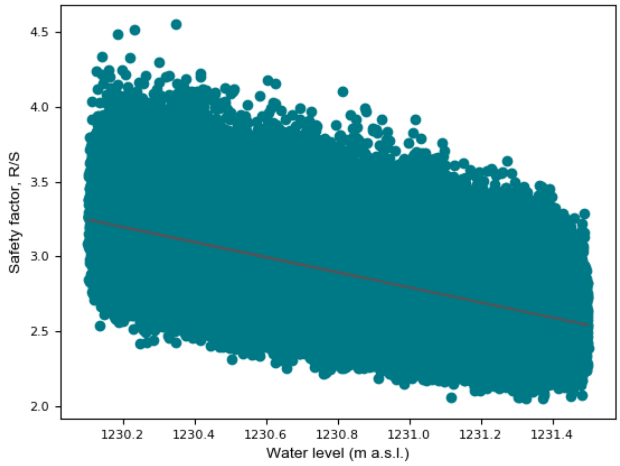
f_y	0.01	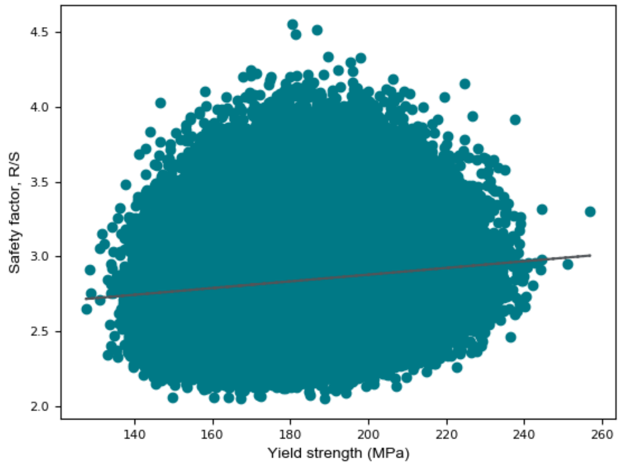

b_{eff1}	0.01	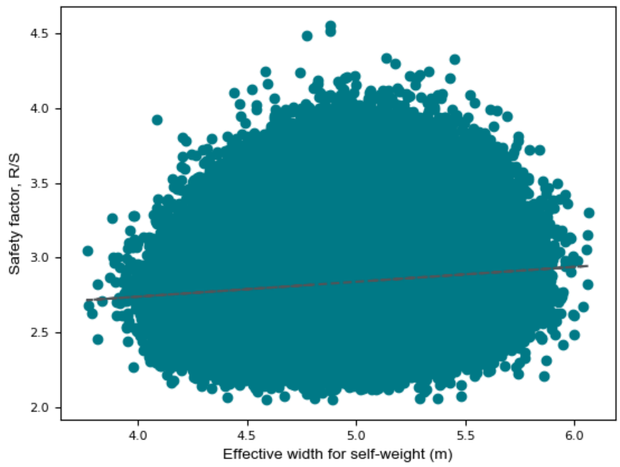
γ_b	0.01	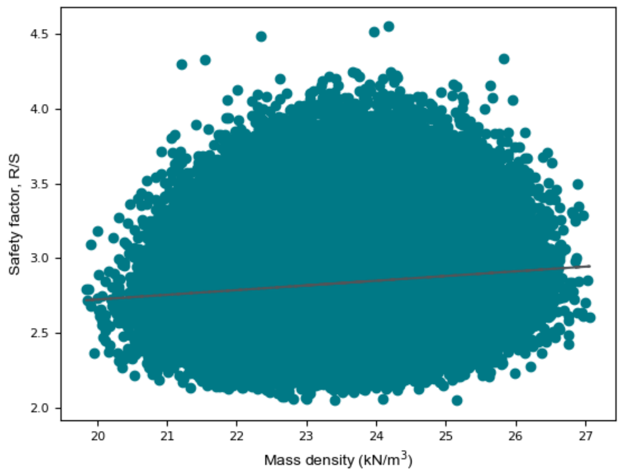
h_o/v_o	0.00	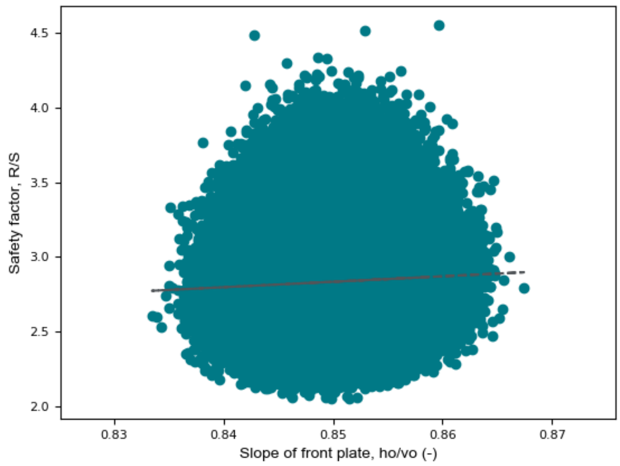

APPENDIX B REPORT – DAM EIKREBEKKEN

REPORT

DSHP – ENERGI NORGE AS, PHASE II
PROBABILISTIC ANALYSIS OF EIKREBEKKEN

REPORT

Project name:

DSHP – ENERGI NORGE AS, PHASE II

Document name:

PROBABILISTIC ANALYSIS OF EIKREBEKKEN

Project number:	12372
Document number:	12372-OO-R-001
Date:	14.01.2020
Revision:	01
Number of pages:	84
Prepared by:	Johannes Osorio Mydland
Controlled by:	Thomas Konow
Approved by:	Thomas Konow

Revision	Date	Reason for Issue	Prep. by	Contr. by	Appr. by
01	2020.01.13	First version	JOM	THK	THK

Table of Content

Appendix

A) Random variables used in calculations

B) Interpretation of measured data

1 SUMMARY

This report is a continuation of the sub-project Probabilistic Analyses of dams Phase II and is a part of the project "Damsikkerhet i et helhetlig perspektiv" (DSHP). The following report contains the study and results from probabilistic analyses done by Dr. Techn. Olav Olsen of dam Eikrebekken and was carried out during the fall 2019 on behalf of Energy Norway and E-CO Energy.

Previous work indicates that probabilistic analyses is a viable method for documenting capacity with regards to stability of dams. However, further work is required before it can be accepted as an alternative method for dams. Firstly, a specified reliability must be established in order to document adequate capacity, either defined as a reliability index β or probability of failure p_f. Secondly, the underlaying assumptions related to this specified reliability must also be determined.

Experience from the work carried out in 2017 of dam Reinoksvatn showed that the method proposed for calculating the applied water load (i.e. design water levels) in Probabilistic Model code for Concrete dams (PMCD) is not suitable for all dams. Furthermore, the stochastic modelling of ice load was also an issue due to limited capability of the software, which in turn lead to a simplification of the ice load.

The main motivation of this report was to test the underlaying assumptions with regards to probabilistic modelling and how it reflected the reliability of dams. The second motivation was to show how testing and increased knowledge, i.e. less uncertainty, can improve the calculated structural reliability.

Both FORM and Crude Monte Carlo analyses has been performed for two cross-sections with different assumptions regarding the stochastic modelling of ice load, design flood level and the contribution from cohesion and rock bolts.

A simplified base case was established based on deterministic analyses and was used as a reference when comparing probabilistic results. Due to initial conservative assumptions, the calculated reliability index for the base case, and thereby most cases, was rather low and in the order of $\beta \approx 2$, with sliding as a failure mechanism. It was also shown that by reducing the uncertainty due to hypothetical testing and new assumptions of the water load, the calculated reliability index for sliding was increased to roughly $\beta \approx 4$. It's also believed that it can be further increased by accounting for macro-asperity, foundation roughness and shear capacity due to a upstream slab trench in the foundation.

For further work it's in generally recommended to establish a common methodology for handling water load and ice load that it's more suitable for all dams.

For the slab buttress dam at Eikrebekken, the probabilistic calculations indicate that assumptions for sliding capacity is the most important single variable. Further study of the sliding capacity is therefore recommended.

2 DAM DESCRIPTION – EIKREBEKKEN

2.1 Location

The dam is located at the border of Hemsedal and Gol municipality in Norway as shown in Figure 2-1. Both municipalities are a part of the region Hallingdal which is one of the major valleys of eastern Norway. The valley is typically U-shaped and renown for skiing during the winter. Key data is summarized in Table 2-1.

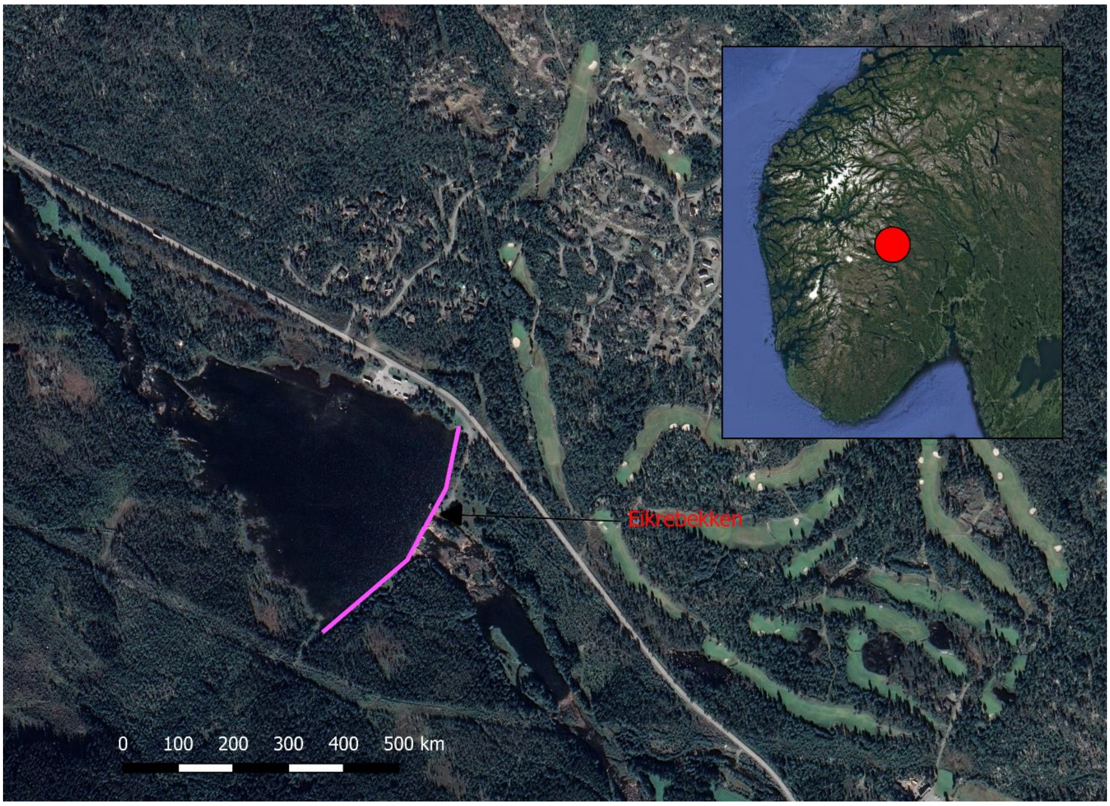

> *Figure 2-1: Overview location of Eikrebekken (Google Maps).*

The dam is located on the river Hemsil with a catchment area of about 896 km² in total. The largest reservoir in the area is Flævatn. Flævatn is also intake for the powerplant Hemsil I, that discharges to Eikrebekken reservoir, as indicated in Figure 2-2. Other reservoirs in the catchment area are the lakes Vavatn and Flatsjø. This implies that the inflow of water at Eikrebekken is heavily influenced by the regulation of upstream reservoirs. This further implies that the structural reliability of the dam is affected by the water regulation of upstream reservoirs and can in principle be improved or worsened depending on the regulation.

Based on the location and the characteristics of the catchment area, it's hypothesis that flooding will mostly occur due to extreme rainfall or rain combined with snow melting. This is further discussed in Appendix B;.

> *Table 2-1: Key data of Eikrebekken dam (Norconsult, 2004)*

Reservoir	
Catchment area	896 km²
HRV	566.0 m a.s.l.
Reservoir volume	0.7 mill m³
Dam length	~ 583 m
Maximum dam height	~ 12.5 m
Hatches:	
- 2 flood gates (radial gates)	$b\ x\ h = 9.4m\ \times 4.7m$
- 1 bottom drainage (slide gate)	$b\ x\ h = 3.0m\ \times 2.1m$
- 2 intake hatches (slide gates)	$b\ x\ h = 1.7m\ \times 3.5m$
Building year	1958-59
Consequence Class (OED, 2009)	2

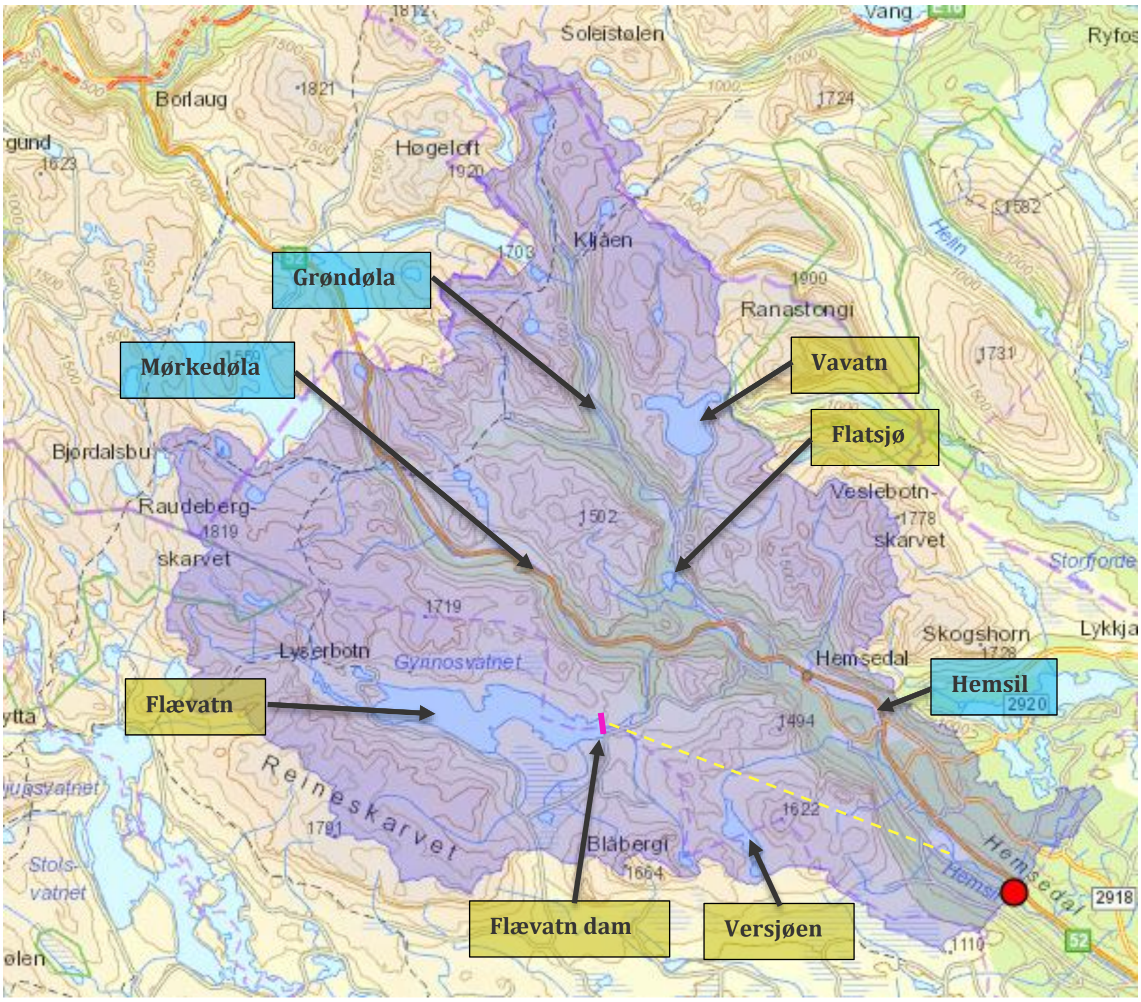

> *Figure 2-2: Catchment area tied to Eikrebekken (NEVINA, 10.12.2019).*

2.2 Construction

The dam is a conventional concrete slab buttress dam constructed between 1958-59. On each side of the buttress dam, there is a concrete gravity section between the slab buttress and then an embankment dam at the far end to the abutment. Due to time restraint the focus in this report is on two selected buttress sections in the dam. However, the overall structural reliability of the dam should account for every part of section in a complete analysis. I.e. every buttress plus the gravity and embankment sections should be included in a total analysis.

For a slab buttress dam, it's often assumed that once a buttress fails, the whole dam section fails. This assumption implies that there is little redundancy in the structure. This is of the type "weakest link" concept and is modelled as a series system with an overall failure probability of $p_f = P(F_1 \cup F_2 \cup \ldots \cup F_N)$, where F_i is the failure event of one section. The lower bound of reliability can be found by assuming that failures are uncorrelated $p_f = 1 - \prod_{i=1}^{n}(1 - P(F_i))$, and the upper bound of reliability is determined from assuming fully correlated system, $p_f = \max P(F_i)$. Since the sections are assumed to be somewhat correlated, this will improve the reliability. Thus, the overall reliability will never be better than the section with the lowest reliability.

> *Table 2-2: Dam components and characteristics described in Norwegian (Norconsult, 2004).*

	Damtype	Lengde (m)	Topp dam (kt)	Anmerkninger
Søndre del (Høyre del)	Fyllingsdam Massivdam Platedam Overløpsdam	12 2,0 183,75 35,0	567,5 567,3 567,3 566,0	Høyde ved topp tetning Høyde ved topp brystning Høyde ved topp brystning Høyde på overløpskrone.
Midtre del	Overløpsdam Flomløp Overløpsdam m/bunnløp Platedam m/inntak	45,0 20,0 30,0 50,0	566,0 ca. 566,6 566,0 567,3	Høyde på overløpskrone Høyde på topp luker Høyde på overløpskrone Høyde ved topp brystning
Nordre del (Venstre del)	Platedam Massivdam Fyllingsdam	118,75 2,0 ca.85	567,3 567,3 567,3	Høyde ved topp brystning Høyde ved topp brystning Høyde ved topp tetning

In Table 2-2 the different parts of dam Eikrebekken are listed in Norwegian. The plan overview of the dam is shown below in Figure 2-3. The dam is mainly a concrete slab buttress structure with the following three different cross sections along the dam: (i) section without spillway, (ii) overflow spillway and (iii) the gated spillway. The buttresses are placed at intervals of c/c 5 m. The slab joints are placed in every other hollow section where the slab moment is zero. The slab thickness is 300 mm at the top and increases with 30 mm every vertical meter. The slab has an inclination of vertical to horizontal ratio equal to 5:4.

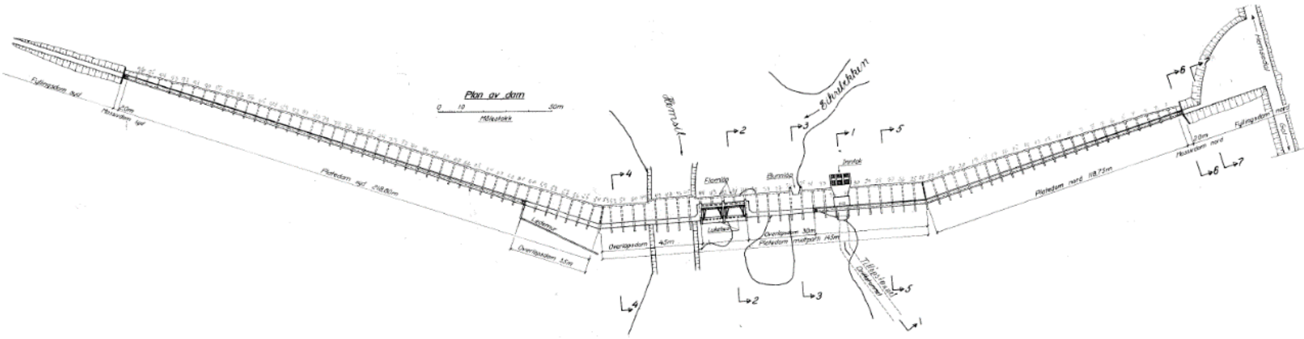

> *Figure 2-3: Plan overview of Eikrebekken – Drawing F-7776.*

It's assumed that the slab transfers the exterior load, water pressure, directly to the buttresses. I.e. no forces are transferred from the slab to the bedrock trench. Note that the trench will increase the horizontal capacity but is not included in the analyses. Initially three cross sections were selected to study the safety level. Due to difficulties with parametrizing the hydrostatic loads at the radial gate caused by gate failure, it was not further studied. Besides, establishing the probability of gate failure is difficult and thus the methodology would be similar as the case of DFV without rock bolts by assuming a failed state. See section 4.4, 5.2 and 5.5 for calculation and comparison with and without rock bolts.

The cross-section P.47 (overflow spillway and bridge), and P.55 (general cross-section) were selected for probabilistic analyses. The geometry is shown in Figure 2-4. The buttress is a concrete wall with a thickness of 300 mm in the top and increases with 22 mm every vertical meter. On the downstream side there is prefabricated vertical "frost" wall resting on the bedrock to reduce effects of large temperature variations throughout the dam, particularly during the winter season. Inside the dam, buttresses have cut-outs for inspections galleries in two levels.

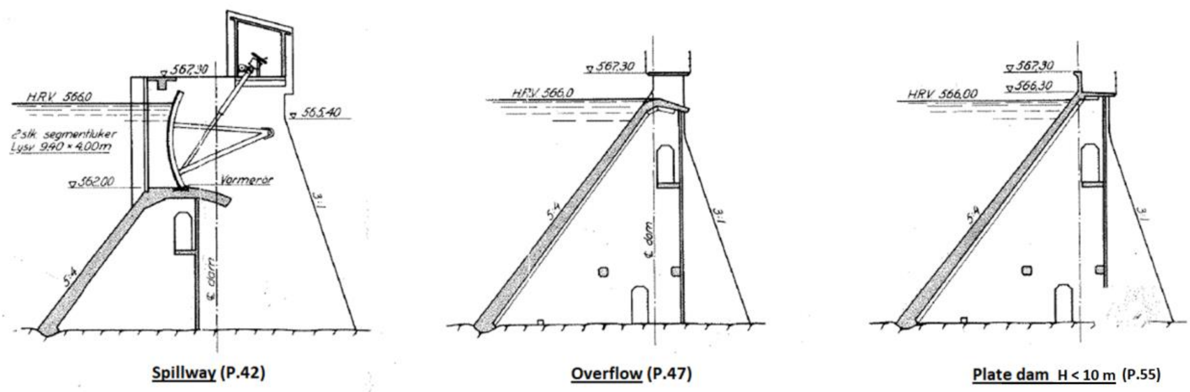

> *Figure 2-4: Cross section used in deterministic and probabilistic analyses.*

Due to the choice of calculation model, which is described in 4.1, the parametrization of geometry is limited. To improve the geometry of P.47, a CAD model was created to estimate the total volume and centre of gravity of the cross-section. Afterwards the geometry was corrected in the model by adding and subtracting for the uncounted mass and is a source of error in the calculation results. Preferably the correct geometry which accounts for cut-outs, footbridge and etc. will be implemented in the future. The geometry of section P.55 has not been similarly adjusted due to limited time. The geometry used in the analyses are shown Figure 2-5.

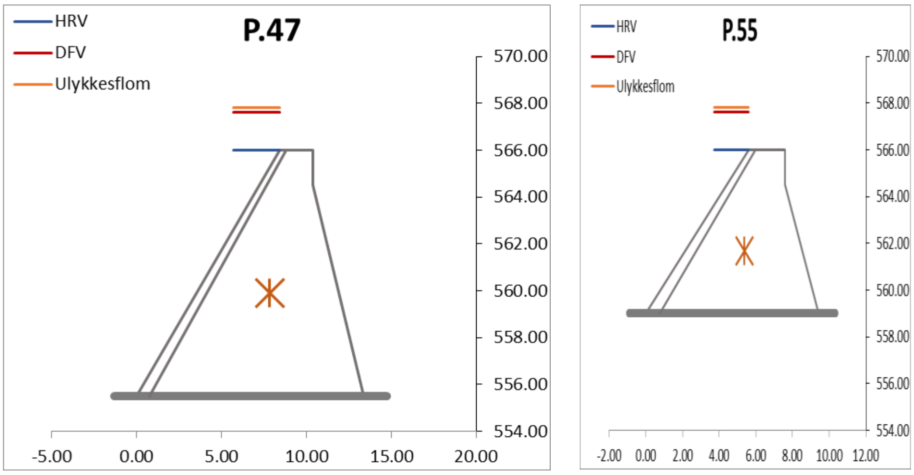

> *Figure 2-5: Geometry of calculation model used in probabilistic analyses.*

The concrete used is C25 in the slab and C20 in the buttresses, while KS40 reinforcment is used in the dam and as rock bolts. St. 37 smooth rebar is used as secondary reinforcement in the construction. The concrete cover is 50 mm in the slab and otherwise 40 mm.

It's indicated in the blue prints that the bedrock is especially shaped for good foundation, and it's stated in the reassessment report (Norconsult, 2004) that the bedrock is of good quality.

2.3 Flood calculations

The results from the newest flood calculations for Hemsil 2 (Multiconsult, 2014) is shown in Table 2-3. It was determined from the flood inundation mapping by NVE of the river.

> *Table 2-3: Design flood determined in 2014 (Multiconsult, 2014).*

Flood situation	Inflow [m³/s]	Discharge flow [m³/s]	Water level [m a.s.l]
Q_{1000}	875	872	567.61
$Q_{PMF} = 1.5 \times Q_{1000}$	1206	1201	567.81
Flood gate failure	875	872	567.73

The area parameters used in the hydrological simulations are shown in Table 2-4, and the parameters used in the recommended flood frequency analyses (one day duration) are shown in Table 2-5.

> *Table 2-4: Catchment area parameters used in simulation (Multiconsult, 2014).*

	Eikrebekken
A [km²]	334,6
H_{25} [m]	1361
H_{75} [m]	882
dH [m]	479
L_F [km]	44,3
H_L [m/km]	10,8
A_{SE} %	0,02
q_N [l/skm²]	23,8
K1 [1/h]	0,108
K2 [1/h]	0,029
T [mm]	14

> *Table 2-5: Recommended data series for flood frequency calculations (Multiconsult, 2014).*

Name	ID	Period	Area [km²]	Distribution	Q_M [m³/s]	Q_M [l/s/km²]	Q_{500}/ Q_M	Q_{1000}/ Q_M
Storeskar	12.215	1987-2010	120	EV1 (Gumbel)	36.5	304.5	2.7	2.9

2.3.1 Spillway capacity

Errors was observed in the spillway capacity curves reported from Multiconsult both in the equations and the calculated results. An attempt was made to recalculate the spillway capacity according to the guidelines (NVE, 2005). However, the calculations have not been verified.

The flood capacity is determined by water level, operation of flood gates, overflow spillway capacity (110 m long), and overtopping of the dam crest. Results from the flood calculations are shown together with the capacity in Figure 2-6. From the curve one can see that large increase in the reservoir inflow does not necessarily lead to large increase in water level due to the reservoir flood discharge regulated by the floodgates.

The spillway discharge curve is used in the calculations in an attempt to calculate the extreme value distribution for the water level based on measured data. The reservoir is small compared to the inflow and discharge. Routing of the inflow can therefore be neglected.

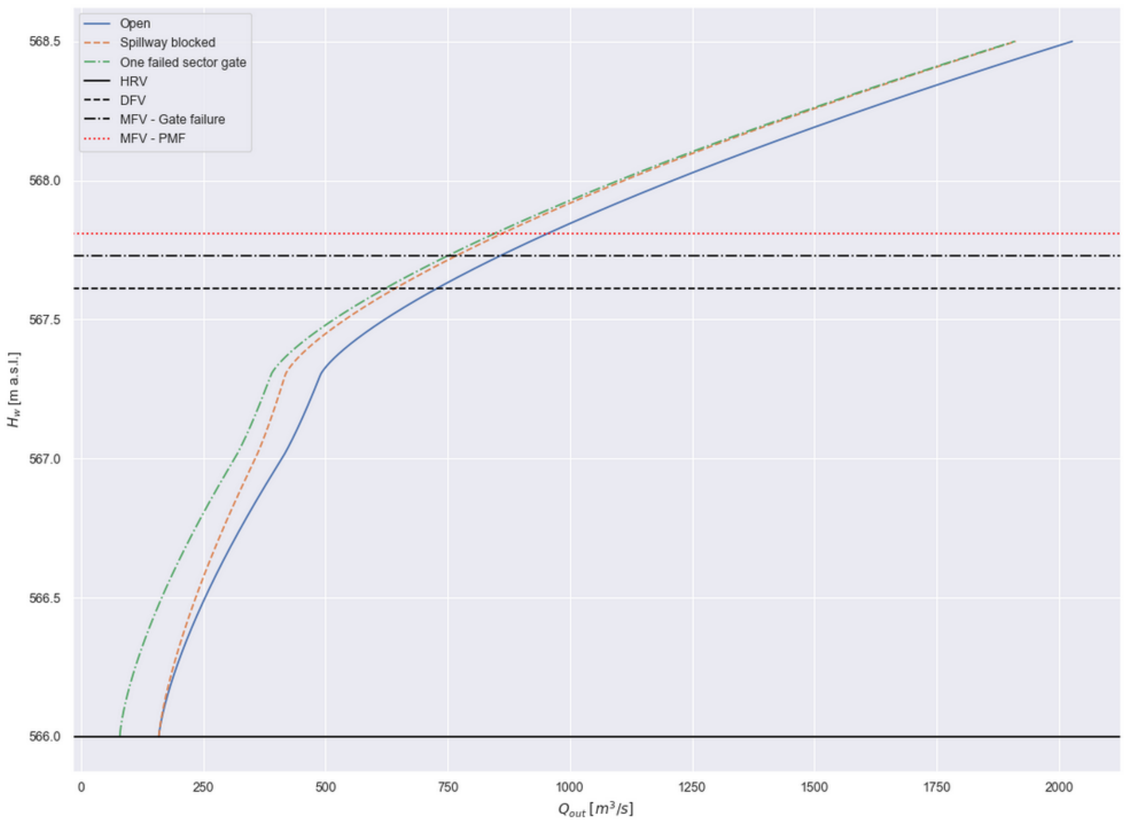

> *Figure 2-6: Simplified spillway capacity used in calculations.*

2.4 Deterministic calculations

For comparison some initial deterministic calculations were performed for P.47 and P.55. This was also done to compare the results with previous stability calculations from the reassessment of the dam (Norconsult, 2004).

The most notable change since the reassessment is that the DFV has increased from 567.05 m to 567.61 m. Some variation in the results can also be expected due to different modelling of the geometry and possible incline rock bolts. The results for P.47 are summarized below. In the case of P.47 where the dam height is over 7 m, the safety factor with bolts is also calculated for comparison with probabilistic analyses.

> *Table 2-6: Deterministic results of global equilibrium of P.47 (10.5m) no bolts - Dr. Techn. Olav Olsen*

LIMIT STATE			OVERTURNING		SLIDING	
			Safety factor	Requirement	Safety factor	Requirement
ULS:	HRV + ice load		1.78	1.40	1.28	1.4
ULS:	DFV	Q_{1000}	2.07	1.40	1.37	1.4
ALS:	MFV	Q_{PMF}	2.04	1.30	1.35	1.1

> *Table 2-7: Deterministic results of global equilibrium of P.47 (10.5m) no bolts - Norconsult*

LIMIT STATE			OVERTURNING		SLIDING	
			Safety factor	Requirement	Safety factor	Requirement
ULS:	HRV + ice load		1.65	1.40	1.19	1.4
ULS:	DFV	Q_{1000}	2.01	1.40	1.32	1.4
ALS:	MFV	Q_{PMF}	1.86	1.30	1.25	1.1

> *Table 2-8: Deterministic results of global equilibrium of P.47 (10.5m) with bolts - Dr. Techn. Olav Olsen*

LIMIT STATE			OVERTURNING		SLIDING	
			Safety factor	Requirement	Safety factor	Requirement
ULS:	HRV + ice load		2.01	1.40	1.41	1.4
ULS:	DFV	Q_{1000}	2.30	1.40	1.48	1.4
ALS:	MFV	Q_{PMF}	2.26	1.30	1.46	1.1
ALS:	DFV without bolts	Q_{1000}	2.07	1.10	1.37	1.1

> Table 2-9: Deterministic results of global equilibrium of P.47 (10.5m) with bolts - Norconsult

LIMIT STATE			OVERTURNING		SLIDING	
			Safety factor	Requirement	Safety factor	Requirement
ULS:	HRV + ice load		1.77	1.40	1.38	1.4
ULS:	DFV	Q_{1000}	2.17	1.40	1.55	1.4
ALS:	MFV	Q_{PMF}	2.04	1.30	1.43	1.1
ALS:	DFV without bolts	Q_{1000}	1.98	1.10	1.31	1.1

> Table 2-10: Deterministic results of global equilibrium of P.55 (7m) - Dr. Techn. Olav Olsen

LIMIT STATE			OVERTURNING		SLIDING	
			Safety factor	Requirement	Safety factor	Requirement
ULS:	HRV + ice load		1.76	1.40	1.32	1.4
ULS:	DFV	Q_{1000}	2.32	1.40	1.54	1.4
ALS:	MFV	Q_{PMF}	2.27	1.30	1.51	1.1
ALS:	DFV without bolts	Q_{1000}	1.91	1.10	1.30	1.1

> Table 2-11: Deterministic results of global equilibrium of P.55 (7m) Norconsult

LIMIT STATE			OVERTURNING		SLIDING	
			Safety factor	Requirement	Safety factor	Requirement
ULS:	HRV + ice load		1.60	1.40	1.43	1.4
ULS:	DFV	Q_{1000}	2.32	1.40	1.80	1.4
ALS:	MFV	Q_{PMF}	2.05	1.30	1.60	1.1
ALS:	DFV without bolts	Q_{1000}	1.94	1.10	1.33	1.1

The deterministic results for the load combination of HRV and 100 kN/m ice load is critical with respect to sliding. The friction coefficient is set to 50°, which is the highest value that can be used without proper documentation according to the guidelines (NVE, 2005). As stated in the reassessment, this method is not entirely accurate since the bedrock is especially prepared to increase the friction capacity. Furthermore, the trench in the bedrock where the front slab rests also may increase the sliding capacity if properly accounted for, and this can require documentation by i.e. FEM analysis.

3 PROBABILISTIC INPUT PARAMETERS

3.1 Stochastic loads and return periods

In general loads are random of nature and will vary with time. An example of this is the monthly mean and maximum trends shown in Figure 3-1. Most often the environmental loads exhibit some periodical trend due to seasonal variation. It's thus often common to relate the loads to a 1-year reference period, which is recommended in the PMCD.

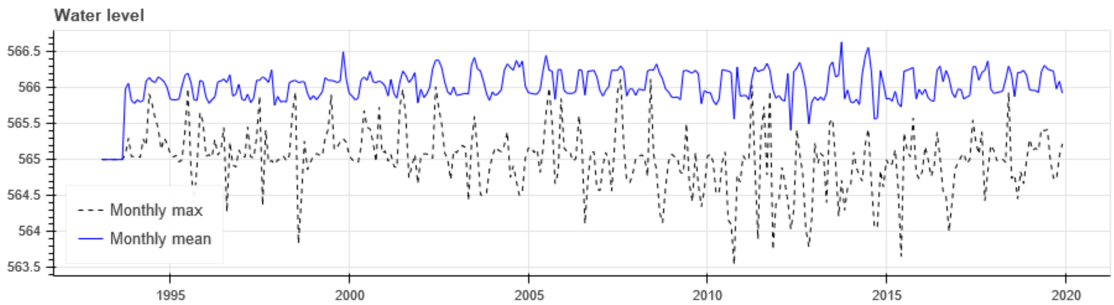

> *Figure 3-1: Monthly mean and maximum trend of the water level at Eikrebekken.*

It's also known that the structural capacity may change with time due to material degradation and general wear and tear. A principal figure of the stochastic time-dependent processes in a reliability calculation are illustrated below in Figure 3-2. Mathematically the probability of failure will thus also vary with time. For simplicity it's here assumed that the capacity R is constant with time, and a time-integrated approach related to return periods is utilized for the load S.

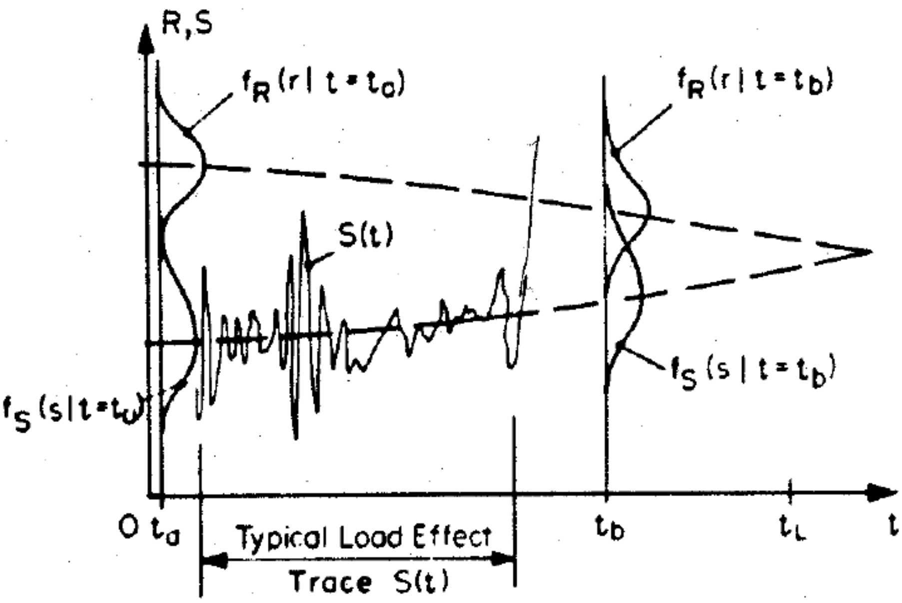

> *Figure 3-2: General time-dependent reliability problem (JCSS, 2000)*

A common approach when estimating the structural reliability is by using extreme value theory. If measurements are available, one can do statistical analysis and determine appropriate stochastic distributions. Alternatively, if a characteristic value is known for a certain return period (from guidelines or regulation), one can try fit stochastic distributions by assuming some spread, as shown in Figure 3-3.

In both cases this will lead to uncertainty when selecting the distribution. One of the major benefits with probabilistic methods is that the uncertainty can be incorporated to such calculations. However, this is a challenge when establishing design code. As discussed in chapter 9.4 (Melchers & Beck, 2018), the code work usually deals with predictions of some possible future. Therefore, reasonable conservative parameters and probability density functions should be used when establishing target values for the reliability.

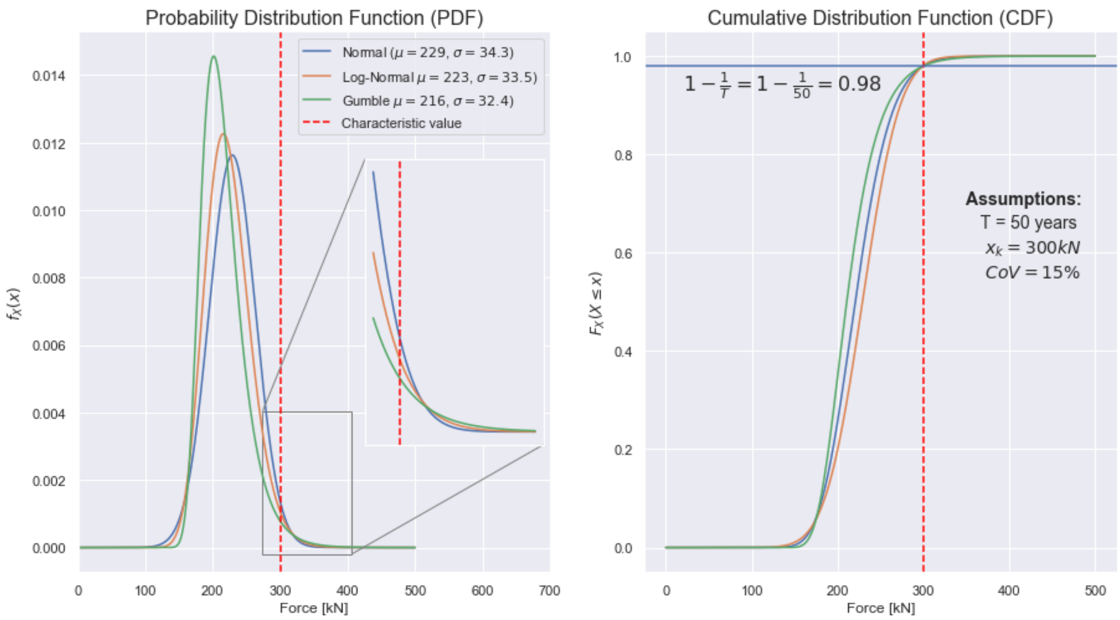

> *Figure 3-3: Stochastic distributions fitted to 50 year return period of an arbitrary characteristic load.*

When evaluating the structural reliability, the tail sensitivity of the external load is often governing for the failure probability. This is a natural outcome of such an analysis due to lack of data at extreme values.

This is a particular challenge with regard to flood calculation in Norway, due to the long return period required by the regulation. The return period is set to T=1000 years for consequence class 2, 3 and 4, and T=500 years for consequence class 1. The statistical chance of observing a flood corresponding to T=100 within 100 years of measurement is merely 63% (NVE, 2011). In most cases the available dataset is either non-existing or much less than 50 years, which is a source for large degree of uncertainty.

3.2 Water level

As the main purpose of a dam is to retain water, special attention should be given to the modelling of the random hydrostatic water load. It's here assumed that the uplift of a dam is fully correlated with the upstream water level and can thus be described by the same parameter, the water column H_w. This is a simplification since, among other, there might be a time lag between the two forces depending on the permeability between the dam and foundation.

Experience from previous probabilistic analysis of the dam Reinoksvatn (Dr. techn. Olav Olsen, 2017) showed that the proposed method in PMCD (Wilde & Johansson, 2016) is not suitable for multi-annual reservoirs. The basic assumption that the water level is at HRV (maximum allowed regulated water level) when considering the yearly maximum water level is false in such cases. This shows that a more generalized method is required in order to take account for individual variations of different dams.

In the case of dam Hensfoss (Norconsult, 2018) normal distribution was used to describe the variation of HRV and DFV (design flood water level). However, this method does not necessarily reflect the structural reliability accurately as described in section 3.1.In both Reinoksvatn and Hensfoss, the measured water level has been interpreted differently and utilized in the probabilistic calculations differently. A generalized approach should accommodate this issue.

Furthermore, it's advantageous that a general method for the water load can easily be combined with other stochastic processes like spillway gate failure and reduced discharge due to blockages. A Norwegian saying is that one accident never comes alone, and experience show that major accidents often is a combination of several abnormal incidents or errors. One example is the failure of Roppa dam, where the commissioning of the dam was delayed. This resulted in a delayed and slow reservoir filling such that the bottom outlet gate was exposed to thawing/freezing effects and thereby damaging the moraine core and foundation. In addition, the dam failure occurred on the morning the 17th of May, which is a national holiday in Norway.

Another desirable effect of a generalized method is the possibility of including effects from regulation of upstream reservoirs, since this can greatly impact the total reliability of a dam, particularly if the dam is dependent on flood gates. One example is by mitigating potential disasters by drawing down major upstream reservoirs prior to heavy rainfall. This is generally a requirement in the operating license but is not taken into account in the flood calculations.

Initially, for simplicity normal distribution with a high variance was assumed for HRV, DFV and MFV in the probabilistic analyses. The purpose was to study the impact on the structural reliability and later improving the results by incorporating new knowledge, i.e. reducing the uncertainty. Measured water level and water discharge from Eikrebekken has been studied and interpreted. Based on the recorded measurements an attempt was made to establish an extreme value distribution for the water level based on the back calculated maximum water inflow (Hydra) and spillway capacity.

3.2.1 HRV

The highest regulated water level is here referred to with the Norwegian acronym HRV. Similarly, the lowest regulated water level is referred to as LRV. These water levels are defined in the licence for the reservoir and defines the water level interval for normal operation. The average water level during operation will also depend on the type of reservoir. In the case of multi-annual reservoir, the water level is generally lower than HRV. This is the case for i.e. Reinoksvatn (Dr. techn. Olav Olsen, 2017). In the case of a run-of-river hydro power plants the water level can be fairly constant around HRV in order to ensure maximum efficiency and output.

The defined water level at HRV is of large importance when evaluating the safety of a dam. The Norwegian dam safety regulation states that in flood calculations the initial water level shall be set to either HRV or the maximum water level if HRV is not defined. Furthermore, the HRV is commonly used in stability calculations as a permanent water level and combined with ice pressure. These assumptions can in certain cases be very conservative, especially with respect to flood routing since regulation of the upstream watercourse is completely ignored. In these cases, the design flood based on a 1000-year precipitation will have much lower return period than 1000-years flood. This implies that the design flood will have different return periods for different dam, i.e. the design criteria for dams are not consistent.

For the initial calculations the variance was subjectively assumed to be $\sigma = 1.415\ m$ by the analyst, with a mean value of HRV, $\mu = 566\ m.a.s.l.$ In retrospect it turns out that the variance is extremely unrealistic. However, the initial assumption is a great example of how ignorance, inexperience and general lack of knowledge influences the calculated probability of failure. This example illustrates the sensitivity and importance of spillway capacity versus the increase in water level.

The data received from Eikrebekken shows that the average water level is between 566 and 564 m.a.sl. with an average approximately 1m below HRV as shown below in Figure 3-4. The water discharge is determined by the spillways (110 m long overflow spillway and two flood gates) and the discharge through the power plant. In 2005 and 2006 the generators were upgraded which can be seen from Figure 3-5.

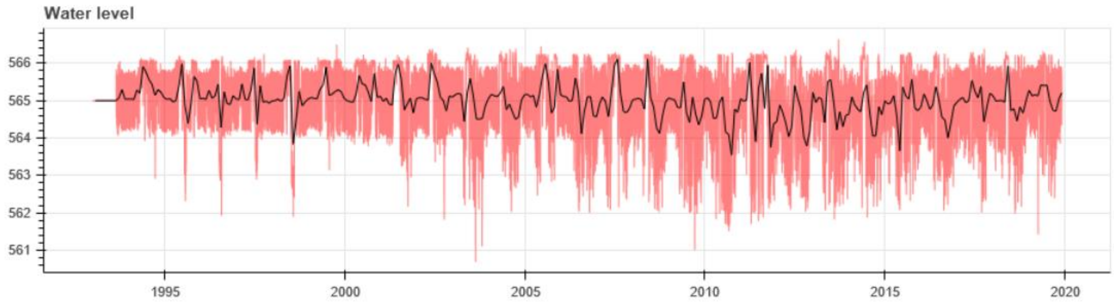

> *Figure 3-4: Monthly average water level from 1993-2020.*

Figure 3-5 shows a bimodal distribution which is often the cause of two processes occurring. In this case the first peak shows that the water level is normally around 565 m a.s.l with some variance and is mainly controlled by the water consumption of the power plant. The second peak represents the incidents where flooding occurs. The flood gates are programmed to open when the water level reaches 566.18 m a.s.l. and will then try to keep this water level.

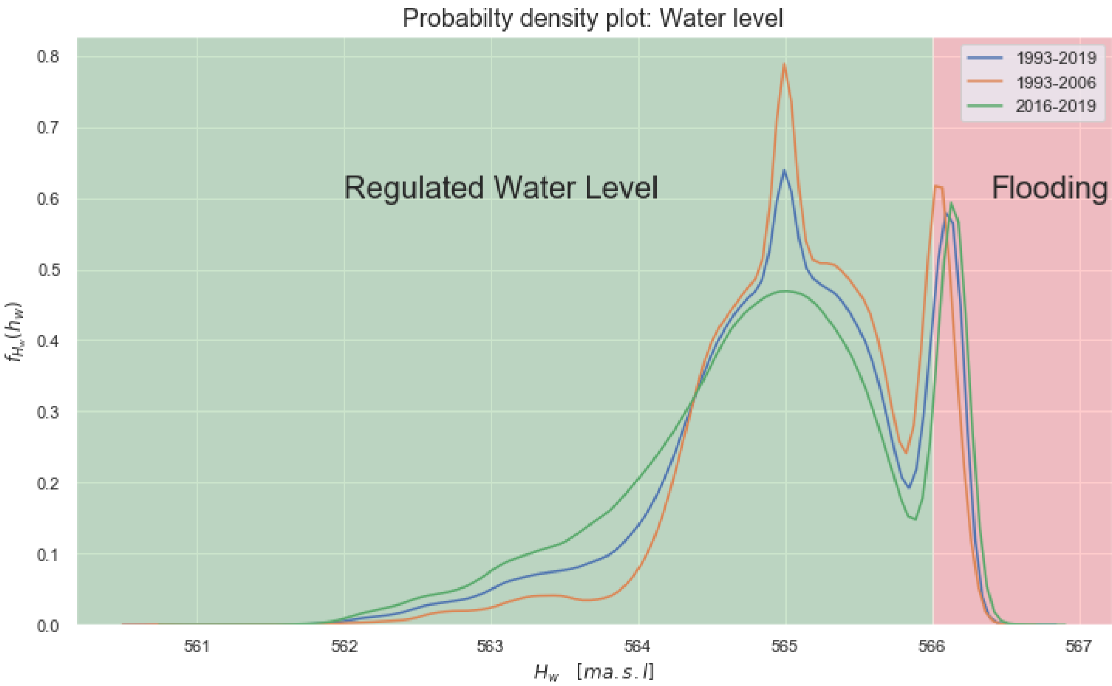

> *Figure 3-5: PDF of water level during the recorded time periods.*

Similarly by looking at the monthly mean (black curve in Figure 3-4) one can construct a histogram for the average water level which is shown in Figure 3-6. The first two moments, μ and σ, of the dataset gives a mean value of 564.88 $m\ a.s.l$ and a variance of 0.46 m, which is considerably lower than the once used in the initial calculations (HRV). One can also observe in the figure that the dataset is not entirely symmetric, thus causing some deviation when comparing with a corresponding normal distribution. Due to time-restraint these values have not been used in updated calculations and is believed to considerably decrease the failure probability for load case II, "HRV + Ice load" (see section 4.4).

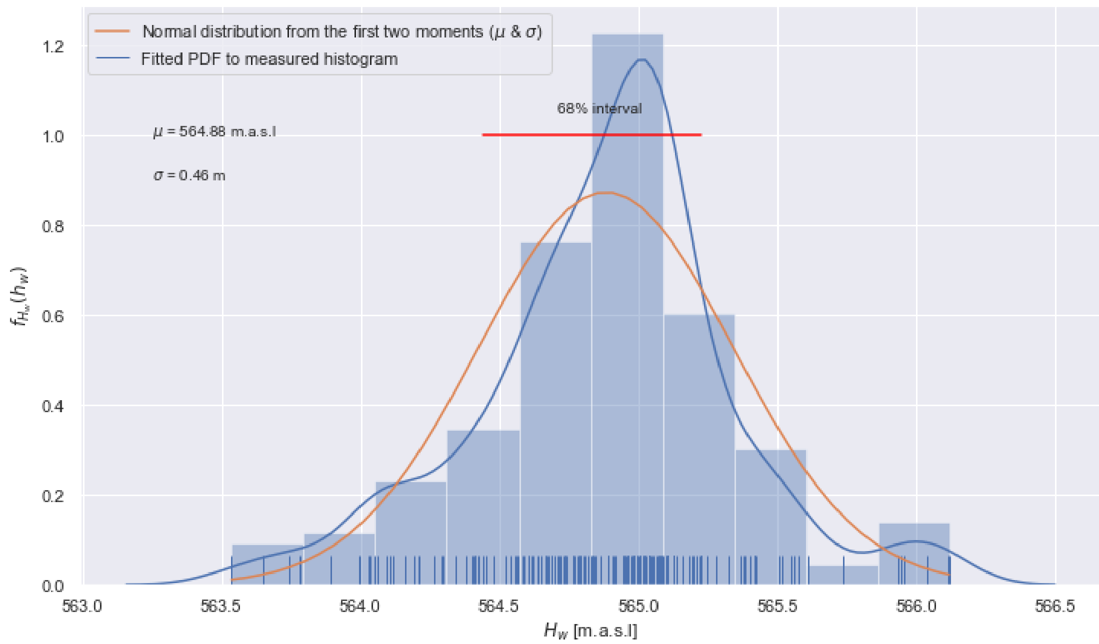

Figure 3-6: Monthly average of water level.

3.2.2 DFV

In deterministic design the characteristic hydrostatic water level during flooding is calculated for a given duration by defining the design inflow flood, Q_{DIM} and the spillway capacity. The variable Q_{DIM} is connected to the return period defined by the consequence class of the dam. It's the task of a hydrologist to determine the appropriate value. This is associated with a large source of uncertainty and a correct estimate of the design flood is therefore extremely challenging.

The guidelines for flood calculation (NVE, 2011) suggest several methods for estimating this value (frequency analyses, regional analyses, precipitation-discharge models, etc.). Often the major challenge is to acquire appropriate measurements and data to accurately evaluate the possible flood size for a given area.

Ideally the uncertainty from flood calculations should be incorporated in the probabilistic analyses. The easiest solution is to use the stochastic parameters and accompanying distributions determined from a flood frequency analysis. In addition to possible lack of representative data, the uncertainty due to large return periods is also a major challenge. Figure 3-7 shows the best fit of four different distributions using L-moments and Maximum Likelihood. As can be seen in the figure, the different methods deviate considerably at large return periods.

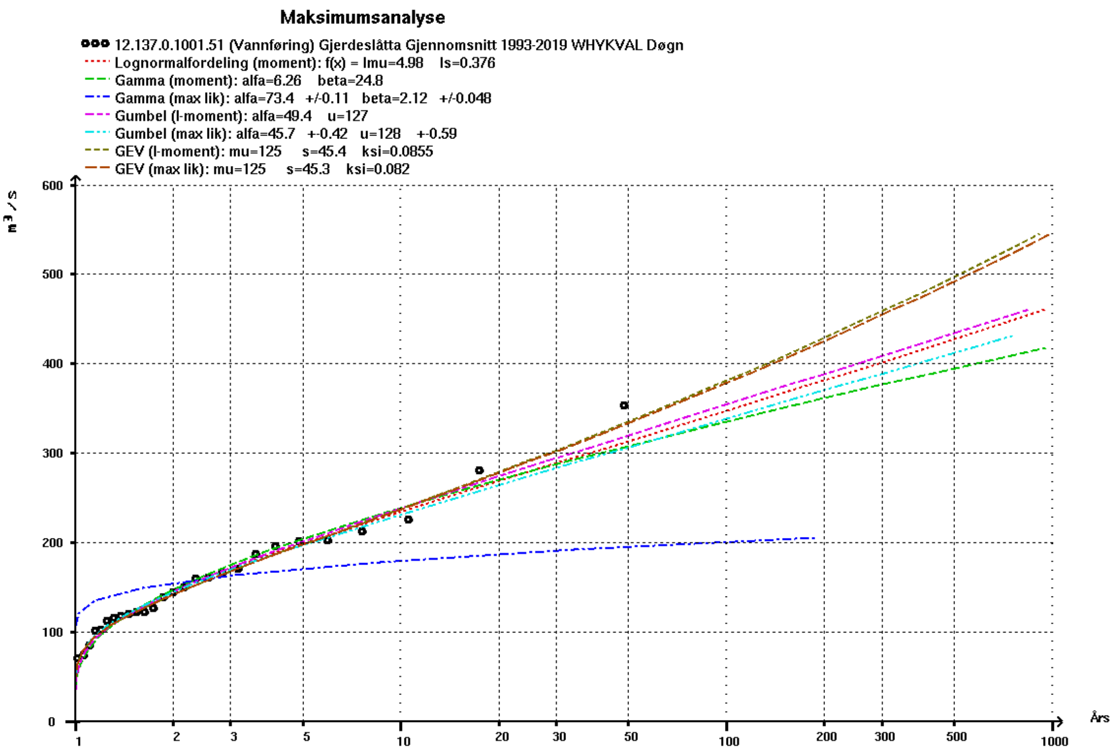

> *Figure 3-7: Best fit of different distributions using L-moments and Maximum Likelihood methods.*

Another possible solution for determining the design inflow flood can be done by using a hydrological model, which ideally is calibrated to measurements in field. This can be constructed in several ways and no preferred method is suggested here. The benefit of such a model is that different scenarios of precipitation can then be simulated, and the total response can afterwards be used to statistically evaluate the design flood with the overall uncertainty associated with the method of calculation.

For the initial calculations a normal distribution $\mathcal{N}(\mu = 567.61, \sigma = 2.84)$ has been used in the probabilistic analyses, which is highly unrealistic variance. In order to improve the calculations, an attempt was made to establish an extreme value distribution for the water level during flooding.

The extreme flood level was determined by firstly assuming that the reservoir inflow is approximately the same as the outflow. Note that this is only valid for small reservoirs, which is the case here. The outflow is the sum of spillways and power plant discharge as shown in Figure 3-8. Secondly, extreme value analysis was afterwards performed on the reservoir inflow series in Hydra (NVE software) to fit different distributions which is shown in Figure 3-7. As a proof of concept, the Gumbel distribution based on maximum likelihood was selected in order to further evaluate the extreme distribution of the water level, with the input parameters $\alpha = 45.7$ and $u = 128$.

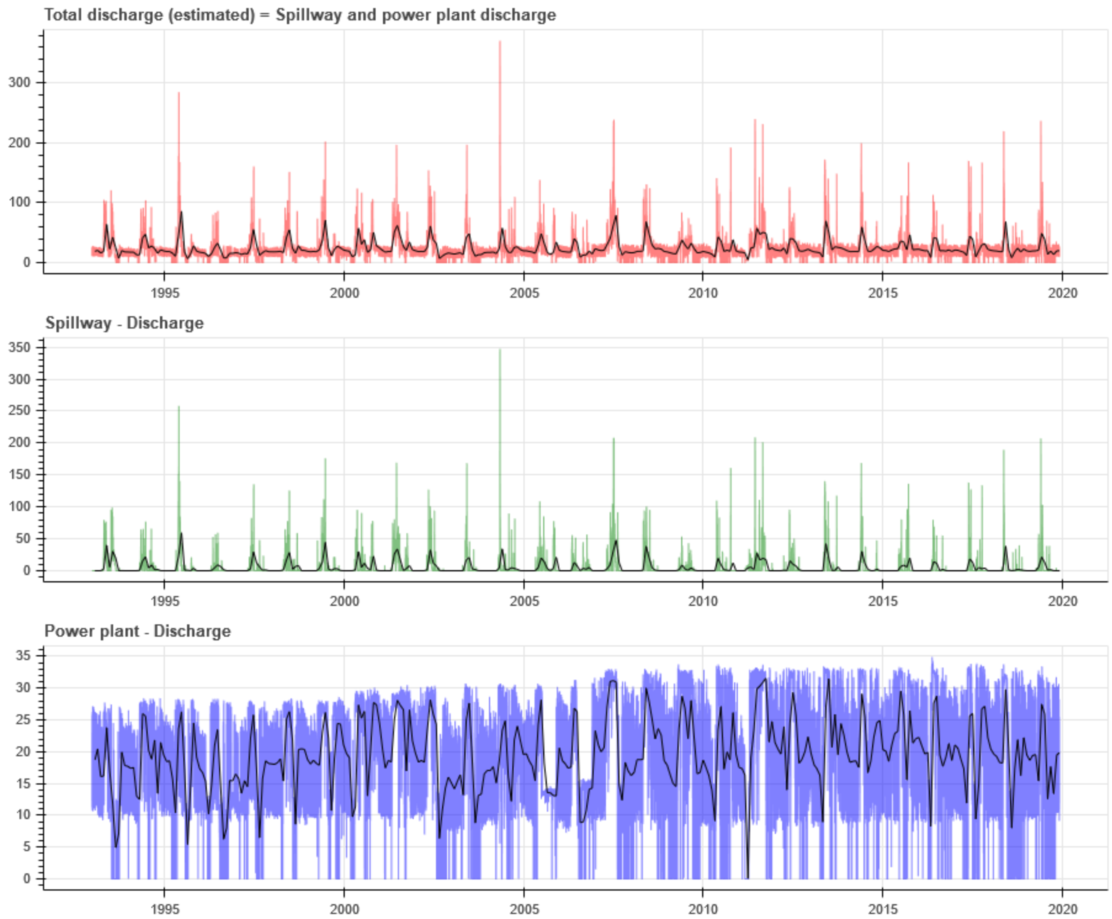

> *Figure 3-8: Measured discharge from spillways and power plant.*

From the unblocked spillway capacity curves as shown in Figure 2-6, the stochastic water level based on the extreme water inflow was calculated (assuming time independence). Since the water level is determined by the power plant discharge below HRV, this was included by assuming a gaussian process for the power plant discharge. These results are shown in the Figure 3-9 and are is similar to the one measured on site, except that the probability of flooding is higher due to extreme value theory. For comparison the probabilistic distribution recommended in the flood analysis (Multiconsult, 2014) of Storeskar has been included in the figure.

The mean design flood from the measured data and assuming blocked spillways gives 567.36 m a.s.l. compared to 567.61 m a.s.l. from the flood calculations (section 2.3). In comparison the design flood from Storeskar gives 566.78 m a.s.l. after scaling compared to the calculated 567.52 m a.s.l. in the flood calculations. Assuming the flood report is correct, this implies that the method is not entirely accurate. The method is also not adequate for all dams due to the assumption of time independence, i.e. inflow is equal to the outflow. Note that the unblocked spillway capacity is used here in the calculations as a proof of concept.

Ideally the extreme water distribution for Eikrebekken would now be used in probabilistic analyses. For the moment one cannot define arbitrary distribution in the Python script, thus for simplicity the distribution was truncated (i.e. cut-off) at HRV. This results in a higher failure probability, since the chance of observing larger floods increases due to scaling of the PDF, $\int_{-\infty}^{\infty} f(x)\,dx = 1$. The extreme water level distribution after truncation was afterwards for simplicity fitted to a Gumbel distribution, $\mu = 566.207$ and $\sigma = 0.152$, which further increases the probability of failure as can be seen in Figure 3-10.

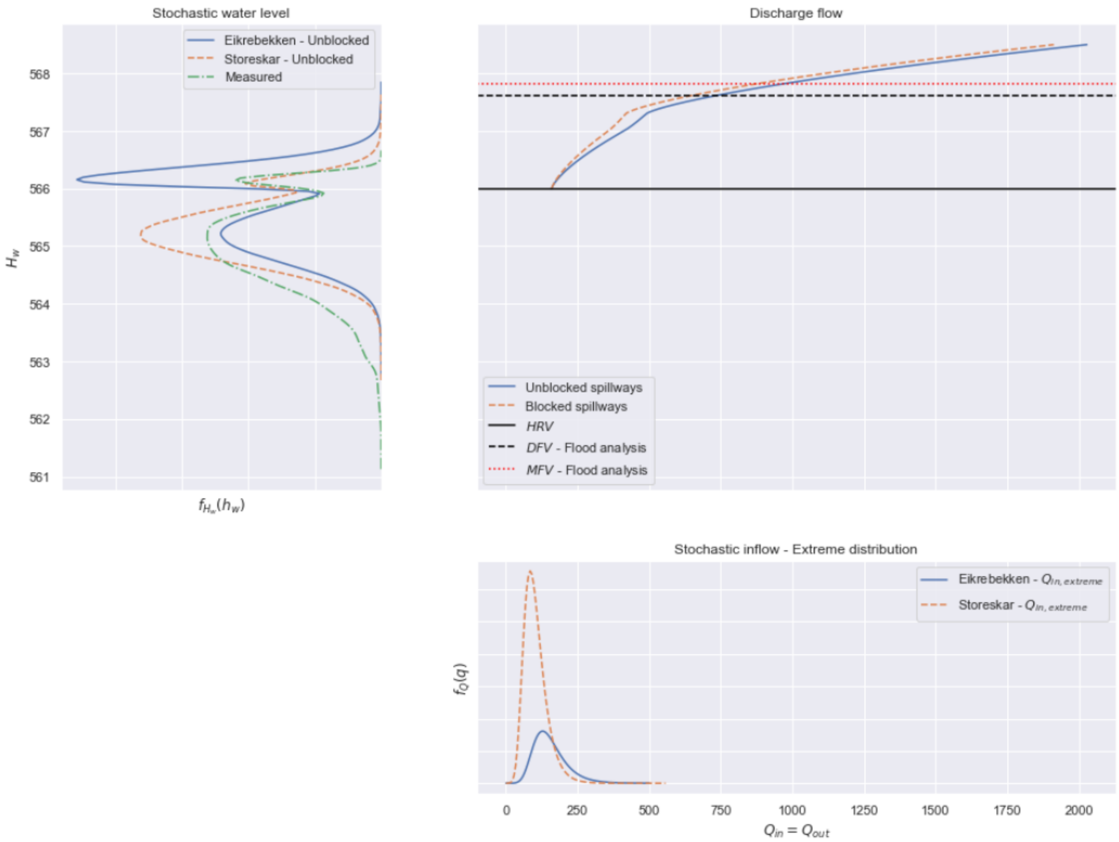

> *Figure 3-9: Water level calculated from extreme distribution inflow assuming unclogged spillways.*

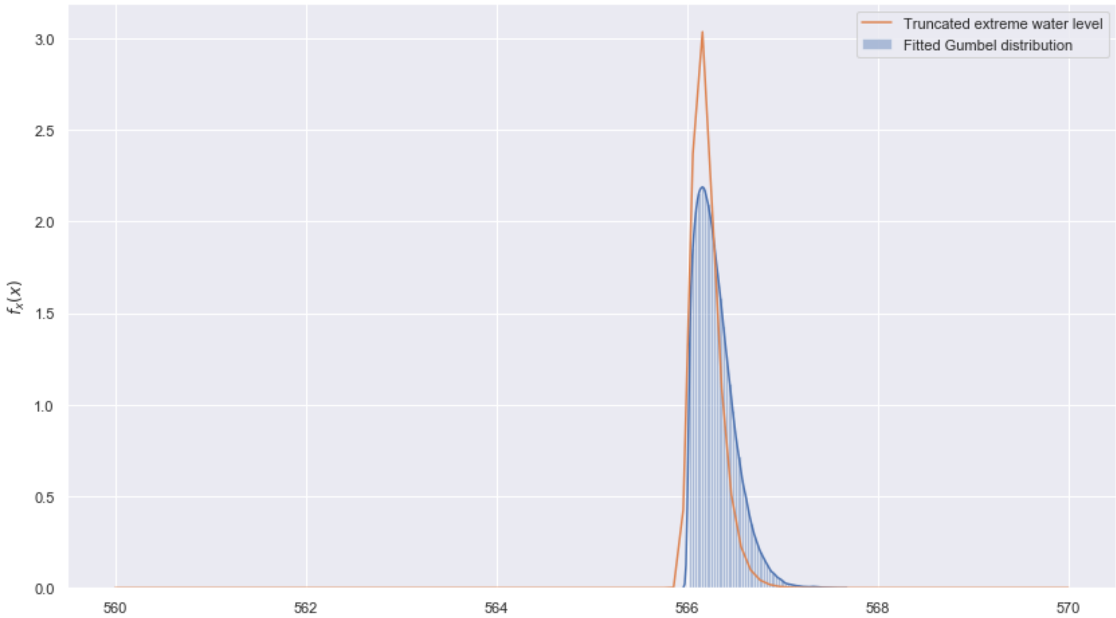

> *Figure 3-10: Gumbel distribution fitted to truncated extreme water level distribution at Eikrebekken.*

3.2.3 MFV

The maximum flood water level is a highly theoretical value which is based on Probable Maximum Precipitation (PMP) and other conservative assumptions in the hydrological model. In essence this method gives the maximum possible water level and can therefore be seen as a sort of truncation of the reservoir inflow Q, given that a distribution can be established. With this mindset one could relate the inflow Q_{PMF} to a return period, which is similar to the simplified approach for dams in consequence class 2 where $Q_{PMF} = 1.5 \times \; Q_{1000}$.

It's recommended in the guidelines for flood calculations that the MFV is calculated based on precipitation-discharge models (NVE, 2011), and is usually about $1.5 - 3.0$ times the $Q_{1000}$for a given catchment area.

To the author knowledge it's not customary to evaluate the uncertainty of the hydrological model nor the parameters used in the calculations. One possible option could be to establish random variables for the input, sample some results (example Monte Carlo) and afterwards estimate the uncertainty based on the spread of the results. Using the two first moments and assuming normal distribution for Q_{PMF} one can possibly (depending on the reservoir) then relate the PMF inflow to MFV by using the spillway capacity curves shown in Figure 2-6.

3.3 Ice load

As described in PMCD part II:2 (Wilde & Johansson, 2016), the ice load is difficult to predict due to lack of good measurement of the ice load, large local variation in temperature, topographic boundary influence, water fluctuation and loads imposed by wind and flowing water. Furthermore, the ice load mechanism is often overlooked and assumed to be a constant static load, when it in fact reduces rapidly with small deformations (Arntsen, Bretas, & Petrich, Simulering av bruddutvikling i murdammer som følge av islast, 2017).

The stochastic load distribution for the ice load proposed in PMCD is based on a master thesis which summarizes the maximum measured ice-loads that was found in the literature (Adolfi & Eriksson, 2013). The purpose was to establish a global probability density function for the ice-load. One should note that the measurements are mainly of newer date, since older measurements are not representative, as described in the thesis. One should also note that loads are mostly from studies done in Canada.

A log-normal distribution has been fitted directly on the data gathered. Note that the data contains mostly yearly max values and no correction is done for the latter. The fitting leads to a mean value of $\mu = 81kN/m$ and $\sigma = 86kN/m$ when assuming log-normal distribution. This results in a probability of 3.72% of an ice-load being above $250kN/m$, which is considered to be highly unlikely. According to RIDAS in Sweden, the horizontal load has an intensity of 50-200 kN/m depending on the geographic location, altitude above sea level and local conditions. In Norway the ice load is normally assumed to be between 100-150 kN/m. To the authors knowledge the justification of these ice loads are currently not known.

In order to make practical use of the log-normal distribution described above, it is suggested in the thesis and PMCD to right truncate the distribution. The reasoning is that there is a physical limitation due to ice buckling. The effect of truncation can be seen in Figure 3-11. For comparison an ice-load with less variation, $\sigma = 10\ kN/m$, is shown in the same figure. Due to uncertainties in the buckling capacity the truncation is in addition assumed to be normally distributed as illustrated in Figure 3-12. However, one should be aware that such a truncation is usually not common in structural reliability and tends to cause numerical problems since the function is non-smooth at this point. With respect to tail-sensitivity (see section 3.1) the truncation can also directly influence the failure probability if the initial Most Probable Point (MPP) is outside the truncation domain. In such cases the results will be very sensitive to the truncation assumptions.

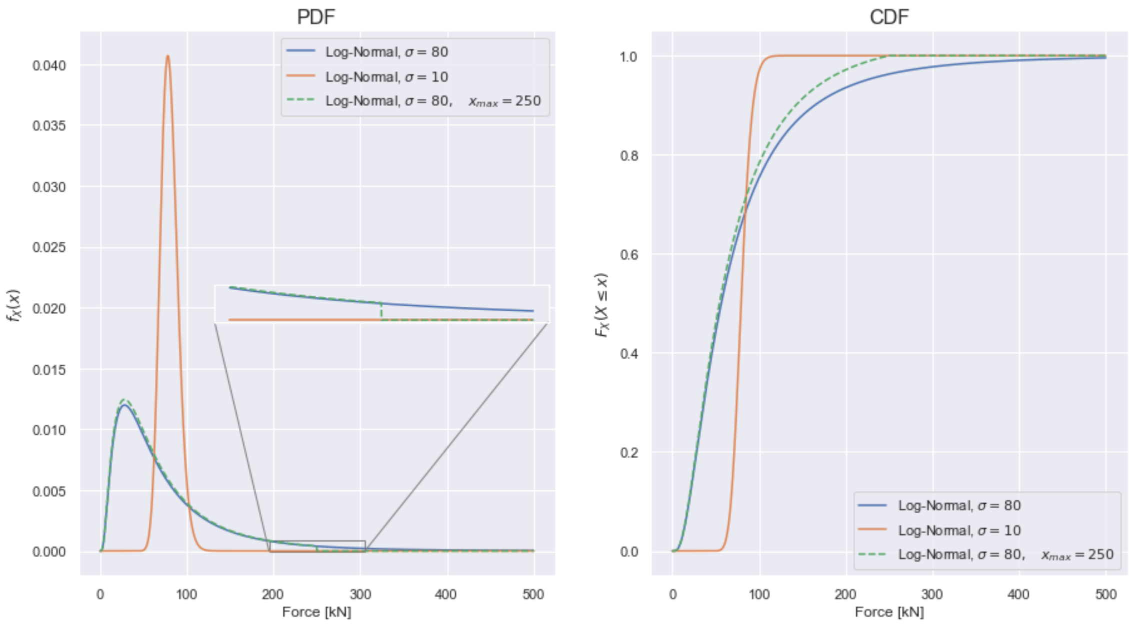

> *Figure 3-11: PDF and CDF of different Ice-load assumptions.*

It's well known that for many dams that the ice-load is governing when calculating stability for small dams in Norway, and as described above is not fully understood. In later years NORUT (soon SINTEF Narvik) and other partners are currently involved in research to study the effects of ice-load and the final report is expected to be available in early 2020. Other research confirms that it can be difficult to measure the ice load due to inaccurate measurements (difficult temperature calibration) and spatial variation. Furthermore, although the stresses can be quite high (above 200 kPa), the maximum ice load at the test site in Narvik have been measured to be around 100 kN/m after several years of measurements (Arntsen, et al., 2019).

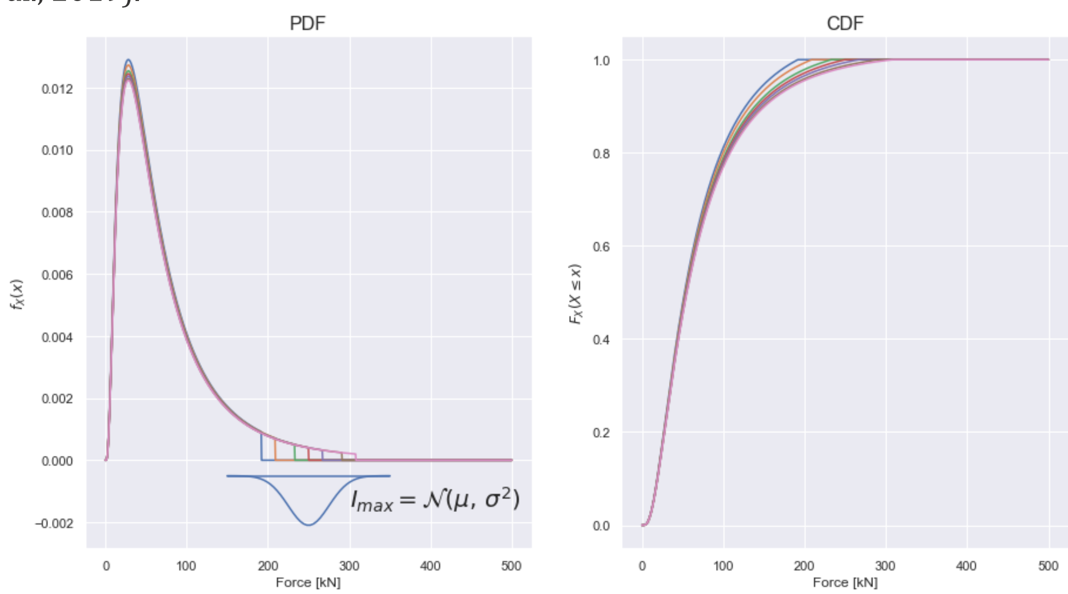

> *Figure 3-12: PDF and CDF of from using normal distributed truncation on the Ice-load distribution.*

The current standard implementation of stochastic ice load is a challenge, both with respect to the actual physical process occurring in nature and the implication of structural reliability in probability analysis. Furthermore, many commercial software cannot handle truncation and thus creating an additional challenge (Westberg, Wilde, Johansson, Bayonas, & Altaerjos-Garcia, 2017).

Since there are several uncertainties regarding the ice-load, three main assumptions have been studied in this report. Firstly, the ice load is modelled as suggested in PMCD with a normally truncated maximum ice load at 250 kN/m with 10% coefficient of variance, as shown in Figure 3-12. Secondly, the non-truncated formulation is used to see the effect of truncation and thereby assess the sensitivity on the results. Lastly a lower variance, as previously applied at dam Hensfoss is utilized (Norconsult, 2018). The idea is that this gives a probability that is more in line with the Norwegian regulation.

In the authors opinion further study of the ice load is necessary in order to promote probabilistic analysis. It's also recommended to collect more information and study the effect of an ice load as a deformation load. This type of analysis would require that the dam is deformable and unfortunately adds to the complexity since stiffness parameters would also be required.

3.4 Friction angle

Previous studies have shown that the friction angle between the dam and the foundation is a vital parameter for sliding capacity. This is to be expected when the friction capacity relates to the Mohr-Coulomb theory. In principle there are several factors contributing to the total friction angle, and one should be precise with which friction angle that is referred to.

For a certain material one can imagine that the there is an internal friction angle. For metals this would commonly be 45° (Ashby & Jones) and for intact rock and soils it would depend on the grain composition. At an interface between two materials or rock joints the friction is normally reduced and is known as a residual friction angle (Grøneng & Nilsen, 2009). Furthermore, the deformation of two objects with irregular surface will cause volume deformation. In most cases the volume increases since there are initially no cracks in the object. This phenomenon is known as dilation and increases the friction capacity. Another similar contribution is the effect of macro-asperities which acts at a larger scale compared to dilation (Steen, 2017).

Pragmatically the sum of these effects can be seen as a total friction angle and is the one commonly used in Norwegian design. In many cases it's hard to define the contribution of each factor, and for simplicity in the calculations a total friction angle is used. The idea behind this is that if the total friction angle is of large importance to the calculated stability, then one should further investigate the contributing factors to improve the structural reliability.

3.5 Geometry

The geometry has been modelled according to Eurocode where $a_d = a_{nom} \pm \Delta a$, where a_{nom} is the nominal measurement, which is here assumed to be according to blue prints. It's also assumed that the deviation in geometry is normally distributed and for simplicity the coefficient of variation is set to 5% for lengths and 1% for inclinations. A drawback with the calculation model is the limitation in the geometry, example no cut-outs, top level of the dam is assumed to vary (not the bottom level), etc. This limitation introduces an error when comparing results with other calculations models and should be addressed in future work.

3.6 Cohesion

While it's known that the contribution of cohesion in the dam foundation can be quite considerable, the effect is normally neglected. This is mainly due to large uncertainties in the capacity and possible spatial variation in the foundation, as it's often unknown whether the bond is intact or not.

The stress-strain relationship is typically very brittle, and the cohesion is mostly lost after "failure". This can occur for small deformations compared to foundation failure. One of the major benefits with probabilistic analysis is that the uncertainty in capacity and the probability of intact bonding can be incorporated in design.

Analysis has been carried out with a similar log-normal distribution used in dam stability for Reinoksvatn (Dr. techn. Olav Olsen, 2017). The mean value is reduced, and the variance is increased to better reflect the uncertainty of cohesion. Non-tensile capacity is assumed, no spatial variability, and it's assumed that the cohesion only contributes where there is contact pressure in the foundation. This is calculated assuming that the dam acts as a cantilever and that Navier-hypothesis is valid, i.e. assuming linear stress distribution. For comparison an analysis without cohesion is also calculated.

3.7 Rock bolt capacity

For smaller dams and lightweight constructions, the rock bolt capacity can give a significant contribution to the stability. The major concern regarding bolts is the bounding, especially with respect to grouting in bedrock during installation. The principal failure modes are shown in Figure 3-13.

As can be deduced from the figure below, the capacity depends on the yield stress, bolt diameter, grout capacity and rock mass capacity. Furthermore, the capacity in a dam depends on the location of the bolt in the cross-section, concrete cover and most importantly on the mobilized strain in the bolt. In the Norwegian guidelines the bolt stress is maximum allowed to be 180 MPa (NVE, 2005). For stability calculations purposes it's commonly assumed that the bolt is fully mobilized at this stress level in limit equilibrium calculations.

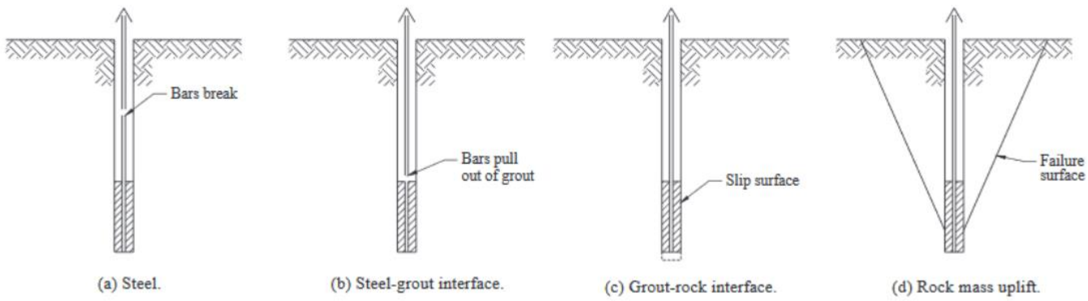

> *Figure 3-13: Principal failure modes of grouted rock anchors (Brown, 2014).*

Furthermore, the guidelines states that the capacity from bolts can only be included if the dam height is less than 7 m. Note that it's expected that this requirement will be revised in the upcoming guideline for concrete dams.

For simplicity the bolt stress is used as a basic variable to represent the bolt capacity, since it directly influences the force acting in the model. A similar log-normal distribution as the one used in Reinoksvatn (Dr. techn. Olav Olsen, 2017) is applied in the analysis of Eikrebekken. This should be reviewed in further work.

Since the focus is on Ultimate Limit State (ULS) and not Serviceability Limit State (SLS) the guideline requirement of maximum dam height of 7 m is disregarded in these analyses. For comparison analyses without bolts have also been carried out.

The bolt capacity is here calculated as a function of the allowed bolt stress and diameter and assumed that the force is vertical. The increase in the horizontal capacity is also assumed to be the result of increased vertical weight, and not from the shear capacity of the bolt as is in Eurocode. One possible explanation for this method is that once a deformation has occurred the bolt stress acts as a prestress on the dam. However, this method is debatable and might be revised if the regulations conforms to Eurocode regulation.

4 PROBAILISTIC MODELING

4.1 Calculation model

For simplicity the in-house developed model (excel file) for dam stability calculations has been used in probabilistic analyses. The idea was to start simple, pinpoint key random variables and refine the model by eventually performing calculations with a deformable body as in previous studies. One could thereby also study the effect of different modelling assumptions. Due to limited amount of time, the latter part has not been performed. The calculation is based on limit equilibrium, which is common practice in Norway and therefore more suited when directly comparing deterministic and probabilistic results.

However, in recent years Finite Element Analysis (FEA) has become increasingly popular and one can thereby more correctly simulate the true physical behaviour of the dam. This often increases the complexity by introducing more variables and thereby increasing the computational time. In the authors opinion one should strive to achieve a correct model that is representative with respect to the actual behaviour of the dam. An example of this is whether or not the ice load can be modelled as a deformation load, and if the bolt capacity should be modelled as a spring instead of a static force. The advantages should always be compared to the required effort and resources.

The limit equilibrium model assumes a linear sliding plane at the foundation, and the roughness must therefore be taken into account in the friction angle if included. A drawback with the model is that one cannot easily model gate failure, and the model only calculates the sliding capacity at the assumed foundation, which is not necessarily the weakest plane. The analyses are thus restricted to only consider global equilibrium (EQU), while failure in the concrete (STR) or rock (GEO) is not considered. The latter could be easily determined in a FEA with plastic material models, although this would be extremely time-consuming and is therefore believed to be impractical in most cases.

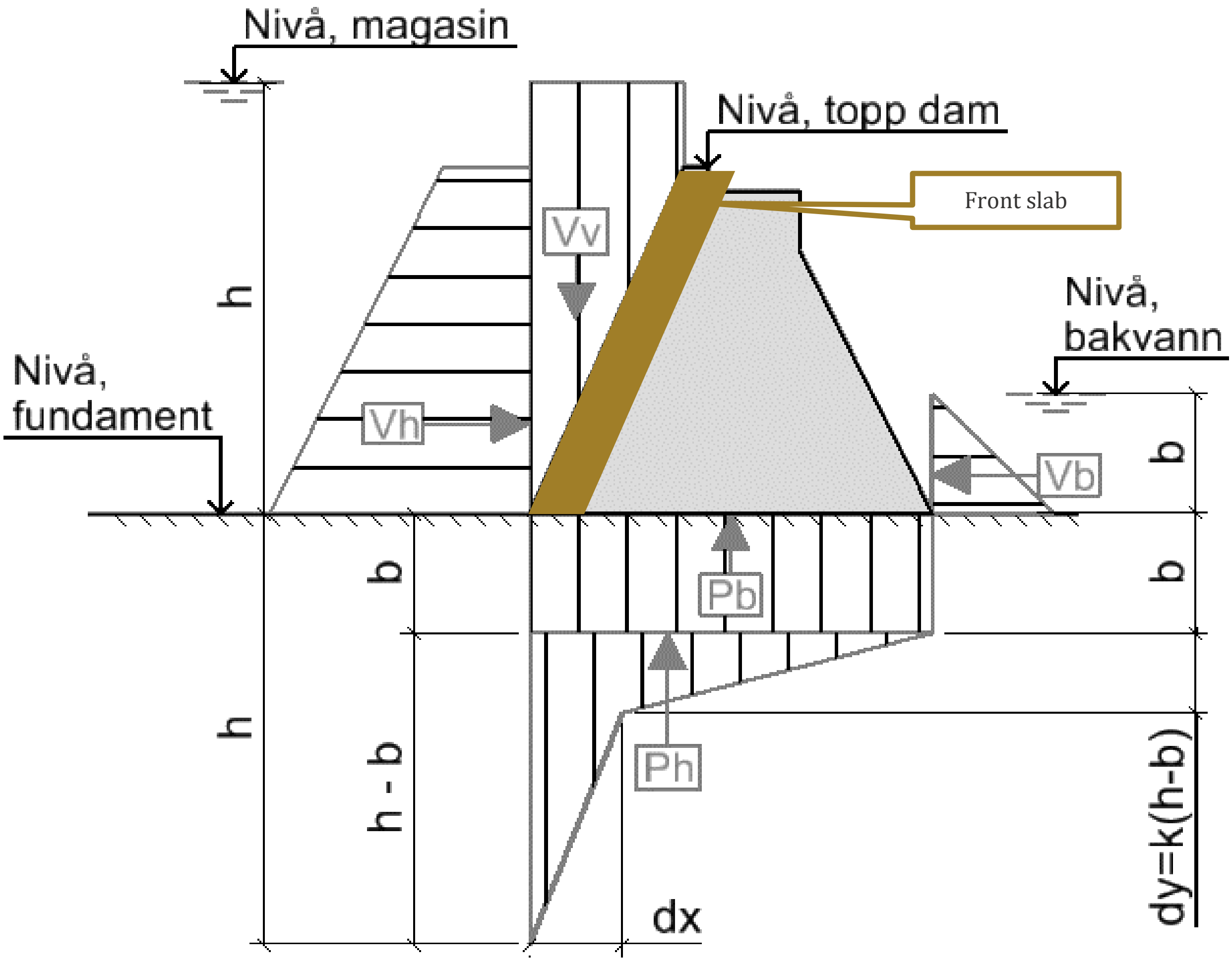

> *Figure 4-1: Principle drawing of the model used in both deterministic and probabilistic calculations.*

A principle drawing of the loads acting on the dam is shown in Figure 4-1. Note that the pore pressure is assumed to vary linear across twice the thickness of the slab. This is a common assumption for slab buttress dams. The ice load also acts 0.25 m below HRV as according to the guideline (NVE, 2003), and both the bolt and ice loads are assumed to be a constant static force, i.e. no change with deformation and time.

4.2 Basic random variables

Ideally only the fundamental variables which are required to best model the safety reliability of a dam should be included in a probabilistic calculation. This is both to reduce the computational complexity and to focus on the factors which actually matters in terms of safety. Note that this will depend on the calculation model that is utilized.

In these analyses the term *sensitivity* is related to the α-vector from a FORM analysis, which is briefly described in section 4.5. This value relates to the uncertainty for a given analysis and the sign tells if the contribution of a variable is positive or negative. The sum of squares is $\sum \alpha_i^2 = 1$. One can thereby determine which variables that has the highest impact on the reliability result.

One should note that total uncertainty is a function of both the calculation model and the uncertainty of a variable. The first part can be thought of as determining the gradient of the limit state function, evaluated at the origin μ. This is also commonly known as sensitivity in structural analysis, which differs here. An example is that the calculation model may be sensitive to the water density. However, since the density of water is rather certain, the total contribution is thus low and can be neglected in reliability analysis.

For some cases it's unclear which parameters that has the highest influence on the safety level. In such cases a probabilistic method is very attractive since the engineer is forced to judge the uncertainty of each parameter and afterwards conclude which parameters should be further studied, which can be the most difficult task in the analysis. In Figure 4-2 one can observe that variables of larger influence tend to group together while variables of minor importance indicate a more random pattern.

The main purpose of using a simple calculation model was to start with as many variables as reasonable and identify which parameters that has the highest influence on the reliability. Variables of minor importance can thus be left out of the analysis due to negligible contribution. Note that generally more variables are needed in a more refined model and that correlation between variables should be evaluated carefully.

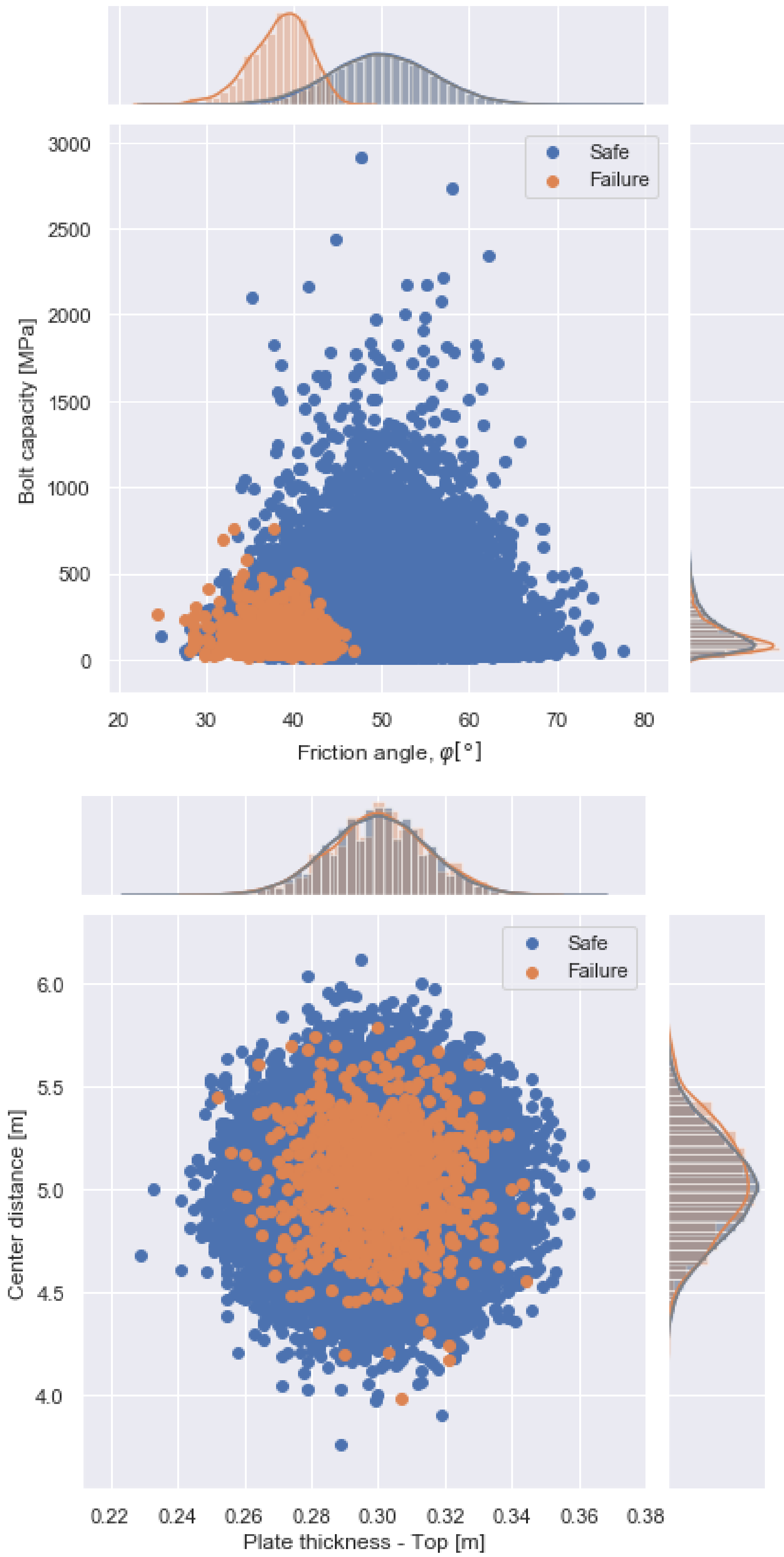

Parameter	α_i^2	Design value
Friction angle	63.8 %	40.645
Bolt Capacity	1.8%	110.029
Plate thickness Top	0%	0.300
Center distance	0.3%	5.026

Figure 4-2: Sensitivity plots from Crude Monte Carlo analysis and comparison with same selected sensitivity values α from FORM analysis of with same assumptions shown in table to the right.

4.3 Limit states

Due to the limited capability of the calculation model only equilibrium (EQU) is evaluated within a probabilistic framework. Besides, the Norwegian dam safety regulation is mostly concerned with this part and has explicit requirements for the global equilibrium with respect to concrete dams. For other cases such as material strength (STR), geotechnical stability (GEO) and fatigue (FAT) one is referred to the Norwegian standard which currently is the Eurocode, where it's allowed to do design by probabilistic method. Note that uplift (UPL) is normally included in the equilibrium calculation, while hydraulic failure (HYD) is mostly of special concern regarding earth and rock filled dams.

The global equilibrium is controlled for sliding and overturning. The limit state functions are formulated such as they are in accordance with common practice in Norway (NVE, 2005).

$$G_{rotation}(\mathbf{x}) = \mathrm{S_{overturning}} - 1 = \frac{\mathrm{M_{stabilizing}}}{\mathrm{M_{destabilizing}}} - 1$$

$$G_{sliding}(\mathbf{x}) = S_{sliding} - 1 = \frac{\mathrm{c} \cdot A_c + \sum F_y \cdot \tan(\varphi)}{\sum \mathrm{F_x}} - 1$$

Where:

$\mathbf{x} = [x_1, x_2, x_3, \dots, x_n]^T$, are the basic variables used in probabilistic calculations
c, cohesion (basic variable if included)
A_c, surface area with contact pressure (function of $\mathbf{x}$)
$\sum F_y$, sum of vertical load (function of $\mathbf{x}$)
$\sum F_x$, sum of horizontal load (function of $\mathbf{x}$)
$\tan(\varphi)$, friction coefficient (basic variable)

The total probability of failure is thus the combined failure probability of both limit state functions. This is handled directly with the use of simple Monte Carlo methods, while the Equivalent Planes methods can be used for FORM analysis which is exact for two limit state functions (Roscoe, Diermanse, & Vrouwenvelder, 2015). If the failure probability for one limit state is much lower compared to the other, its contribution can be neglected.

4.4 Load combinations

Although external loads normally vary with time, it's common practice to use load combinations to evaluate the safety level. The idea is that the load effect from each load action can be added together. This is similar to the partial factor method, where the safety level is defined by multiplying each load action with a partial load factor and afterwards combined to determine a design load effect (Eurocode 0).

The most common load combination used in Norwegian dam design is listed below. It's stated in the dam safety regulation that the most unfavourable load combination shall be used in design (OED, 2009). The load combinations are similar in setup as in Eurocode where there is normally one leading action for each combination in ULS, and a special incident in each ALS.

I. DFV + reduced spillway capacity (ULS)
II. HRV + Ice load (ULS)
III. HRV + Temperature (ULS)
IV. PMF (ALS)
V. DFV + rock bolts inactive (ALS)
VI. DFV + gate failure (ALS)
VII. HRV + clogged drainage (ALS)
VIII. Earthquake (ALS)

For simplicity the four-load combination I, II, IV and V has been implemented in the probabilistic analyses.

One side note is that HRV, DFV and PMF each defines a water level which can be related to a frequency in time. One can thus similarly to Eurocode imagine that the water levels are as external loads and the load scaling factor ψ is an outcome of the hydrological model and spillway capacity.

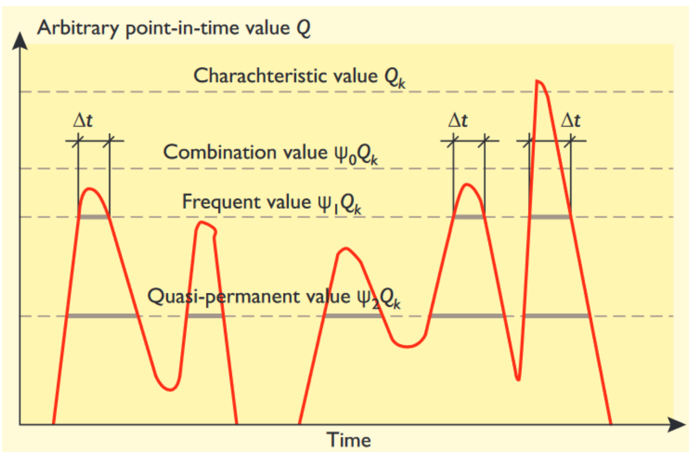

> *Figure 4-3: EN1990 frequency classification of variable actions (Gulvanessian, 2001).*

4.5 Numerical methods used in calculation

Both FORM and Crude Monte Carlo has been used in the probabilistic calculations. The benefit of performing a FORM analyses is the reduced computational time required to achieve a reasonable answer compared to Monte Carlo methods. However, convergence can be challenging, especially when many random variables are involved and can lead to wrong answers. Furthermore, the FORM analysis linearizes the limit state function and can thus over- or underestimate the probability of failure depending on the curvature of the failure domain.

Monte Carlo is a family of methods, and the simplest one is the Crude Monte Carlo method. Here random variables are generated in accordance with the specified correlation, used in the calculation model and afterwards the sum of failure indicates the failure probability. This method is very robust and can give some insight to the mathematical properties of the reliability level even with few iterations. For exact answers the method is extremely time-consuming, and the number of iterations required to approximately estimate the failure probability is very dependent on the actual failure probability.

Since each Monte Carlo result is binary (safe or failure), this can be seen as a Bernoulli distribution. The sum of a Bernoulli sequence gives a binomial distribution. This can be used to approximate the necessary required iterations to evaluate the failure probability as shown below.

$$\hat{p}_f = \frac{N_f}{N}, \text{ where } N_f \text{ are points that have failed}$$

$$\sigma^2_{p_f} = \frac{p_f \cdot q}{N} \Rightarrow \hat{\sigma}_{\hat{p}_f} = \sqrt{\frac{\hat{p}_f(1-\hat{p}_f)}{N}}$$

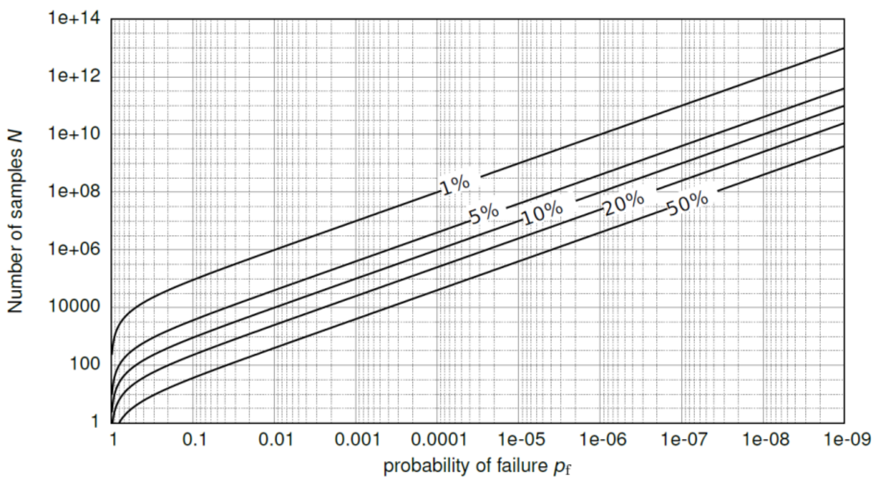

> *Figure 4-4: Number of samples N required for different coefficient of variation $\delta\hat{p}_f$ assuming p_f is very small (SOFiSTik, 2018).*

The figure clearly shows how the number of sample points and coefficient of variation varies with the probability of failure. Typical convergence from Crude Monte Carlo calculation is shown in Figure 4-5.

In each probabilistic analysis 1 million iterations have been calculated. From the figure above this gives a coefficient of variation of 1% if the probability of failure is 0.01 ($\beta = 1.28$) and about 35% coefficient of variation for a failure probability of 1e-6 ($\beta = 4.75$). For this reason, the monte simulations are used in combination with FORM analysis.

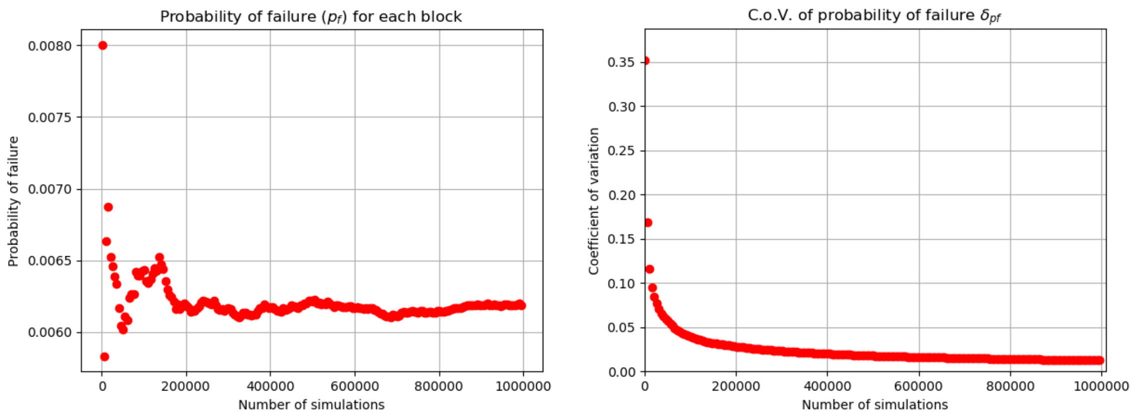

> *Figure 4-5: Typical convergence plots of $\hat{p}_f$ and $\delta\hat{p}_f$ from Crude Monte Carlo simulations.*

The FORM method is an elegant mathematical formulation for determining the Most Probable Point (MPP) which in turn is used to estimate the probability of failure. This is done by (i) selecting a start point (normally from mean values), (ii) transforming the variables to uncorrelated variables in the normal-space, (iii) calculating the gradient of the limit function, (iv) iterate to new point, and (v) repeat this procedure until convergence is satisfied. For improved convergence one can adjust the starting point, change the step length or increase the tolerance for convergence.

This method is mathematically exact if the transformed limit function is linear in the normal-space. Note that the limit state function can be non-linear due to the transformation of the random variables. The transformation from the original to the standard normal space with the Most Probable Point is shown in Figure 4-6. The distance from the origin to MPP is the reliability index β and the direction is given by the gradient vector α.

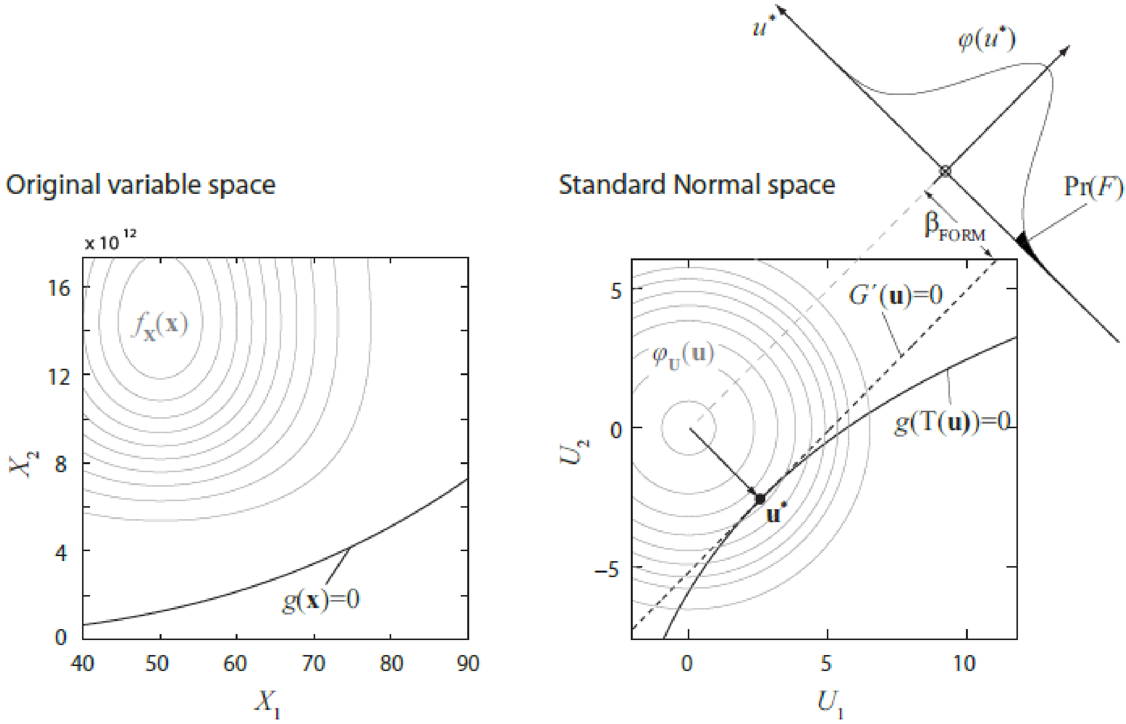

> *Figure 4-6: Illustration of the original space and the standard normal space shown with non-linear limit state function and MPP at* $\mathbf{u}^*$ *(SOFiSTik, 2018)*

The python library PyRe coded by Jürgen Hackl (https://github.com/hackl/pyre) has been modified and used to perform structural reliability analyses. The library is connected to the calculation model in excel, as described in section 4.1 and a custom distribution for a right-truncated log-normal has been added to the code.

The code is based on the FERUM (Finite Element Reliability Using Matlab) which originates from University of California, Berkeley. The software is much used in academia and is thus assumed to be mathematically correct and numerically stable Furthermore, the coupling of excel with PyRe has been verified with simple analytical structural reliability problems provided in the RELY module by SOFiSTiK.

5 RESULTS

Since the purpose of these calculations are to evaluate different assumptions and show how reduction in uncertainty reflects the calculated safety level, the reliability results shown here should not be interpreted as correct results. It's important to note that the calculated probability of failure, or β, are the result of some underlaying assumptions which can in certain cases be very conservative. It's especially important to recognize this distinction when comparing the calculated safety level with predefined target values. This is even more important if the reliability target values are to be calibrated from probabilistic results.

The two cross-sections P.47 and P.55 have been analysed using different assumptions. Different ice load distribution, effects of bolts and cohesion, and the outcome from using extreme water level distribution have been evaluated. A base case according to PMCD and previous work is established and used as a reference. It's assumed in the base case that the bolts are active in both sections, even though the dam height is over 7 m in P.47.

A hypothetical case where the friction angle for P.47 has been tested and evaluated is calculated. The idea behind the analysis was to show how a reduction in the mean value and variance, i.e. $\mu = 45°$ and $\sigma = 2.25°$ instead of $\mu = 50°$ and $\sigma = 6°$, can still improve the safety level if the uncertainty is reduced.

The random variables used as input in the calculations are described in 0. Note, in some FORM analyses the inactive variables are removed in order to improve convergence which can be seen in the sensitivity results and colouring of plots. To limit the amount of results shown in the figures, 50 000 samples are randomly selected. If the failure probability is very low, the number of samples is increased to better illustrate the cause of failure.

The combined probability from sliding and overturning calculated in FORM analyses are not calculated as described in section 4.3 due to time constraint. However, if the probability of sliding is much higher than overturning, which often is the case here, the overturning can be neglected due to negligible contribution.

5.1 P47 - Simplified analysis

A simple analysis with only two basic variables was carried out to illustrate some key concepts in the following results. The non-truncated ice load and the friction was assumed to be random variables, while the rest of the variables was set to be constant. Only the load case II of "HRV + Ice load" has been evaluated in this case.

One million simulations (1e6) was run with this configuration and used to estimate the probability of failure using Crude MC. The calculated safety factors are shown in Figure 5-1 and the joint plot of the variables in Figure 5-2. FORM analyses were performed with default values and afterwards adjusted based on the crude Monte Carlo results. The reliability index, probability of failure, MPP and the sensitivity of the variables are shown in Table 5-1 for each calculation. Note that the Crude Monte Carlo Method results in a higher failure probability due to the combined failure domain of each limit state.

Table 5-1: Summary of key values from FORM and Crude Monte Carlo

Results	First attempt FORM	Second attempt[1] FORM	Crude Monte Carlo
Sliding	$\beta = 2.23$ $p_f = 0.0128$ $\varphi = 50.006 \approx \mu_\varphi$ $F_{ice} = 362.60\ kN/m$ $\alpha_\varphi = 0$ $\alpha_{F_{ice}} = 100\%$	$\beta = 1.73$ $p_f = 0.0418$ $\varphi = 41.96$ $F_{ice} = 140.62\ kN/m$ $\alpha_\varphi = 60\%$ $\alpha_{F_{ice}} = 40\%$	$\beta \approx 1.57423$ $p_f \approx 0.0577$ $\delta p_f \approx 0.0040$
Overturning	$\beta = 2.58$ $p_f = 0.0049$ $\varphi = 50.006 \approx \mu_\varphi$ $F_{ice} = 486.36\ kN/m$ $\alpha_\varphi = 0$ $\alpha_{F_{ice}} = 100\%$		

1) Starting point for friction angle was reduced to 40 degrees based on MC results.

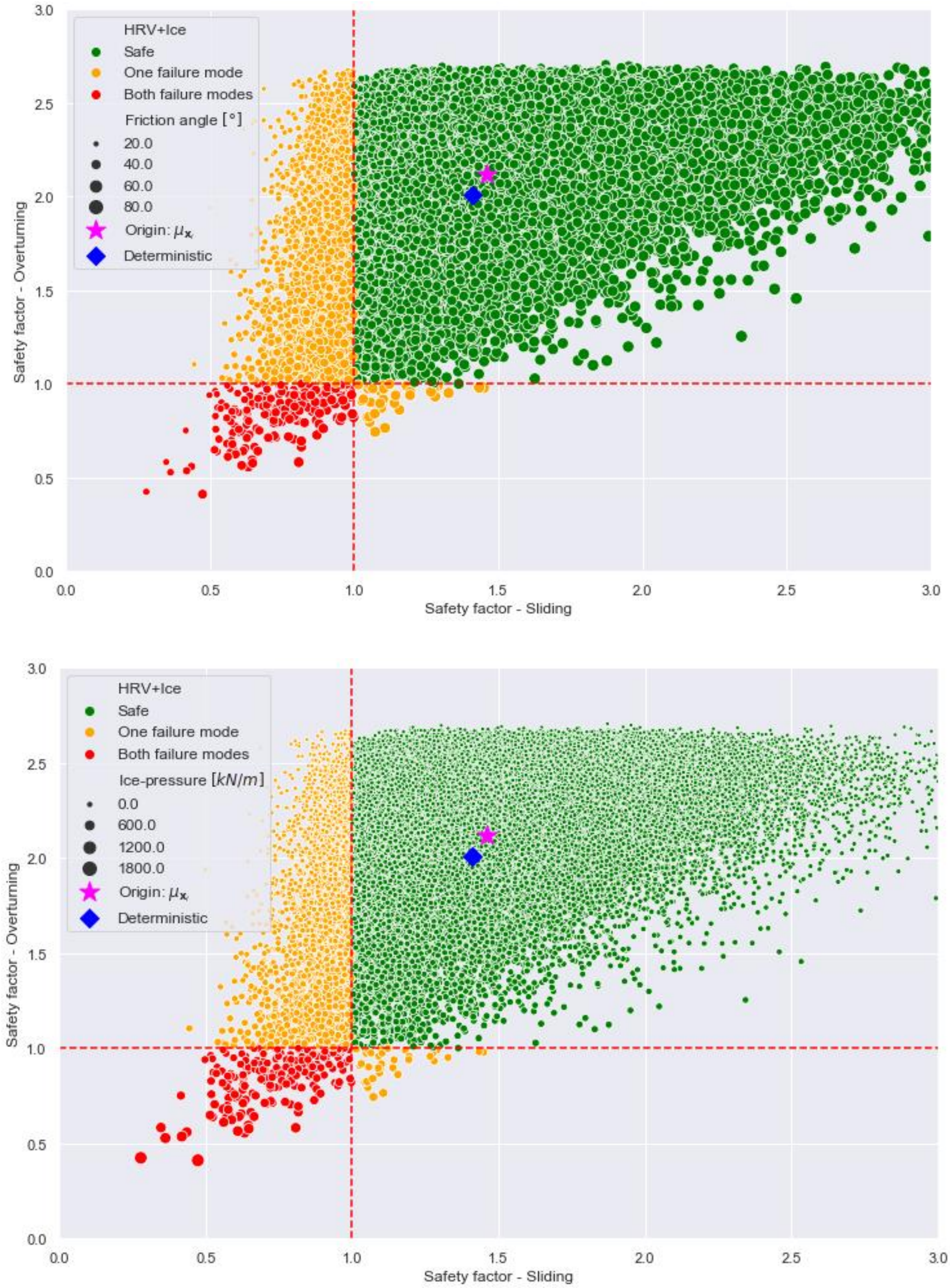

> *Figure 5-1: Calculated safety factor from Crude MC with size representing (a) the friction angle and (b) the ice load used in each calculation.*

From Figure 5-1 (a) one can observe that a low friction angle gives a high chance for failure to occur. One can also observe that the friction angle has no impact on the overturning as expected. A reduction in the variance would lead to less points failing due to sliding and thus would improve the reliability of the structure.

Similarly, one can see in Figure 5-1 (b) that failure due to overturning is largely caused by extreme ice loads in this case. Furthermore, the figure shows that failure in friction can also occur with a low ice load if the friction angle is sufficiently low, something that is confirmed by Figure 5-2. This figure is also very useful in the absence of recorded failure modes, since the central tendency of the point cloud and distance to failure would also give some indication of the structural reliability.

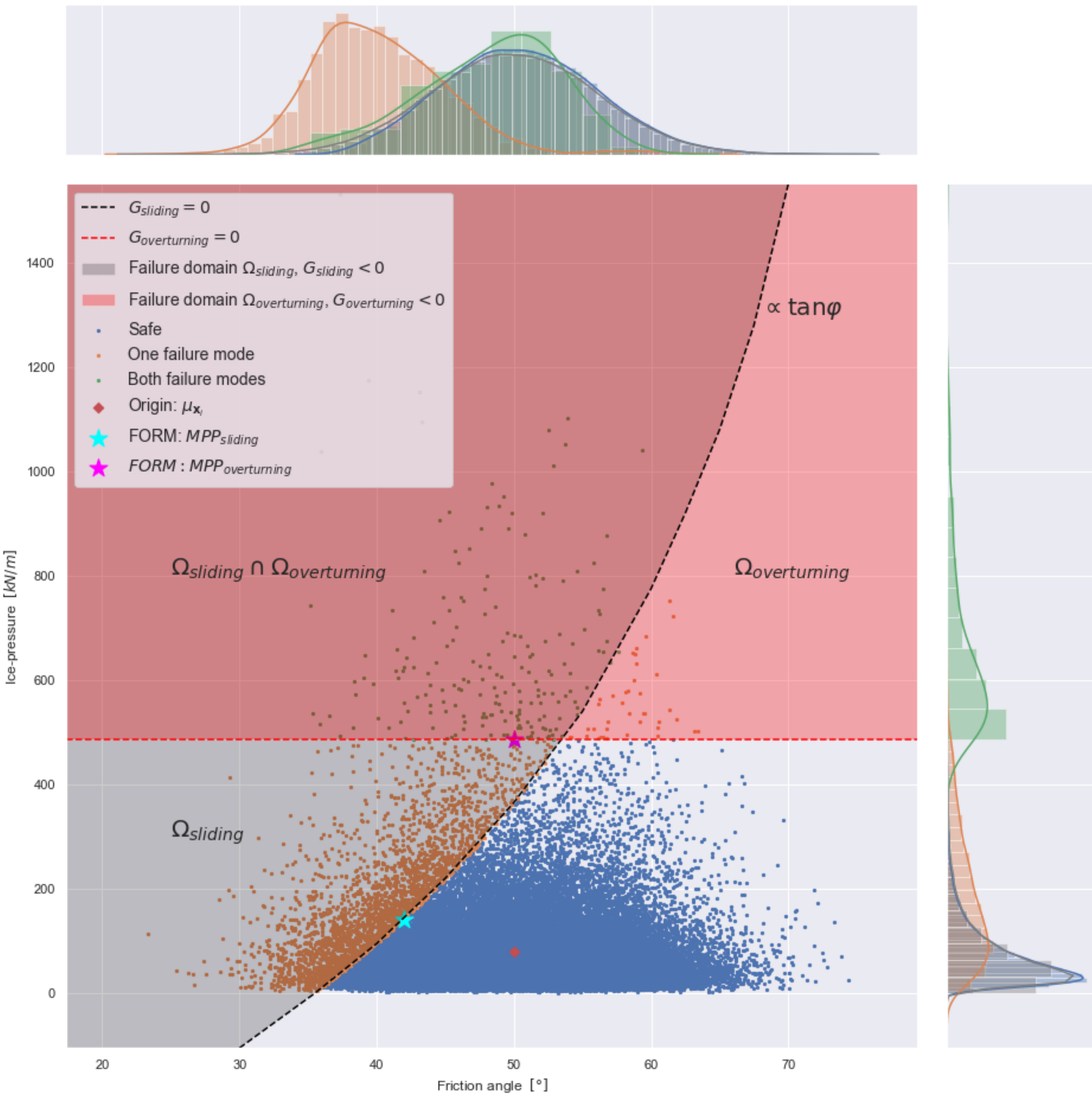

> *Figure 5-2: Joint plot of the two variables used in calculation. The limit states functions can be deduced from the location of the failed points and from the marginal distribution of the failed simulations.*

The joint plot shown in Figure 5-2 is a very useful since one can deduce which parameters that has the highest influence on the reliability as mentioned in section >. With two random variables one can easily identify the limit state functions of sliding $G_{sliding}(\boldsymbol{x})$ and overturning $G_{overturning}(\boldsymbol{x})$. The functions show that the overturning has a constant threshold for a maximum ice load and is independent of the friction angle. On the other hand, the sliding capacity is proportional with the friction angle and is thus a function of both parameters.

In the case of a variable HRV the threshold of $G_{overturning}(\boldsymbol{x})$ would be more difficult to interpret since the figure would show a slice of a multidimensional failure domain. In this instance one could plot the points in 3D to remedy this effect, however this is an issue in general when many variables are involved.

The figure also clearly depicts that there is an intersection of the joint failure domain $\Omega_{sliding}$ and $\Omega_{overturning}$ which needs to be considered when calculating the total probability of failure. The MPP and the mean value point is also shown in the figure, and the distance between a given MPP and the "origin" suggest the size of the reliability index. Note that this is not entirely accurate since the reliability index is the distance in standard normal space and not the original space.

For simplicity the number of failure modes was calculated and divided into 3 categories. 0, 1 and 2, which describes the number of failure modes observed in a given calculation. In retrospect the failure modes should have been divided into 4 categories with a distinction between sliding and overturning. This information is utilized when calculating the probability density function shown on the sides of the figure. The blue PDF shows the input distribution in the calculations, while the orange PDF is from one failure mode. Preferably this would be subdivided between overturning and sliding. Lastly the green PDF shows the combined distribution where both sliding and overturning occurs.

The different PDFs gives valuable information when examining and interpreting the data. Firstly, one can easily verify if the correct distribution was used in the calculation. Secondly the peak of the PDF for a given failure mode indicates the whereabouts of the MPP. Lastly the difference between the PDFs corresponds to the sensitivity given in Table 5-1 and can thus be used when calibrating FORM analyses. Note that a better fit between the MPP and the peak of the PDFs would probably be achieved if the failure mode was categorized by the actual failure mode.

Similar approach and interpretation are used when examining the probabilistic analyses with several variables. This example also indicates that one can reasonably estimate the failure probability using FORM.

5.2 P.47 – Base case

For the base case bolts and cohesion are included in the calculations. The ice load is normally truncated using the values in PMCD which corresponds to a 1 m ice thickness. Based on the master thesis (Adolfi & Eriksson, 2013) there is no basis for the scaling of the ice load, thus is not considered in this analysis. Furthermore, the water levels are given an unreasonably high variance due to ignorance of the analyst. The combined effects results in a low calculated reliability level as summarized in Table 5-2. However, the results also show how the reduced uncertainty by examining the important parameters can improve the structural reliability. Table 5-3 is an example of the calculated values from a FORM analysis of load case I. Due to excessive amount of data, only the sensitivity plots are shown for the other results as in Figure 5-3.

> *Table 5-2: Summary of calculated probability of failure and corresponding reliability index.*

	LOAD COMBINATION	FORM OVERTURNING	FORM SLIDING	CRUDE MONTE CARLO
I	**DFV + clogged spillways (ULS)**	$p_f = 2.5e-8$ $\beta = 5.4495$	$p_f = 0.0254$ $\beta = 1.953$	$p_f = 0.0176$ $\beta = 2.1050$
II	**HRV + Ice load (ULS)**	$p_f = 4.8e-8$ $\beta = 5.3354$	$p_f = 0.0165$ $\beta = 2.131$	$p_f = 0.0134$ $\beta = 2.2120$
IV	**MFV (ALS)**	$p_f = 3.7e-8$ $\beta = 5.379$	$p_f = 0.0278$ $\beta = 1.914$	$p_f = 0.0193$ $\beta = 2.0691$

> *Table 5-3: Summary of value at MPP, gradient vector and sensitivity values for load case I using FORM.*

	Sliding			Overturning		
Variables	x_{MPP}	α_i	α_i^2	x_{MPP}	α_i	α_i^2
Conc_density	23.955	-0.035	0.001	23.867	-0.037	0.001
phi	**40.645**	**-0.799**	**0.638**	50.006	-0.000	0.000
cohesion	56.556	-0.186	0.034	67.120	-0.000	0.000
bolt_capacity	110.029	-0.135	0.018	72.168	-0.150	0.022
HRV	566.001	-0.000	0.000	566.001	-0.000	0.000
DFV	**570.651**	**0.548**	**0.300**	**582.667**	**0.973**	**0.947**
PMF	567.813	-0.000	0.000	567.813	-0.000	0.000
Ice_load	53.851	-0.000	0.000	54.984	-0.000	0.000
c/c	5.026	0.053	0.003	5.038	0.028	0.001
inc_upstream	0.799	-0.040	0.002	0.797	-0.070	0.005
inc_downstream	0.330	-0.004	0.000	0.329	-0.032	0.001
b_crown	1.997	-0.017	0.000	1.940	-0.110	0.012
h_vert_down	1.501	0.004	0.000	1.511	0.027	0.001
plate_t_top	0.300	-0.008	0.000	0.299	-0.009	0.000
plate_t_bot	0.600	0.007	0.000	0.608	0.046	0.002
column_t_top	0.350	-0.008	0.000	0.349	-0.006	0.000
column_t_bot	0.657	-0.046	0.002	0.656	-0.022	0.000
top_height	565.996	-0.019	0.000	565.954	-0.081	0.007

5.2.1 Load case I – DFV + blocked spillways

It can be seen in Figure 5-3 that the limit state functions have different sensitivites as one would expect. The analysis shows that the four main driving variables for the sliding reliability is the friction angle (capacity), DFV (exterior load), and lastly the bolt stress and cohesion (capacity). The figure indicates that the biggest impact on the uncertainity in terms of reliability would come from investigating the friction angle. On the other hand, the sensitvity plot for the overturning shows that the largest contributor of the uncertainity is the external load. Since the reliability is much lower for the sliding versus overturning, the focus should be on the sliding capacity.

Figure 5-4 confirms that sliding is primairly of interst, and that the failure is mainly caused by low friction angle. Thus by either increasing the mean friction angle or only reducing the variance, one would expect the realiabilty to increase based on this figure. The first case would result in an horizontal shift towards the right, while the latter case would reduce the spread of the scatter points in the horizontal axis and thereby reducing the chance of failure. One can also observe that the bolts primarily influences the overturning capacity, while the presence of a large cohesion can improve the sliding reliability.

The results in FORM have been compared with the jointplots from Crude Monte Carlo simulations. In certain cases the FORM analyses has converged wrongly, and in such situations the jointplots have been used to calibrate the starting point used in FORM. The jointplots Figure 5-6 and Figure 5-7 is in accordance with the sensitivty plots shown in Figure 5-3. Similar plots have been constructed for all of the variables and have been compared to the sensitvity plots from FORM analyses. Due to excessive amount of figures these are not included in the report, and mainly the sensitvity plots from FORM analyses are shown for the rest of the results.

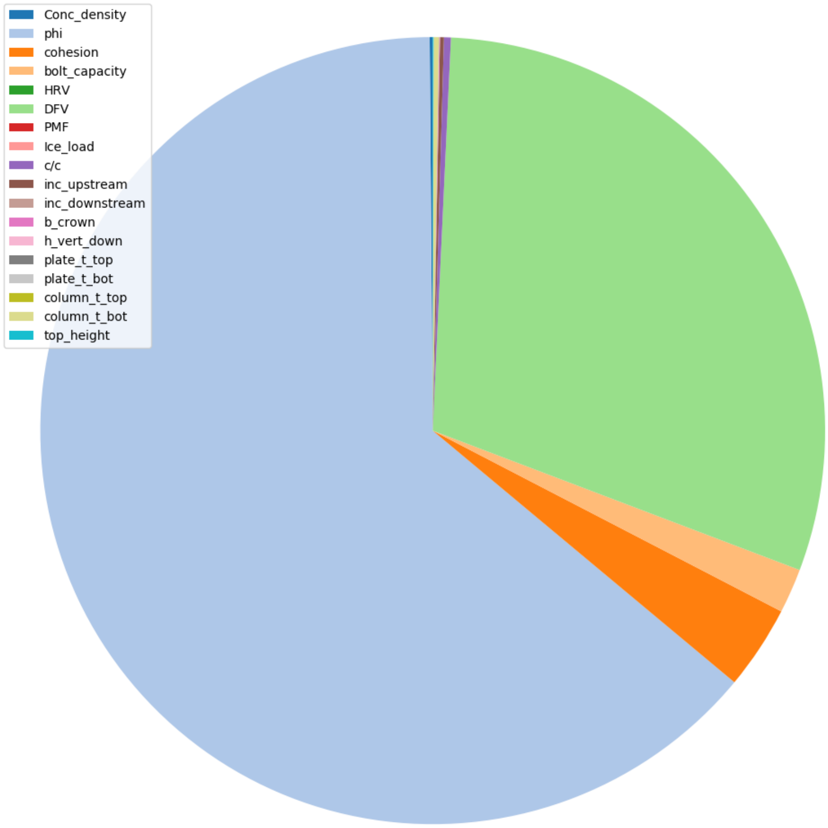

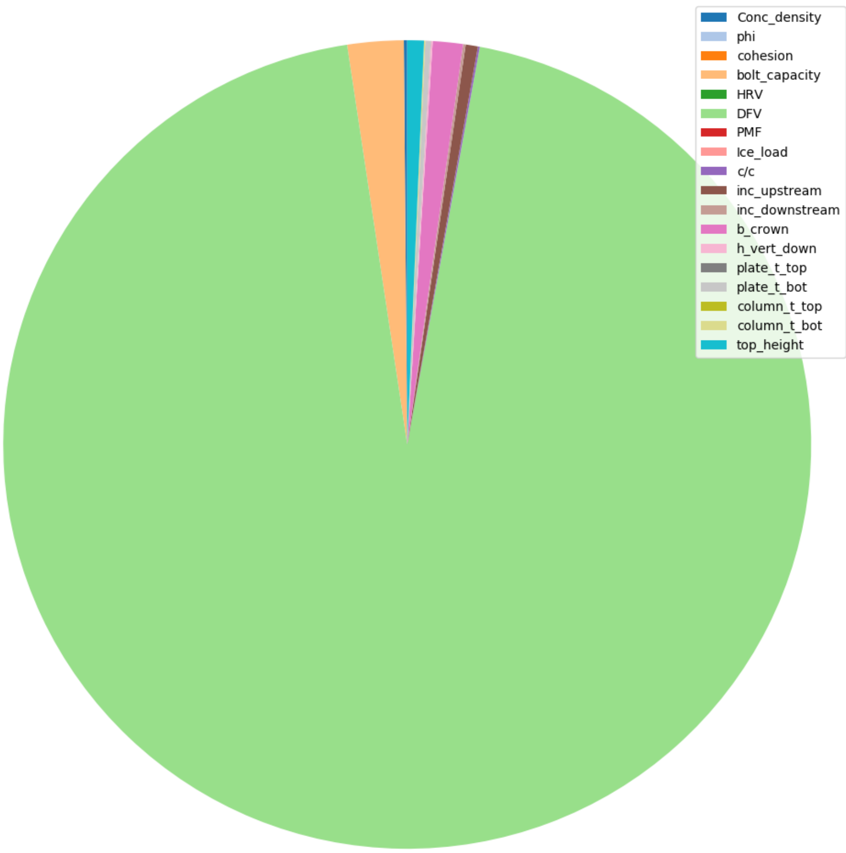

> *Figure 5-3: Sensitivity plots of basic variables (a) Sliding, (b) Overturning for load case I.*

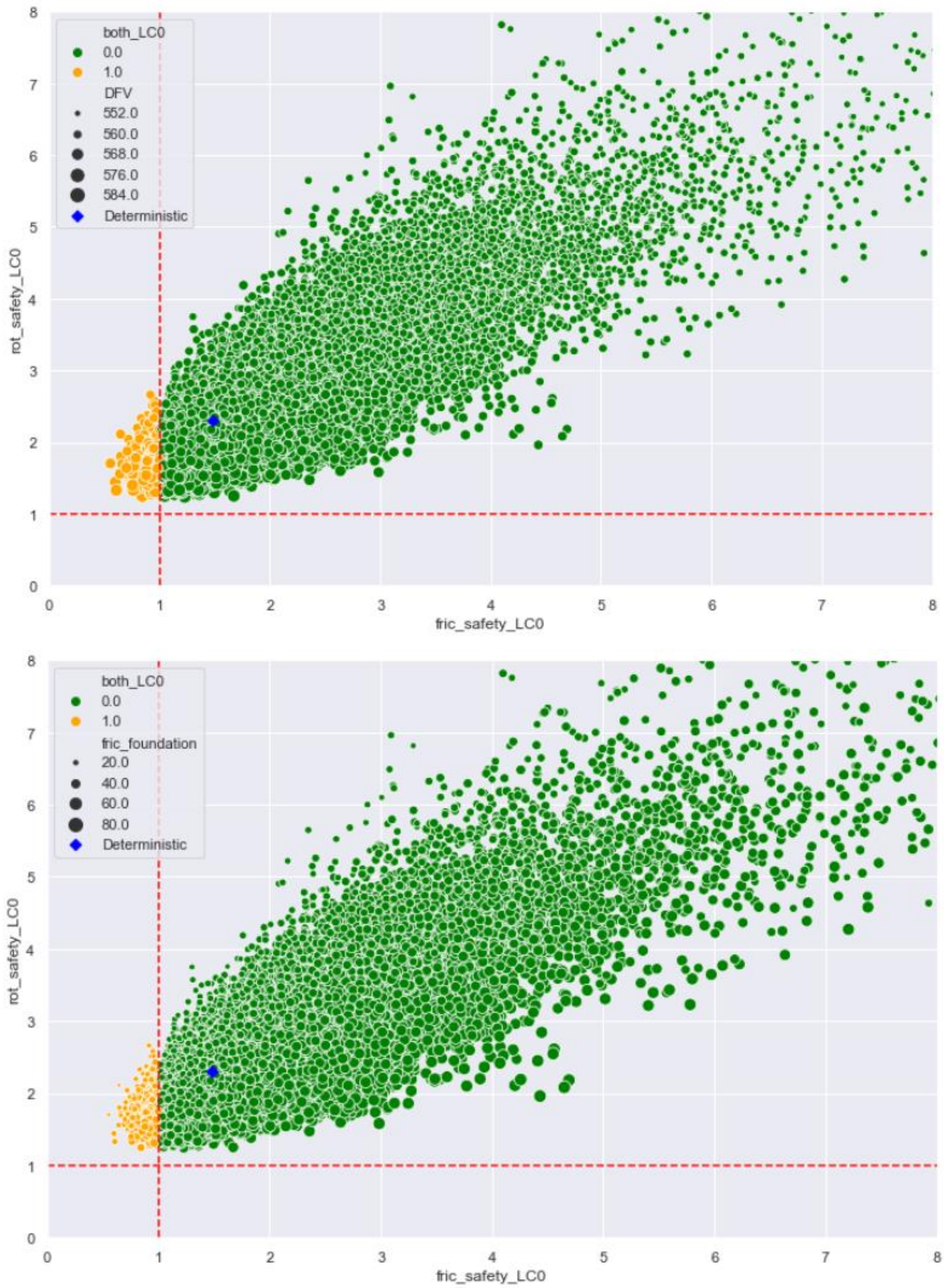

> *Figure 5-4: Safety factor from Monte Carlo simulations (a) DFV, (b) Friction angle for load case I.*

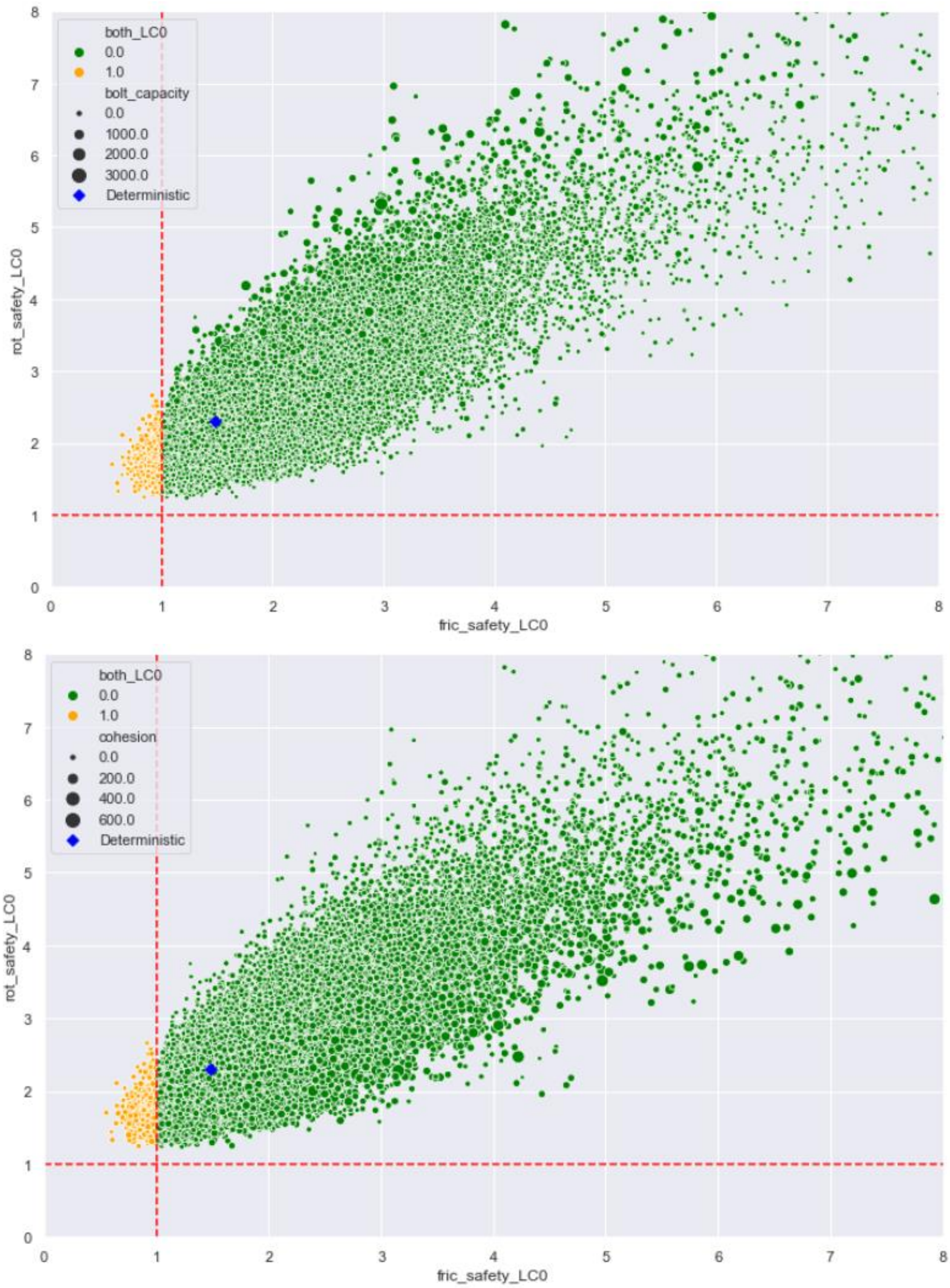

> *Figure 5-5: Safety factor from Monte Carlo simulations (a) Bolt stress, (b) Cohesion for load case I.*

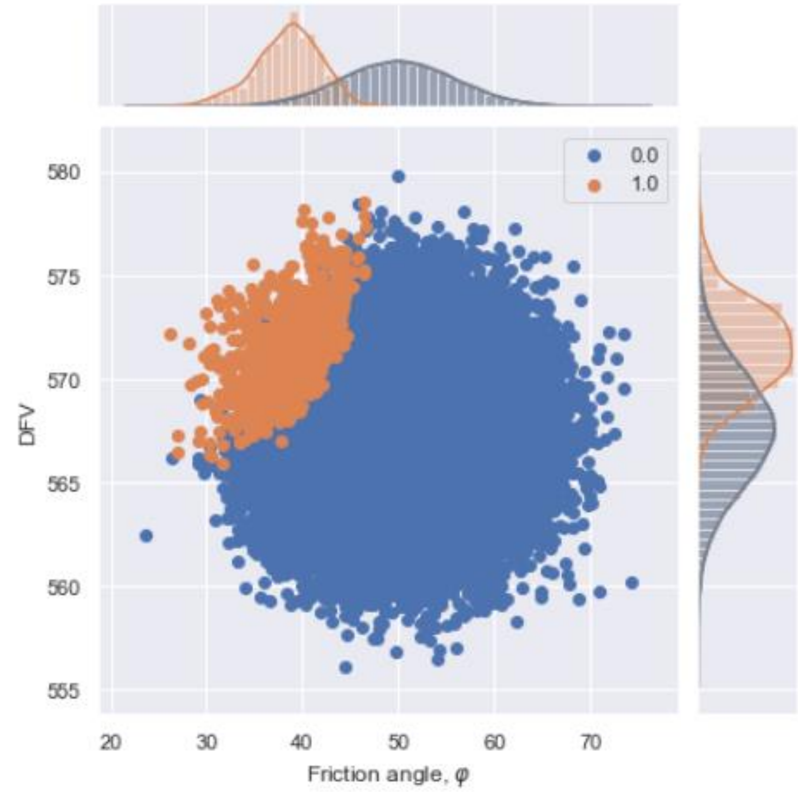

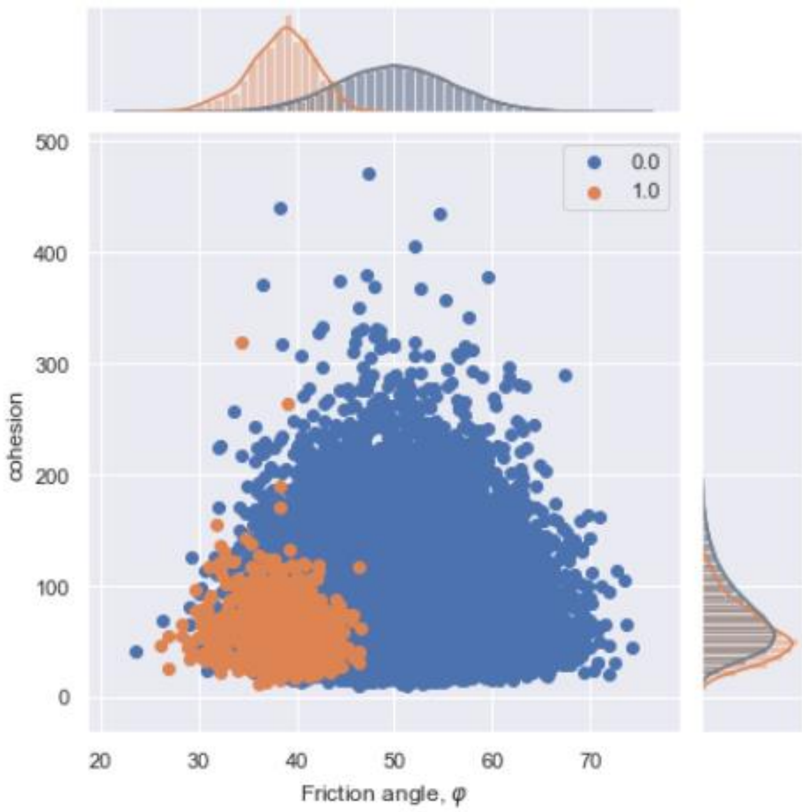

> *Figure 5-6: Jointplot from Monte Carlo simulations for load case I.*

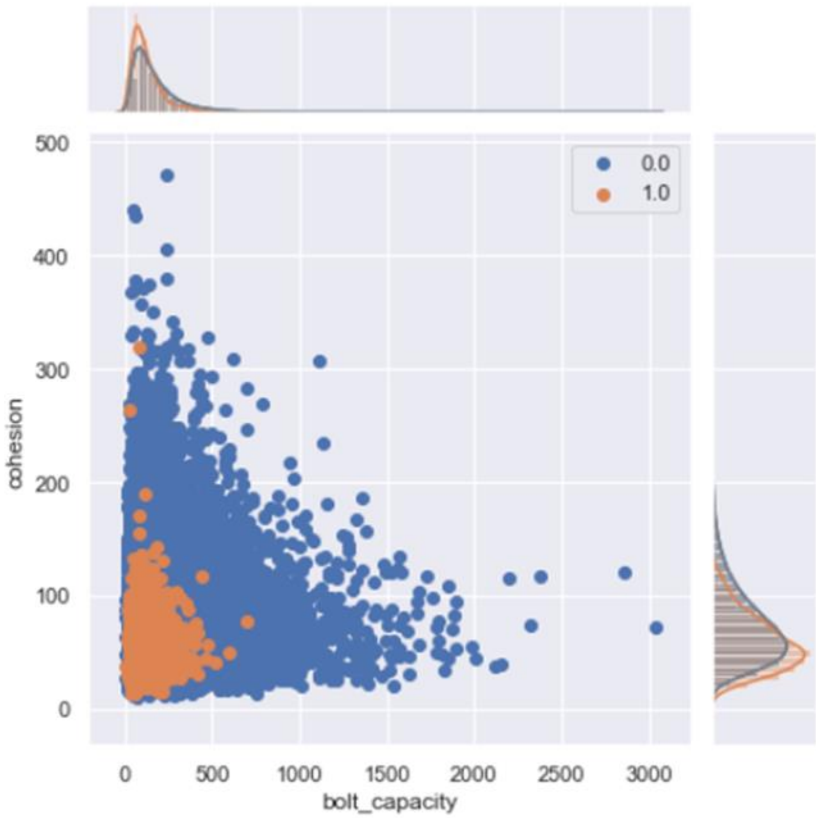

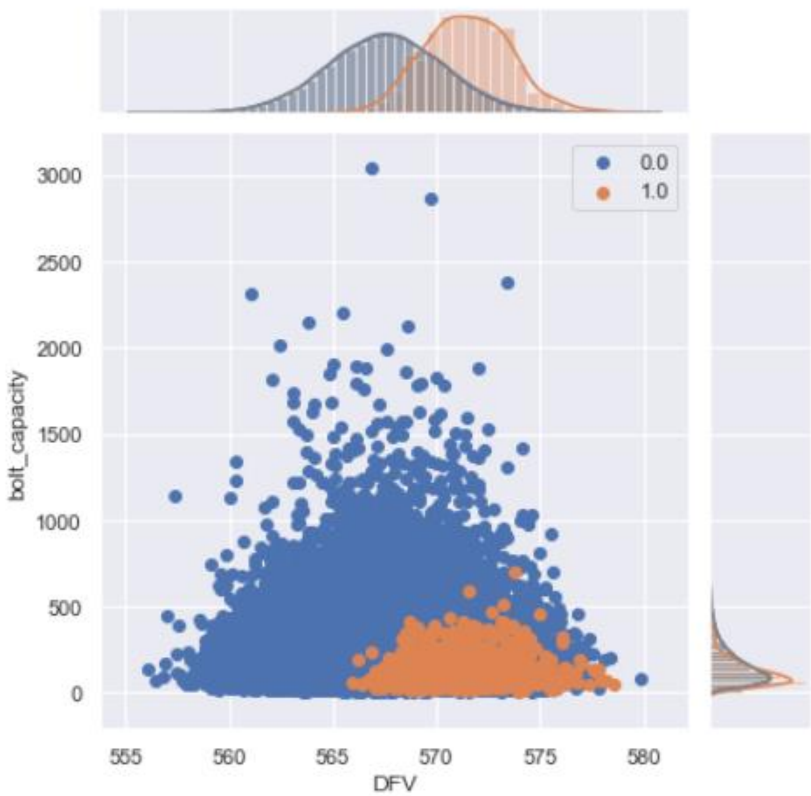

> *Figure 5-7: Jointplot from Monte Carlo simulations for load case I.*

5.2.2 Load case II – Ice load + HRV

When the ice load is truncated, the main contributors to the uncertainty are the friction angle for sliding, and the ice load and HRV for both sliding and overturning as indicated with bold text in Table 5-4. One can also observe in Figure 5-9 that the ice load has the highest impact on the overturning. Similarly, the HRV has a high impact on the overturning since the position of the ice load is determined by the water level. One can thus for load case I conclude the investigating the friction angle will improve the reliability. Furthermore, improved knowledge of the ice load and HRV can also increase the reliability.

> *Table 5-4: Summary of value at MPP, gradient vector and sensitivity values for load case II using FORM.*

	Sliding			Overturning		
Variables	x_{MPP}	α_i	α_i^2	x_{MPP}	α_i	α_i^2
Conc_density	23.939	-0.043	0.002	23.685	-0.088	0.008
phi	**41.022**	**-0.703**	**0.494**	50.006	-0.000	0.000
cohesion	55.370	-0.191	0.037	67.120	-0.000	0.000
bolt_capacity	103.607	-0.161	0.026	48.952	-0.249	0.062
HRV	**566.974**	**0.322**	**0.104**	**571.748**	**0.761**	**0.579**
Ice_load	**137.199**	**0.573**	**0.329**	**241.362**	**0.506**	**0.256**
c/c	5.033	0.061	0.004	5.086	0.065	0.004
inc_upstream	0.799	-0.036	0.001	0.793	-0.168	0.028
inc_downstream	0.330	-0.004	0.000	0.329	-0.045	0.002
b_crown	1.996	-0.020	0.000	1.916	-0.157	0.025
h_vert_down	1.501	0.005	0.000	1.515	0.038	0.001
plate_t_top	0.300	-0.010	0.000	0.298	-0.021	0.000
plate_t_bot	0.600	0.001	0.000	0.607	0.045	0.002
column_t_top	0.350	-0.009	0.000	0.349	-0.014	0.000
column_t_bot	0.656	-0.052	0.003	0.651	-0.052	0.003
top_height	565.993	-0.030	0.001	565.905	-0.170	0.029

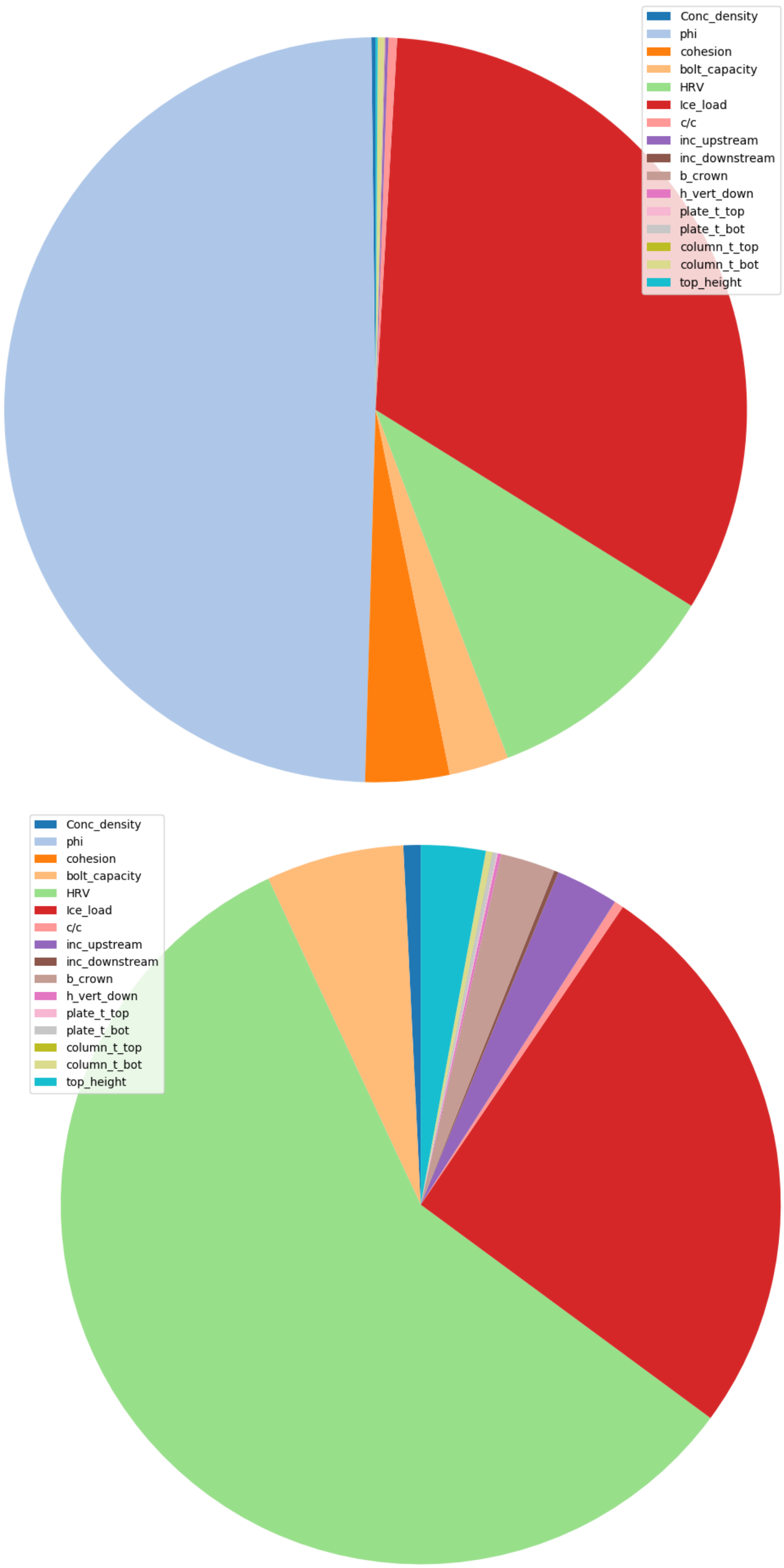

> *Figure 5-8: Sensitivity plots of basic variables (a) Sliding, (b) Overturning for load case II.*

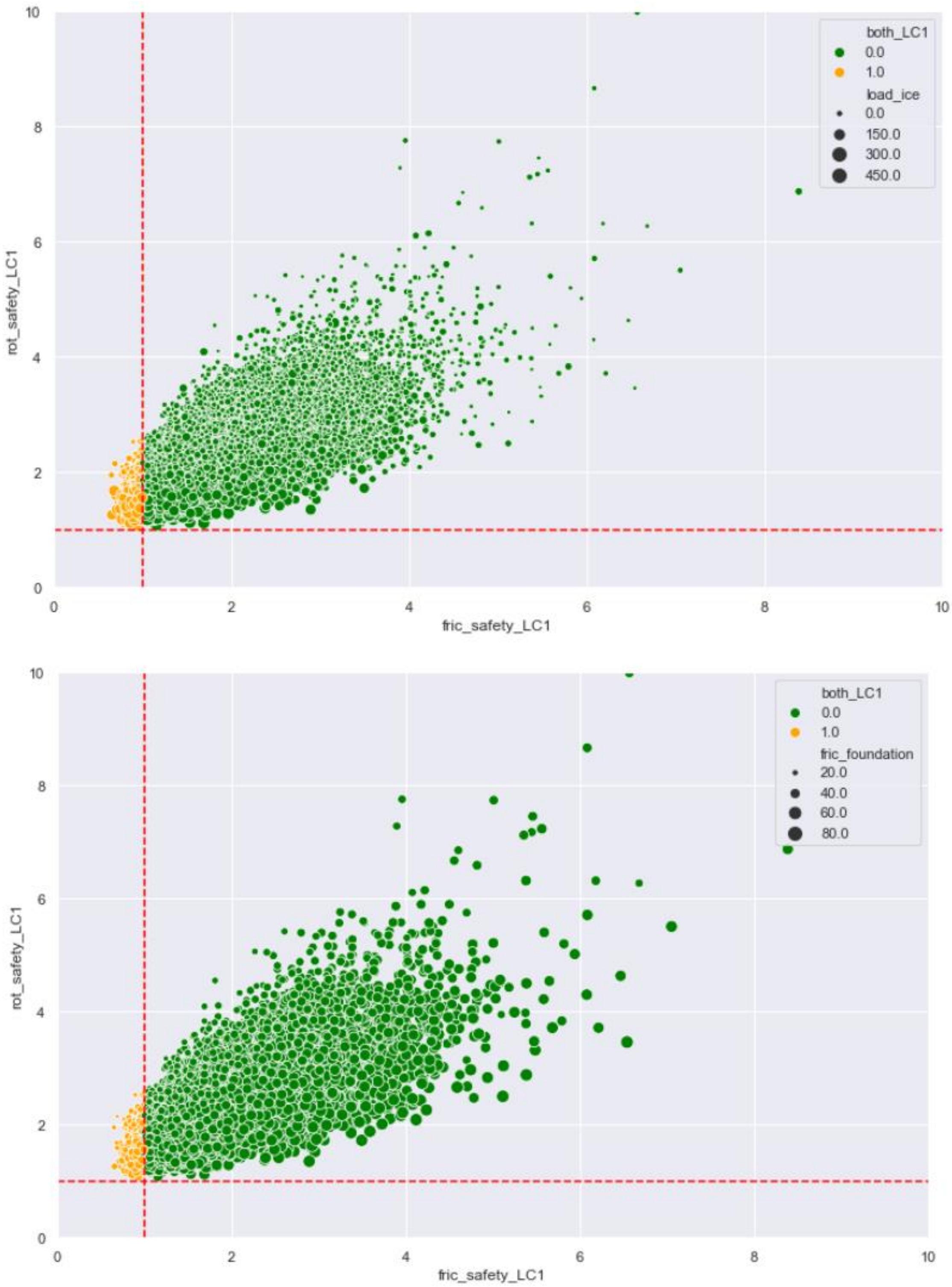

> *Figure 5-9: Safety factor from Monte Carlo simulations (a) Ice load, (b) Friction angle for load case II.*

5.2.3 Load case IV – PMF

Since this is an ALS situation one would normally accept a higher probability of failure since the event in itself is unlikely. Note that the results are similar as for Load case I and II and shows the importance of comparing the reliability with the correct target values.

The sensitivity plot in Figure 5-10 also shows that the friction angle and the exterior load MFV are the driving variables for the uncertainty. One can thus conclude form the previous load cases that in order to improve the reliability of the structure, attention should be given to the sliding capacity. By testing the friction angle and cohesion, studying the macro-asperities, and possibly including the shear capacity of the slab one would expect to achieve a much higher reliability against sliding.

One can also note that the MPP value of PMF is well above the calculated MFV in the flood report for overturning. This indicates that the reliability can be even higher due to stabilizing effect from possible tail water. In the case of sliding the most probable water level which causes failure is about 3 m above the calculated MFV in the flood report. The variables with the highest uncertainties are shown with bold text in Table 5-5.

> *Table 5-5: Summary of value at MPP, gradient vector and sensitivity values for load case IV using FORM.*

	Sliding			**Overturning**		
Variables	x_{MPP}	α_i	α_i^2	x_{MPP}	α_i	α_i^2
Conc_density	23.956	-0.035	0.001	23.869	-0.037	0.001
phi	**40.778**	**-0.804**	**0.646**	50.006	-0.000	0.000
cohesion	56.838	-0.184	0.034	67.120	-0.000	0.000
bolt_capacit	110.426	-0.136	0.018	72.555	-0.151	0.023
HRV	566.001	-0.000	0.000	566.001	-0.000	0.000
DFV	567.613	-0.000	0.000	567.613	-0.000	0.000
PMF	**570.758**	**0.542**	**0.293**	**582.676**	**0.973**	**0.947**
Ice_load	54.513	-0.000	0.000	55.125	-0.000	0.000
c/c	5.026	0.053	0.003	5.037	0.028	0.001
inc_upstream	0.799	-0.040	0.002	0.797	-0.070	0.005
inc_downstre	0.330	-0.004	0.000	0.329	-0.032	0.001
b_crown	1.997	-0.017	0.000	1.941	-0.110	0.012
h_vert_down	1.501	0.004	0.000	1.511	0.027	0.001
plate_t_top	0.300	-0.008	0.000	0.299	-0.009	0.000
plate_t_bot	0.600	0.007	0.000	0.607	0.046	0.002
column_t_top	0.350	-0.008	0.000	0.349	-0.006	0.000
column_t_bot	0.657	-0.046	0.002	0.656	-0.022	0.000
top_height	565.996	-0.019	0.000	565.954	-0.081	0.007

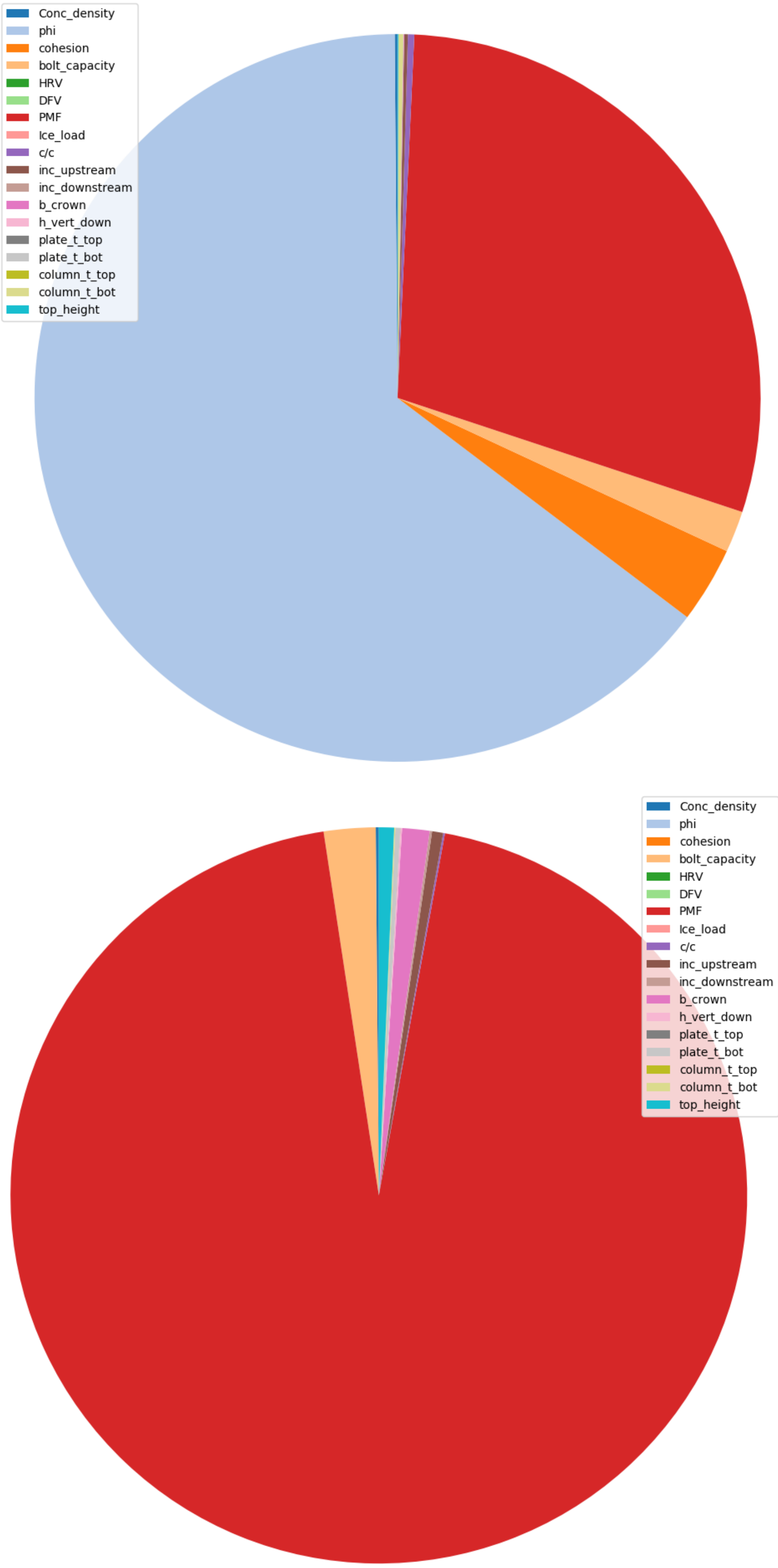

> *Figure 5-10: Sensitivity plots of basic variables (a) Sliding, (b) Overturning for load case IV.*

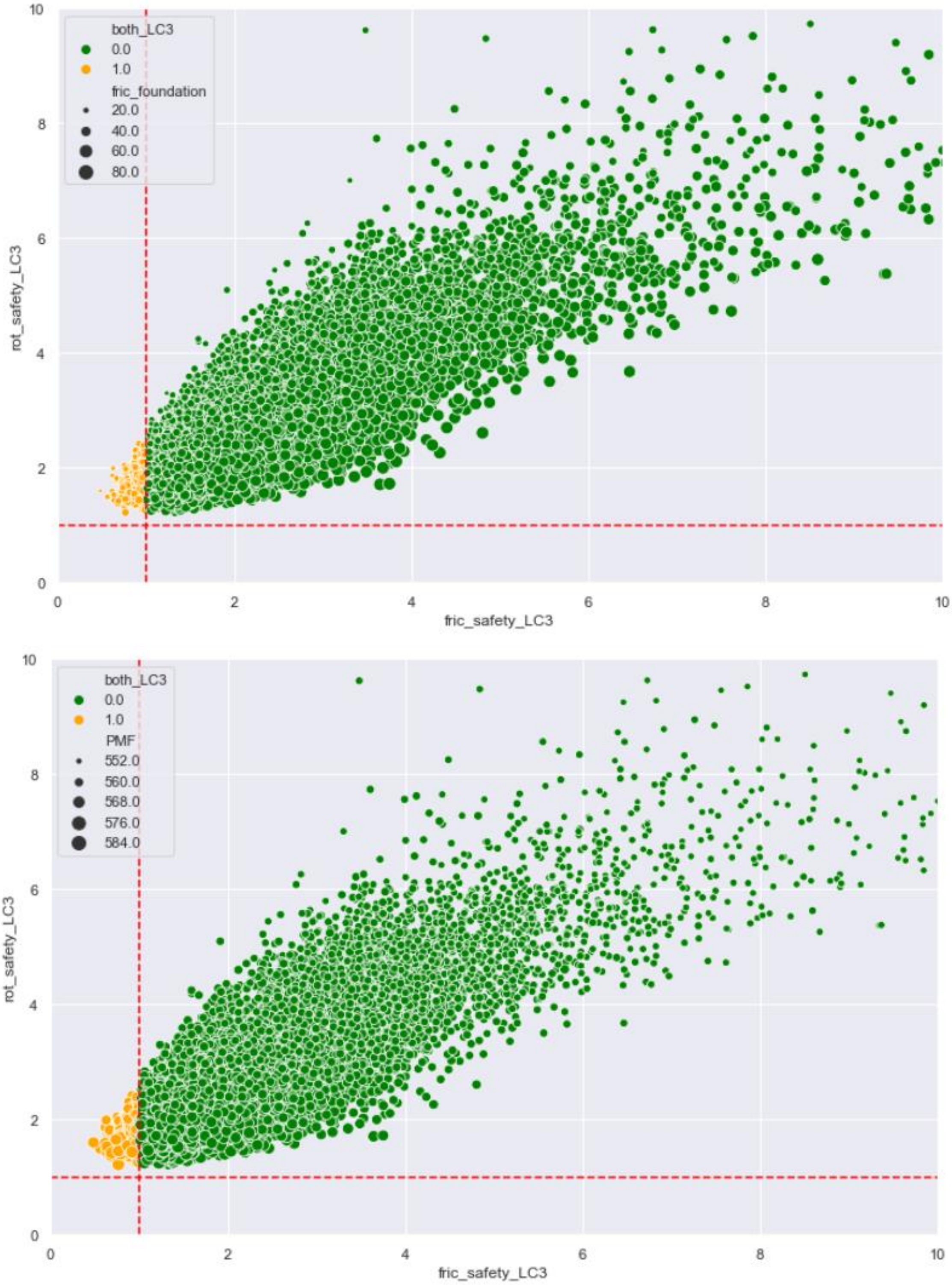

> *Figure 5-11: Safety factor from Monte Carlo simulations (a) Friction angle, (b) MFV/PMF load case IV.*

5.3 P.47 – Non truncated ice load

This analysis was chosen for comparison due to its simplicity in modelling the ice load. As mentioned in section 3.3, the truncation of the ice load can be challenging depending on the software. One may thus be tempted to run probabilistic analyses without truncating the distribution. Furthermore, the results will show how the truncation will influence the reliability and whether additional attention should be given to this effect if included.

The values shown in Table 5-6 shows that similar results are achieved for the load cases I and IV as in the base case and is therefore not further discussed. It can be seen for load case II that the truncation does in fact influence the result both for the sliding and overturning. The most probable ice load calculated by FORM with respect to overturning is 434.8 kN/m compared to 241.4 kN/m with truncation. This shows that the expected value prior to truncation is considerably higher. One can thus conclude that the truncation of the distribution is of high importance when considering ice loads in probabilistic dam analyses.

Figure 5-12 and Figure 5-13 both shows that the uncertainty of ice load is indeed of high importance for the reliability and it majorly affects the reliability of overturning. Although truncation of the ice load due to buckling is a reasonable assumption, the phenomenon is arguably not sufficiently well enough understood. Thus, by including this in the calculations one should be well aware of its limitations and how it effects the calculated reliability.

> *Table 5-6: Summary of calculated probability of failure and corresponding reliability index.*

	LOAD COMBINATION	FORM OVERTURNING	FORM SLIDING	CRUDE MONTE CARLO
I	**DFV + clogged spillways (ULS)**	$p_f = 2.5e-8$ $\beta = 5.449$	$p_f = 0.0254$ $\beta = 1.953$	$p_f = 0.0176$ $\beta = 2.1063$
II	**HRV + Ice load (ULS)**	$p_f = 0.0065$ $\beta = 2.4852$	$p_f = 0.0242$ $\beta = 1.974$	$p_f = 0.0286$ $\beta = 1.901$
IV	**MFV (ALS)**	$p_f = 3.7e-8$ $\beta = 5.379$	$p_f = 0.0278$ $\beta = 1.914$	$p_f = 0.0195$ $\beta = 2.0653$

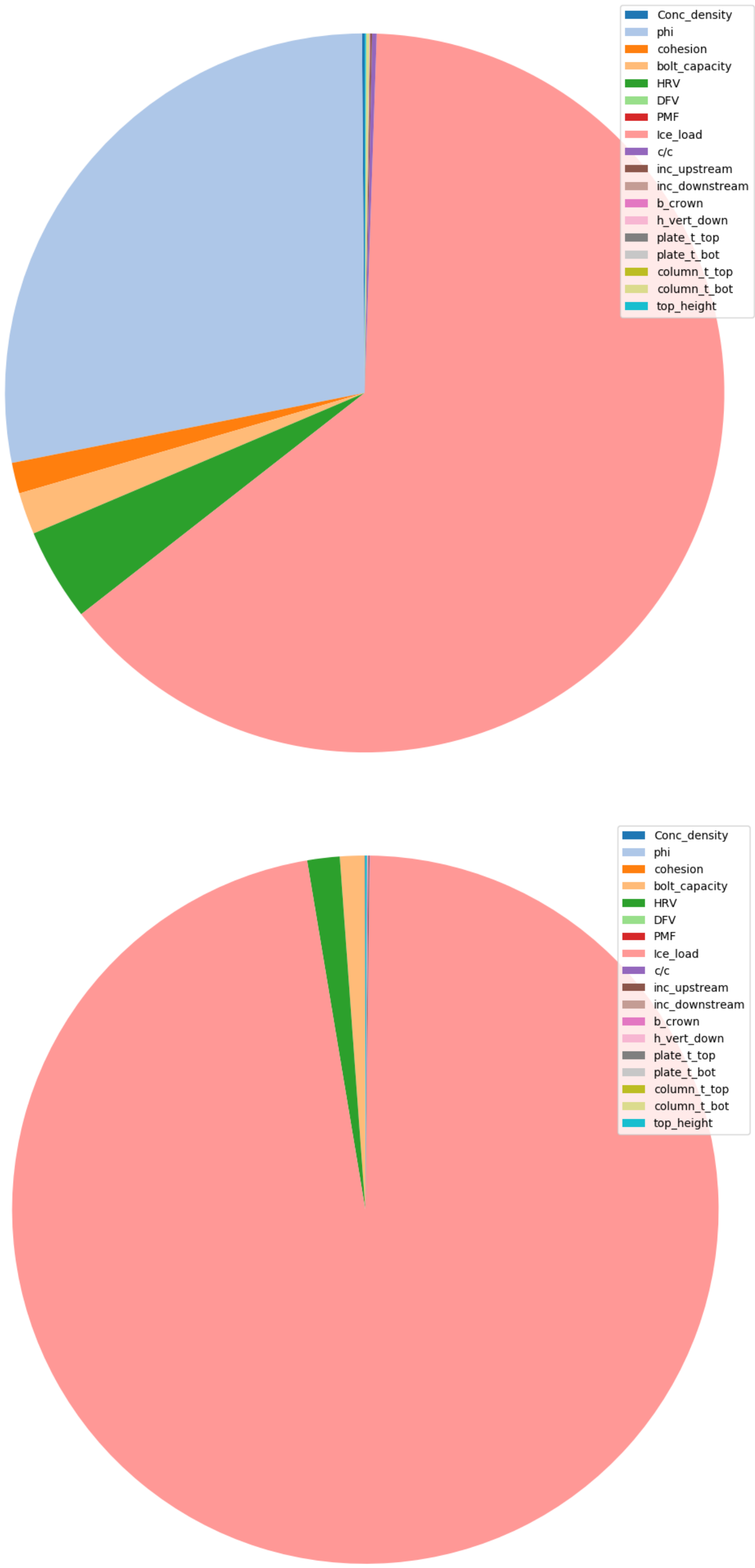

> *Figure 5-12: Sensitivity plots of basic variables (a) Sliding, (b) overturning for load case II.*

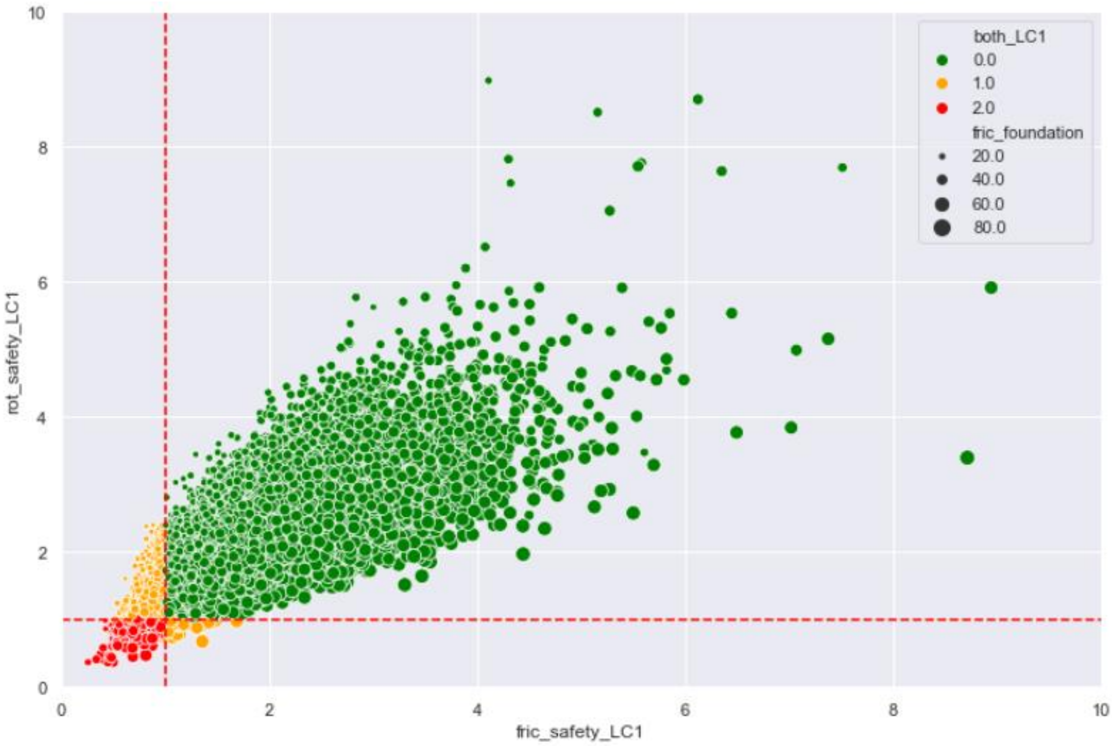

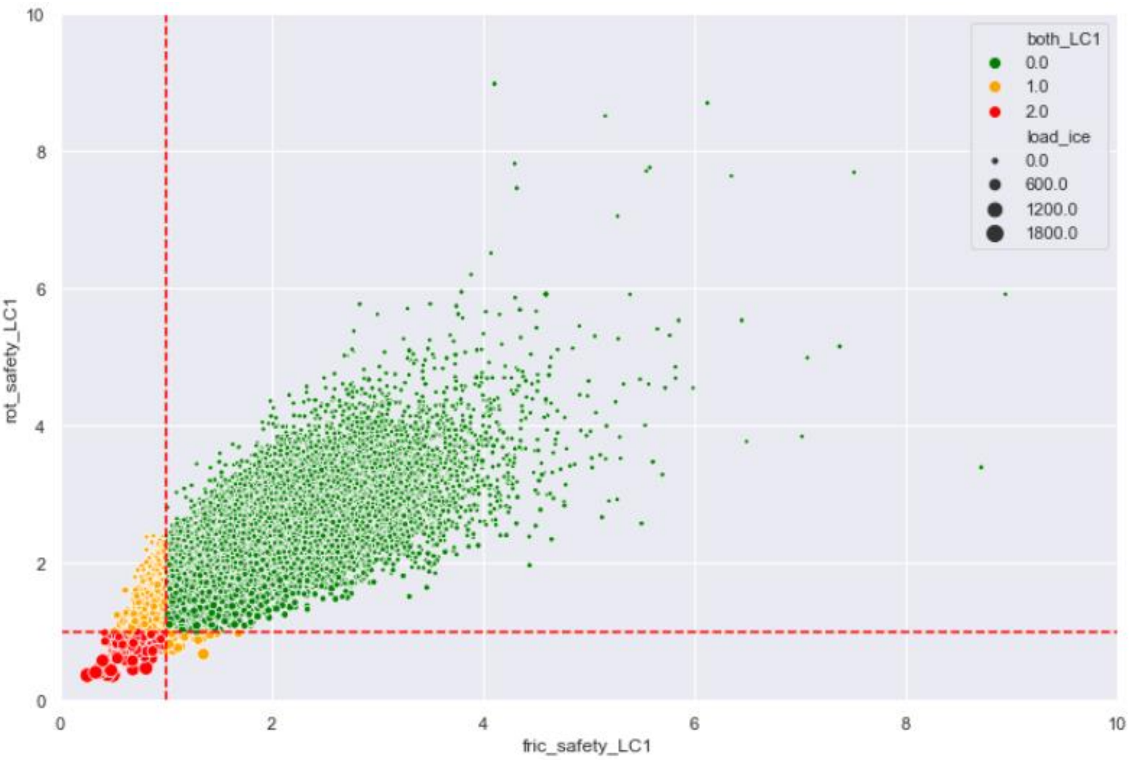

> *Figure 5-13: Safety factor from Monte Carlo simulations (a) Friction angle, (b) ice load for load case II.*

5.4 P.47 – Ice load distribution with low variance

Since the proposed ice load distribution in PMCD gives much higher ice-loads than compared to the guidelines used in Norway, a simple fix is to reduce the variance as with dam Hensfoss (Norconsult, 2018). The reduced variance improves the reliability considerably as can be seen in Table 5-7, especially for overturning.

The sensitivity plots from FORM analyses in Figure 5-14 shows that the uncertainty in sliding caused by ice load is negligible and is of less importance then the HRV for overturning. Figure 5-15 also confirms that the ice load is of less importance for the calculated reliability. Although the stochastic ice load described here more appropriately reflects the Norwegian guidelines for ice load, it's difficult to validate this load since the basis is not publicly available. It's expected that further research of the ice load mechanism, at i.e. Norut, will improve our knowledge.

> *Table 5-7: Summary of calculated probability of failure and corresponding reliability index.*

	LOAD COMBINATION	FORM OVERTURNING	FORM SLIDING	CRUDE MONTE CARLO
I	**DFV + clogged spillways (ULS)**	$p_f = 2.5e-8$ $\beta = 5.4495$	$p_f = 0.0254$ $\beta = 1.953$	$p_f = 0.0174$ $\beta = 2.110$
II	**HRV + Ice load (ULS)**	$p_f \approx 0$ $\beta = 12.62$	$p_f = 0.0067$ $\beta = 2.471$	$p_f = 0.0101$ $\beta = 2.321$
IV	**MFV (ALS)**	$p_f = 3.7e-8$ $\beta = 5.379$	$p_f = 0.028$ $\beta = 1.914$	$p_f = 0.0194$ $\beta = 2.0671$

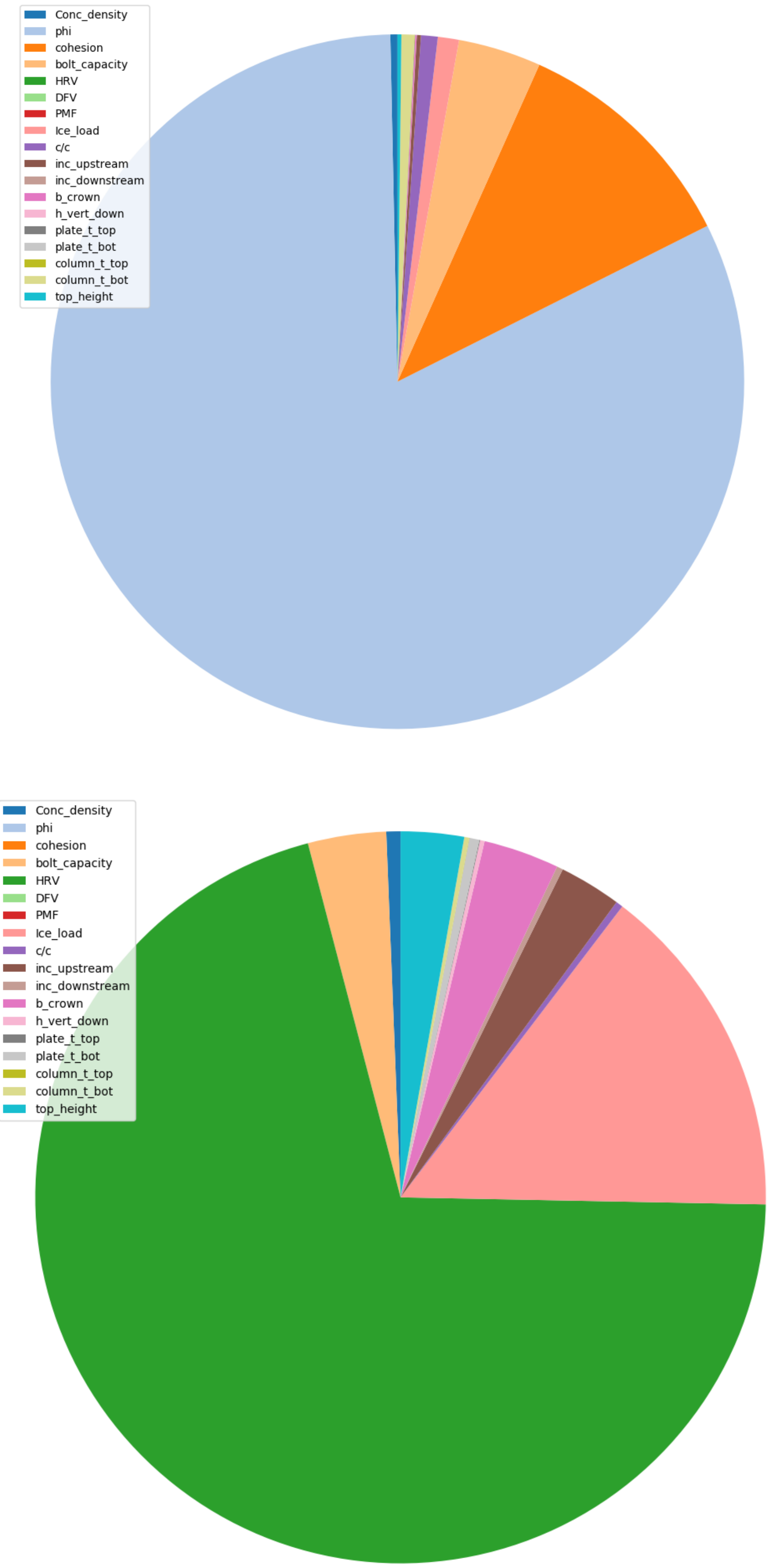

> *Figure 5-14: Sensitivity plots of basic variables (a) Sliding, (b) Overturning for load case II.*

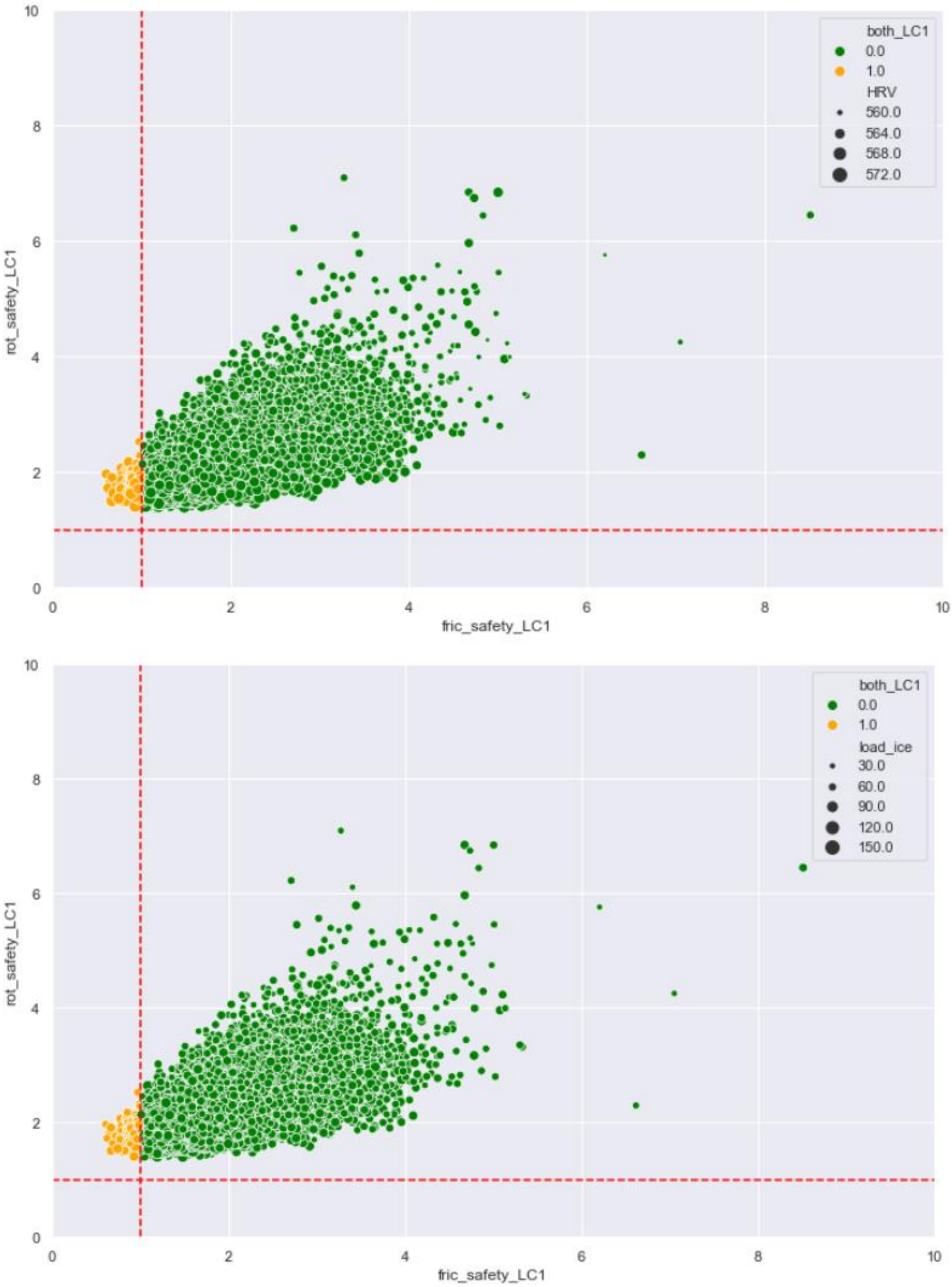

> *Figure 5-15: Safety factor from Monte Carlo simulations (a) Friction angle, (b) ice load for load case II.*

5.5 P.47 – No contribution from rock bolt

In the case of no rock bolts, one can observe in Table 5-8 that the reliability reduces as expected. The change is subjectively judged to be small and indicates that there are other variables that are more important to the structural reliability.

> *Table 5-8: Summary of calculated probability of failure and corresponding reliability index.*

	LOAD COMBINATION	FORM OVERTURNING	FORM SLIDING	CRUDE MONTE CARLO
I	**DFV + clogged spillways (ULS)**	$p_f = 1.1e-7$ $\beta = 5.1853$	$p_f = 0.0401$ $\beta = 1.748$	$p_f = 0.0311$ $\beta = 1.864$
II	**HRV + Ice load (ULS)**	$p_f = 7.0e-7$ $\beta = 4.825$	$p_f = 0.0436$ $\beta = 1.710$	$p_f = 0.0290$ $\beta = 1.895$
IV	**MFV (ALS)**	$p_f = 1.6e-7$ $\beta = 5.114$	$p_f = 0.030$ $\beta = 1.880$	$p_f = 0.0340$ $\beta = 1.825$

5.6 P.47 – No cohesion

It can be seen in Table 5-9 that the cohesion does in fact contribute to the sliding reliability considerably, compared to rock bolts. The cohesion is according to common practice neglected due to its uncertainty. However, with probabilistic methods this can be accounted for and considerably improve the reliability against sliding.

> *Table 5-9: Summary of calculated probability of failure and corresponding reliability index.*

	LOAD COMBINATION	FORM OVERTURNING	FORM SLIDING	CRUDE MONTE CARLO
I	**DFV + clogged spillways (ULS)**	$p_f = 2.5e-8$ $\beta = 5.4495$	$p_f = 0.070$ $\beta = 1.475$	$p_f = 0.0542$ $\beta = 1.605$
II	**HRV + Ice load (ULS)**	$p_f = 4.8e-8$ $\beta = 5.3354$	$p_f = 0.056$ $\beta = 1.589$	$p_f = 0.0543$ $\beta = 1.605$
IV	**MFV (ALS)**	$p_f = 3.7e-8$ $\beta = 5.379$	$p_f = 0.074$ $\beta = 1.443$	$p_f = 0.0583$ $\beta = 1.569$

5.7 P.47 – Extreme value water level distribution

As previously mentioned, the variance on the water level used in the base case is extremely unrealistic. This leads to an overall low calculated structural reliability. In order to improve the analysis, one could therefore reduce the variance of the water level. The question would then rather be "What is the variance of the estimated design flood?". But the design flood is in fact tied to a stochastic process as discussed in section 3.1, and the method of utilizing a return period is semi-probabilistic approach (Melchers & Beck, 2018). The method proposed here is therefore to relate the measured water level on-site to the flooding probability using extreme value theory.

The method for determining the extreme water level distribution is described in section 3.2.2. One should note that this is one alternative method than the one proposed in PMCD, and there might be unknown issues which makes this method unsuitable for probabilistic analysis.

The results in Table 5-10 clearly shows that the reliability is improved using these assumptions. However, this is believed to be primarily caused by the reduction of both the mean value and the variance, rather than the method itself.

Figure 5-16 shows that the spread in result is much lower compared the ones in Figure 5-4. Furthermore, one can see in Figure 5-17 that the uncertainty caused by the assumed water level is of much lower interest compared to the friction angle and cohesion.

> *Table 5-10: Summary of calculated probability of failure and corresponding reliability index.*

	LOAD COMBINATION	FORM OVERTURNING	FORM SLIDING	CRUDE MONTE CARLO
I	**DFV + clogged spillways (ULS)**	$p_f \approx 0$ $\beta = 8.372$	$p_f = 0.0007$ $\beta = 3.183$	$p_f = 0.0006$ $\beta = 3.263$
II	**HRV + Ice load (ULS)**	$p_f \approx 0$ $\beta = 9.830$	$p_f = 0.0086$ $\beta = 2.383$	$p_f = 0.0049$ $\beta = 2.583$
IV	**MFV (ALS)**	$p_f \approx 0$ $\beta = 31.52$	$p_f = 0.0076$ $\beta = 2.430$	$p_f = 0.0054$ $\beta = 2.549$

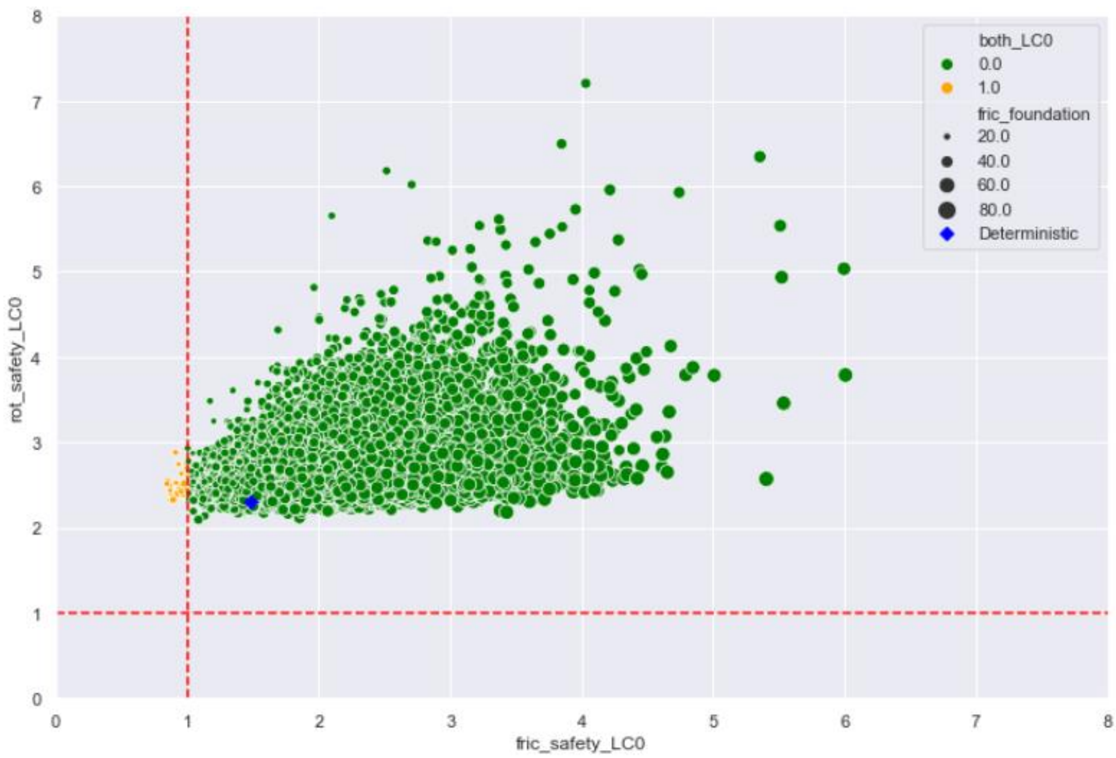

> *Figure 5-16: Safety factor from Monte Carlo simulations of friction angle for load case I.*

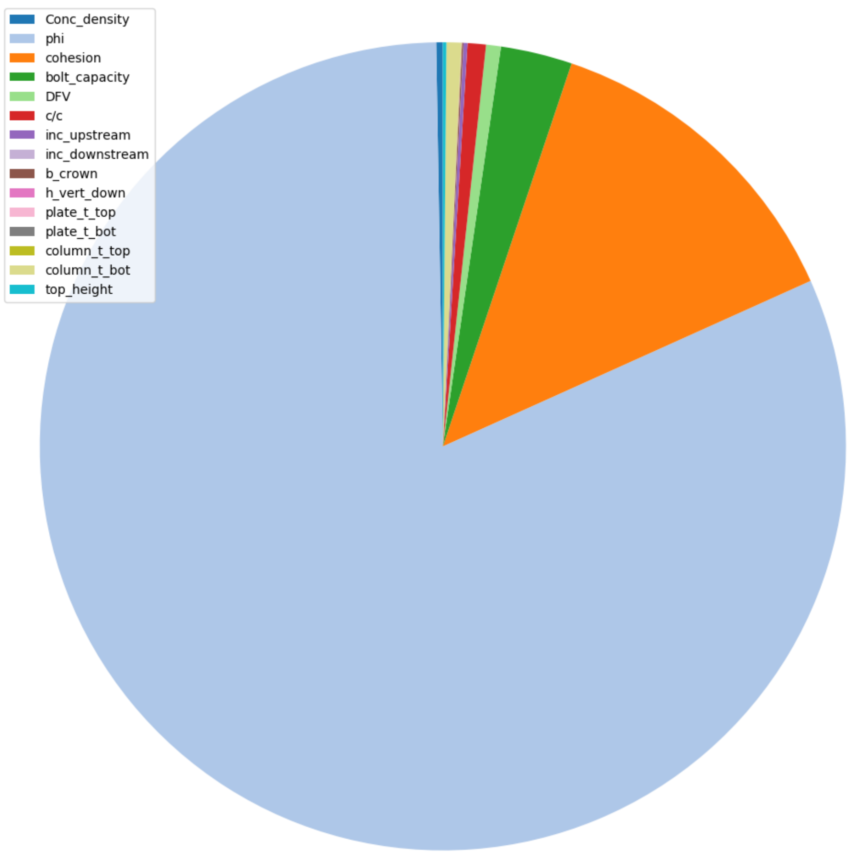

> *Figure 5-17: Sensitivity plots of basic variables of sliding for load case I.*

5.8 P.47 – Thought experiment - Friction test combined with extreme water level distribution

It's common in practice to assume that testing materials will result in a higher capacity, since one can be less conservative in the parameter estimation. In the case of friction coefficient this might not necessarily be the case for dam stability. The purpose of this analysis is to show that even though the mean value of the friction angle is reduced due to some hypothetical testing, the increased certainty of this value can still lead to improved results in the calculated reliability.

It's here assumed that the extreme water level distribution from section 5.7 is valid. The results in Table 5-11 shows that the sliding is substantially improved for load case I and IV. In the case of load case II the limiting variable is now the ice load which can be seen in Figure 5-18.

> *Table 5-11: Summary of calculated probability of failure and corresponding reliability index.*

	LOAD COMBINATION	FORM OVERTURNING	FORM SLIDING	CRUDE MONTE CARLO
I	**DFV + clogged spillways (ULS)**	$p_f \approx 0$ $\beta = 9.169$	$p_f = 2.5e-6$ $\beta = 4.562$	$p_f = 2e-6$ $\beta = 4.611$
II	**HRV + Ice load (ULS)**	$p_f \approx 0$ $\beta = 9.740$	$p_f = 0.007$ $\beta = 2.425$	$p_f = 0.0045$ $\beta = 2.613$
IV	**MFV (ALS)**	$p_f \approx 0$ $\beta = 21.17$	$p_f = 0.0005$ $\beta = 3.297$	$p_f = 0.0005$ $\beta = 3.282$

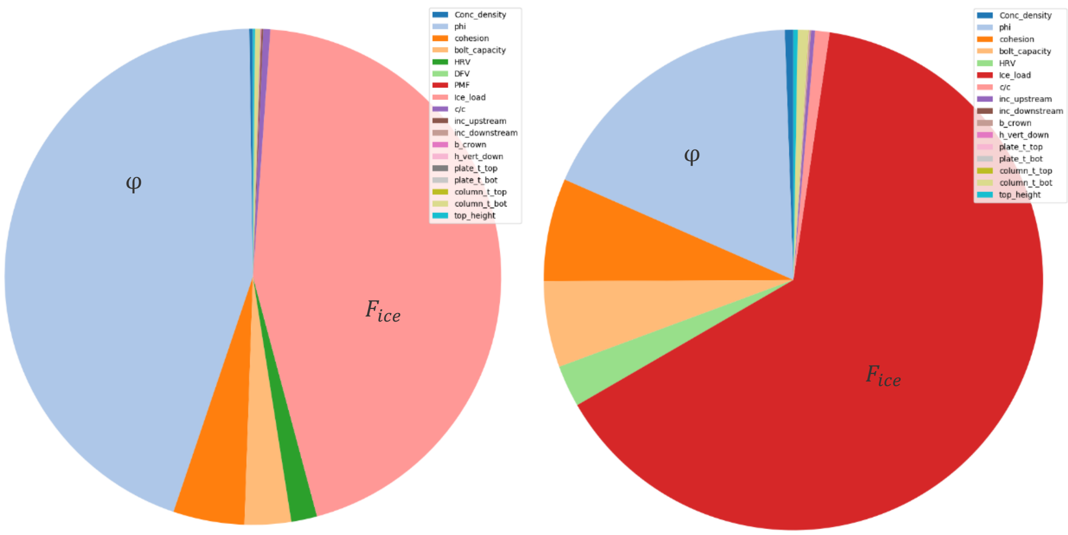

> *Figure 5-18: Sensitivity plots of basic variables of sliding for load case II (a) before and (b) after friction testing.*

5.9 P.55

The results for cross-section P.55 are similar to the ones obtained at P.47. The results are thus not further discussed here and simply summarized in Table 5-12 to Table 5-17.

5.9.1 Base case

> *Table 5-12: Summary of calculated probability of failure and corresponding reliability index.*

	LOAD COMBINATION	FORM OVERTURNING	FORM SLIDING	CRUDE MONTE CARLO
I	**DFV + clogged spillways (ULS)**	$p_f = 4.4e-5$ $\beta = 3.923$	$p_f = 0.0250$ $\beta = 1.961$	$p_f = 0.0167$ $\beta = 2.127$
II	**HRV + Ice load (ULS)**	$p_f = 0.0096$ $\beta = 2.340$	$p_f = 0.0460$ $\beta = 1.685$	$p_f = 0.0382$ $\beta = 1.772$
IV	**MFV (ALS)**	$p_f = 5.8e-5$ $\beta = 3.853$	$p_f = 0.0277$ $\beta = 1.916$	$p_f = 0.0186$ $\beta = 2.083$

5.9.2 Non truncated ice load

> *Table 5-13: Summary of calculated probability of failure and corresponding reliability index.*

	LOAD COMBINATION	FORM OVERTURNING	FORM SLIDING	CRUDE MONTE CARLO
I	**DFV + clogged spillways (ULS)**	$p_f = 4.3e-5$ $\beta = 3.923$	$p_f = 0.0249$ $\beta = 1.961$	$p_f = 0.0165$ $\beta = 2.133$
II	**HRV + Ice load (ULS)**	$p_f = 0.035$ $\beta = 1.810$	$p_f = 0.0661$ $\beta = 1.505$	$p_f = 0.0681$ $\beta = 1.490$
IV	**MFV (ALS)**	$p_f = 5.8e-5$ $\beta = 3.853$	$p_f = 0.0277$ $\beta = 1.916$	$p_f = 0.0186$ $\beta = 2.084$

5.9.3 Ice load distribution with low variance

> *Table 5-14: Summary of calculated probability of failure and corresponding reliability index.*

	LOAD COMBINATION	FORM OVERTURNING	FORM SLIDING	CRUDE MONTE CARLO
I	**DFV + clogged spillways (ULS)**	$p_f = 4.3e-5$ $\beta = 3.923$	$p_f = 0.0250$ $\beta = 1.961$	$p_f = 0.0166$ $\beta = 2.129$
II	**HRV + Ice load (ULS)**	$p_f = 6.5e-7$ $\beta = 4.838$	$p_f = 0.0246$ $\beta = 1.967$	$p_f = 0.0168$ $\beta = 2.125$
IV	**MFV (ALS)**	$p_f = 5.8e-5$ $\beta = 3.853$	$p_f = 0.0277$ $\beta = 1.916$	$p_f = 0.0187$ $\beta = 2.082$

5.9.4 No bolts

> *Table 5-15: Summary of calculated probability of failure and corresponding reliability index.*

	LOAD COMBINATION	FORM OVERTURNING	FORM SLIDING	CRUDE MONTE CARLO
I	**DFV + clogged spillways (ULS)**	$p_f = 0.0002$ $\beta = 3.577$	$p_f = 0.0489$ $\beta = 1.655$	$p_f = 0.0380$ $\beta = 1.774$
II	**HRV + Ice load (ULS)**	$p_f = 0.030$ $\beta = 1.883$	$p_f = 0.0926$ $\beta = 1.325$	$p_f = 0.0966$ $\beta = 1.301$
IV	**MFV (ALS)**	$p_f = 0.0002$ $\beta = 3.506$	$p_f = 0.054$ $\beta = 1.610$	$p_f = 0.0416$ $\beta = 1.733$

5.9.5 No cohesion

> *Table 5-16: Summary of calculated probability of failure and corresponding reliability index.*

	LOAD COMBINATION	FORM OVERTURNING	FORM SLIDING	CRUDE MONTE CARLO
I	**DFV + clogged spillways (ULS)**	$p_f = 4.4e-5$ $\beta = 3.923$	$p_f = 0.0710$ $\beta = 1.468$	$p_f = 0.0526$ $\beta = 1.620$
II	**HRV + Ice load (ULS)**	$p_f = 0.0096$ $\beta = 2.340$	$p_f = 0.0922$ $\beta = 1.327$	$p_f = 0.0889$ $\beta = 1.347$
IV	**MFV (ALS)**	$p_f = 5.8e-5$ $\beta = 3.853$	$p_f = 0.0763$ $\beta = 1.430$	$p_f = 0.0568$ $\beta = 1.582$

5.9.6 Extreme value water level distribution

> *Table 5-17: Summary of calculated probability of failure and corresponding reliability index.*

	LOAD COMBINATION	FORM OVERTURNING	FORM SLIDING	CRUDE MONTE CARLO
I	**DFV + clogged spillways (ULS)**	$p_f \approx 0$ $\beta = 10.35$	$p_f = 4.5e-5$ $\beta = 3.918$	$p_f = 3e-5$ $\beta = 4.013$
II	**HRV + Ice load (ULS)**	$p_f = 0.0015$ $\beta = 2.972$	$p_f = 0.0283$ $\beta = 1.906$	$p_f = 0.0199$ $\beta = 2.056$
IV	**MFV (ALS)**	$p_f \approx 0$ $\beta = 15.54$	$p_f = 0.0029$ $\beta = 2.755$	$p_f = 0.0019$ $\beta = 2.889$

6 CONCLUSION

6.1 Results

The deterministic results show that the safety factor against sliding is generally low, which is confirmed by the probabilistic analyses. For the slab buttress dam, Eikrebekken, the reliability can be improved considerably by increasing the knowledge of the sliding failure mode in the interface between dam structure and foundation.

In general, the proposed ice loads for probabilistic analyses in PMCD gives high loads compared to the Norwegian guidelines. It is also shown that the truncation is of large importance since it skews the result in a non-conservative direction. Thus, further study of the stochastic process of ice load is required.

An approach for determining the design flood level based on extreme value theory from data on site is proposed with the assumption $Q_{in} = Q_{out}$. The calculations show that by decreasing the uncertainty of the water level, the reliability is improved.

6.2 Further work

The calculation model used in the analyses is limited and based on the limit equilibrium. There are limitations to the geometry (no cut-outs and etc) which is a source of failure in the calculations. Furthermore, it's known that the ice load is deformation controlled, and it thus recommended to study this effect with numerical methods like Finite Element.

Target values for the reliability needs to be defined in order to document capacity with probabilistic design. This also requires that the underlaying assumptions tied to the target values needs to be defined. Examples are the calculation method stochastic flood level, contribution from rock bolts and cohesion, etc.

Since the reliability of the structure changes with time due to increased knowledge of the structure, requirements in the regulations and a due to general degradation of the structure, one could possibly relate this to a "bathtube curve" which is more common for reliability of components. By defining appropriate hazard curve for degradation, and similar curves for improvements, one can estimate the life expectancy for a given structural reliability.

Appendix A; RANDOM VARIABLES USED IN CALCULATIONS

A.1 *Concrete density*

Distribution	Normal
μ	24 kN/m³
σ	$0.70 \cdot 0.04 \cdot \mu = 0.672 \text{kN/m}^3$

Description:

It's assumed a constant correlation ρ_m between to points in two different members, but within "one building" (JCSS, 2001) is valid for a slab buttress dam. Thus, the recommended coefficient of variation is reduced with a factor of 0.7 in the calculations.

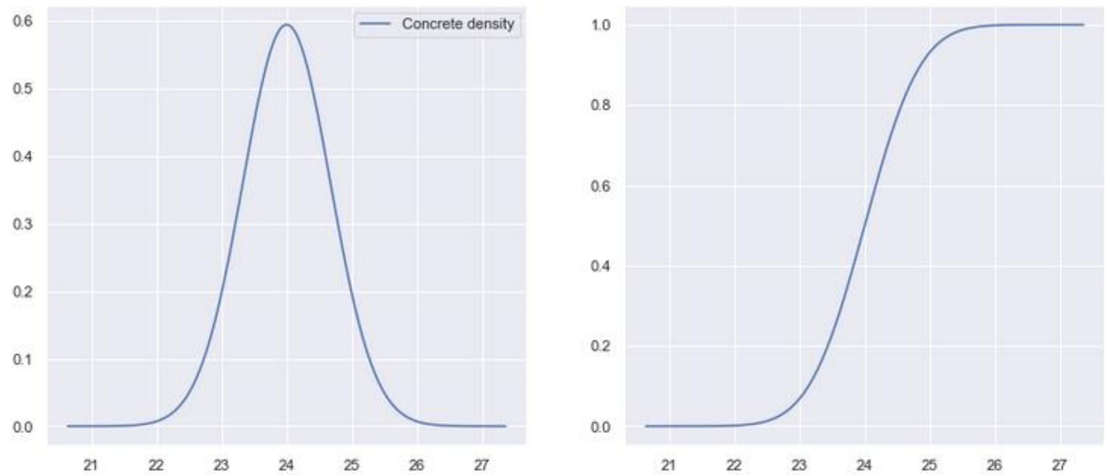

A.2 *Friction angle*

Distribution	Normal
μ	50 ° | 45 °
σ_{prior} $\sigma_{"Tested"}$	$0.12 \cdot \mu = 6°$ $0.05 \cdot \mu' = 2.25°$

Description:

It's assumed that the characteristic friction angle in the guidelines refers to the mean value. The variance is set high to account for the uncertainty in dilatancy, macro-asperities and similar contributions. A hypothetical case where the friction angle has been studied is also assumed for one probabilistic analysis.

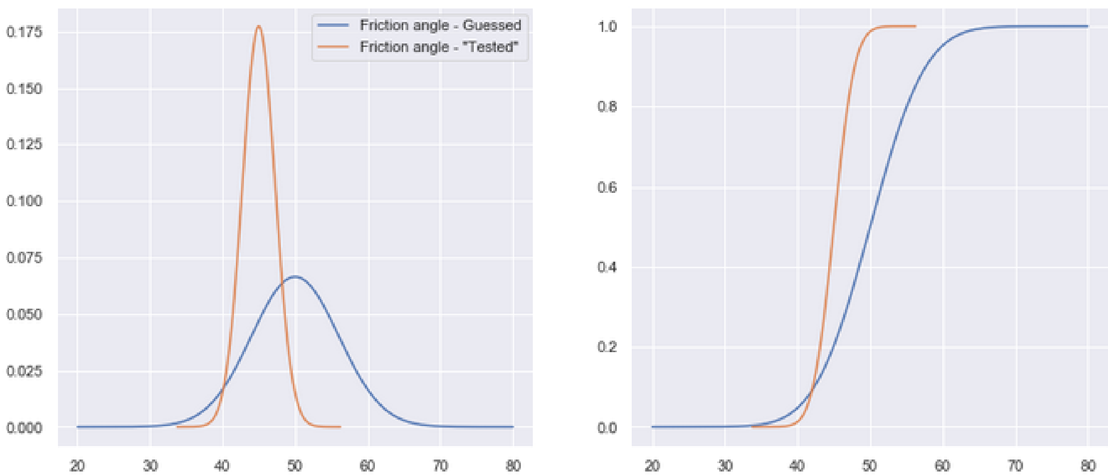

A.3 *Cohesion*

Distribution	Lognormal
μ	75 kPa
σ	$0.5 \cdot \mu = 37.5\ kPa$

Description:

The cohesion is similar to the one used at dam Reinoksvatn (Dr. techn. Olav Olsen, 2017). The mean value is reduced, and a higher variance is chosen to better reflect the uncertainty of cohesion at site. Further study of the cohesion in literature and calculations (spatial variability) is recommended for further work.

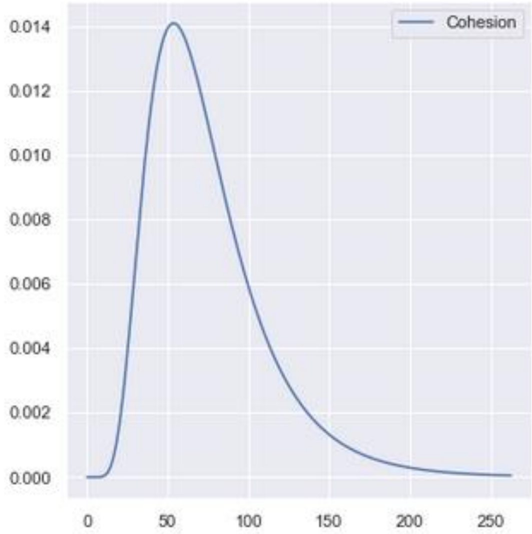

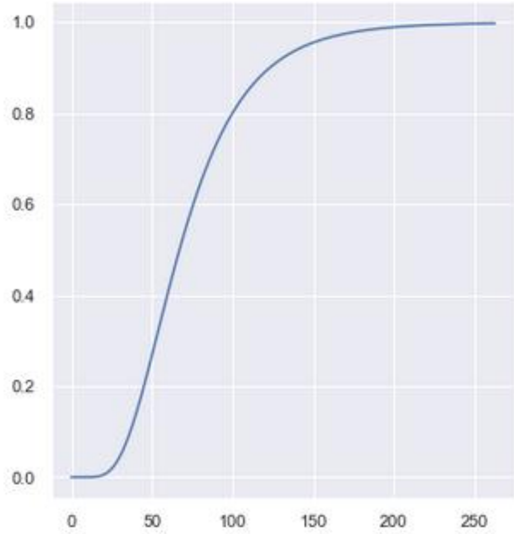

A.4 *Rock Bolt stress*

Distribution	Lognormal
μ	180 MPa
σ	$0.89 \cdot \mu = 160.2\ MPa$

Description:

For simplicity only the rock bolt stress is used as a basic variable since it directly influences the load in calculations. The recommended bolt stress from the guidelines (NVE, 2005) is assumed as a mean value with a high coefficient of variance. This should be studied and compared with actual bolt capacity according to Eurocode, or other criteria.

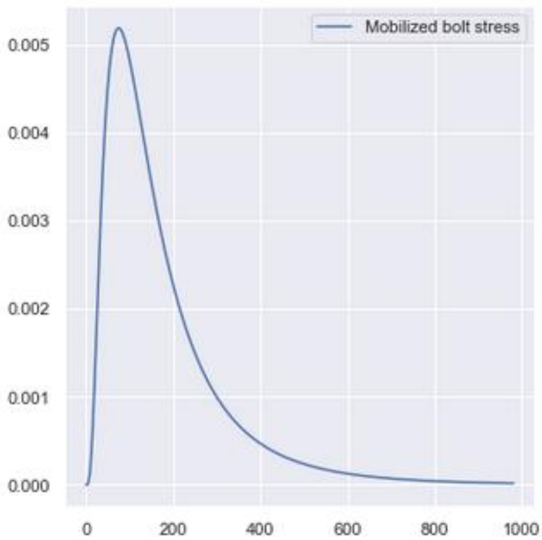

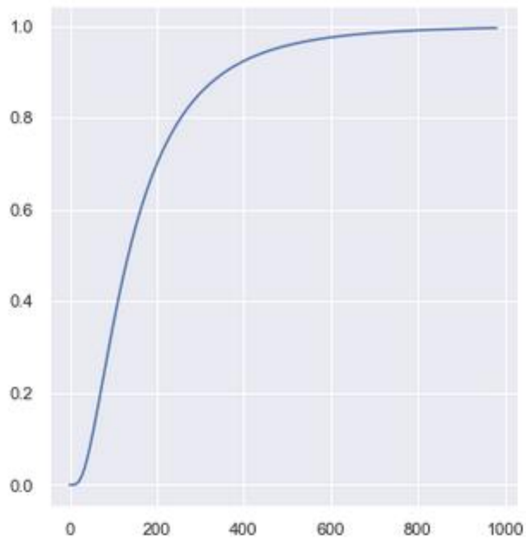

A.5 *HRV*

Distribution	Normal
μ	566 m a.s.l
σ	1.415 m

Description:

The defined HRV is assumed as mean value, and the variance is subjectively chosen by the analyst prior to examining the spillway capacity and water level measurements on site.

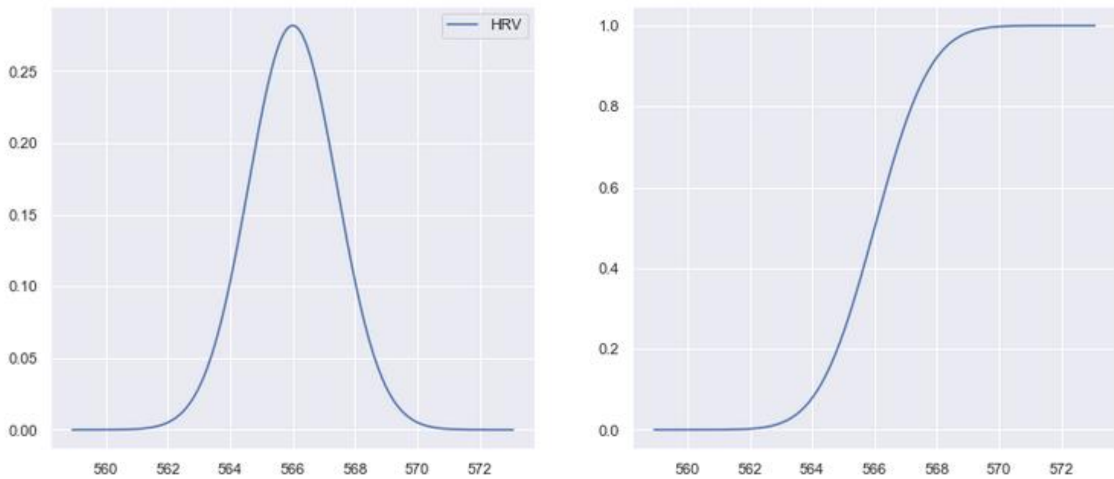

A.6 *DFV*

Distribution	Normal
μ	567.61 m a.s.l
σ	2.838 m

Description:

The defined DFV is assumed as mean value, and the variance is subjectively chosen by the analyst prior to examining the spillway capacity and water level measurements on site.

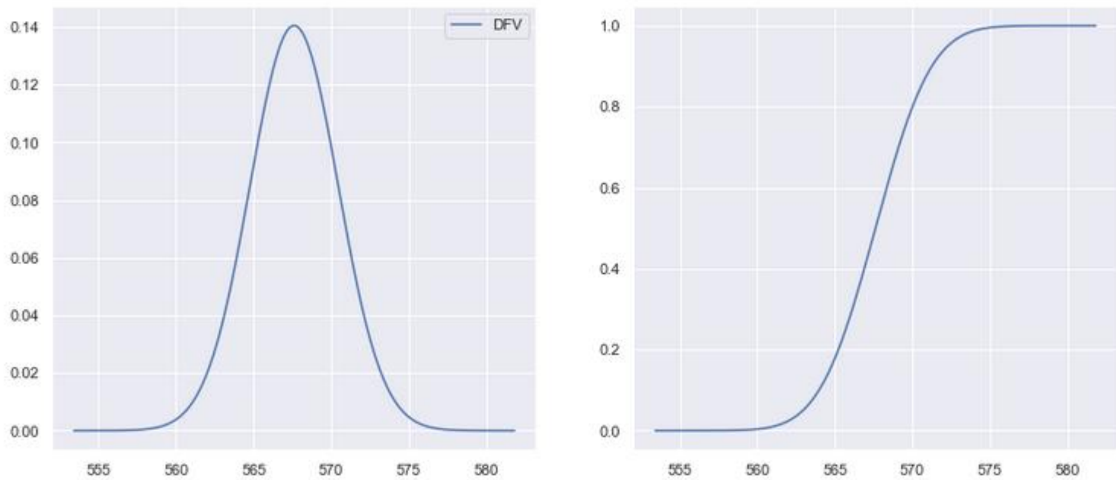

A.7 *MFV*

Distribution	Normal
μ	567.81 m a.s.l
σ	2.839 m

Description:

The defined MFV from PMF is assumed as mean value, and the variance is subjectively chosen by the analyst prior to examining the spillway capacity and water level measurements on site.

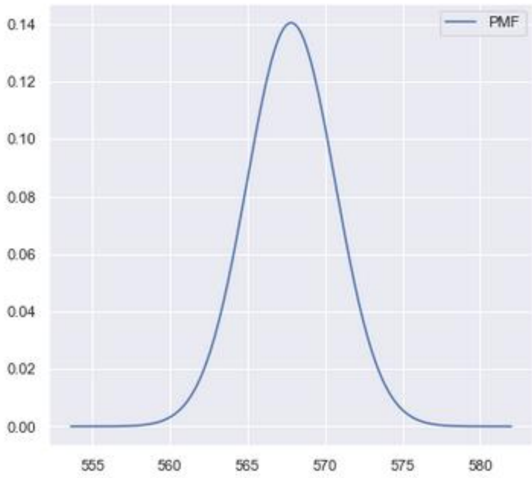

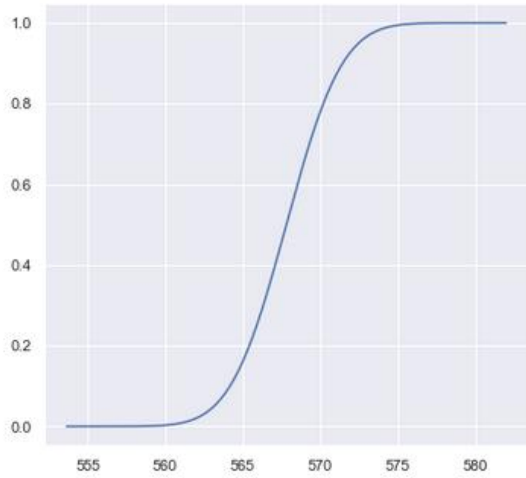

A.8 *Ice load*

Distribution	Lognormal*
μ	80 kN/m
σ	80 | 10

Description:

Three different assumptions for the ice load have been studied in this report. The recommended ice load with truncation, without truncation and ice load with reduced variance is assumed in the probabilistic analyses.

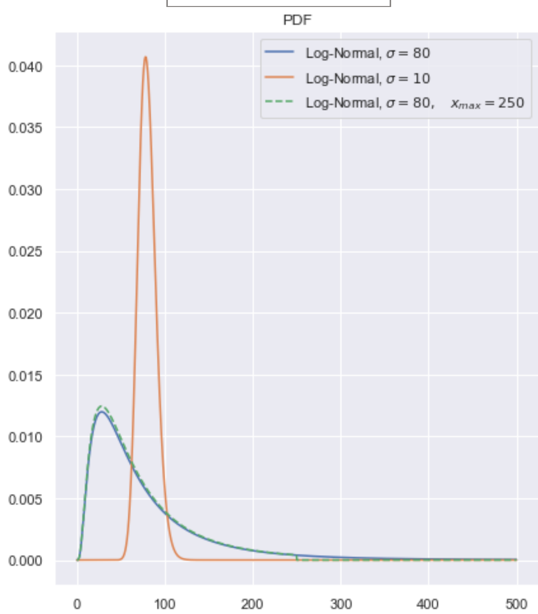

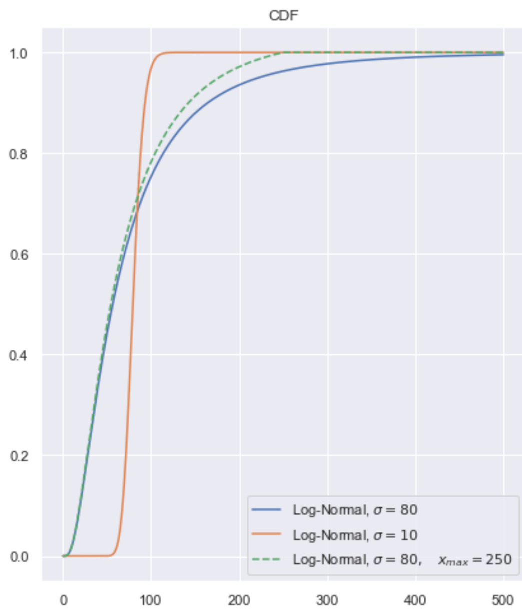

A.9 *Centre to centre distance*

Distribution	Normal
μ	$5\ m$
σ	$0.05\mu = 0.25m$

Description:

The nominal distance is subjectively assumed of the analyst to vary with 5% of the mean value.

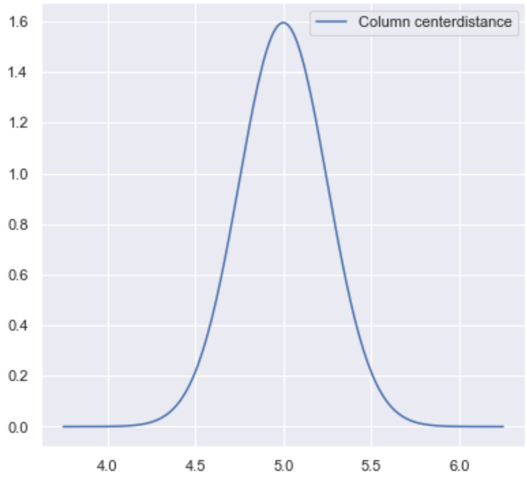

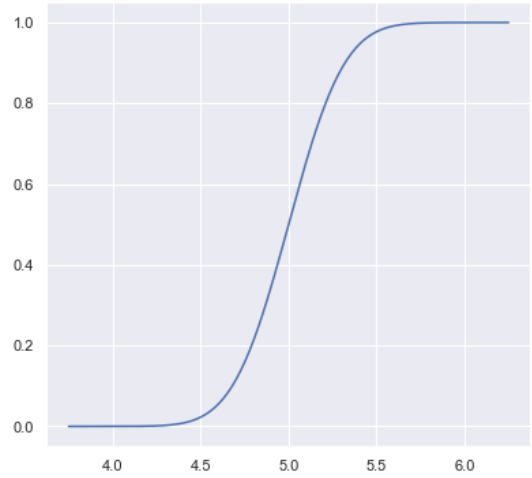

A.10 *Inclination - Upstream*

Distribution	Normal
μ	0.8
σ	$0.01\mu = 0.008$

Description:

The nominal inclination is subjectively assumed of the analyst to vary with 1% of the mean value.

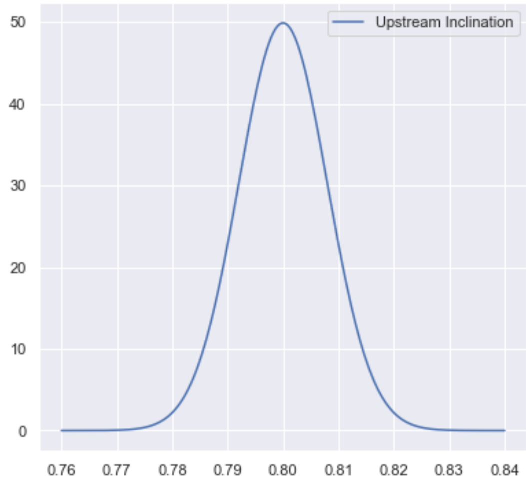

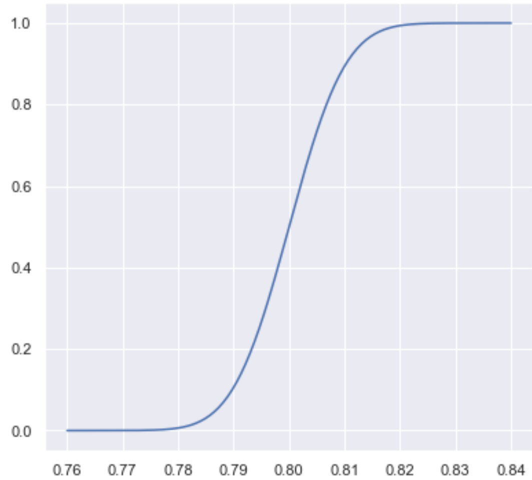

A.11 *Inclination - Downstream*

Distribution	Normal
μ	0.33
σ	$0.01\mu = 0.0033$

Description:

The nominal inclination is subjectively assumed of the analyst to vary with 1% of the mean value.

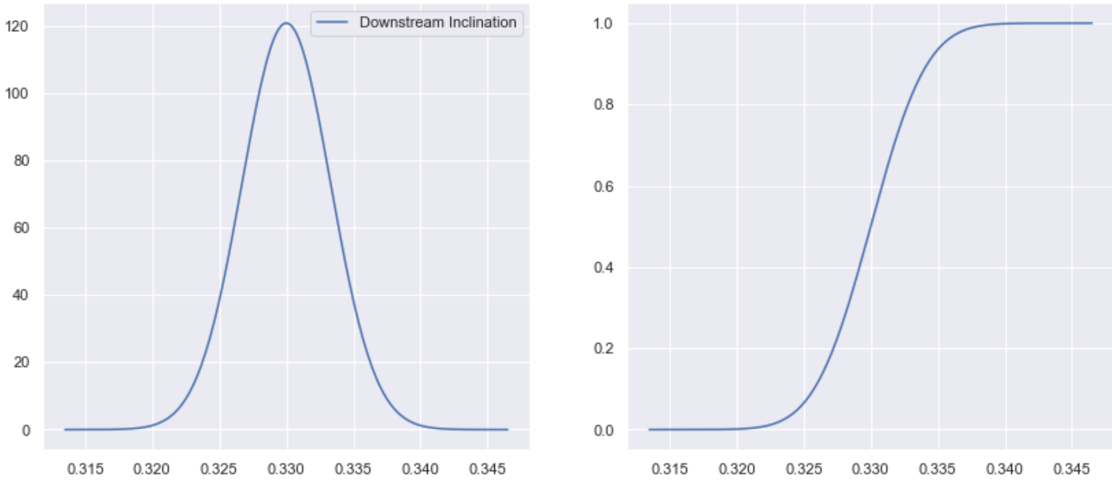

A.12 *Crest width*

Distribution	Normal
μ	$2.0\ m$
σ	$0.05\mu = 0.1m$

Description:

The nominal distance is subjectively assumed of the analyst to vary with 5% of the mean value.

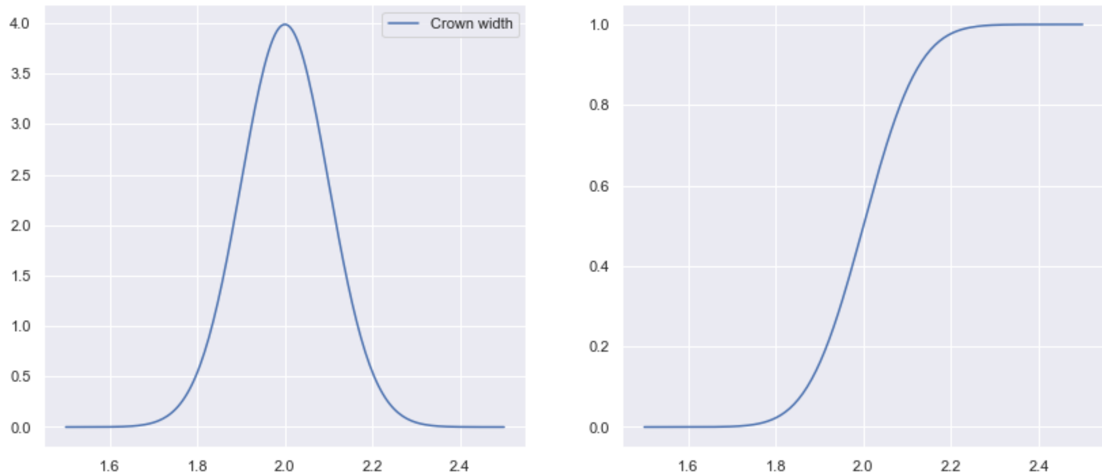

A.13 *Vertical upstream height*

Distribution	Normal
μ	$1.5m$
σ	$0.05\mu = 0.075m$

Description:

The nominal distance is subjectively assumed of the analyst to vary with 5% of the mean value.

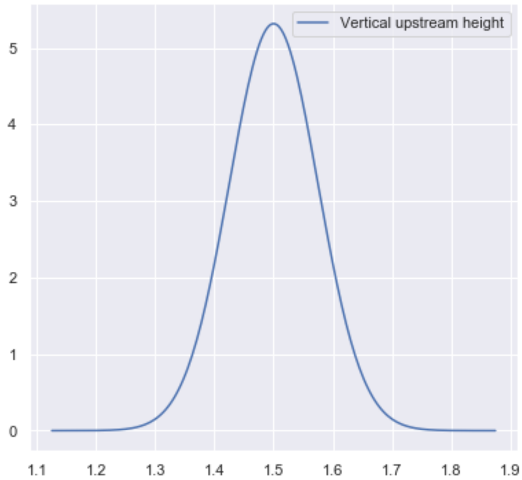

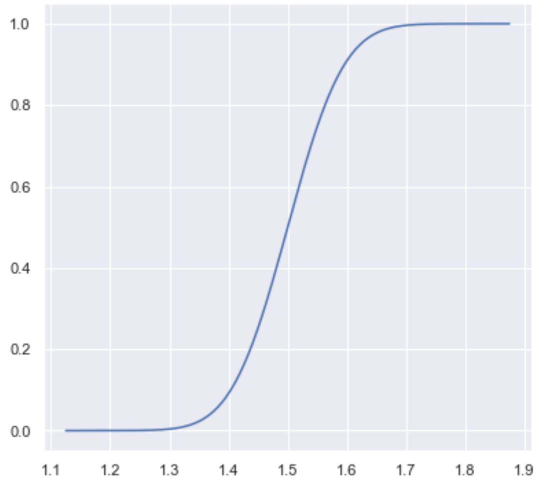

A.14 *Plate thickness - Top*

Distribution	Normal
μ	$0.30\ m$
σ	$0.05\mu = 0.015\ m$

Description:

The nominal distance is subjectively assumed of the analyst to vary with 5% of the mean value.

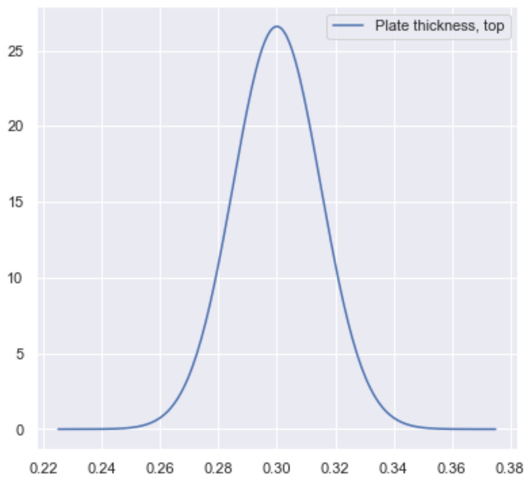

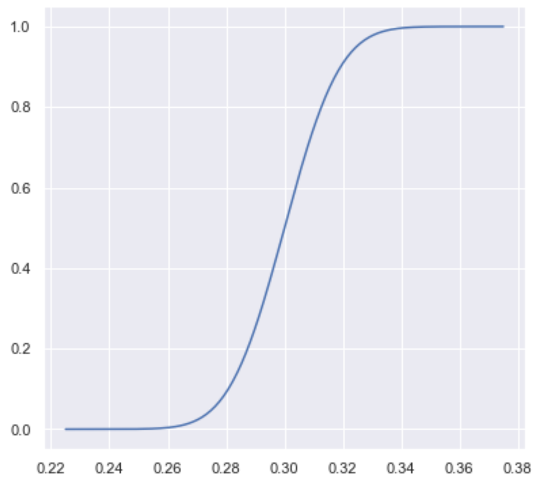

A.15 *Plate thickness - Bottom*

Distribution	Normal
μ	$0.60m$
σ	$0.05\mu = 0.03m$

Description:

The nominal distance is subjectively assumed of the analyst to vary with 5% of the mean value.

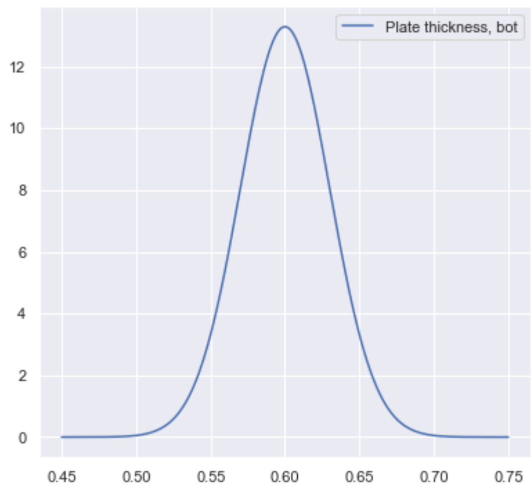

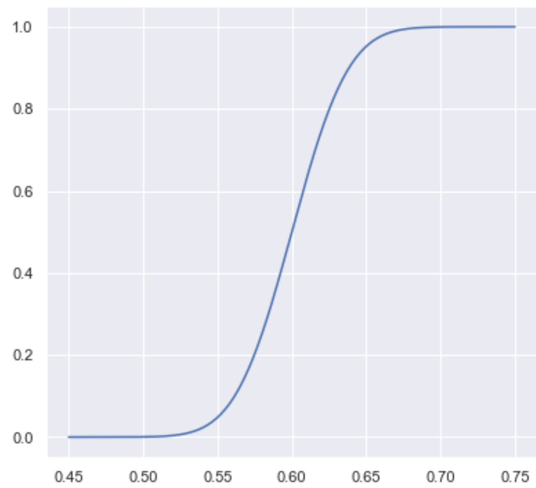

A.16 *Column thickness - Top*

Distribution	Normal
μ	$0.35m$
σ	$0.05\mu = 0.0175m$

Description:

The nominal distance is subjectively assumed of the analyst to vary with 5% of the mean value.

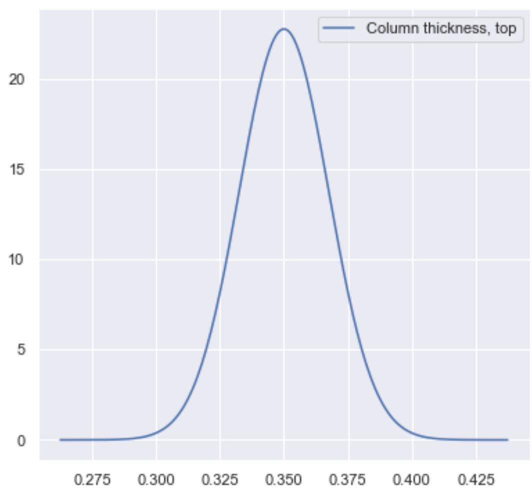

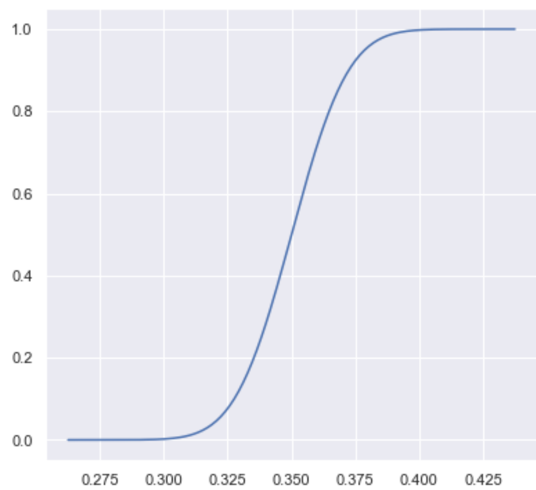

A.17 *Column thickness - Bottom*

Distribution	Normal
μ	$0.66m$
σ	$0.05\mu = 0.033m$

Description:

The nominal distance is subjectively assumed of the analyst to vary with 5% of the mean value.

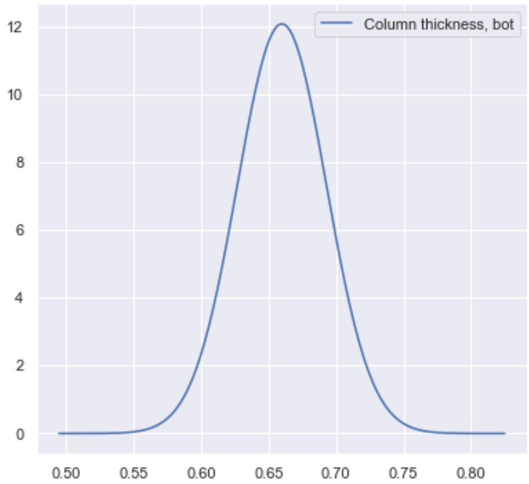

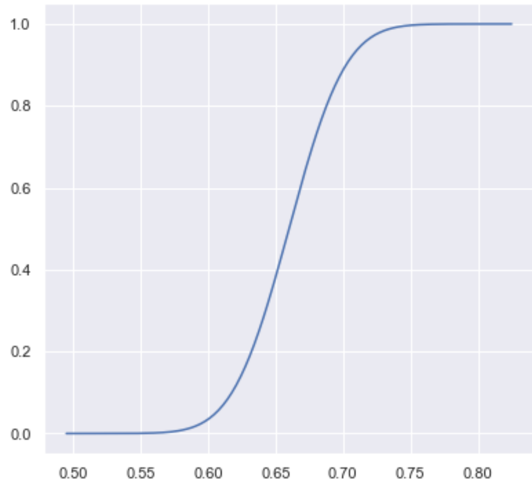

A.18 *Top height (I.e. total dam height)*

Distribution	Normal
μ	566
σ	$0.01 \times 10.5m = 0.105m$

Description:

The dam height is subjectively assumed of the analyst to vary with 1% of the nominal (assumed) height. Note that the same value has wrongly been used for P.55, where the dam height is 7 m. It's recommended for further work that the dam height is rather determined by the bottom level, and not the top which is the case here.

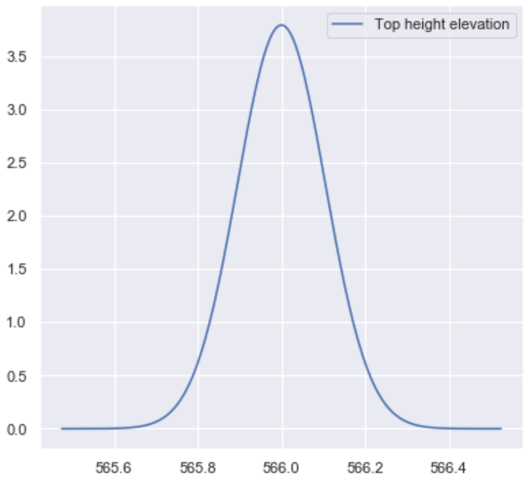

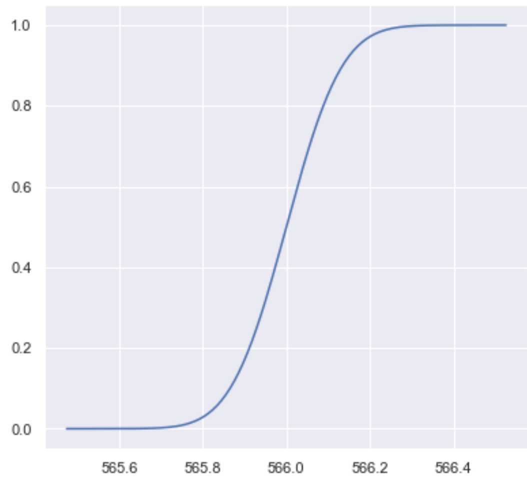

Appendix B; Interpretation of measured data

The data received from E-CO Energi AS contains measured data of the water level, water outflow in spillways and water consumption to the power generators. The available digitized dataset dates back to 1993 and up to 28.11.2019, which gives a total of 26 years of data.

The data set has been interpreted using mainly the Python libraries of Numpy, Pandas, Matplotlib, Scipy, Seaborn and Bokeh in Jupyter Notebook. The complete dataset and the average monthly trend are shown below in Figure 6-1. From the figure one can observe that the water level is rarely above HRV at 566 m a.s.l. The second subplot indicates that flooding occurs fairly periodic with varying extreme measurements. The last subplot shows that the water consumption is irregular and sometimes drops to zero. Furthermore, the plot shows that the power generators was upgraded around 2005 and 2006 which lead to an increase in the maximum capacity.

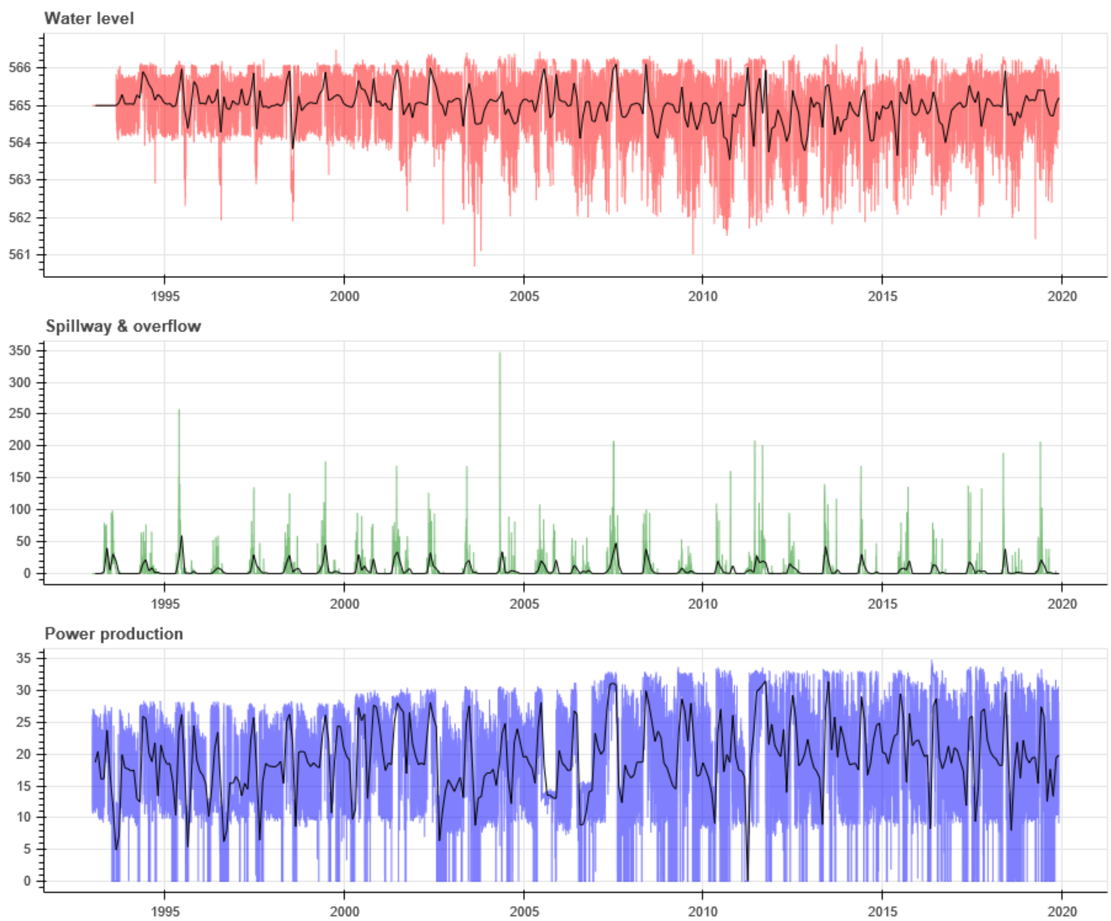

> *Figure 6-1: Received dataset shown with monthly average trend.*

On further inspection of an individual year one can typically observe that the water level plataues during flooding as in Figure 6-2. This is the result of the radial gates which tries to automatically regulate the water level at 566.18 m a.sl. Attempts to backcalculate the measured overflow from the measured water was not possible, and the validity of the measurements can thus not be confirmed. The measurements are from digital recordings and are here assumed to be correct.

The yearly trend typically shows that flooding occurs around may to july each year and sporadically during the fall. The first floods are believed to be a large degree caused by snow melting. Flooding later in the year often occurs more randomly and is believed to be mainly caused by rainfall.

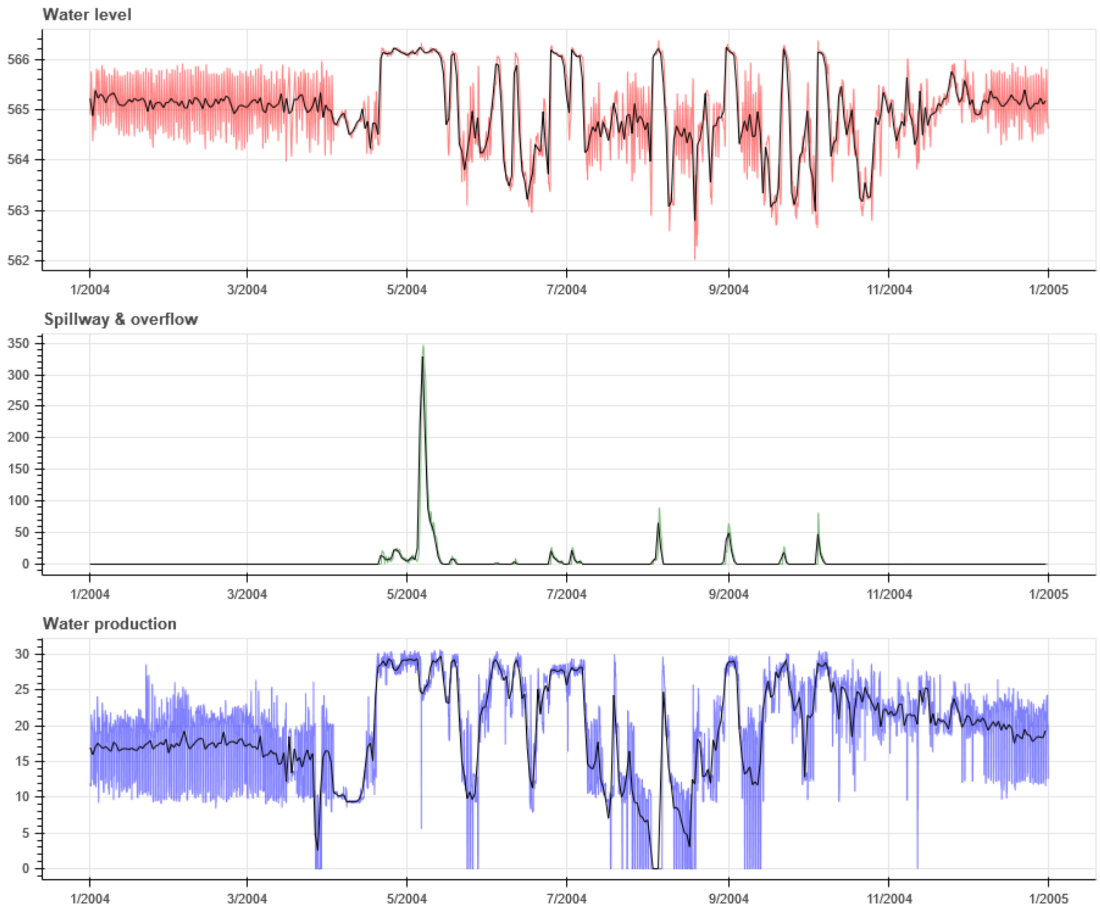

> *Figure 6-2: Yearly measurement at Eikrebekken 2004 with daily mean trend.*

By dividing the measured data into bins one can measure the frequency and construct probability density plots as shown in Figure 6-3, Figure 6-4 and Figure 6-5. The first figure shows a bimodal distribution and is caused by two processes occuring. During normal operation the water level is regulated and thus most often around 565 m a.s.l. In the case of flooding the water level is often kept close to 566.18 m a.s.l.

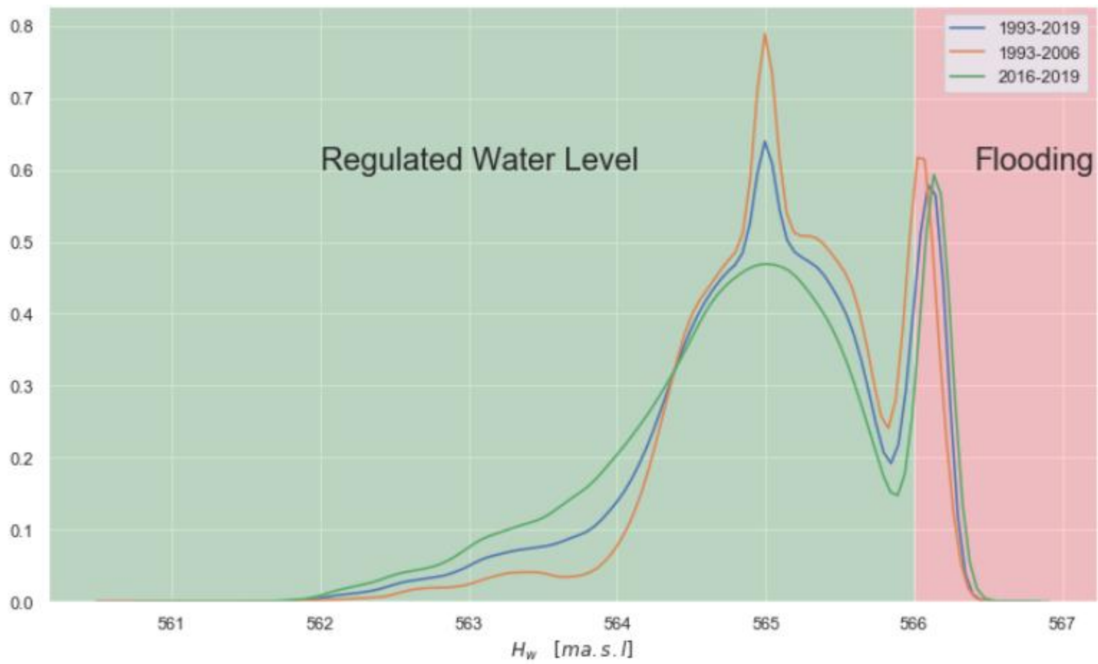

> *Figure 6-3: Probability density plot of measured water level at Eikrebekken.*

Similary one can observe that the water loss in spillways, shown in Figure 6-4, is seldomly above 100 m^3/s and has the highest probability close to zero. The figure also indicates that the upgrade done in 2005-2006 has had a little impact on the discharge capacity.

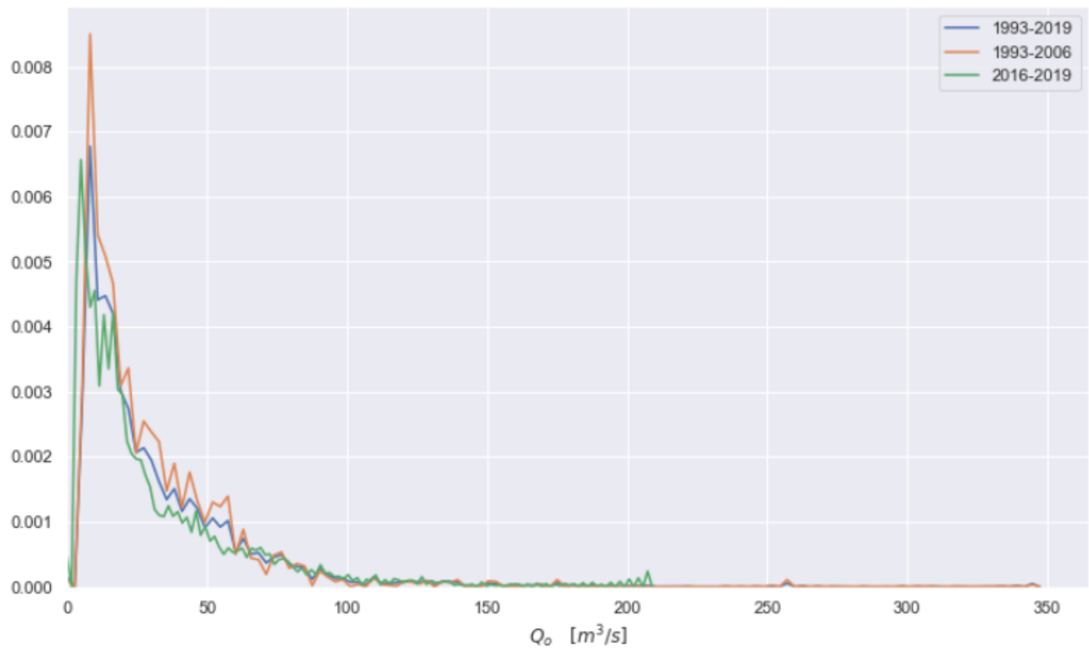

> *Figure 6-4: Probability density plot of measured water outflow in spillways.*

Figure 6-5 clearly shows a change in the water consumption due to the upgrade in 2005-2006. By inspecting the water consumption before and after the upgrade one can observe 4 distinct peaks. The first peak at zero tells that there is some chance that both power generators are turned off. While the second and third peak is assumed to be caused by running one or two generators. The last peak is believed to be the result of the two generators running at maximum capacity, which can be seen to have been increased after the upgrade.

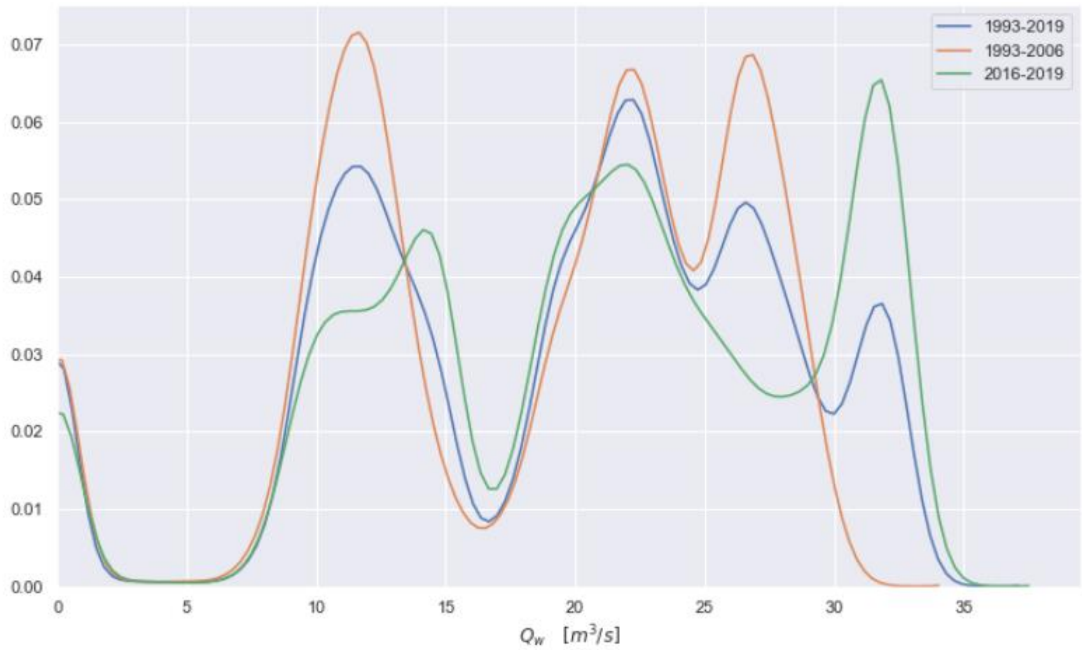

> *Figure 6-5: Probability density plot of measured water consumption to power generators.*

The monthly variation has also been studied and the monthly maximum variation is shown in Figure 6-6. It can be seen that the maximum variation is small during the winter months desember to march in the water level. The highest variation is observed in april and october. While for the measured water outflow the highest variation is in may and june.

Based on the received data one can backcalculate the water inflow if the the height contours of the reservoir is known. If the the reservoir is small compared to the water inflow, it's typical to assume that the reservoir change can be neglected, i.e. $Q_{in} = Q_{out}$. This dataseries can afterwards be used to calculate extreme flooding situtations by extreme value theory and can be used to compare to flood calculations for the given catchment area.

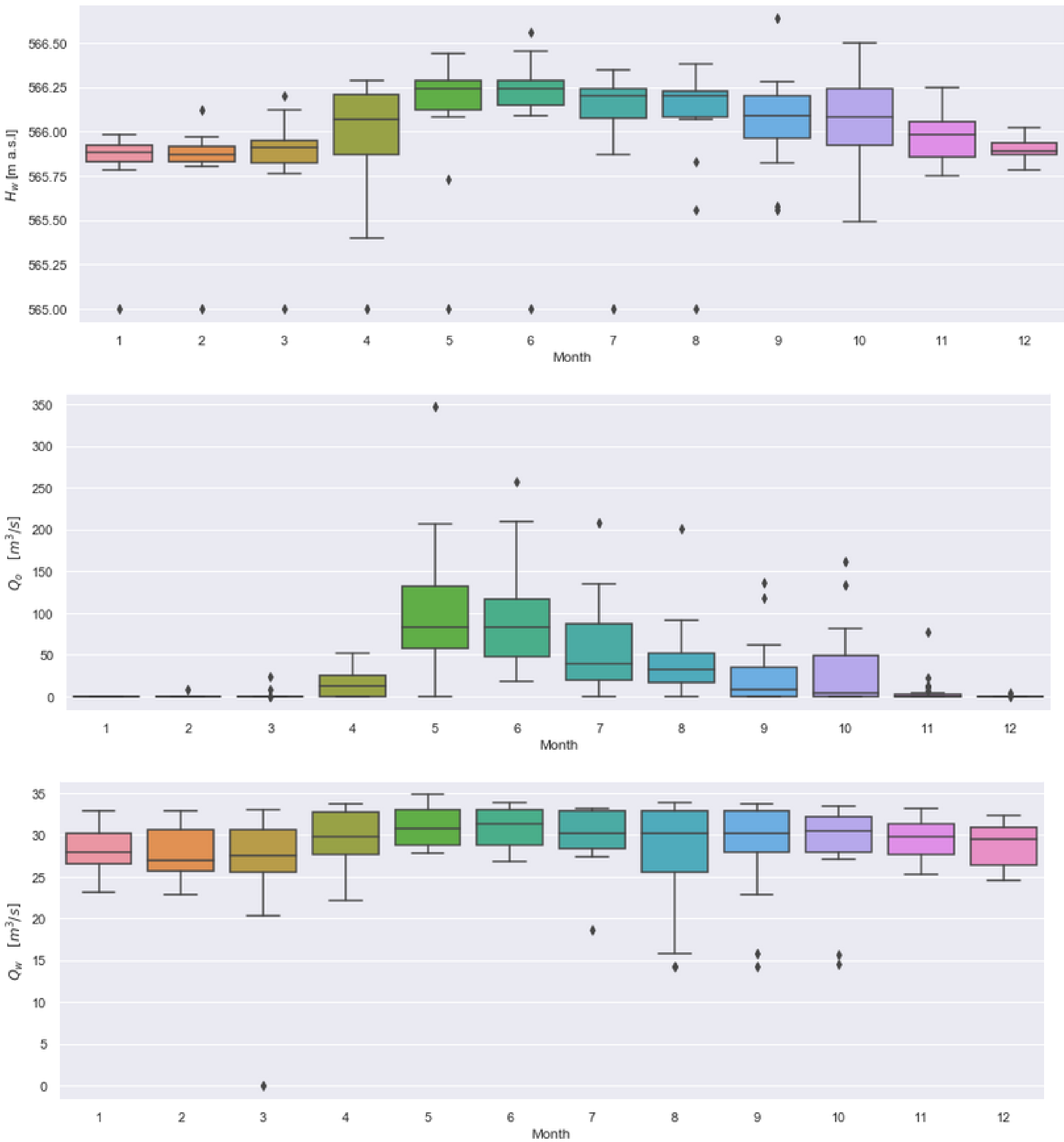

> *Figure 6-6: Whiskers plot of max monthly variation of the measured dataset.*